

Louisiana State University LSU Digital Commons

LSU Doctoral Dissertations

Graduate School

2006

Retention and Transport of Arsenic in Soils

Hua Zhang

Louisiana State University and Agricultural and Mechanical College, hzhang4@lsu.edu

Follow this and additional works at: https://digitalcommons.lsu.edu/gradschool_dissertations

Recommended Citation

Zhang, Hua, "Retention and Transport of Arsenic in Soils" (2006). *LSU Doctoral Dissertations*. 3194.
https://digitalcommons.lsu.edu/gradschool_dissertations/3194

This Dissertation is brought to you for free and open access by the Graduate School at LSU Digital Commons. It has been accepted for inclusion in LSU Doctoral Dissertations by an authorized graduate school editor of LSU Digital Commons. For more information, please contact gradetd@lsu.edu.

RETENTION AND TRANSPORT OF ARSENIC IN SOILS

A Dissertation

Submitted to the Graduate Faculty of the
Louisiana State University and
Agricultural and Mechanical College
in partial fulfillment of the
requirement for the degree of
Doctor of Philosophy

in

The Department of Agronomy and Environmental Management

by

Hua Zhang

B.S., HuaZhong Agricultural University, 1999

M.S., Chinese Academy of Sciences, 2002

December, 2006

ACKNOWLEDGEMENTS

At this opportunity the author wishes to express his most sincere gratitude and appreciation to Dr. H.M. Selim, Caldwell Endowed Professor of Soils, for his valuable guidance and genuine interest as research advisor and chairman of the examination committee. Deep appreciation is also extended to other members of the committee, Dr. Donald D. Adrian, Dr. Ronald D. DeLaune, Dr. Jim J. Wang, Dr. William Blanford, and Dr. Nan D. Walker for their support and constructive suggestions.

I wish to thank the Department of Agronomy and Environmental Management for the wonderful experience I have had during my study period. I also would like to express my appreciation for my fellow graduate students: Brain Naquin, and Lixia Liao, for their help and friendship. I would like to thank Jackie Prudente for her ICP expertise. Thank all student workers who have spent time with me, especially the late Elizabeth Thompson, you will always be remembered.

Funding for this research was supported by the Louisiana Agricultural Experiment Station and the Department of Environmental Quality (DEQ), Section 319.

I would like to acknowledge my wife, Xueli Gao for her patience and understanding. I would like to give my final thanks to my parents for their support throughout my life.

TABLE OF CONTENTS

ACKNOWLEDGEMENTS	ii
LIST OF TABLES	vi
LIST OF FIGURES	viii
ABSTRACT	xii
CHAPTER	
1. INTRODUCTION	1
1.1 Statement of Problem.....	2
1.2 Objectives	2
1.3 References.....	3
2. ARSENIC IN SOILS: A REVIEW.....	4
2.1. Introduction.....	4
2.2. Environmental Toxicity of Arsenic	4
2.3. Arsenic in Soils.....	6
2.3.1 Background Concentrations.....	6
2.3.2 Arsenic Sources	6
2.3.2 Soil Arsenic Regulations.....	10
2.3.4 Chemical Speciation	11
2.4. Adsorption-Desorption of Arsenic in Soils.....	12
2.4.1 Adsorption Mechanisms	12
2.4.2 Adsorption Envelopes.....	17
2.4.3 Adsorption Isotherms.....	19
2.4.4 Competing Anions	21
2.4.5 Kinetic Adsorption-Desorption.....	24
2.5. Dissolution – Precipitation.....	28
2.5.1 Dissolution of Primary Minerals.....	28
2.5.2 Reductive Dissolution of Metal Oxides	29
2.5.3 Coprecipitation and Surface Precipitation with Metal Oxides.....	31
2.5.4 Precipitation with Sulfides.....	32
2.6. Reduction-Oxidation.....	32
2.6.1 Thermodynamics.....	33
2.6.2 Oxidation by Metal Oxides.....	34
2.6.3 Reduction by Sulfides	35
2.6.4 Biotransformation	35
2.6.5 Kinetics of Arsenic Reduction-Oxidation in Soils.....	36
2.7. Transport of Arsenic under Dynamic Flow Condition	37
2.8. Movement of Arsenic in Field	41
2.9. Remediation of Arsenic Contaminated Soils.....	44
2.10. Summary	46
2.11. References.....	47

3. KINETICS OF ARSENATE ADSORPTION-DESORPTION IN SOILS	59
3.1 Introduction.....	59
3.2 Materials and Methods.....	62
3.3 Multireaction Model	65
3.4 Results and Discussion	67
3.4.1 Nonlinear Sorption Isotherms.....	67
3.4.2 Adsorption Kinetics	73
3.4.3 Desorption Hysteresis and Binding Phases.....	75
3.4.4 Multireaction Modeling.....	77
3.5 Summary and Conclusions	82
3.6 References.....	85
4. MODELING THE TRANSPORT AND RETENTION OF ARSENIC(V) IN SOILS	88
4.1 Introduction.....	88
4.2 Material and Methods	90
4.3 Results and Discussion	94
4.3.1 Kinetic Sorption.....	94
4.3.2 Tracer Breakthrough Curves.....	98
4.3.3 Arsenate Breakthrough Curves.....	100
4.3.4 Multireaction Transport Modeling.....	101
4.3.5 Inverse MRM Modeling	103
4.4 Summary and Conclusions	110
4.5 References.....	111
5. COMPETITIVE SORPTION KINETICS OF ARSENATE AND PHOSPHATE IN SOILS	113
5.1 Introduction.....	113
5.2 Material and Methods	115
5.3 Results and Discussion	116
5.3.1 Adsorption Isotherms.....	116
5.3.2 Competitive Adsorption.....	118
5.3.3 Adsorption Kinetics	122
5.3.4 Desorption and Sequential Extraction	126
5.3.5 Selectivity Coefficients.....	128
5.3.6 Multi-reaction Modeling.....	130
5.4 Summary and Concluions	132
5.5 References.....	133
6. MODELING ARSENATE-PHOSPHATE RETENTION AND TRANSPORT IN SOILS: A MULTI-COMPONENT APPROACH	136
6.1 Introduction.....	136
6.2 Model Formulation	138
6.3 Materials and Methods.....	142
6.4 Results and Discussion	143
6.4.1 Competitive Sorption Isotherms	143
6.4.2 Sorption Kinetics	145

6.4.3 Multi-Component Retention Kinetics.....	147
6.4.4 Breakthrough Curves	155
6.4.5 Transport Modeling	163
6.5 Summary and Conclusions	167
6.6 References.....	168
7. COLLOID MOBILIZATION AND ARSENITE TRANSPORT IN SOIL COLUMNS.....	170
7.1 Introduction.....	170
7.2 Material and Methods	173
7.2.1 X-ray Diffraction	173
7.2.2 Miscible Displacement Experiments	174
7.2.3 Sequential Extraction	175
7.3 Results.....	175
7.3.1 Soil Characteristics	175
7.3.2 Arsenite Transport	177
7.3.3 Arsenic Retention in Soils	181
7.3.4 Mobilization of Colloidal Particles.....	181
7.3.5 Release of Fe and Al.....	184
7.4 Discussion.....	187
7.4.1 Colloid Mobilization.....	187
7.4.2 Release of Fe Oxides under Anarobic Condition	189
7.4.3 Arsenite Transport	191
7.4.4 Environmental Implications.....	192
7.5 Summary and Conclusions	192
7.6 References.....	193
8. SUMMARY AND CONCLUSIONS	196
VITA	200

LIST OF TABLES

Table 3.1 Selected physical and chemical properties of the studied soils.	63
Table 3.2 Estimated Freundlich- and Langmuir- equation parameters (with standard error) for arsenate adsorption at different reaction times	70
Table 3.3 Fitted two-phase fully reversible MRM parameters (with standard error) for adsorption and desorption kinetics of As(V) in soils.....	81
Table 3.4 Fitted three-phase reversible-irreversible MRM parameters (with standard error) for adsorption and desorption kinetics of As(V) in soils.....	81
Table 4.1 Column soil physical parameters for As(V) and tritium miscible displacement experiments for single and double pulses. Values of the dispersion coefficient were estimated from tritium breakthrough results.	93
Table 4.2 Comparison of the goodness-of-fit of a two-phase kinetic reversible and consecutive irreversible model requires 3 parameters model formulation ($M4 = k_1, k_2, \text{ and } k_3$) for Olivier soil.....	95
Table 4.3 Comparison of parameters and goodness-of-fit determined from fitting eight different MRM model formulations to kinetic adsorption data.....	96
Table 4.4 Root mean squared errors (RMSE) of predicted and optimized arsenate breakthrough curves (BTCs) across all soil columns and eight different MRM formulations (M1-M8).	104
Table 5.1 Estimated Freundlich and SRS parameters for 24 h adsorption of arsenate and phosphate	119
Table 5.2 Estimated MRM parameters for the kinetic adsorption of arsenate in the presence of various concentrations of phosphate.....	131
Table 5.3 Estimated MRM parameters for the kinetic adsorption of phosphate in the presence of various concentrations of arsenate	131
Table 6.1 Soil physical parameters for miscible displacement experiments. Values of the dispersion coefficient were estimated from tritium breakthrough results.	144
Table 6.2 Estimated single component MRM parameters (with standard errors) for adsorption kinetics of arsenate and phosphate.....	148
Table 6.3 Estimated single component MRM parameters (with standard error) obtained from nonlinear optimization with As(V) BTCs.....	164
Table 7.1 Column soil physical parameters for miscible displacement experiments. Values of the dispersion coefficient were estimated from tritium breakthrough results.	176

Table 7.2 XRD determined mineral composition of coarse (0.2-2 μm) and fine ($<0.2\mu\text{m}$) fractions of sodium-dispersible clay (SDC) and water-dispersible clay (WDC) for Olivier and Windsor soils	176
--	-----

Table 7.3 Cumulative amount of As, Fe, and Al leached out and amount of As retained in soil columns	179
---	-----

LIST OF FIGURES

Figure 3.1 A schematic diagram of the multireaction transport model (MRM). Here C is concentration in solution, S_e , S_k , S_i and S_s are the amounts sorbed on equilibrium, kinetic, consecutive and ccurrent irreversible sites, respectively, where K_e , k_1 , k_2 , k_3 and k_s are the respective rates of reactions.	66
Figure 3.2 Isotherms of arsenate adsorption on different soils. Symbols are for different reaction times of 24, 72, 168, 336, and 504 h (from bottom to top). Solid curves depict results of curve-fitting with Freundlich equation.....	69
Figure 3.3 Freundlich parameter N (top), coefficient K_F (middle), and Langmuir adsorption maxima S_{max} (bottom) as a function of total amount of citrate-bicarbonate-dithionite (CBD) extractable Fe and Al content.	72
Figure 3.4 Arsenate concentration in solution versus time during adsorption-desorption for different soils. Symbols are for different initial concentrations (C_0) of 5, 10, 20, 40, 80, and 100 mg L ⁻¹ (from bottom to top). Solid curves are two-phase MRM simulations using parameters obtained from nonlinear optimization with adsorption data.	74
Figure 3.5 Isotherms of arsenate desorption from different soils based on successive dilution after the last adsorption step for different initial concentrations (C_0) of 20, 40, 80, and 100 mg L ⁻¹ . The solid and dashed curves depict results of curve-fitting with Freundlich equation for 504 h adsorption, and desorption isotherms, respectively.	76
Figure 3.6 Recoveries of arsenic from desorption and sequential extractions as percentages of total adsorption amounts for different soils. Different patterns illustrate arsenic distribution among the following pools: P1 = desorbed during successive desorption, P2 = extracted with 1M NaH ₂ PO ₄ , P3 = extracted with 0.2 M ammonium oxalate, and P4 = digested with 4 M HNO ₃ . Different groups indicate initial concentrations (C_0) of 5, 10, 20, 40, 80, and 100 mg L ⁻¹	78
Figure 3.7 Arsenate sorbed versus time during adsorption-desorption for Olivier and Windsor soils. Symbols are for initial concentrations (C_0) of 5, 10, 20, 40, 80, and 100 mg L ⁻¹ (from bottom to top). Solid curves are two-phase MRM simulations using parameters obtained from nonlinear optimization with adsorption data.....	83
Figure 3.8 Arsenate sorbed versus time during adsorption-desorption for Sharkey soil. Symbols are for different initial concentrations (C_0) of 5, 10, 20, 40, 80, and 100 mg L ⁻¹ (from bottom to top). Solid curves are three-phase MRM simulations using parameters obtained from nonlinear optimization with adsorption data.....	84
Figure 4.1 Tritium breakthrough curves for soils. Solid curves depict results of curve-fitting with convection dispersion equation (CDE) for non-reactive solutes	92

Figure 4.2 Comparison of MRM model formulations M1-M8 for predicting As(V) breakthrough curves for Olivier soil (top) and Windsor soil (bottom). Model parameters were those from the batch kinetic experiment (Table 4.3).	99
Figure 4.3 Comparison of MRM model formulations M1-M8 model for predicting As(V) breakthrough curves for Olivier soil column 101. Model parameters were obtained using nonlinear inverse modeling.....	105
Figure 4.4 Comparison of MRM model formulations M1-M8 for predicting As(V) breakthrough curves for Olivier soil column 102. Model parameters were obtained using nonlinear inverse modeling	106
Figure 4.5 Comparison of MRM model formulations M1-M8 for predicting As(V) breakthrough curves for Windsor soil column 103. Model parameters were obtained using nonlinear inverse modeling	107
Figure 4.6 Comparison of MRM model formulations M1-M8 for predicting As(V) breakthrough curves for Windsor soil column 104. Model parameters were obtained using nonlinear inverse modeling	108
Figure 4.7 Comparison of predictions and simulations using MRM model formulation M8 for predicting As(V) breakthrough curves for Sharkey soil column 105	109
Figure 5.1 Arsenate [As(V)] and phosphate (P) adsorption isotherms at 24 h of reaction for Olivier, Sharkey, and Windsor soils. The lines depict results of curve-fitting with Freundlich equation.....	120
Figure 5.2 Competitive sorption between arsenate and phosphate at 24 h of reactions for Olivier, Sharkey, and Windsor soils. The initial concentrations of arsenate were 0.13 mM	121
Figure 5.3 Arsenate concentrations in solution as a function of reaction time during adsorption on Olivier, Sharkey, and Windsor soils in the presence of various concentrations of phosphate. The initial concentrations of arsenate were 0.13 mM. The initial concentrations of phosphate were 0, 0.32, 1.3, and 3.2 mM. The lines depict results of MRM simulation.....	124
Figure 5.4 Phosphate concentrations in solution as a function of reaction time during adsorption on Olivier, Sharkey, and Windsor soils in the presence of various concentrations of arsenate. The initial concentration of phosphate was 0.32 mM. The initial concentrations of arsenate were 0, 0.13, and 1.3 mM. The lines depict results of MRM simulation.	125
Figure 5.5 Recoveries of arsenic from desorption and sequential extractions for different soils. Different patterns illustrate arsenic distribution among the following pools: P1 = desorbed during successive desorption, P2 = extracted with 0.2 M ammonium oxalate, and P3 = digested with 4 M HNO ₃ . Different groups indicate different initial phosphate concentrations of 0, 0.32, 1.3, and 3.2 mM	127

Figure 5.6 Selectivity coefficients of arsenate to phosphate as a function of reaction time for Olivier, Sharkey, and Windsor soils. Initial concentrations were 1.3 and 3.2 mM for arsenate and phosphate, respectively	129
Figure 6.1 Calculated competitive sorption isotherms for Olivier soil using SRS equation with sorption parameters given in Table 5.1	146
Figure 6.2 Arsenate concentrations versus reaction times for Olivier and Windsor soils. Symbols are for different initial As(V) concentrations of 0.067, 0.13, 0.27, 0.53, 1.07, and 1.33 mM. Solid and dashed curves are single component multireaction model (MRM) simulations with kinetic parameters given in Table 6.2	149
Figure 6.3 Phosphate concentrations versus reaction times for Olivier and Windsor soils. Symbols are for different initial phosphate concentrations of 0.32, 1.29, and 3.23 mM. Solid and dashed curves are single component multireaction model (MRM) simulations with kinetic parameters given in Table 6.2	150
Figure 6.4 Arsenate concentrations versus reaction times with the presence of various concentrations of phosphate for Olivier and Windsor soils. The initial concentrations of arsenate were 0.13 mM. Symbols are for different initial phosphate concentrations of 0, 0.32, 1.3, and 3.2 mM. Solid and dashed curves are multi-component multi-reaction model (MCMRM) simulations with parameters given in Table 6.2.....	152
Figure 6.5 Phosphate concentrations versus reaction times with the presence of various concentrations of arsenate for Olivier and Windsor soils. The initial concentration of phosphate was 0.32 mM. Symbols are for different initial arsenate concentrations of 0, 0.13, and 1.3 mM. Solid and dashed curves are multi-component multi-reaction model (MCMRM) simulations with parameters given in Table 6.2	153
Figure 6.6 Competitive sorption kinetics of arsenate and phosphate on Windsor soils. a) The initial concentrations of arsenate were 0.13 mM. Symbols are for different initial phosphate concentrations of 0, 0.32, 1.3, and 3.2 mM. b) The initial concentration of phosphate was 0.32 mM. Symbols are for different initial arsenate concentrations of 0, 0.13, and 1.3 mM. Solid and dashed curves are multi-component multi-reaction model (MCMRM) simulations with parameters given in Table 6.2	154
Figure 6.7 Experimental As(V) breakthrough curves (BTCs) in Olivier soil without addition of phosphate. Solid curves are single-component multi-reaction model (MRM) predictions made with the kinetic parameters derived from the batch experiment data (Table 6.2), whereas the dashed curves depicts the results of nonlinear optimization of BTCs to the MRM model	156
Figure 6.8 Experimental As(V) breakthrough curves (BTCs) in Olivier soil without addition of phosphate. Solid curves are single-component multi-reaction model (MRM) predictions made with the kinetic parameters derived from the batch experiment data (Table 6.2), whereas the dashed curves depicts the results of nonlinear optimization of BTCs to the MRM model (Table 6.3).	157

Figure 6.9 Experimental As(V) and P breakthrough curves (BTCs) in Olivier soil (column 102). Solid curves are multi-component multi-reaction model (MCMRM) predictions made with the kinetic parameters derived from the batch experiment data (Table 6.2), whereas the dashed curves are MCMRM simulation with kinetic parameters obtained from single component As(V) transport experiment (column 101, see Table 6.3).	158
Figure 6.10 Experimental As(V) and P breakthrough curves (BTCs) in Olivier soil (column 103). Solid curves are multi-component multi-reaction model (MCMRM) predictions made with the kinetic parameters derived from the batch experiment data (Table 6.2), whereas the dashed curves are MCMRM simulation with kinetic parameters obtained from single component As(V) transport experiment (column 101, see Table 6.3).	159
Figure 6.11 Experimental As(V) and P breakthrough curves (BTCs) in Windsor soil (column 105). Solid curves are multi-component multi-reaction model (MCMRM) predictions made with the kinetic parameters derived from the batch experiment data (Table 6.2), whereas the dashed curves are MCMRM simulation with kinetic parameters obtained from single component As(V) transport experiment (column 104, see Table 6.3).	160
Figure 6.12 Experimental As(V) and P breakthrough curves (BTCs) in Windsor soil (column 106). Solid curves are multi-component multi-reaction model (MCMRM) predictions made with the kinetic parameters derived from the batch experiment data (Table 6.2), whereas the dashed curves are MCMRM simulation with kinetic parameters obtained from single component As(V) transport experiment (column 104, see Table 6.3).	161
Figure 7.1 Breakthrough curves (BTC) of total (<20 μ m) and dissolved (<0.2 μ m) arsenic for Olivier and Windsor soil columns. Arrows indicate pore volumes when flow interruptions occur.....	178
Figure 7.2 The percentage recoveries of arsenic as against to the total input as determined from sequential extractions of soils from different column depths. Agents used for extractions were: Exchangeable (1M NaCl), Strongly sorbed (1M NaH ₂ PO ₄), Precipitated (0.2M ammonium oxalate), and Recalcitrant (16 N HNO ₃).	180
Figure 7.3 Effluent turbidity during injection of 10 mg L ⁻¹ As(III) in 0.01M NaCl followed by leaching with deionized water for Olivier and Windsor soil columns. Arrows indicate pore volumes when flow interruptions occur.....	182
Figure 7.4 X-ray diffractograms (XRD) of colloids in the composite effluent solution of Olivier soil column.....	183
Figure 7.5 Mobilization of total (<20 μ m) and dissolved (<0.2 μ m) iron fractions from Olivier and Windsor soil columns. Arrows indicate pore volumes when flow interruptions occur.....	185
Figure 7.6 Mobilization of total (<20 μ m) and dissolved (<0.2 μ m) aluminum fractions from Olivier and Windsor soil columns. Arrows indicate pore volumes when flow interruptions occur.....	186

ABSTRACT

Arsenic transport in soils and aquifers is highly dependent on the adsorption-desorption reactions in the solid phase. Results from our kinetic batch experiments indicated that adsorption of arsenate [As(V)] was highly nonlinear and strongly kinetic. Desorption of As(V) were hysteretic in nature and a significant amount of As(V) was irreversibly adsorbed on all soils. Results from column experiments indicated strong As(V) retardation followed by slow release or extensive tailing of the breakthrough curves (BTCs). Sharp decrease in As(V) concentration during flow interruption verified the extensive non-equilibrium condition which was likely due to the dominance of kinetic retention processes. We evaluated several multireaction model (MRM) formulations for its prediction capability of As(V) retention and transport in soils and concluded that nonlinear reversible along with a consecutive or concurrent irreversible reactions were the dominant mechanisms. The use of batch rate coefficients for the predictions of As(V) BTCs underestimated the extent of retention and overestimated the extent of As(V) mobility for all soils. When utilized in an inverse mode, the MRM model provided good predictions of As(V) BTCs.

The competition between arsenate and phosphate (P) has the potential of increasing arsenic mobility and bioavailability in soils. Our kinetic batch studies demonstrated that rates and amounts of As(V) adsorption by soils were significantly reduced by increasing P additions. In a separate experiment, the presence of P in soils increased mobility of As(V) in saturated columns. The use of flow interruptions verified the dominance of time-dependent sorption during As(V) and P transport in soils. We further extended the MRM model to simulate retention and transport of multiple solutes in soils. The formulated multicomponent multireaction model was capable of predicting the competition effect of P on As(V) retention and transport given appropriate kinetic coefficients.

The mobilization of colloidal particles and its effect on the transport of arsenite [As(III)] was investigated using miscible displacement experiments. Mobilization of colloidal amorphous material and enhanced transport of As(III) was observed when the input solution was replaced with deionized water. Peaks of colloid generation coincided with the peak concentrations of Fe, indicating mobilization of Fe oxides and facilitated transport of As(III).

CHAPTER 1: INTRODUCTION

Arsenic (As) is a highly toxic element widely present in soil, water, and plant at trace level. USEPA classified arsenic as a human carcinogen contaminant and the maximum contaminant level (MCL) in drinking water was lowered from 50ppb to 10ppb in 2001 (USEPA, 2001). Arsenic in groundwater above the environmental standard have been observed in many countries including Bangladesh, India, Vietnam, China, and US, which was attributed to either geologic or anthropogenic sources (Smedley and Kinniburgh, 2002). The occurrence of arsenic in groundwater of Bangladesh from the dissolution of arsenic containing aquifer material caused massive poisoning of the people living in that area (BGS, 2001). In addition, the increasing use of arsenic containing compounds as pesticides, herbicides, wood preservatives, and livestock feed additives have introduced large amounts of arsenic into soils (Smith et al., 1998). The possible release and transport of arsenic from soils to groundwater pose a potential threat to human health. The better understanding of the fate of arsenic in soil environment is urgently required for environment risk assessment and remediation plan.

Efforts have been made in modeling the fate of arsenic in the soil environment as influenced by physical, chemical, and biological processes (Smith and Jaffe. 1998). Significant amount of research was conducted to investigate the geochemical behavior of arsenic under various environmental conditions. Numerous laboratory and field studies demonstrated that complex chemical (e.g., adsorption-desorption, precipitation-dissolution, and biotransformation) and physical (e.g., advection and dispersion) processes involved in regulating the behavior of arsenic in soil, sediment, aquifer, and surface water environment (Smedley and Kinniburgh, 2002). The heterogeneous nature of the geological materials multiplied the complexity of predicting the fate of arsenic existed or released in natural environment. While our understanding

of arsenic cycle was greatly improved in the last several decades, the influence of various environment factors and their combinations on the retention and transport of arsenic has not been fully explored.

1.1 Statement of Problem

Generally, the transport of arsenic in aerated soils is controlled by the adsorption-desorption processes. Various soil chemical properties, such as Fe/Al contents, pH, redox potential, and competing anions (phosphate, silicate, carbonate, etc), influence the adsorption and desorption of arsenic on/from soils (Smith et al., 1998). In addition, the physical properties such as porosity, aggregates, flow velocity, and residence time may also impact the transport of arsenic in soils. In order to predict the fate of arsenic in soil environment, it is necessary to study the adsorption-desorption in soils under flowing condition.

There is large demand from the public as well as regulatory agencies for the quantitative assessment of environmental risk associated with arsenic contamination. Unfortunately, the modeling attempts to simulate the transport of arsenic in geologic porous media were not very successful due to the nonlinear and nonequilibrium nature of arsenic reactions in soils (Smith and Jaffe. 1998). The incorporation of the complex geochemistry reactions into the solute transport model is a challenging task facing environmental scientists.

1.2 Objectives

In this study, kinetic batch experiments and miscible displacement experiments were conducted to quantify the retention and transport of arsenate [As(V)] and arsenite [As(III)] in soils with different properties. The results from our experiment were simulated with numerical models that incorporate equilibrium and kinetic reactions with solute transport equation. The specific objectives of this study are: 1) to study the adsorption-desorption kinetics of arsenate

[As(V)] in three soils using both kinetic batch experiments and numerical simulation with equilibrium-kinetic multireaction (MRM) model; 2) to study the nonequilibrium transport of As(V) with saturated miscible displacement experiment and multireaction transport simulation; 3) to study the effect of phosphate on the adsorption-desorption kinetics and transport of arsenate in soils; 4) to extend the existing MRM model to simulate the competitive sorption between As(V) and P during transport in soils; and 5) to study the effect of colloidal mobilization on arsenic transport in soils.

1.3 References

BGS, 2001. Arsenic contamination of groundwater in Bangladesh. In Kinniburgh D.G and Smedley, P.L.,(Eds.), British Geological Survey (Technica Report, WC/00/19. 4 Volumes). British Geological Survey, Keyworth.

Smedley, P.L., and D.G Kinniburgh. 2002. A review of the source, behaviour and distribution of arsenic in natural waters. *Applied geochem.* 17, 517-568.

Smith, E., R. Naidu, and A.M. Alston. 1998. Arsenic in the soil environment: A review. *Adv. Agronomy* 64:149-195.

Smith, S.L., and P.R. Jaffe. 1998. Modeling the transport and reaction of trace metals in water-saturated soils and sediments. *Water Resour. Res.* 34, 3135-3147.

USEPA. 2001. National primary drinking water regulations; Arsenic and clarifications to compliance and new source contaminants monitoring; Final rule. *Federal Register*. Vol. 66. No. 14. 6975-7066. Jan 22. 2001. U.S. Gov. Print Office, Washington D.C.

CHAPTER 2: ARSENIC IN SOILS: A REVIEW

2.1. Introduction

Increasing amounts of arsenic (As) are being introduced into soil and water environments as a result of natural and anthropogenic processes. USEPA classified arsenic as a human carcinogen contaminant and lowered the maximum contaminant level (MCL) in drinking water from 50ppb to 10ppb (USEPA, 2001). The elevated level of arsenic was found in many soils due to applications of arsenic compounds such as pesticides, herbicides, wood preservatives, and livestock feed additives (Smith et al., 1998). In United State, arsenic is a contaminant of concern (COC) at 568 Superfund sites, making it the second most common common inorganic contaminant on the National Priority List (USEPA, 2002). Contamination of ground and surface water by arsenic from soils and aquifers pose significant threat to human health (WHO, 2004).

Tremendous research effort was devoted to unraveling the complex geochemical reactions of arsenic in natural environment in last several decades, reflected by the huge volumes of literatures published in this area. The scientific knowledge about the fate and behavior of arsenic in heterogeneous soil systems greatly expanded in recent years. This literature review highlights recent advances in understanding the sources, distribution, reaction, bioavailability, and mobilization of arsenic in soil environment.

2.2. Environmental Toxicity of Arsenic

The toxicity of arsenic depends on its chemical form. Organic arsenic compounds are much less toxic than inorganic arsenic. Among the inorganic arsenic, arsine gas (AsH_3) is the most toxic form. However, arsine gas rarely exists in natural environment. Two dominant arsenic forms in natural environment, arsenate and arsenite, are highly toxic. As a molecular analog of phosphate, arsenate blocks oxidative phosphorylation, short-circuiting life's main energy

generation system. Arsenite is even more toxic by binding to sulfhydryl groups, impairing the function of many proteins (Oremland and Stolz, 2003).

The targets of arsenic toxicity are the respiratory system, the circulatory system, the skin, the nervous system, the reproductive system, etc. Acute arsenic poisoning affects central nervous system, blood vessels, kidney, and can cause death in one to three days (Reigart and Roberts, 1999). Drinking water rich in arsenic over a long period leads to arsenic poisoning or arsenicosis. The health effects of arsenicosis include skin problems (such as color changes on the skin, and hard patches on the palms and soles of the feet), skin cancer, cancers of the bladder, kidney and lung, diseases of the blood vessels of the legs and feet, and possibly also diabetes, high blood pressure and reproductive disorders (WHO, 2003). The U.S. Environmental Protection Agency (USEPA) classified arsenic as Group A (human carcinogen) contaminant. Several incidence of arsenic poisoning have been reported in Bangladesh (Nickson, et al., 1998), India (Acharyya et al., 1999), Vietnam (Berg et al., 2003), China (Smedley and Kinniburgh, 2002), Taiwan (Chen et al., 1994), and United States (USGS, 2004). The culprit of arsenic poisoning in those cases can be arsenic in drinking water from geological sources, arsenic released from industrial sources or mining activities, or arsenic in contaminated food (Mandal and Suzuki, 2002).

Arsenic enters human body via respiration of arsenic in dust and fumes and ingestion of arsenic in water, soil, and food (Mandal and Suzuki, 2002). The air exposure of arsenic is generally low. However, combustion of arsenic containing coal may result in locally high arsenic level in some area. Drinking arsenic contaminate water is the major route of arsenic poisoning around the world. Millions of people are suffering from the toxic effects of arsenic due to drinking of arsenic rich ground water (Smedley and Kinniburgh, 2002). Soil ingestion is another important pathway of arsenic poisoning, especially for children (Rodriguez and Basta, 1999).

Furthermore, arsenic may accumulate in crops, vegetables, and fruits grown on contaminated soil (Meharg and Hartley-Whitaker, 2002). Consumption of arsenic polluted food is also a serious threat to human health.

2.3. Arsenic in Soils

2.3.1 Background Concentrations

Background concentrations of arsenic in soils vary among soil types, depending on the parent materials from which the soil is derived. According to the National Geochemical Survey conducted by USGS, arsenic concentrations of most soils in the U.S. are well below 10 mg kg^{-1} (USGS, 2004). Researchers reported that background arsenic concentrations of soils in Australian and New Zealand is $0.2\text{-}30 \text{ mg kg}^{-1}$, and they suggested environmental investigation for the concentrations greater than 20 mg kg^{-1} (Barzi et al., 1996). The study of Bradford et al. (1996) showed that the geometric mean of arsenic concentration in 50 soils from California was 2.8 mg kg^{-1} , with a range of $0.6\text{-}11.0 \text{ mg kg}^{-1}$. Similarly, Chen et al. (2002) reported that the mean arsenic concentration of Florida soils was 0.42 mg kg^{-1} , ranging from 0.01 to 50.6 mg kg^{-1} , with considerable difference between soil types. The survey of soils in Mississippi found the mean arsenic concentration was 8.25 mg kg^{-1} , with a range of 0.26 to 24.43 mg kg^{-1} (Pettry and Switzer, 2001). It is observed that soil arsenic concentration may correlate with clay content, pH, cation exchange capacity, organic matter content, and most significantly Fe and Al concentration (Bradford et al. 1996; Pettry and Switzer, 2001; Ori et al., 1993; Chen et al., 2002).

2.3.2 Arsenic Sources

The main sources of arsenic in soils come from arsenic containing parent material. The mean value of arsenic abundance in crustal rocks is around 2 mg kg^{-1} with considerable variance

between different types of rocks. Among more than 245 As-containing minerals, about 60% are arsenates, 20% sulfides and sulphosalts, and the other 20% include arsenides, arsenites, and oxides. Arsenic minerals commonly occurred in the environments are arsenopyrite, orpiment, realgar, enargite (Cu_3AsS_4), arsenides (Cu_3As), colbaltite (CoAsS), and proustite (Ag_3AsS_3). The weathering of those arsenic containing minerals brings dissolved arsenic into soil and water environment, like what happens in Ganges Delta.

Arsenic is found to be associated with various types of mineral deposits, especially sulfide ore. It is often present at the $0.02\text{--}0.03 \text{ g g}^{-1}$ level in copper and lead ores and can be as high as 0.11 g g^{-1} in gold ores (Foster et al., 1998; Paktunc et al., 2003). Arsenide (arsenic minerals have oxidation state between 0 and -3) minerals such as cobalt arsenides [skutterudite (CoAs_3)], Nickel arsenides [niccolite (NiAs) and rammelsbergite (NiAs_2)] are important in the extractive metallurgy of Co, Ni, Pt, Ir. The mining process of Pb, Cu, Zn, Co, Ni, and Au may produce tailing of high residual arsenic concentration due to the presence of arsenic minerals in the ores, such as arsenopyrite (FeAsS), arsenolite (As_2O_3), olivenite ($\text{Cu}_2\text{OHAsO}_4$), mimetite ($\text{Pb}_5\text{Cl(AsO}_4)_3$), cobaltite (CoAsS), etc. Soil arsenic concentration near the mining dump site is reported as high as $30,000 \text{ mg kg}^{-1}$, though the levels rapidly decreased with distance away from the dump (O'Neill, 1990). Bowell (1993) reported the concentration of arsenic extracted from soils at the Ashanti mine, Ghana varied from 2 to $35,600 \text{ mg/kg}$.

Large amounts of arsenic containing coal are combusted in power plants worldwide. Combustion of coals add arsenic containing fly ashes into the atmosphere, which eventually accumulate in soils and water (Qafoku et al., 1999; Ishak et al., 2002; Sakulpitakphon, 2003). Generally, arsenic may present in coals at concentrations from 2 to 84 mg kg^{-1} , depending on the geological background. However, high concentrations of arsenic of arsenic (1500 mg kg^{-1})

within the brown coal from the former Czechoslovakia were reported (Bencko and Symon, 1977). Even higher concentration of arsenic ($100\text{--}9,000\text{ mg kg}^{-1}$) within the coal was reported in Guizhou, China as a result of epigenetic mineralization (Liu et al., 2002).

Approximately 90 percent of industrial arsenic in the U.S. is currently used as a wood preservative. Arsenic containing compounds such as chromated copper chromate (CCA), ammoniacal copper arsenate (ACA), and ammoniacal copper zinc arsenate (ACAA) have been extensively used as wood preservatives in reducing bacterial, fungal, and insect decay in woods. CCA has been the dominant chemical used to treat wood for decks and other outdoor uses, constituting 75% of the pressure treatment wood market by volume. The treated woods commonly contain $1,000\text{--}5,000\text{ mg kg}^{-1}$ arsenic. Arsenic in those wood preservatives could diffuse into adjacent soil and leach into ground water. Chirenje et al. (2003) showed that mean soil arsenic concentration as high as 23 mg kg^{-1} close to CCA-treated wood structures compared with less than 3 mg kg^{-1} at distance about 1.5 m away. Similarly, Rahman et al. (2004) concluded that arsenic diffused from CCA-treated wood to adjacent garden soil and found that the vegetable crops grown in these gardens can accumulate significant concentrations of arsenic. On March 17, EPA granted the cancellation and use termination requests affecting virtually all residential uses of CCA-treated wood after December 30, 2003 (USEPA, 2003).

Compounds containing arsenic had been extensively used as pesticides, insecticides, herbicides, soil sterilants, silvicides, and desiccants in cotton, orchards, silviculture, and turf since late 1800s. The commonly used arsenical pesticide include inorganic compounds such as lead arsenate (PbAsO_4), calcium arsenate (CaAsO_4), magnesium arsenate (MgAsO_4), zinc arsenate (ZnAsO_4), zinc arsenite ($\text{Zn(AsO}_2)_2$), and Paris green [$\text{Cu(CH}_3\text{COO)}_2 \cdot 3\text{Cu(AsO}_2)_2$], as well as organic compounds such as DMAA [dimethylarsonic acid, $(\text{CH}_3)_2\text{AsO}_2\text{H}$], MSMA

[monosodium methane arsenate, $\text{CH}_3\text{AsO}_3\text{HNa}$], MAMA [Monoammonium methane arsonate, $\text{CH}_3\text{AsO}_2\text{NH}_4\text{OH}$], and MAA [Methylarsonic acid, $\text{CH}_3\text{AsO}_2(\text{OH})_2$] (Reigart and Roberts, 1999). Woolson et al. (1971) reported that surface soil in orchards with history of arsenic containing pesticide application averaged $165 \text{ mg As kg}^{-1}$ comparing to soils without arsenic input averaged 13 mg As kg^{-1} . In Louisiana, calcium arsenate (CaAsO_4) was typically used as desiccants to allow cotton to be easily harvested after defoliation prior to 1968 (Ori, et al., 1993; Bednar et al., 2002). Even though many arsenical pesticides have been prohibited in the United States as a result of government regulation, considerable amount of arsenic are retained by soils. In Denver, Colorado, half century after applied an arsenical herbicide ($\text{As}_2\text{O}_3 + \text{PbAsO}_4$) on turf, arsenic still occur in residential soils at concentrations up to 1440 mg kg^{-1} (Folkes et al., 2001).

In the poultry industry of the U.S., organic arsenic compounds such as roxarsone (3-nitro-4-hydroxyphenylarsonic acid) are commonly feed to broiler chicken to control coccidial intestinal parasites and improve feed efficiency. Little of these organoarsenicals is retained in the meat and most of the arsenic is rapidly excreted in the manure. Thus poultry litter containing $10\text{--}40 \text{ mg kg}^{-1}$ arsenic has been largely recycled as organic amendment to the agriculture fields. It is reported that $20,000\text{--}50,000 \text{ kg}$ of arsenic is annually introduced into the environment by the chicken farmers along the eastern shore of the United States (e.g., Delaware, Maryland, and Virginia) (Arai, et al., 2003). Han et al. (2004) found that after 25 years of application of arsenic containing poultry litter, arsenic accumulated from 2.68 mg kg^{-1} for the non-amended soils to 8.4 mg kg^{-1} for the amended soils.

From 1906 to 1962, dipping solutions containing $1,400$ to $2,200 \text{ mg kg}^{-1}$ arsenic were widely used among thousands of cattle-dipping vats throughout southern U.S. including Louisiana to eradicating a transmitting disease called “southern cattle fever”. These practices

have resulted in the contamination of soils and ground water by arsenic leaching and disposal from those cattle dipping vats (Thomas, et al., 1999). McLaren et al. (1998) reported that surface soils surrounding cattle dips in Australia with a history of arsenicals usage were contaminated with arsenic ranged up to 3,542 mg kg⁻¹.

2.3.2 Soil Arsenic Regulations

Despite the widespread soil contamination of arsenic, there is no nationwide accepted cleanup standard for arsenic due to soil heterogeneity and policy interpretation (Davis et al., 2001). A survey conducted by the Association for the Environmental health of Soils (AEHS, 1999) revealed that there were large variations among the soil arsenic regulations set by different states across the US. They reported the notification levels of 2-61 mg kg⁻¹, soil screening levels of 0.1-250 mg kg⁻¹ for residential area and 2.4-200 mg kg⁻¹ for industrial sites, cleanup levels of 0.1 to 250 mg kg⁻¹ for residential area and 0.85-1000 mg kg⁻¹ for industrial sites for the 34 states participated in the survey. In addition, the rationale used for setting the regulation levels was widely diversified, including related regulation limits, background levels, human health risk, and migration to groundwater. From their survey of Records of Decisions (RODs), Davis et al. (2001) divided the studied sites into four risk categories: industrial, residential, background and ecological risk-based decisions with 84% of the sites were risk-driven and 16% were background-driven. They reported that a wide range of soil-arsenic cleanup standard for residential risk goals (2-305 mg kg⁻¹) and a narrower background-based clean up goal of 8-21 mg kg⁻¹. In addition, there was no apparent temporal trend but considerable geographic differences were observed for arsenic RODs.

2.3.4 Chemical Speciation

Arsenic can exist in many organic and inorganic forms, depending on the original sources and dominant reactions in soils. Arsenic can form organic compounds by methylation as a biological process, producing both trivalent and pentavalent organoarsenic compounds (O'Neill, 1990; Smith et al., 1998). However, the most important compounds are the arsenate and arsenite, because they are highly soluble in water and more toxic than other arsenic compounds. Distribution of arsenate and arsenite is largely determined by adsorption and redox reactions in soils, which will be discussed in the following sections.

Because of the heterogeneous properties of soils, various chemical reactions can happen after arsenic entered soil environment. Since arsenic in sediments and soils is bound with solid phases at different strengths, the total arsenic concentration is not necessarily a good indicator of its potential mobility and bioavailability. Several sequential chemical extraction methods have been proposed to apportion soil arsenic into various pools based on the types of extractant used. Those sequential extraction methods have been extensively used to characterize the mobility and bio-availability of arsenic in sediments and soils and regarded as operational (Woolson et al., 1973; McLaren et al., 1998; Keon et al., 2001; Rodriguez et al., 2003; Matera and Hecho, 2001; Han et al., 2004). Nevertheless, most extraction procedures was originated from the method of Tessier et al. (1979), which chemically fractions heavy metals into ion-exchangeable, surficially adsorbed, precipitated, organic chelated, and occluded chemical pools. Considering the chemical similarity between As and P, the soil P fraction procedure of Chang and Jackson (1957) was also adapted to examine arsenic availability in soils.

Although selective chemical extraction could provide empirical determination of the dominant constituents retaining As in contaminated soils, the procedure do not provide the

specific information about interfacial reactions between As and various soil constituents.

Spectroscopic techniques have been applied to determine the sorption reactions occurring in heterogeneous geological material (Foster, 2003). Spectroscopic analysis including Fourier transformed infrared (FTIR), raman Spectroscopy, X-ray photoelectron spectroscopy, extended X-ray absorption fine structure (EXAFS), X-ray absorption near-edge spectroscopy (XANES) were able to determine the electronic energy levels of atoms or molecules in the system. Therefore, they are useful in determine the structure of a particular solid phase at molecular level. Extensive researches have been conducted in this area and the reader is referred to Foster (2003) for a comprehensive review.

2.4. Adsorption-Desorption of Arsenic in Soils

2.4.1 Adsorption Mechanisms

A wide range of interactions including ion exchange, surface complexation, and precipitation contribute to the removal of arsenic from aquatic solution by solid constituents. However, the majority of arsenic present in soils is sorbed onto the surface of the solid matrix. Adsorption process, especially sorption onto metal oxide surfaces, controls the arsenic distribution in contaminated soils (Smith et al., 1998). Soil minerals such as metal oxides, clay minerals and calcite, have the capacity of adsorbing arsenic anions. It is well established that iron and aluminum oxides and hydroxides have much higher sorption capacity and stronger bond strength for arsenic than other soil constituents. Generally, arsenate and arsenite anions are strongly adsorbed as inner-sphere surface complexes through a ligand exchange mechanism. Inner-sphere surface complexes are formed through strong chemical bond between the surface functional group and As(V) or As(III) anions without water molecule between them. During the surface complexation, an anion or molecular called “ligand” was replaced by arsenic anion

(Sparks, 1995). Inner-sphere complexes can be monodentate or bidentate, depend on the number of oxygen bonded to the metal atom.

Several extended X-ray adsorption fine structure spectroscopy (EXAFS) studies have shown that As(V) formed monodentate and/or bidentate complexes on iron oxides surfaces via a ligand exchange for OH₂ and OH⁻ in the coordination spheres of surface structural Fe atoms. Waychunas et al. (1993, 1995) using EXAFS studied adsorption and coprecipitation of arsenate onto ferrihydrite and crystalline FeOOH polymorphs. Their result showed clear evidence of formation of inner sphere bidentate arsenate complexes on surfaces of ferrihydrite ($R_{\text{As-Fe}} = 3.25 \pm 0.02 \text{ \AA}$) and crystalline FeOOH polymorphs ($R_{\text{As-Fe}} = 3.28 \pm 0.01 \text{ \AA}$). However, at low arsenate coverage, monodentate complex occupied a comparable proportion on ferrihydrite surface ($R_{\text{As-Fe}} = 3.60 \pm 0.03 \text{ \AA}$) but not crystalline FeOOH polymorphs. Sun and Doner (1996) employed Fourier Transform infrared (FTIR) spectroscopy to investigate arsenate and arsenite adsorption onto goethite surface. They concluded that most arsenate and arsenite forms binuclear bridging complexes by replacing two singly coordinated surface OH groups. The EXAFS study of Fendorf et al. (1997) showed that a monodentate complex ($R_{\text{As-Fe}} = 3.59 \text{ \AA}$), a bidentate-binuclear complex ($R_{\text{As-Fe}} = 3.29 \text{ \AA}$), and a bidentate-mononuclear complex ($R_{\text{As-Fe}} = 2.85 \text{ \AA}$) formed on goethite surface. Their result confirmed that monodentate complex was favored at low arsenic surface coverage while bidentate-binuclear complex occupied highest proportion at highest arsenic coverage. Grossl et al. (1997) measured chemical relaxation via conductivity detection during pressure-jump relaxation experiment and they concluded that arsenate adsorption on goethite is a two-step process resulting in the formation of inner-sphere bidentate complex. EXAFS study of Manning et al. (1998) showed that As(III) formed bidentate binuclear bridging complexes on goethite surfaces ($R_{\text{As(III)-Fe}} = 3.378 \pm 0.014 \text{ \AA}$). Goldberg and Jonhson

(2001) using FTIR investigated arsenate and arsenite adsorption on amorphous iron and aluminum oxides. Their conclusion was that arsenate form inner-sphere surface complexes on both amorphous Fe and Al oxides, while arsenite form inner-sphere and outer-sphere surface complexes on amorphous Fe oxides and outer-sphere surface complexes on Al oxides. O'Reilly et al. (2001) conducted EXAFS study to investigate residence time effect on arsenate adsorption on goethite. They concluded that arsenate bound to goethite surface as bidentate binuclear complex ($R_{As-Fe} = 3.30 \text{ \AA}$). The molecular environment did not significantly affected by the residence time. The EXAFS spectra of arsenate sorption on hematite (Arai et al., 2004) showed the coexistence of bidentate mononuclear ($R_{As-Fe} = 2.78\text{-}2.86 \text{ \AA}$) and bidentate binuclear complexes ($R_{As-Fe} = 3.29 \text{ \AA}$) on hematite surface.

The surface of Fe and Al oxides possess variable or pH-dependent charge. When pH value equals PZC, the positive and negative charge of the mineral surface are equal. Shift in PZC with increasing anion concentration can be seen as a evidence of strong specific anion adsorption and inner sphere surface complexation. Electrophoretic mobility measures of Anderson et al. (1976) indicated PZC change to lower pH values as arsenate adsorption increased on amorphous Al hydroxide surface. Pierce and Moore (1980) observed PZC of amorphous iron hydroxide decreased from 8.0 without arsenite to 7.28 with $440 \mu\text{M L}^{-1}$ arsenite and increase in background electrolyte concentration did not significantly affect arsenite adsorption. The titration curve produced by Jain et al. (1999) demonstrated that adsorption of arsenate resulted in PZC reduction from 8.5 of pure ferrihydrite to 6.1, adsorption of arsenite resulted in a slightly less reduction of 1.5. Their results showed that at lower pH, arsenite adsorbed on ferrihydrite might produce protonated Fe-O-As bond and monodentated bonding mechanism might play an increasing role during arsenate adsorption with increasing pH. Goldberg and Johnston (2001) found PZCs of

amorphous iron oxide significantly shifted to increasingly lower pH with increasing As(V) or As(III) concentration, but the same results were not observed on amorphous Al oxide. They also showed that ionic strength has little or no effect on As(V) and As(III) adsorption on amorphous Al and Fe oxides.

Adsorption of anions forming inner-sphere complexes normally shows little or no dependence on ionic strength (Hingston et al., 1967). Studies of Goldberg and Johnson (2001), Manning and Goldberg (1996) have showed that ionic strength have little effect on arsenite adsorption on Al and Fe oxides at the range of 0.02 to 0.1M. They observed that ionic strength have greater effect on arsenite than arsenate, indicating arsenite is more weakly bound. Manning and Goldberg (1997) showed that sorption of both As(V) and As(III) on soils slightly increased with increasing ionic strength. They suggested that this was caused by the variety of mineral surfaces other than Fe oxides. Smith et al. (1999) found increasing ionic strength greatly increased As(V) sorption on soils above pH 3, and the contrary hold true for pH below 3. The difference between the results probably caused by the higher arsenic concentration (0.20 mmol L⁻¹) used by smith et al. (1999). They explained that with the increasing net negative charge above point zero charge (PZC) when ionic strength increases.

Relatively few studies have been conducted to investigate arsenic adsorption on phyllosilicate clay minerals. Direct spectroscopic information on arsenic chemical bonding at clay mineral surface is not yet available. Since arsenic present mostly in solution as oxyanions, it is believed that arsenic adsorption by negatively charged clay minerals are limited to exposed octahedral cations on broken clay particle edges, which is relatively small. Frost and Griffin (1977) investigated As(V) and As(III) adsorption on kaolinite and montmorillonite. They explained arsenic adsorption with nonspecific anion exchange mechanism. Manning and

Goldberg (1996, 1997) studied arsenate and arsenite adsorption on kaolinite, montmorillonite, and illite. Their results showed that arsenic adsorption on clay surfaces was highly dependent on pH but independent of ionic strength. They suggested to understand the mechanism of arsenic adsorption on clay mineral, the determination of clay crystal edge properties such as edge surface site density (SOH_T), PZC_{edge} would be necessary. Lin and Puls (1999) investigated As(V) adsorption and desorption of six clay minerals and suggested that at high loadings, arsenate might precipitate and form a hydroxy-arsenate layer on some 1:1 layer clays (halloysite). Isomorphous substituted iron in some clays may contribute to arsenic sorption. Adsorption with surface hydroxyl groups might be the most important mechanism for arsenic adsorption on other clay minerals. Generally, clay minerals with higher surface area can absorb more arsenic (Lin and Puls, 1999).

Other substances present in soil matrix such as calcite, sulfide, and organoclay matters may also contribute to arsenic adsorption. Goldberg and Glaubig (1988) studied arsenate adsorption on calcite and concluded that at high pH range (>9), soil carbonates may play an important role in arsenate adsorption. Bostick and Fendorf (2003) studied arsenite sorption on iron sulfides. They found that at low surface coverage, arsenite retention by sulfides conformed to a Langmuir isotherm. Generally, the existence of soil organic matter (SOM) can reduce arsenic adsorption since they can compete for adsorption site on mineral surface (Grafe et al., 2001) or form aqueous complex with arsenic (Redman et al., 2002). However, study of Saada et al. (2003) showed evidence that humic acid nitrogen groups can form organoclay with clay mineral and resulted in enhanced the arsenic adsorption capacity.

2.4.2 Adsorption Envelopes

The effect of solution pH on arsenic adsorption processes have been extensively investigated on numerous pure minerals as well as whole soils (Frost and Griffin, 1977; Pierce and Moore, 1982; Goldberg and Glaubig, 1988; Xu et al., 1988; Manning and Goldberg, 1996; Manning and Goldberg, 1997; Smith et al., 1999; Goldberg, 2002; Dixit and Hering, 2003). Solution pH controls two fundamental factors, mineral surface potential and arsenic speciation, which in turn impacts arsenic adsorption on mineral surfaces. Metal oxides and other minerals possess pH-dependent variable surface charges. At pH below point zero charge (PZC), adsorption of H^+ excess of that of OH^- , the surface become positively charged. the negative potential of mineral surface increases with increasing pH value. On the other side, there exists pH-pKa dependence of both arsenate ($pK_a^1=2.3$, $pK_a^2=6.8$, and $pK_a^3=11.6$) and arsenite ($pK_a^1=9.2$, and $pK_a^2=12.7$). At neutral pH range, arsenate exists as negatively charged $H_2AsO_4^-$ and $HAsO_4^{2-}$, and the negative potential tend to increase as pH increases. In contrast to arsenate, arsenite mostly exists as zero charged $H_3AsO_3^0$ below pH 9.2. The interaction between PZC of soil minerals and pK_a of arsenate or arsenite determine the adsorption envelope, i.e., amount of adsorption as a function of pH (Hingston, et al., 1967).

Anderson et al. (1976) showed that arsenate had maximum adsorption on amorphous aluminum hydroxide around pH 4.3 and amount of adsorption decrease with increasing pH above 4.3. Frost and Griffin (1977) found arsenate sorption by kaolinite and montmorillonite exhibited a maximum at pH 4-6, arsenite adsorbed steadily from pH 4 to 9 on kaolinite and peaked at pH 7 on montmorillonite. Pirce and Moore (1980, 1982) showed that arsenite adsorption on amorphous Fe hydroxide had an maximum around pH 7. Manning and Goldberg (1996,1997) observed arsenate adsorption maxima were approximately pH 5.0 for kaolinite, 6.0

for montmorillonite, and 6.5 for illite. In contrast to As(V), As(III) generally have lower adsorption at low pH, at exhibited maximum adsorption between pH 7.5 and pH 9.5 for this three minerals. Raven et al. (1998) found adsorption envelope on ferrihydrite exhibited broad adsorption maxima extending from approximately from pH 6.8 to pH 9.4 for arsenite and pH 5.2 to pH 7.0 for arsenate. Goldberg (2002) showed that arsenate has a maximum adsorption on oxides and clays at low pH and then decreases with increasing pH above pH 9 for Al oxides, pH 7 for Fe oxides, and pH 5 for clays; whereas arsenite adsorption on all oxide and clays showed a parabolic trend with maximum sorption around pH 8.5. Dixit and Hering (2003) observed that arsenate sorption on amorphous Fe oxide (HFO) and goethite decreased with increasing pH. The arsenite sorption peaks for HFO, goethite, and magnetite were 6-9, 7-9, and >9, respectively.

Arsenate adsorption on a calcareous, montmorillonite soil increased with increasing pH with a maximum around pH 10.5 (Goldberg & Glaubig, 1988). As(III) and As(V) adsorption envelope of three California soils (Fallbrook, Wasco, and Wyo) displayed patterns similar to that of containing individual mineral compounds (Manning and Goldberg, 1997). Smiths et al. (1999) investigated effect of pH on arsenate and arsenite on four Australian soils. They found with increasing pH, arsenate sorption decreased but arsenite sorption increased. Under oxidized conditions, Masscheleyn et al. (1991) found soluble arsenic concentration at pH 8 were as much as 3 times higher than that of pH 5.

Surface complexation models have been shown to be capable of describing chemical reactions of ion adsorption on minerals (Goldberg, 1992). Constant capacitance model was fitted to the envelope of arsenic adsorption on several pure minerals to obtain the surface complexation constant which can be used to predict the adsorption behavior of arsenic. However, model predictions can only qualitatively describe the shape of adsorption curves (Goldberg & Glaubig,

1988; Manning and Goldberg, 1996; Manning and Goldberg, 1997; Goldberg, 2002; Williams et al., 2003). A diffuse double layer (DDL) model was also used to describe the arsenic sorption edges on various oxides (Goldberg and Johnson, 2001; Manning and Goldberg, 1996; Dixit and Hering, 2003). Using binding mechanisms observed from spectroscopy results, Hiemstra and van Riemsdijk (27) simulated adsorption of arsenate on metal oxides with a multi-site surface complexation model.

2.4.3 Adsorption Isotherms

Sorption of arsenate and arsenite on whole soils had been conducted with traditional batch equilibration method. Amount of arsenic adsorption on soils was found to be significantly correlated with extractable Al and Fe contents and other soil properties such as clay content and pH value. Jacobs et al. (1970) found that As(V) adsorption increased with increasing content of Fe oxide and the removal of Fe and Al oxides eliminated or appreciably reduced As(V) adsorption in soils. In addition, the research of Wauchope (1975) showed that besides Fe and Al content, soil clay content can also affect arsenate and methylarsonate adsorption. The batch experiment conducted by Livesey and Huang (1981) showed that arsenate retention proceed through adsorption mechanism but not precipitation and the adsorption maxima linearly related to extractable Fe and Al, and clay content. Elkhatab et al. (1983a) found that the Freundlich parameters from arsenite adsorption were most closely related to Fe percentage and soil pH. Similarly, Sakata (1987) demonstrated that distribution coefficient (K_d) for As(III) was significantly related with the dithionite extractable Fe content in the soils. Furthermore, Manning and Goldberg (1997) demonstrated that soils with highest extractable Fe and clay had the highest affinity to both As(V) and As(III) and As(V) adsorbed more strongly than As(III) under most

conditions. It is confirmed by Smith et al. (1999) that soils generally sorbed more As(V) than As(III).

Equilibrium batch experiment, conducting by equilibrating arsenic solution with mineral or soil solid for a certain amount of time at constant temperature, was usually carried out to study the adsorption capacity of arsenic. The relationship between the equilibrium concentration in the aquatic solution and the amount adsorbed on the solid surface are commonly described with adsorption isotherms. The L-type and H-type isotherms are usually employed to describe the arsenic adsorption on mineral and soil surfaces. Both types are highly nonlinear and indicative of high affinity chemical adsorption.

To numerically describe the nonlinear adsorption behavior of arsenic, isotherms generated from batch experiments were fitted to equilibrium sorption models including Langmuir equation (Manning & Goldberg, 1997; Livesey & Huang, 1981; Pierce and Moore, 1980; Darland and Inskeep, 1997), and Freundlich equation (Elkhatib, 1984a; Puls & Powell, 1992; Smiths et al., 1999; Williams et al., 2003). Anderson et al. (1975) employed Langmuir curve to fit data of arsenate adsorption on amorphous aluminum hydroxide. Their K_L and ω equal $5.62 \pm 0.42 \mu\text{mol/L}$, and $1179 \pm 0.22 \mu\text{mol/g}$, respectively. The Freundlich isotherm of arsenite adsorption on A and Bt horizons of five West Virginia soils (Elkhatib et al., 1984b) had K_f and n values among 19.2-102.0 and 0.399-0.958, respectively. Both Langmuir and Freundlich equations were employed by Manning and Goldberg (1997) to describe As(III) and As(V) adsorption on Wasco, Fallbrook, and Wyo soils. The K_L , ω , K_f , and n values were 0.183-0.300, 37.4-279 $\mu\text{mol/kg}$, 19.0-209, and 0.612-0.772 for As(III), 0.043-0.554, 235-298 $\mu\text{mol/kg}$, 14.4-355, and 0.786-0.867 for As(V), respectively.

2.4.4 Competing Anions

Both As(V) and As(III) are specifically adsorbed on surface Fe and Al oxides by forming inner-sphere complex. These two arsenic oxyanions may compete with each other for adsorption sites. Jain and Loeppert (2000) reported that with As(V) and As(III) concentrations $<2.08 \text{ mmol As kg}^{-1} \text{ Fe}$ each, the effect of As(V) on As(III) sorption on ferrihydrite was more pronounced than vice versa, whereas at higher concentrations $3.47 \text{ mmol As kg}^{-1} \text{ Fe}$ each, As(V) did not influence As(III) adsorption but As(III) significantly reduced As(V) adsorption. Goldberg (2002) concluded that at pH lower than 8, arsenate have higher adsorption capacity on minerals and soils than arsenite and competition between arsenate and arsenite is relatively small. Dixit and Hering (2003) concluded that at lower pH (<7), arsenate sorption is more favorable than arsenite on amorphous Fe oxide and goethite, also the opposite hold true at $\text{pH}>7$.

Many anions or molecules present in soils can compete with arsenic for adsorption sites by ligand exchange mechanism. The most extensively studied competitive ligand is phosphate anion, considering arsenate and phosphate have similar chemical properties. Numerous studies have shown that the existence of phosphate substantially suppressed the sorption of arsenate on minerals and soils (Livesey and Huang, 1981; Roy et al., 1986; Melamed et al., 1995; Darland and Inskeep, 1997; Violante and Pigna, 2002; Smith et al., 2002; Williams et al., 2003; Dixit and Hering, 2003).

Arsenate and phosphate are specifically adsorbed on a similar set of surface sites, although evidence showed some sites are only available for either As(V) or P (Hingston et al. 1992). The competition between phosphate and arsenate depends on the surface properties of the adsorbent, intensity of As and P, and pH. Manning and Goldberg (1996ab) showed that when present in equal molar concentrations ($3.7 \times 10^{-7} \text{ mol L}^{-1}$), the adsorption envelope of phosphate

and arsenate on goethite, gibbsite, kaolinite, montmorillonite, and illite were similar. As(V) and P appears to compete for a similar set of surface sites. However, some sites were uniquely available for adsorption of either As(V) or P. As a result, the presence of P reduced arsenic adsorption on those minerals. Jain and Loeppert (2000) the effect of phosphate on arsenate adsorption on ferrihydrite was greater at high pH than at low pH, whereas the opposite hold true for arsenite. Zhao and Stanforth (2001) confirmed that arsenate and phosphate equally adsorbed on goethite when added simultaneously. When added sequentially, the desorption process was kinetically controlled, with a fraction of both As(V) and P remained non-exchangeable. Violante and Pigna (2002) demonstrated that kaolinite, gibbsite, boehmite, allophane, and non-crystalline Al hydroxide have a greater affinity of phosphate than arsenate. On the contrary, goethite, pyrolusite, birnessite, nontronite, smectite, and ferrihydrite have greater affinity of As(V), while other minerals such as vermiculite and illite have similar affinity to As(V) and P. Dixit and Hering (2003) observed that the fractions of both As(V) and As(III) bound to amorphous Fe oxide and goethite were substantially reduced in the presence of phosphate.

Several equilibrium adsorption experiments have been conducted on soils to investigate the competitive effect of phosphate. The extraction of soil sorbed phosphate by arsenate was studied by Barrow (1972). They showed that the amount of phosphate extracted by arsenate increased with increasing pH, showing a platform between pH 6.7 and pH 9. Livesey and Huang (1981) reported that addition of P (10^{-4} to 10^{-2} mol L⁻¹) substantially suppressed arsenic sorption on soils. It was demonstrated that the adsorption of arsenate was significantly reduced by phosphate but arsenate have little effect on phosphate adsorption on three soils, Cecil clay, EPA-14, and Catlin silt loam (Roy et al., 1986). The competitive coefficient they calculated was 1.66 to 2.76 for phosphate displacing arsenate (α_{As-P}), 0.11-0.35 for arsenate displacing phosphate (α_P).

As). Peryea (1995) observed phosphate induced arsenic release from orchard soils contaminated with PbAsO_4 pesticide, with a mechanism of specific $\text{PO}_4\text{-AsO}_4$ exchange. The study of Reynolds et al. (1999) demonstrated that under anaerobic conditions, the presence of phosphate have very little effect on the solubility of arsenic. In addition, Smith et al. (2002) reported that the competitive effect of P was more evident in soils with low arsenic sorption capacity. They concluded that binding energy is not the major factor controlling the effect of P and As.

Carbonate anions is commonly present at high concentration in soil solution and ground water. Appelo et al. (2002) using surface complexation model calculated carbonate and ferrous ion sorption on ferrihydrite and their displacing effect on sorbed arsenate and arsenite. Their calculation demonstrated that sorption of particularly carbonate at common soil concentrations reduced the sorption capacity of arsenic on ferrihydrite significantly. In contrast, Arai et al. (2004) surprisingly observed carbonate enhanced As(V) sorption on hematite surface. But when pH was held constant, dissolved carbonate effect was negligible. They suggested that the effect of dissolved carbonate on As(V) adsorption were influenced by the reaction conditions.

In natural systems, the presence of dissolved organic carbon (DOC) may compete with arsenic for adsorption site on mineral surfaces and inhibit arsenic adsorption. Grafe et al. (2001) showed that the presence of humic acid (HA) and fulvic acid (FA) reduced As(V) adsorption on goethite surface at a maximum of 27% and 17%, respectively, while citric acid (CA) had no effect. As(III) adsorption was inhibited by all three organic acids in the order of $\text{CA} > \text{FA} \approx \text{HA}$. Redman et al. (2002) observed natural organic matter (NOM) dramatically delayed the sorption kinetic and diminished the sorption maximum of both arsenate and arsenite on hematite. The introduction of NOM displaced sorbed As(V) and As(III) from hematite surface, on the other

side, arsenic similarly displaced NOM from hematite surface. They also observed the formation of aqueous complexes between NOM and arsenate or arsenite.

Silicic acid, another ubiquitously occurring ligand in natural systems, have high affinity to Fe oxides. Waltham and Eick (2002) found that the presence of 1.0mM silicic acid reduced 40% of the arsenite adsorption on goethite, whereas it only decreased arsenate adsorption rate but not the total quantity.

It is reported that the existence of other ligands such as carbonate, dissolved organic acid, citric acid, and silicic acid inhibited the sorption of As(V) and As(III) on goethite at a much lower level (Crafe, et al. 2001; Waltham and Eick, 2002). Several studies have verified that other anions naturally occurring in soil solution, such as Cl^- , NO_3^- , and SO_4^{2-} , have almost no effect on arsenic retention and transport (Livesey and Huang, 1981; Peryea, 1995; Qafoku et al. 1999; Smith et al., 2002).

The type of cations occurring in soil system may have impact on arsenic adsorption. Some cations may form ion-pair with arsenic oxyanions, resulting in decreasing arsenic activity in solution and decreasing retention on soil surfaces. Another effect is that the sorption of some cations on mineral surface may decrease the negative charge on mineral surface and increase adsorption of arsenic oxyanions. Smith et al. (2002) observed that the sorption of both As(V) and As(III) was enhanced by the presence of Ca^{2+} instead in the solution compared with Na^+ .

2.4.5 Kinetic Adsorption-Desorption

Traditionally, arsenic sorption has been studied with equilibrium batch experiments conducted within a short period of reaction time. Few studies investigated the effect of long residence time on adsorption of arsenic in soils. However, a long slow but significant reaction phase may exist due to diffusion into interparticle and intraparticle spaces, sites of different

reactivity, or surface precipitation. The kinetics of arsenic adsorption-desorption must be understood if accurate predictions are to be made about the fate of arsenic in soil environment (Sparks, 1989).

Studies demonstrated that adsorption of arsenic on mineral surfaces is perhaps a two phase reaction with a large amount of arsenic rapidly uptake by adsorbent during a very short initial time, followed by a long plateau phase that can extend to years. For example, Fuller et al. (1993) found that the arsenate adsorption on ferrihydrite was almost instantaneous (<5 min) followed by continued uptake for at least 8 days. Grossl et al. (1997) using pressure-jump technique studied kinetic of arsenate adsorption on goethite and they proposed that the reaction is a two-step process with an initial ligand exchange reaction leading to the formation of monodentate surface complex and a second ligand exchange reaction resulting in the formation of bidentate surface complex. Raven et al. (1998) studied arsenite and arsenate adsorption on ferrihydrite at reaction time of 0.083 to 96 h and found the reactions almost complete in the first 2 h. They suggested that arsenic adsorption on ferrihydrite were diffusion controlled and best described by the parabolic diffusion equation. O'Reilly et al. (2002) studied arsenate adsorption on goethite over a period of 4 min up to 12 mo. They found 93% (pH=6) and 97% (pH=4) of the As(V) was removed from solution in the initial 24 h, and the rest of the arsenic was slowly adsorbed in the following one year. Arai and Sparks (2002) found at pH 4.5, it took 3 days to complete As(V) adsorption on aluminum oxide, while at pH 7.8, reaction continued for over 1 year. Furthermore, they observed arsenic adsorption on hematite was initially fast and followed by a slower uptake process with increasing time (Arai et al., 2004). However, there were considerable variations between experimental observed reaction rates of arsenic adsorption on different minerals. Anderson et al. (1976) showed that over 90% of arsenate adsorption on

amorphous Al oxides took place before 1 h. Pierce and Moore (1980) concluded that 99% of As(III) adsorption on amorphous Fe oxide had taken place after 2 h of reaction and the reaction was complete after 24 h. Manning and Goldberg (1996) showed arsenate adsorption on kaolinite, montmorillonite, and illite remained nearly constant after reacted for 8 h. Waltham and Eick (2002) showed that both As(III) and As(V) adsorption on goethite were essentially complete within 2h.

Because of the intrinsic chemical and physical heterogeneity of soils, it is more difficult to describe and predict the kinetics of arsenic adsorption on soil matrix. Most studies have demonstrated that residence time have significant effect on arsenic retention by soils. Similar to the observations on mineral surfaces, it is widely reported that arsenic sorption is a biphasic process with an initial rapid reaction followed by a long slow phase. For example, Livesey and Huang (1981) concluded that As(V) adsorption on soils were rapid initially and a small increase in adsorption occurred after 24 h. Elkhatib et al. (1984b) studied kinetic of As(III) adsorption on surface and subsurface soils and fitted their results with an Elovich equation and a modified Freundlich equation. They concluded that initial reaction was rapid with more than 50% of As(III) sorbed on soils in the first 0.5 h. Their regression results showed that reaction rate can be related to soil clay content or Fe oxide content. Similarly, Carbonell-Barrachina et al. (1996) found that As(III) sorption on soils was initially rapid and sorption rate decreased with time. Their results showed that sorption process continued during 50hrs of reaction. Smiths et al. (1999) showed that As(V) retention by soils was initially rapid, attained apparent equilibrium in less than 1 h, followed by a steady and slow rate for the 72 h investigated. Williams et al. (2003) conducted long-term As(V) adsorption experiment on a iron oxide containing subsurface soil. They concluded that As(V) sorption exhibit biphasic pattern with a rapid period before 48hr,

followed with a slow process over next several weeks. The K_d value after three weeks was three to four times that after one week. Darland and Inskeep (1997) demonstrated that the adsorption of As(V) on iron oxide containing sand continued for at least 96 hours. More recently, Brouwer et al. (2003) showed that K_d of As(V) for soils increased on average 1.8 fold between day 2 and 7 after reaction. Manning and Suarez (2002) showed that the rate of As(III) adsorption on soils was closely dependent on soil properties including extractable metals, soil texture, specific surface area, and pH.

In contrast to adsorption studies, relatively few work have been done to investigate desorption or release of arsenic from the soil minerals or soils. Research has shown that sorption of arsenic is highly hysteric and sorbed arsenic is not easily removable from the soil matrix. However, the effects of residence time on desorption of arsenic from soil minerals or soils are not clear yet. Lin and Puls (2000) found that desorption of As(III) and As(V) from clay minerals was significantly decreased with increasing aging time. They explained this phenomena with the diffusion of arsenic into internal sorption sites, which is not readily accessible by the bulk solution. O'Reilly (2001) showed that a significant amount of As(V) bound to goethite (>60%) is not readily desorbable by PO_4^{3-} after 5 months of reaction. However, they found residence time (0.7h to 4846h) have little effect on As(V) desorption from goethite in the presence of 6mM PO_4^{3-} at pH 4 and 6. In contrast, Arai and Sparks (2002) found that As(V) desorption from aluminum oxide surfaces decreased with increasing reaction time (3 day to 1 year). Furthermore, their EXAFS studies provided microscopic evidence of rearrangement of surface complexes and surface precipitation. The different results may due to the different desorption solution they used, O'Reilly used high concentration of phosphate while Arai and Sparks used a complex solution containing 0.096M NaCl, 1mM sodium sulfate, and 2mM organic buffer.

Desorption or release of arsenic from soil surface is a much more complex process. Jacobs et al. (1970) the extractability of As(V) sorbed by soil decreased with increasing equilibration time. The time required to reach equilibrium of arsenic in soils varied from 1 to 6 months depending on soil texture and arsenic level. Woolson et al. (1973) showed that the solubility As(V) applied to soils decreased with time and reached an equilibrium in about 4-6 weeks. Elkhatib (1984a) concluded that arsenite desorption soils was quite hysteretic with only a small fraction of the sorbed As(III) released after 5 desorption steps with deionized water. Barrachina et al. (1996) stated that As(III) sorption was a reversible process and their data showed about 50% of the sorbed arsenic can be released from soil after 5 desorption steps in 36hrs. They suggested that the difference might be explained with different sorption capacity of the soils they used. Lombi et al. (1999) evaluated the kinetics and reversibility of As(III) and As(V) sorption by Fe-oxide-coated sand and several soils. They demonstrated that a significant portion of arsenic was converted to less mobile form as demonstrated by the decreased amount of As in the easily extractable form and the increasing As in the more recalcitrant form.

Data from adsorption-desorption kinetic experiment can be described by a series of kinetic equations, which will be extensively discussed in the following chapter. However, few researchers have investigated the kinetic of arsenic adsorption-desorption in soils. Elovich equation and modified Freundlich equation was the only model used to describe the kinetic of arsenic sorption on soils (Elkhatib et al., 1984; Barrachina et al., 1996).

2.5. Dissolution – Precipitation

2.5.1 Dissolution of Primary Minerals

Most arsenic originally present in the parent material is in the form of chemically reduced minerals such as realgar, orpiment, and arsenopyrite (Oremland and Stolz, 2003). The

weathering process can oxidize arsenic to arsenite or arsenate minerals. As a result, arsenic in secondary minerals is mainly composed of arsenate. Because of the high solubility of metal-arsenate or metal-arsenite compounds (e.g. Ca, Fe, Mn, and Al), high concentrations of As(V) or As(III) will be released into aqueous phase through mineral dissolution.

The kinetics of the oxidation and dissolution of arsenic bearing sulfide minerals have been studied under various environmental conditions (dissolved oxygen, pH, temperature, carbonate, et al.). In general, the dissolution arsenic from sulfide minerals is a slow process than can last for thousands of years. Considerable amount of arsenic will be released into aqueous solution during this process. Kim et al. (2000) reported that under anaerobic conditions, the carbonation of arsenic sulfide minerals (orpiment, realgar) released stable arseno-carbonate complexes $[\text{As}(\text{CO}_3)_2^-]$, $[\text{As}(\text{CO}_3)(\text{OH})_2^-]$ into groundwater. The oxidation of amorphous As_2S_3 and AsS , orpiment, and realgar was studied by Lengke and Tempel (2001, 2002, 2003, 2005) with mixed flow reactors and numerical simulation and the reaction rates as functions of dissolved oxygen, pH, and temperature were given. Walker et al. (2006) observed the congruent dissolution of arsenopyrite by oxygen under pH 6.3-6.7. They found the reaction kinetics was not oxygen dependent.

2.5.2 Reductive Dissolution of Metal Oxides

Under strongly acidic and strongly reducing conditions, iron oxides may be dissolved either biotically or abiotically. It is believed that arsenic associated (adsorbed or precipitated) with oxides will release to aqueous solution during iron oxide dissolution (Smedley and Kinniburgh). Pederson et al. (2006) observed the release of arsenic during the reduction of ferrihydrite, lepidocrocite, and goethite. For ferrihydrite and goethite, they attributed the release of arsenic with the desorption process resulted from reduced surface area of iron oxides during

dissolution. In contrast, they found the arsenic was released from lepidocrocite before the Fe release. An interesting study by Herbel and Fendorf (2005) investigated the mobilization of arsenic under dynamic flow conditions in ferric hydroxide coated sands inoculated with arsenate reducing bacteria (*Surfurosprillum barnesii* strain SES-3). They suggested that the release of arsenic into the aqueous phase is associated with the mineralogical transformation of iron oxides resulted from the microbial reduction.

Even though the sediments in the Ganges Delta contains only modest level of arsenic ($0.4 - 10 \text{ mg kg}^{-1}$), arsenic concentrations of drinking water from shallow tubewells are commonly much higher than the WHO guideline level of 0.01 mg L^{-1} , ranging from less than $0.25 \text{ } \mu\text{g L}^{-1}$ to more than $1600 \text{ } \mu\text{g L}^{-1}$ (WHO, 2001). Scientists have suggested several explanations for the presence of dissolved arsenic. Oxidation of arsenic-bearing pyrite induced by lowered water table in dry season irrigation pumping was initially considered as the reason of arsenic dissolution (Chowdhury et al. 1999). However, more recent evidences have shown that the reduced dissolution of arsenic-rich iron oxyhydroxides was the more possible reason of arsenic releasing (Nickson et al., 1998; McArthur et al., 2001; Harvey et al., 2002). Several hypotheses were proposed to explain this process. McArthur et al. (2001) believed that iron oxides were reduced by microbial degradation of buried peat since the last ice age. Harvey et al. (2002) suspected that the dissolved organic carbon (DOC) introduced into young alluvial aquifers during recharge of irrigation pumping could lead to the reducing dissolution of iron oxides. However, those findings are controversial, debate on the sources of arsenic and process of arsenic mobilization still continues.

2.5.3 Coprecipitation and Surface Precipitation with Metal Oxides

Generally, precipitation only contributes a little portion of the arsenic retention except in highly contaminated soils (e.g. soil around acid mine). If present at very high concentrations, direct precipitation or coprecipitation of arsenic with solid phase Al, Fe, Mn, Mg, and Ca might occur. For example, Masscheleyn et al. (1991) indicated that under reduced conditions, the formation of $\text{Mn}_3(\text{AsO}_4)_2$ may control the dissolved As(V). Voigt et al. (1996) observed natural precipitation of mineral hoernesite $[\text{Mg}_3(\text{AsO}_4)_2 \cdot 8\text{H}_2\text{O}]$ in a contaminated soil. Juillota et al. (1999) reported the precipitation of 1:1 Ca arsenate (weilite CaHAsO_4 , haidingerite $\text{CaHAsO}_4 \cdot \text{H}_2\text{O}$, and pharmacolite $\text{CaHAsO}_4 \cdot 2\text{H}_2\text{O}$) and in a minor amounts, Ca-Mg arsenate [picropharmacolite $(\text{Ca,Mg})_3(\text{AsO}_4)_2 \cdot 6\text{H}_2\text{O}$] in a contaminated industrial site. Foster et al. (1998) showed the formation of scorodite $[\text{FeAsO}_4 \cdot 2\text{H}_2\text{O}]$ in mine waste using extended x-ray adsorption fine-structure spectroscopy (EXAFS). Grafe et al. (2004) reported the formation of adamite like $[\text{Zn}_2(\text{AsO}_4)\text{OH}]$ precipitation on goethite when As(V) and Zn were simultaneously introduced in high surface density ratio. Violante et al. (2006) reported the formation of poorly crystalline aluminum-arsenate precipitates (a boehmite-like mineral) as influenced by pH, As/Al ratio, and aging. They suggested that arsenate appeared to be occluded within the network of short range ordered material.

Recent studies suggested that surface precipitation, i.e., three dimensional growth of a particular surface phase, may occur for arsenate. The theory of surface precipitation suggests that anions adsorbed on mineral surfaces attract dissolved Fe or Al. The adsorbed Fe or Al in turn adsorbs more anions, result in a multilayer adsorption. Contradicting stories were reported from the kinetic and spectroscopic studies. Waychunas et al. (4) ruled out the possibility of arsenate surface precipitation on ferrihydrite with their EXAFS data. However, the possibility of Al-AsO₄

surface precipitate formation was not excluded from the spectroscopic studies of arsenate adsorption on Al oxides (Arai and Sparks, 2002). The possibility of surface precipitation of As(V) on ferrihydrite was suggested by Zhao and Stanforth (2002) through kinetic studies. More recently, Jia et al. (2006) demonstrated the formation of poorly crystalline ferric arsenate surface precipitates (a scorodite-like mineral) under undersaturated condition at low pH. Pedersen et al. (2006) reported that the arsenate was initially associated with the surface of more reactive iron oxides (ferrihydrite and lepidocrocite) but incorporated into the crystalline structure during Fe^{2+} catalyzed transform of those iron oxides into recrystallization products (goethite and magnetite).

2.5.4 Precipitation with Sulfides

Under highly reduced condition and with the presence of sulfide, arsenic sulfide precipitation may occur. Using X-ray adsorption near edge structure (XANES), Reynolds et al. (1999) identified the precipitation of FeAsS in Santa and Palouse soils after 14d of flooding and those FeAsS precipitation was largely destroyed upon re-aeration. Under acidic and reduced conditions, Wilkin and Ford (2002) reported that disordered orpiment or alacranite precipitations formed after the reaction between soluble arsenic and H_2S . Bostick and Fendorf (2003) studied arsenite sorption on troilite (FeS) and pyrite (FeS_2) and they identified surface precipitation of arsenopyrite (FeAsS) using X-ray absorption spectroscopy (XAS).

2.6. Reduction-Oxidation

Soil oxidation-reduction reaction plays an important role in determining arsenic solubility, mobility, bio-availability and toxicity. Under natural environmental conditions, arsenate [As(V)] and arsenite [As(III)] are the most abundant forms of arsenic (Smith et al., 1998). In soils and water systems, As(V) is dominant under aerobic condition and As(III) under anoxic or anaerobic condition. But, because the redox reactions between As(V) and As(III) are

relatively slow, both oxidation forms are often found in soils regardless of pH and Eh (Masscheleyn et al., 1992). Given the dissociation constants for arsenic acid [As(V)] ($pK_a^1=2.20$, $pK_a^2=6.97$, $pK_a^3=11.53$) and arsenious acid [As(III)] ($pK_a^1=9.22$, $pK_a^2=12.13$, $pK_a^3=13.4$), the stable forms of arsenic are $H_2AsO_4^-$, $HAsO_4^{2-}$, $H_3AsO_3^0$, and $H_2AsO_3^-$ under natural pH conditions (Goldberg, 2002).

2.6.1 Thermodynamics

The distribution and transformation between arsenate [As(V)] and arsenite [As(III)] is largely controlled by the redox condition of the soil environment. Besides soil redox potential (Eh or pe), other factors such as pH, Fe and Mn oxides, sulfides, organic matter, and microbial activity also impact reduction and oxidation of arsenic. The oxidation-reduction reactions of arsenic can be chemical or biological, depending on the substances present in the environment. The oxidation of arsenite by oxygen occurs at extremely slow rate. Several minerals, such as Mn oxides, sulfides, can either catalyze the redox reaction or be a direct oxidant or reductant. Certain microbes (prokaryotes) use arsenic oxyanions as energy source, either by oxidizing arsenite or by reducing arsenate. The species of arsenic in solution usually are not at equilibrium status because of slow rates of redox reactions.

Eh and pH diagrams were commonly used to describe the distribution of arsenic species under various soil conditions. Bohn (1976) provided an Eh-pH diagram of solid and gaseous arsenic state in the presence of oxygen, water, and sulfur. They concluded that at equilibrium As_2O_5 , As_4O_5 , and As_2S_3 are stable solids, while H_3AsO_4 , $HAsO_2$ and $As_2S_3^{3-}$ are stable solution species over the range of possible soil redox conditions. Masscheleyn et al. (1991) investigated arsenic speciation and solubility of a contaminated soil under different Eh and pH combinations. Their data showed that reducing soil condition ($Eh < 0mV$) greatly enhanced the solubility of

arsenic, and the majority of soluble arsenic was presented as As(III). The effect of redox on distribution of arsenic species was simulated with thermodynamic data. Result showed that As(V) species are more abundant at $pe+pH>9$, while As(III) forms dominate with $pe+pH<7$ (Sadiq et al., 1983; Sadiq, 1997).

2.6.2 Oxidation by Metal Oxides

There is considerable evidence that mineral surfaces can play an important role in transformation between As(V) and As(III). Oscarson et al. (1981, 1983) showed that manganese(IV) oxides can effectively oxidize As(III) into As(V). The depletion of As(III) follows first order kinetics with rate constant of 7.42×10^{-5} , 5.25×10^{-5} , and 1.2×10^{-7} for birnessite, cryptomelane, and pyrolusite, respectively. No oxidation of As(III) in solution was observed after 48h reaction with suspensions of illite, montmorillonite, kaolinite, vermiculite, ferruginous smectite, microcline, orthoclase, or calcite (Oscarson, 1981a). The X-ray photoelectron spectroscopy evidences showed no redox reaction between Fe(III) oxide and As(III) happened within 72 h (Oscarson, 1981b). Scott and Morgan (1995) found that As(III) oxidation by synthetic birnessite is rapid, with a time scale of minutes. They explained this reaction with a four step multiprocess surface mechanism, 1) adsorption of As(III); 2) electron transfer from As(III) to Mn(IV); 3) release of As(V); 4) release of Mn(II), with the adsorption as the slowest step. Sun and Doner (1997) observed that 20% of As(III) sorbed on goethite surface was oxidized into As(V) after 20 days of incubation. Their result showed that birnessite was an active oxidant of As(III) both in solution and on the goethite surface. Manning and Goldberg (1997) showed that alkaline solution ($pH>9$) without mineral solids caused homogeneous oxidation of As(III) to As(V). Heterogeneous oxidation of As(III) to As(V) was observed on the kaolinite and illite surface but they attributed that to the MnO_2 present in clay minerals. Manning

et al. (1998) investigated As(III) sorption on goethite surface with EXAFS. No As(V) was observed and they concluded that As(III) sorbed on goethite surface was stable. Lin and Puls (2000) demonstrated that oxidation of As(III) to As(V) occurred at the clay surface, whereas no reduction of As(V) to As(III) was observed. Using speciation with XANES spectroscopy, Manning (2005) reported recently that As(III) was either partially or completely oxidized to As(V) on soil surface, whereas no reduction of As(V) was observed.

2.6.3 Reduction by Sulfides

Under highly reduced condition, sulfide minerals can reduce As(V) to As(III). Rochette et al. (2000) showed arsenate reduction by dissolved hydrogen sulfide is a rapid reaction that follows 2nd order kinetics with rate constant, $k=8.9 \times 10^{-2} \text{ s}^{-1}$, that is more than 300 times greater at pH 4 than at pH 7. A intermediate product $\text{H}_x\text{As}_3\text{S}_6^{x-3}$ was identified and persisted in solution for several days.

2.6.4 Biotransformation

Microorganisms in soils and natural waters have significant implications for the speciation and behavior of arsenic. Biotransformation of arsenic by soil microbial activities are of great interest because of their possible applications for the bioremediation of contaminated soils. Numerous bacteria, fungi, and algae organisms that are capable of reducing or oxidizing arsenic have been identified and isolated. A comprehensive review on biotransformation of arsenic can be found in the book “environmental chemistry of arsenic” by Frankenberger (2001). Macur et al. (2004) showed that bacteria capable of either oxidizing As(III) or reducing As(V) coexist and are ubiquitously present in soil environment. Their unsaturated column study showed that As(III) was readily oxidized into As(V), whereas no apparent As(V) reducing was observed.

Few studies have been conducted to investigate the effect of microbial activity on arsenic adsorption. Langner and Inskeep (2000) investigated microbial reduction of arsenate in the presence of ferrihydrite. They found that a As(V) reducing, glucose-fermenting microorganism was able to rapidly reduce the aqueous As(V) to As(III) but not able to reduce As(V) adsorbed on ferrihydrite surface. Although the aqueous As(V) was highly reduced, the desorption rate of As(V) from ferrihydrite is too slow to cause increase of arsenic solubility. Moreover, Langner et al. (2001) observed the rapid oxidation (first-order rate constant of 1.2 min^{-1}) of As(III) to As(V) in stream waters from geothermal springs with the presence of live organisms and high Fe/Al content.

2.6.5 Kinetics of Arsenic Reduction-Oxidation in Soils

Because of the slow kinetics of redox reaction of arsenic, both As(V) and As(III) are often found in the soil environment regardless of the redox conditions. Masscheleyn et al. (1991) reported the persistence of arsenate under reducing condition and As(III) under oxidizing condition, which was attributed to the slow reaction kinetics. McGeehan and Naylor (1994) have shown that the reduction of As(V) to As(III) was highly dependent on the sorption process of arsenic. Onken and Hossner (1996) identified both convergence from arsenite to arsenate and arsenate to arsenite in the soil solution under flooded conditions. Manning and Suarez (2002) observed that heterogeneous oxidation of As(III) to As(V) was controlled by soil properties including pH, content of Al, Fe and Mn oxides. Takahashi et al. (2004) found that arsenic quickly released from flooded paddy soils as a result of reductive dissolution of Fe hydro(oxide) accompanied with reduction from As(V) to As(III).

Other substances occurring in soils may influence redox chemistry of arsenic, even though the mechanisms of those effects have not been revealed. For example, Reynolds et al.

(1999) reported that the addition of H_2PO_4^- enhanced arsenic reduction rate in Palouse and Santa soils. Senn and Hemond (2002) demonstrated that the existence of nitrate under anaerobic condition can oxidize As(III) into As(V). The accumulation of nitrate also produced more As-sorbing Fe(III) oxides. As a result, the presence of nitrate reduced the toxicity of arsenic.

2.7. Transport of Arsenic under Dynamic Flow Condition

The majority of the experimental studies on the fate and behavior of arsenic were conducted in well mixed batch systems. Relatively few experiments have been conducted under dynamic flow conditions. The miscible displacement techniques have been widely proposed to study the transport of arsenic in natural porous media since the experiment condition in column studies could more closely mimic the behavior of contaminants in heterogeneous geological material.

The transport of arsenic in heterogeneous natural soils was largely controlled by the adsorption-desorption of arsenic on the surface of solid matrix. Several studies demonstrated that the highly nonlinear (concentration-dependent) and kinetic (time-dependent) adsorption-desorption resulted in non-equilibrium transport of arsenic in natural soils. Melamed et al. (1995) observed highly asymmetry As(V) breakthrough curves (BTCs) from columns of an Oxisol and they suggested that the physical and chemical non-equilibrium exist in the soil matrix during arsenic movement through the columns. Kuhlmeier (1997a) investigated the transport of As in columns of silty sands or coarse sands and calculated the time- and concentration- dependent distribution coefficient (K_d) values. In a separate column experiment conducted with a heavily contaminated clayey soil, Kuhlmeier (1997b) observed the slow release of arsenic as a result of kinetically controlled or rate limited mass transfer of arsenic. More over, Darland and Inskeep (1997ab) found that As(V) transport exhibited significant retardation, tailing, and poor recovery

and they excluded the possibility of physical or transport related non-equilibrium through the symmetrical BTCs of conservative tracer. The non-equilibrium of As(V) transport in a heterogeneous subsurface soil with high arsenic sorption capacity was demonstrated by Williams et al. (2002).

Because of the non-equilibrium nature of the arsenic transport in soil, the flow velocity or residence time might significantly impact the transport of arsenic. Puls and Powell (1992) observed that the distribution factors (K_d) determined from column transport experiments increased from 1.4 L kg⁻¹ for flow rate (q) of 3.4 m d⁻¹ to 3.0 L kg⁻¹ for $q = 1.7$ m d⁻¹. Darland and Inskeep (1997a) demonstrated that increasing pore volume velocity from 0.2 cm h⁻¹ to 90 cm h⁻¹ resulted in a nearly ten folds increase of As(V) recovery from saturated sand columns. Similarly, Williams et al. (2003) reported that that As(V) mobility in a heterogeneous subsurface soil was significantly enhanced by the increasing of pore water velocity (0.53 to 1.6 cm min⁻¹) as demonstrated by the decreased retardation in the BTCs. The significant enhancing effect of increasing pore water velocity on the transport of As(III) was demonstrated by Radu et al. (2005). Nikolaidis et al. (2004) studied the mobility of arsenic in contaminant lake sediments with continuous column leaching and they also found that the significant more arsenic was removed at high flow rate (0.1 cm min⁻¹) than low flow rate (0.01 cm min⁻¹). Radu et al. (2005) studied the effect of pore water velocity (0.23 and 2.3 cm/min) on the transport of As(III) in saturated columns of goethite-coated sand. Their results demonstrated that the increasing pore water velocity increased the mobility of As(III).

A number of saturated column studies have been conducted to evaluate the impact of various chemical conditions on the transport of arsenic in natural soils. Hiltbold et al. (1973) studied the transport of monosodium methanearsonate (MSMA) in surface and subsurface

Dothan loamy sand, hartsells fine sandy loam, and Decatur silt loam with column experiment. The breakthrough curves (BTC) of surface soils showed relatively little retardation, whereas long retardation periods were observed in the BTCs from the subsoils. The distribution coefficients (K_d) values calculated from batch and column showed big discrepancy and they attributed that to the shorter residence time within column. Williams et al. (2003) found increasing ionic strength from 0.01M to 0.1 M extended As(V) adsorption. They explained that the increase in ionic strength lessens the electrostatic repulsion power between the negatively charged surface and oxyanion hence may increase the adsorption of arsenic onto mineral surface.

Miscible displacement experiments provided evidence that the presence of P in soils greatly enhanced arsenic mobility. Woolson et al. (1973) leached a Dunkirk fine sand soil, containing 625 mg As L⁻¹ as a result of PbAsO₄ application, with 0.05M KH₂PO₄. 77% of the arsenic originally present in soil was released and the more water soluble arsenic was extracted from soil residual after leaching. The significant enhanced transport of As(V) through columns of an aggregated Oxisol by the increasing addition of phosphate was demonstrated by the left shifted BTCs observed by Melamed et al. (1995). Similarly, Peryea and Kammereck (1997) found that the application of phosphate significantly mobilized arsenate and resulted in near 50% loss of soil arsenic after 10 pore volume displacements. Qafoku et al. (1999) studied the effect of competitive anions (phosphate and sulfate) arsenic transport through a packed Cecil soil column amended with fly ash. They found that with addition of calcium phosphate, arsenate concentration in leachate increased almost ten times compared to calcium sulfate addition. The displacement of As(V) by phosphate under dynamic flow conditions were reported by several other researchers (Darland and Inskeep 1997b; Williams et al. 2003; Radu et al. 2005). Column studies were also employed to study the effect of carbonate on arsenic transport. Radu et al.

(2005) studied the effects of high aqueous carbonate concentrations on the transport of arsenic in synthetic iron oxide-coated sand columns. They found that increasing carbonate concentrations had relatively little effect on the adsorption and transport of As(III) and As(V) even when present in much higher concentrations than phosphate. Williams et al. (2003) found that the presence of 0.1mM CO₃ slightly increased As(V) transport in columns of subsurface soil.

Miscible displacement experiments demonstrated that As(V) was generally more mobile under high pH due to decreased adsorption. For example, Darland and Inskeep (1997b) found that increasing pH from 4.5 to 8.5 dramatically shifted As(V) BTC to left. A more symmetrical BTC was observed at pH 8.5 as a result of the increasing As(V) mobility. Similar effect of pH was observed by Williams (2002) on a subsurface soil with high iron content. In contrast, Radu et al. (2005) reported that the breakthrough of As(III) was more rapid at pH 4.5 than at pH 9, resulted from increased adsorption of As(III) under high pH.

The reductive dissolution of iron oxide and subsequent release of sorbed or precipitated arsenic were proposed as the mechanisms of arsenic contamination of aquifers in Bangladesh (Smedley and Kinniburgh, 2002; Pedersen et al., 2006). Isenbeck-Schroter et al. (2002, 2004) conducted natural gradient tracer test of arsenic transport in ground water at Cape Cod, Massachusetts. They observed significant oxidation of As(III) to As(V) and high retardation of arsenic breakthrough in the oxic zone. The transport of both As(III) and As(V) was faster in the suboxic zones as compared to the oxic zones. Herbel and Fendorf (2005) investigated the mobilization of arsenic under dynamic flow conditions in ferric hydroxide coated sands inoculated with arsenate reducing bacteria (*Surfurosprillum barnesii* strain SES-3). They suggested that the release of arsenic into the aqueous phase is associated with the mineralogical transformation of iron oxides resulted from the microbial reduction.

The important role of colloid in facilitating contaminant transport in porous media has been recognized since early 1990s. Traditionally contaminant was assumed to be either immobilized by sorption of solid phase or mobile in aqueous phase. However, evidences had shown that the non-aqueous, mobile colloid could transport the low solubility contaminant for a considerable distance (Honeyman, 1999). Puls and Powell (1992) conducted column experiments with a aquifer material to investigate the possible effect of colloidal iron oxide on facilitating As(V) transport. They observed the substantial mobilization of colloid associated arsenate when flushing the column with deionized water. Ishak et al. (2002) investigated arsenic leaching from fly ash through an intact Applying loamy sand column. Their result showed that arsenic levels present in the leachates roughly correlated with effluent turbidity, which support the supposition that arsenic movement was generally associated with mobilized colloids.

2.8. Movement of Arsenic in Field

The elevated concentrations of arsenic in soils and aquifers have caused concern over the potential pollution of surface and ground water resulting from arsenic release and leaching. Understanding the transport or mobility of arsenic in porous media is required to assess the impact of soils and aquifer arsenic on surface and ground water quality. The geochemical reactions (dissolution-precipitation, adsorption-desorption, and reduction-oxidation) often control the transport of arsenic in soils and sediments.

Downward movement of arsenic has been observed in contaminated soils. Isensee et al. (1973) investigated arsenate residual in Metapeake silt loam 14 years after massive application of arsenical herbicides. Their result showed that a large amount of arsenic remained in soil profile and the concentration decreases with increasing depth, which is indicative of the slow leaching of arsenic. Hiltbold et al. (1973) studied MSMA (monosodium methanearsonate)

transport in surface and subsurface Dothan loamy sand, hartsells fine sandy loam, and Decatur silt loam with field profile sampling and the leaching of MSMA was not observed, possibly because of the relatively short period after the introduction of the herbicide (6 years) and the high As adsorption of the subsoils. Peryea (1994) investigated the vertical distribution of arsenic in an orchard soil contaminated by historical application of lead arsenate insecticides. Their results demonstrated that arsenic was relatively depleted in the surface soil and enriched in subsoil and a significant amount of As (0.07 to 0.63 mmol/kg in soil) were leached to the depth of 120cm, indicating the substantial downward movement of arsenic.

Soils around the historical cattle dipping vats usually contain extremely high concentrations of arsenic. There were fears that arsenic in those contaminated soils may be leached to groundwater and cause the contamination of the drinking water sources. McLaren et al. (1998) investigated soils surrounding cattle dips and the result showed that considerable movement of arsenic down through the soils had occurred. Arsenic in the subsurface soil (20-40cm) near cattle dip sites in Australia can be as high as 2282 mg As kg⁻¹. Generally, the immigration of arsenic has been found to be very slow, controlled by the chemical and physical properties of soils. Kimber et al. (2002) analyzed the shallow ground water around 28 cattle dipping vats in Australia with piezometers. The highest arsenic concentration (5.69 mg L⁻¹) in ground water was found adjacent to a contaminated site with soils of sandy texture. The concentration declined to approximately background ground level with 20m distance from the contaminated site.

Studies demonstrated that the arsenic contained in chromated copper arsenate (CCA) leached from the wood surface to adjacent soil (Chirenje et al. 2003). More over, it is possible that part of the arsenic may eventually released into aquatic environment and cause human health

concern. Allinson et al. (2000) investigated the release of CCA constituents from undisturbed soil monolith lysimeters containing the surface horizon of a mildly acidic, sandy loam soil. They observed that up to 13% of the applied arsenic was detected in the leachate at 15 cm depth and breakthrough was observed 25 days after CCA application. Hingston et al. (2001) conducted literature review on the leaching studies of CCA treated wood and they concluded there is insufficient data to quantitatively predict the leaching rate of elements under various environment conditions (pH, salinity, and temperature). More recently, Khan et al. (2006ab) investigated the leaching of arsenic from CCA-treated wood during service as well as disposal with lysimeter tests. They found cumulatively around 2000 mg arsenic was leached out from landfills in a one year period, with inorganic As(V) and As(III) as the major species.

Because of the complex reaction of arsenic in natural geological materials, it is extremely difficult to numerically simulate the fate of arsenic compounds with consideration of numerous environmental factors (pH, Eh, Fe/Al oxides, competing ligands, et al). Simulation attempts have been made with geochemical models. Smith and Jaffe (1998) formulated a geochemical model which coupled the transport process with various kinetics reactions and simulated the arsenic transport in Benthic sediment. However, because of the uncertainty associated with numerous geochemical parameters, such models can only be viewed as heuristic tools for exploring the possible trends in the fate of contaminants as a result of environment change. More over, Sracek et al. (2004) summarized several examples of forward or inverse geochemical modeling for the fate of arsenic in natural environments. The common strategies employed in those studies were coupling the transport model with surface complexation model to demonstrate the effect of adsorbents, pH, redox potential, and competing ions.

2.9. Remediation of Arsenic Contaminated Soils

The engineering approaches for the remediation of arsenic-contaminated sites include isolation, immobilization, toxicity reduction, physical separation and extraction (Mulligan et al., 2001). Solidification/stabilization (S/S), also known as chemical fixation or encapsulation, is a set of technologies widely applied to treat the soils contaminated with cationic heavy metals. The most common form of S/S uses a cement or pozzolanic binder to convert the contaminated soil to create a monolithic form that limits the contaminant mobility. Akhter et al. (2000) evaluated many combinations of cement binders and reagents in their capability to solidify sandy soils contaminated with arsenic. They reported that a mixture of Type I Portland cement and ferrous sulfate was effective in reducing the leaching of arsenic and improved performance was observed when the soil was pretreated with $\text{FeSO}_4 \cdot 7\text{H}_2\text{O}$ followed by Portland cement. This chemical contaminant strategy was successfully implemented in their field study.

Permeable reactive barrier (PRB) consists of installing a reactive material into the aquifer to induce sequestration and/or transformations of the contaminants and reduce the contaminant concentration in groundwater. Su and Puls (2001, 2003) evaluated several types of zerovalent iron (Fe^0) in their capacity of attenuate arsenic concentration using both batch and column experiments. They suggested that Fe^0 was a promising material for *in situ* remediation of contaminated groundwater with relatively low cost. The use of Fe^0 in treating arsenic contaminated soil and groundwater have attracted extensive attention in last five years and new developments appears on large volumes of literatures in this area. However, to our knowledge, field scale implementations of PRB for arsenic treatment have not been reported.

Monitored natural attenuation (MNA) is proposed as an alternative remediation strategy for soils contaminated with inorganic contaminants such as arsenic. In the EPA Directive (EPA,

1999), MNA is defined as “ physical, chemical, or biological processes that, under favorable conditions, act without human intervention to reduce the mass, toxicity, volume, or concentration of contaminants in soil or ground water”. The establishing of MNA as a potential remediation strategy for a specific contaminated site requires thorough and adequate site-specific characterization data and analysis. Specifically, there are three tiers of “lines of evidence”: 1) historical groundwater and/or soil chemistry data that clearly demonstrate a trend of decreasing contaminant mass and/or concentration; 2) indirect hydrogeologic and geochemical data that demonstrate the type and rate of natural attenuation processes active at the site; 3) direct field or microbiological data that demonstrate the occurrence of a particular natural attenuation process at the site.

Sorption and precipitation are the dominant processes of natural attenuation of arsenic. Biotransformation of arsenic (redox cycling and methylation) can influence those natural attenuation processes. The key issue of natural attenuation of arsenic is the reversibility of arsenic sequestration (sorption/precipitation) into solid phase because the intrinsic toxicity of arsenic was not affected by this immobilization process (Reisinger et al., 2005). Therefore, successful implementation of MNA for arsenic contaminated sites requires detailed site-specific characterization including source identification, plume boundary delineation, time-series monitor of arsenic concentration in soil and groundwater. An extensive list of ancillary data (e.g., pH, redox potential, Fe/Al/Mn contents, soil texture, organic matter) is required for the evaluation of the feasibility of MNA. Reisinger et al. (2005) provided four examples of arsenic contaminated sites where natural attenuation was deemed acceptable by regulators.

Phytoremediation is an emerging technology that uses specially selected and engineered metal-accumulating plants for environmental clean-up. Plants such as Indian Mustard (Pickering

et al., 2000) and brake fern (Ma et al., 2001) have the capability to accumulate arsenic and is considered as an potential method for treating contaminated soils. Since the discovery of arsenic hyperaccumulation capacity of *Pteris vittata* (brake fern), extensive researches have been conducted to investigate its physiological mechanisms and its effectiveness for remediation of arsenic contaminated soils. In addition to naturally selected plants, scientists used biotechnology to develop engineered plants that have the capability of accumulating arsenic. Dhankher et al. (2002) have developed a genetics-based phytoremediation strategy for arsenic where arsenic is hyperaccumulated in a plant transformed with the *arsC* gene [encoding arsenate reductase (*ArsC*)].

2.10. Summary

We summarized the occurrence, source, reaction, mobility, and remediation of arsenic in soils. Generally, the mobility and bioavailability of arsenic in soils is controlled by the adsorption-desorption process. Formation of inner-sphere surface complexes on metal (e.g., Fe, Al, Mn) oxides via ligand exchange is the dominant pathway of arsenic sorption on aerated soils. Generally, the arsenate and arsenite adsorption on Fe/Al oxides decreases with increasing pH. The adsorption of arsenate is higher than arsenite under most pH values whereas more arsenite can be sorbed on high pH values. The sorption isotherms of both As(V) and As(III) are highly nonlinear, i.e., distribution coefficient (K_d) decreases with increasing solution concentration. The time dependent adsorption behavior of arsenic was reported and attributed to the intraparticle diffusion and surface precipitation processes. Anions forming inner-sphere surface complex with metal oxides can compete with arsenic for adsorption sites and increase its mobility. The dissolution and precipitation (e.g., coprecipitation and surface precipitation) of arsenic with metal oxides under aerobic condition and with sulfide under anaerobic condition might

contribute to the retention-release of arsenic in soils. The retention-release of arsenic can be affected by the redox chemistry of arsenic in soils. Briefly, the major inorganic forms of arsenic in the natural soil environment are arsenate [As(V)] under aerobic conditions and arsenite [As(III)] under anaerobic conditions. Because the redox reactions between As(V) and As(III) are relatively slow, both oxidation forms are often found in soils regardless of pH and Eh. Transport of arsenic in soils is controlled by the complex geochemical reactions of arsenic and affected by a large number of environment factors.

2.11. References

- Acharyya, S.K., P. Chakraborty, S. Lahiri, B.C. Raymahashay, S. Guha, and A. Bhowmik. 1999. Arsenic poisoning in the Ganges delta. *Nature* 401:545-545.
- Allinson, G., N.J. Turoczy, Y. Kelsall, M. Allinson, F. Stagnitti, J. Lloyd-Smith, and M. Nishikawa. 2000. Mobility of the constituents of chromated copper arsenate in a shallow sandy soil. *New Zealand J. Agri. Res.* 43, 149-156.
- Anderson, M.A., J.F. Ferguson, and J. Gavis. 1976. Arsenate adsorption on amorphous aluminum hydroxide. *J. Colloid Interface Sci.* 54:391-399.
- Appelo, C.A.J., M.J.J. van der Weiden, C. Tournassat, and L. Charlet. 2002. Surface complexation of ferrous iron and carbonate on ferrihydrite and the mobilization of arsenic. *Environ. Sci. Technol.* 36:3096-3103.
- Arai, Y., D.L. Sparks, and J. A. Davis. 2004. Effects of dissolved carbonate on arsenate adsorption and surface speciation at the hematite-Water interface. *Environ. Sci. Technol.* 38, 817-824.
- Arai, Y., A. Lanzirotti, S. Sutton, J. A. Davis, and D. L. Sparks. 2003. Arsenic speciation and reactivity in poultry litter. *Environ. Sci. Technol.* 37, 4083-4090.
- Arai Y., and D.L. Sparks. 2002. Residence time effects on arsenate surface speciation at the aluminum oxide-water interface. *Soil Sci.* 167, 303-314.
- Association for the Environmental Health of Soils (AEHS). 1999. Study of State Soil Arsenic Regulations. <http://www.aehs.com/surveys/arsenic.pdf>.
- Barrow, N.J. 1974. On the displacement of adsorbed anions from soil: 2. Displacement of phosphate by arsenate. *Soil Sci.* 117, 28-33.
- Bednar, A.J., J.R. Garbarino, J.F. Ranville, and T.R. Wildeman. 2002. Presence of organoarsenicals used in cotton production in agricultural water and soil of the southern United States. *J. Agric. Food Chem.* 50:7340-7344.

- Berg, M., H. C. Tran, T. C. Nguyen, H. V. Phem, R. Scheertenleib, and W. Giger. 2001. Arsenic contamination of groundwater and drinking water in Vietnam: A human health threat. *Environ. Sci. Technol.* 35:2621-2626.
- Bohn, H.L. 1976. Arsenic Eh-pH diagram and comparison to soil chemistry of phosphorus. *Soil Sci.* 121:125-127.
- Bostick, B.C., and S. Fendorf. 2003. Arsenite sorption on troilite (FeS) and pyrite (FeS₂). *Geochim. Cosmochim. Acta* 67:909-921.
- Bowell, R.J. 1994. Sorption of arsenic by iron-oxides and oxyhydroxides in soils. *Applied Geochemistry* 9, 279-286.
- Bradford, G.R., A.C. Chang, A.L. Page, D. Bakhtar, J.A. Frampton, and H. Wright. 1996. Background Concentrations of Trace and Major Elements in California Soils. Kearney Foundation Special Report. Kearney Foundation of Soil Science, Division of Agriculture and Natural Resources, University Of California.
<http://www.envisci.ucr.edu/faculty/chang/kearney/kearneytext.html>
- Brouweria, K.D., E. Smoldersa and R. Merckxa. 2004. Soil properties affecting solid-liquid distribution of As(V) in soils. *Euro. J. Soil Sci.* 55:165-173.
- Carbonell-Barrachina, A.A., F. B. Carbonell, and J. M. Beneyto. 1996. Kinetics of arsenite sorption and desorption in Spanish soils. *Commun. Soil Sci. Plant. Anal.* 27:3101-3117.
- Chang, S.C., and M. L. Jackson. 1957. Fractionation of soil phosphorus. *Soil Sci.* 84:133-144.
- Chen, M., L. Q. Ma, and W. G. Harris. 2002. Arsenic concentrations in Florida surface soils: Influence of soil type and properties. *Soil Sci. Soc. Am. J.* 66:632-640.
- Chen, S.L., S. R. Dzenge, M.H. Yang, K.H. Chiu, G.M. Shieh, and C. M. Wai. 1994. Arsenic Species in Groundwaters of the Blackfoot Disease Area, Taiwan. *Environ. Sci. Technol.* 28:877-881.
- Chirenje, T., L.Q. Ma, M. Chen, and E.J. Zillioux. 2003. Comparison between background concentrations of arsenic in urban and non-urban areas of Florida. *Adv Environ. Res.* 8, 137-146.
- Darland, J.E., and W. P. Inskeep. 1997a. Effects of pore water velocity on the transport of arsenate. *Environ. Sci. Technol.* 31:704-709.
- Darland, J.E., and W. P. Inskeep. 1997b. Effects of pH and phosphate competition on the transport of arsenate. *J. Environ. Qual.* 26:1133-1139.
- Davis, A., D. Sherwin, R. Ditmars, and K.A. Hoenke. 2001. An analysis of soil arsenic records of decision. *Environ. Sci. Technol.* 35: 2401-2406.
- Dhankher, O.P., Y.J. Li, B.P. Rosen, J. Shi, D. Salt, J.F. Senecoff, N.A. Sashti, and R.B. Meagher. 2002. Engineering tolerance and hyperaccumulation of arsenic in plants by combining arsenate reductase and gamma-glutamylcysteine synthetase expression. *Nature Biotech.* 20:1140-1145.

- Dixit, S., and J. G. Hering. 2003. Comparison of arsenic(V) and arsenic(III) sorption onto iron oxide minerals: implication for arsenic mobility. *Environ. Sci. Technol.* 37:4182-4189.
- Elkhatib, E.A., O.L. Bennett, and R.J. Wright. 1984a. Kinetics of arsenite adsorption in soils. *Soil Sci. Soc. Am. J.* 48:758-762.
- Elkhatib, E.A., O.L. Bennett, and R.J. Wright. 1984b. Arsenite sorption and desorption in soils. *Soil Sci. Soc. Am. J.* 48:1025-1030.
- Fendorf S., M.J. Eick, P. Grossl, and D.L. Sparks. 1997. Arsenate and chromate retention mechanisms on goethite. 1. Surface structure. *Environ. Sci. Technol.* 31:315-320.
- Folkes, D.J., S.O. Helgen, and R.A. Little. 2001. Impacts of historic arsenical pesticide use on residential soils in Denver, Colorado. In Chappell, W.R., C.O. Abernathy, and R.L. Calderon. (eds.) *Arsenic exposure and health effects*. Elsevier Sciences, Netherland.
- Foster, A.L., G.E. Brown, and G.A. Parks. 2003. X-ray absorption fine structure study of As(V) and Se(IV) sorption complexes on hydrous Mn oxides. *Geochim. Cosmochim. Acta*, 67:1937-1953.
- Foster, A.L., G.E. Brown, T.N. Tingle, and G.A. Parks. 1998. Quantitative arsenic speciation in mine tailings using X-ray absorption spectroscopy. *Am. Min.* 83:553-568.
- Foster, A.L., G.E. Brown, and G.A. Parks. 1998. X-ray absorption fine-structure spectroscopy study of photocatalyzed, heterogeneous As(III) oxidation on kaolin and anatase. *Environ. Sci. Technol.* 32:1444-1452.
- Frankenberger, W. T. (eds.) 2001. *Environmental chemistry of arsenic*. Marcel Dekker, New York.
- Frost, R.R., and R.A. Griffin. 1977. Effect of pH on adsorption of arsenic and selenium from landfill leachate by clay minerals. *Soil Sci. Soc. Am. J.* 41:53-57.
- Fuller C.C., J.A. Davis, and G.A. Waychunas. 1993. Surface chemistry of ferrihydrite: Part 2. Kinetics of arsenate adsorption and coprecipitation. *Geochim. Cosmochim. Acta* 57:2271-2282.
- Goldberg, S. 1985. Chemical modeling of anion competition on goethite using the constant capacitance model. *Soil Sci. Soc. Am. J.* 49:851-856.
- Goldberg, S. 1986. Chemical modeling of arsenate adsorption on aluminum and iron oxide minerals. *Soil Sci. Soc. Am. J.* 50: 1154-1157.
- Goldberg S., and R.A. Glaubig. 1988. Anion adsorption on calcareous, montmorillonitic soil – Arsenic. *Soil Sci. Soc. Am. J.* 52:1297-1300.
- Goldberg S. 1992. Use of surface complexation models in soil chemical-systems. *Adv. Agron.* 47:233-329.
- Goldberg S., and C.T. Johnston. 2001. Mechanisms of arsenic adsorption on amorphous oxides evaluated using macroscopic measurements, vibrational spectroscopy, and surface complexation modeling. *J. Colloid Interface Sci.* 234:204-216.

- Goldberg, S. 2002. Competitive adsorption of arsenate and arsenite on oxides and clay minerals. *Soil Sci. Soc. Am. J.* 66:413-421.
- Grafe, M., and D.L. Sparks. 2005. Kinetics of zinc and arsenate co-sorption at the goethite-water interface. *Geochim. Cosmochim. Acta*, 69: 4573-4595.
- Grafe, M., M. Nachtegaal, and D.L. Sparks. 2004. Formation of metal-arsenate precipitates at the goethite-water interface. *Environ. Sci. Technol.* 38:6561-6570.
- Grafe, M., M.J. Eick, and P.R. Grossl. 2001. Adsorption of arsenate (V) and arsenite (III) on goethite in the presence and absence of dissolved organic carbon. *Soil Sci. Soc. Am. J.* 65:1680-1687.
- Grossl P.R., M.J. Eick, D.L. Sparks, S. Goldberg, and C.C. Ainsworth. 1997. Arsenate and chromate retention mechanisms on goethite. 2. Kinetic evaluation using a pressure-jump relaxation technique. *Environ. Sci. Technol.* 31:321-326.
- Han , F.X., W.L. Kingery , H.M. Selim , P.D. Gerard , M.S. Cox and J.L. Oldham. 2004. Arsenic solubility and distribution in poultry waste and long-term amended soil. *Sci. Total Environ.*, 320:51-61.
- Harvey, C.F., C.H. Swartz, A.B.M. Badruzzaman, N. Keon-Blute, W. Yu, M.A. Ali, J. Jay, R. Beckie, V. Niedan, D. Brabander, P.M. Oates, K.N. Ashfaq, S. Islam, H.F. Hemond, and M.F. Ahmed. 2002. Arsenic mobility and groundwater extraction in Bangladesh. *Science* 298, 1602-1606.
- Herbel, M., and S. Fendorf. 2006. Biogeochemical processes controlling the speciation and transport of arsenic within iron coated sands. *Chem. Geol.* 228, 16-32.
- Hiemstra, T., and W.H. Van Riemsdijk. 1999. Surface structural ion adsorption modeling of competitive binding of oxyanions by metal (hydr)oxides. *J. Colloid Interface Sci.* 210: 182-193.
- Hiltbold, A.E., B.F. Hajek, and G.A. Buchanan. 1974. Distribution of arsenic in soil profile after repeated application of MSMA. *Weed Sci.* 22:272-275.
- Hingston, F.J., R.J. Atkinson, A.M. Posner, and J.P. Quirk. 1967. Specific adsorption of anions. *Nature (London)* 215, 1459-1461.
- Hingston, F.J., A.M. Posner, and J.P. Quirk. 1971. Competitive adsorption of negatively charged ligands on oxide surfaces. *Disc. Faraday Soc.* 52, 334-342.
- Hingston, F.J., J.P. Quirk, and A.M. Posner. 1972. Anion adsorption by goethite and gibbsite .1. Role of proton in determining adsorption envelopes. *J. Soil Sci.* 23, 177-192.
- Hingston, F.J., A.M. Posner, J.P. Quirk. 1974. Anion adsorption by goethite and gibbsite .2. Desorption of anions from hydrous oxide surfaces. *J. Soil Sci.* 25, 16-26.
- Hingston, J.A., C.D. Collins, R.J. Murphy, and J.N. Lester. 2001. Leaching of chromated copper arsenate wood preservatives: a review. *Environ. Pollut.* 111, 53-66.

Isensee, A.R., W.C. Shaw, W.A. Gretner, C.R. Swansen, B.C. Turner, and E.A. Woollen. 1973. Revegetation following massive application of selected herbicides. *Weed Sci.* 21:409-412.

Ishak, C.F., J.C. Seaman, W.P. Miller, and M. Summer. 2002. Contaminant mobility in soils amended with fly ash and flue-gas gypsum: Intact soil cores and repacked columns. *Water Air Soil Pollut* 134:287-305.

Isenbeck-Schroter, M., R. Hohn, S. Stadler, S. Jann, J. Davis, D. Kent, V. Nieden, C. Scholz, A. Treitner, and R. Jakobsen. 2002. Tracer test with As(III) and As(V) at the Cape Cod site. *Geochim. Cosmochim. Acta* 66: A356-A356.

Jacobs, L.W., J.K. Syers, and D.R. Keeney. 1970. Arsenic sorption by soils. *Soil Sci. Soc. Am. Proc.* 34:750-754.

Jain, A., and R.H. Loeppert. 2000. Effect of competing anions on the adsorption of arsenate and arsenite by ferrihydrite. *J. Environ. Qual.* 29:1422-1430.

Jain, A., K.P. Raven, and R.H. Loeppert. 1999. Arsenite and arsenate adsorption on ferrihydrite: Surface charge reduction and net OH⁻ release. *Environ. Sci. Technol.* 33: 1179-1184.

Jessen, S., F. Larsen, C.B. Koch, and E. Arvin. 2005. Sorption and desorption of arsenic to ferrihydrite in a sand filter. *Environ. Sci. Technol.* 39:8045-8051.

Jia, Y.F., L.Y. Xu, Z. Fang, and G.P. Demopoulos. 2006. Observation of surface precipitation of arsenate on ferrihydrite. *Environ. Sci. Technol.* 40:3248-3253.

Juillot, F., P. Ildefonse, G. Morin, G. Calas, A.M. de Kersabiec, and M. Benedetti. 1999. Remobilization of arsenic from buried wastes at an industrial site: mineralogical and geochemical control. *Appl. Geochem.* 14:1031-1048.

Keon, N. E., C. H. Swartz, D. J. Brabander, C. Harvey, and H. F. Hemond. 2001. Validation of an arsenic sequential extraction method for evaluating mobility in sediments. *Environ. Sci. Technol.* 35:2778-2784.

Khan, B.I., H.M. Solo-Gabriele, T.G. Townsend, and Y. Cai. 2006. Release of arsenic to the environment from CCA-treated wood. 1. Leaching and speciation during service. *Environ. Sci. Technol.* 40:988-993.

Khan, B.I., J. Jambeck, H.M. Solo-Gabriele, T.G. Townsend, and Y. Cai. 2006. Release of arsenic to the environment from CCA-treated wood. 2. Leaching and speciation during disposal. *Environ. Sci. Technol.* 40:994-999.

Kim, M.J., Nriagu, J., and S. Haack. 2002. Carbonate ions and arsenic dissolution by groundwater. *Environ. Sci. Technol.* 34:3094-3100.

Kimber, S.W.L., D.J. Sizemore, and P.E.G. Slavich. 2002. Is there evidence of arsenic movement at cattle tick dip sites? *Aust. J. Soil Res.* 40:1103-1114.

Kuhlmeier, P.D. 1997. Partitioning of arsenic species in fine-grained soils. *J. Air Waste Management Assoc.* 47:481-490.

- Kuhlmeier, P.D. 1997. Sorption and desorption of arsenic from sandy soils: Column studies. *J. Soil Contam.* 6: 21-36.
- Langner, H.W., C.R. Jackson, T.R. McDermott, and W.P. Inskeep. 2001. Rapid oxidation of arsenite in a hot spring ecosystem, Yellowstone National Park. *Environ. Sci. Technol.* 35:3302-3309.
- Langner, H.W., and W.P. Inskeep. 2000. Microbial reduction of arsenate in the presence of ferrihydrite. *Environ. Sci. Technol.* 34:3131-3136.
- Lengke, M.F., and R.N. Tempel. 2005. Geochemical modeling of arsenic sulfide oxidation kinetics in a mining environment. *Geochim. Cosmochim. Acta* 69, 341-356.
- Lin, T.F., and J.K. Wu. 2001. Adsorption of arsenite and arsenate within activated alumina grains: Equilibrium and kinetics. *Water Res.* 35: 2049-2057.
- Lin H.T., M.C. Wang, and G.C. Li. 2002. Effect of water extract of compost on the adsorption of arsenate by two calcareous soils. *Water Air Soil Pollut.* 138:359-374.
- Lin Z., and R.W. Puls. 2000. Adsorption, desorption and oxidation of arsenic affected by clay minerals and aging process. *Environ. Geol.* 39: 753-759.
- Linge K.L. and C.E. Oldham. 2002. Arsenic remobilisation in a shallow wetland: the role of sediment resuspension. *J. Environ. Qual.*, 31:822-828.
- Liu, F., A. De Cristofaro, and A. Violante. 2001. Effect of pH, phosphate and oxalate on the adsorption/desorption of arsenate on/from goethite. *Soil Sci.* 166:197-208.
- Liu, J., B. Zheng, H.V. Aposhian, Y. Zhou, M. Chen, A. Zhang, and M.P. Waalkes. 2002. Chronic arsenic poisoning from burning high-arsenic-containing coal in Guizhou, China. *Environ. Health. Perspective* 110:119-122.
- Livesey, N.T., and P.M. Huang. 1981. Adsorption of arsenate by soils and its relation to selected chemical properties and anions. *Soil Sci.* 131:88-94.
- Lombi, E., W.W. Wenzel, and R.S. Sletten. 1999. Arsenic adsorption by soils and iron-oxide-coated sand: kinetics and reversibility. *J. Plant Nutrition Soil Sci.* 162:451-456.
- Ma, L.Q., K.M. Komar, C. Tu, W.H. Zhang, Y. Cai, and E.D. Kennelley. 2001. A fern that hyperaccumulates arsenic - A hardy, versatile, fast-growing plant helps to remove arsenic from contaminated soils. *Nature* 409:579-579.
- Macur, R.E., C.R. Jackson, L.M. Botero, T.R. McDermott, and W.P. Inskeep. 2004. Bacterial populations associated with the oxidation and reduction of arsenic in unsaturated soil. *Environ. Sci. Technol.* 38:104-111.
- Manning, B. 2005. Arsenic speciation in As(III)- and As(V)-treated soil using XANES spectroscopy. *Microchimica Acta* 151, 181-188.

- Manning, B.A., S.E. Fendorf, and S. Goldberg. 1998. Surface structure and stability of arsenic(III) on goethite: Spectroscopic evidence for inner-sphere complexes. *Environ. Sci. Technol.* 32: 2383-2388.
- Manning, B.A., and S. Goldberg. 1996a. Modeling competitive adsorption of arsenate with phosphate and molybdate on oxide minerals. *Soil Sci. Soc. Am. J.* 60:121-131.
- Manning, B.A., and S. Goldberg. 1996b. Modeling arsenate competitive adsorption on kaolinite, montmorillonite and illite. *Clays Clay Miner.* 44:609-623.
- Manning, B.A., and S. Goldberg. 1997a. Arsenic(III) and arsenic(V) adsorption on three California soils. *Soil Sci.* 162:886-895.
- Manning, B.A., and S. Goldberg. 1997b. Adsorption and stability of arsenic(III) at the clay mineral-Water interface. *Environ. Sci. Technol.* 31: 2005-2011.
- Manning, B.A., and D.L. Suarez. 2000. Modeling arsenic(III) adsorption and heterogeneous oxidation kinetics in soils. *Soil Sci. Soc. Am. J.* 64:128-137.
- Masscheleyn, P.H., R.D. Delaune, and W.H. Patrick. 1991. Effect of redox potential and pH on arsenic speciation and solubility in a contaminated soil. *Environ. Sci. Technol.* 25: 1414-1419.
- Matera V., I. Le Hecho, A. Laboudigue, P. Thomas, S. Tellier, and M. Astruc. 2003. A methodological approach for the identification of arsenic bearing phases in polluted soils. *Environ. Pollut.* 126: 51-64.
- McArthur, J.M., P. Ravenscroft, S. Safiulla, and M.F. Thirlwall. 2001. Arsenic in groundwater: Testing pollution mechanisms for sedimentary aquifers in Bangladesh. *Water Resource Research* 37, 109-117.
- McGeehan, S.L., and D.V. Naylor. 1994. Sorption and redox transformation of arsenite and arsenate in two flooded soils. *Soil Sci. Soc. Am. J.* 58: 337-342.
- McLaren, R.G., R. Naidu, J. Smith, and K. G. Tiller. 1998. Fractionation and distribution of arsenic in soils contaminated by cattle dip. *J. Environ. Qual.* 27:348-354.
- Melamed, R., J.J. Jurinak, and L.M. Dudley. 1995. Effect of adsorbed phosphate on transport of arsenate through an oxisol. *Soil Sci. Soc. Am. J.* 59:1289-1294.
- Miller, J., H. Akhter, F.K. Cartledge, and M. McLearn. 2000. Treatment of arsenic-contaminated soils. II: Treatability study and remediation. *J. Environ. Engin.-ASCE* 126:1004-1012.
- Mulligan, C.N., R.N. Yong, and B.F. Gibbs. 2001. Remediation technologies for metal-contaminated soils and groundwater: an evaluation. *Engin. Geol.* 60:193-207.
- Nickson, R., J. McArthur, W. Burgess, K. M. Ahmed, P. Ravenscroft, and M. Rahman. 1998. Arsenic poisoning of Bangladesh groundwater. *Nature* 395:338-338.
- Nikolaidis, N.P., G.M. Dobbs, J. Chen, and J.A. Lackovic. 2004. Arsenic mobility in contaminated lake sediments. *Environ. Pollut.* 129:479-487.

Nordstrom, D.K. 2002. Public health - Worldwide occurrences of arsenic in ground water. *Science* 296:2143-2145.

National Research Council (NRC). 1977. Arsenic. National Academy of Sciences. Washington, D.C.

National Research Council (NRC). 1999. Arsenic in drinking water. National Academy of Sciences. Washington, D.C.

O'Neill, P. 1995. Arsenic. In *Heavy metals in soils*. 2nd ed. (B.J. Alloway, ed.) 105-121. Blackie, London.

Oremland, R.S., and J. F. Stolz. 2003. The ecology of arsenic. *Science* 300:939-944.

Ori, L. V., M. C. Amacher, and J. E. Sedberry. 1993. Survey of the total arsenic content in soils in Louisiana. *Commun. Soil Sci. Plant Anal.* 24:2321-2332.

O'Reilly, S.E., D. G. Strawn, and D. L. Sparks. 2001. Residence time effects on arsenate adsorption/desorption mechanisms on goethite. *Soil Sci. Soc. Am. J.* 65:67-77.

Oscarson, D.W., P.M. Huang, and W.K. Liaw. 1981. Role of manganese in the oxidation of arsenite by fresh-water lake sediments. *Clays Clay Miner.* 29:219-225.

Oscarson, D.W., P.M. Huang, C. Dofosse, and A. Herbillion. 1981. The oxidation power of Mn (IV) and Fe (III) oxides with respect to As (III) in terrestrial and aquatic environments. *Nature (London)* 291:50-51.

Oscarson, D.W., P.M. Huang, W.K. Liaw and U.T. Hammer. 1983a. Kinetics of oxidation of arsenite by various manganese dioxides. *Soil Sci. Soc. Am. J.* 46:644-648.

Oscarson, D.W., P.M. Huang, and U.T. Hammer. 1983b. Oxidation and sorption of arsenite by manganese dioxide as influenced by surface coatings of iron and aluminum oxides and calcium carbonate. *Water, Air, Soil Pollut.* 20:233-244.

Paktunc, D., A. Foster, and G. Laflamme. 2003. Speciation and characterization of arsenic in Ketzar river mine tailings using X-ray adsorption spectroscopy. *Environ. Sci. Technol.* 37:2067-2074.

Paktunc, D., A. Foster, S. Heald, and G. Laflamme. 2004. Speciation and characterization of arsenic in gold ores and cyanidation tailings using X-ray absorption spectroscopy. *Geochim. Cosmochim. Acta*, 68:969-983.

Pedersen, H.D., D. Postma, and R. Jakobsen. 2006. Release of arsenic associated with the reduction and transformation of iron oxides. *Geochim. Cosmochim. Acta* 70:4116-4129.

Peryea, F.J., and R. Kammereck. 1997. Phosphate-enhanced movement of arsenic out of lead arsenate-contaminated topsoil and through uncontaminated subsoil. *Water Air Soil Pollut.* 93:243-254.

Peryea, F.J., and T.L. Creger. 1994. Vertical-distribution of lead and arsenic in soils contaminated with lead arsenate pesticide-residues. *Water Air Soil Pollut.* 78:297-306.

- Peryea, F.J., 1991. Phosphate-induced release of arsenic from soils contaminated with lead arsenate. *Soil Sci. Soc. Am. J.* 55:1301-1306.
- Pettry D.E., and R.E. Switzer. 2001. Arsenic concentrations in selected soils and parent materials in Mississippi. MAFES Bulletin 104. Office of Agricultural Communications, Mississippi State University.
- Pickering, I.J., R.C. Prince, M.L. George, R.D. Smith, G.N. George, and D.E. Salt. 2000. Reduction and coordination of arsenic in Indian mustard. *Plant Physico.* 122:1171-1177.
- Pierce, M.L., and C.B., Moore. 1980. Adsorption of arsenite on amorphous iron hydroxide from dilute aqueous solution. *Environ. Sci. Technol.* 14:214-216.
- Pierce, M.L., and C.B., Moore. 1982. Adsorption of arsenite and arsenate on amorphous iron hydroxide. *Water Res.* 16:1247-1253.
- Puls, R.W., and R.M. Powell. 1992. Transport of inorganic colloid through natural aquifer material: implication for contaminant transport. *Environ. Sci. Technol.* 26: 614-621.
- Qafoku, N.A., U. Kukier, M.E. Sumner, W.P. Miller, and D.E. Radcliffe. 1999. Arsenate displacement from fly ash in amended soils. *Water, air, and Soil Pollution* 114: 185-198.
- Radu, T., J.L. Subacz, J.M. Phillippi, and M.O. Barnett. 2005. Effects of dissolved carbonate on arsenic adsorption and mobility. *Environ. Sci. Technol.* 39:7875-7882.
- Rahman, F. A., D. L. Allan, C. L. Rosen, and M. J. Sadowsky. 2004. Arsenic availability from chromated copper arsenate (CCA)-Treated wood. *J. Environ. Qual.* 33:173-180.
- Raven, K.P., A. Jain, and R.H. Loeppert. 1998. Arsenite and arsenate adsorption on ferrihydrite: Kinetics, equilibrium, and adsorption envelopes. *Environ. Sci. Technol.* 32:344-349.
- Redman, A.D., D.L. Macalady, and D. Ahmann. 2002. Natural organic matter affects arsenic speciation and sorption onto hematite. *Environ. Sci. Technol.* 36:2889-2896.
- Reigart, J.R. and J. R. Roberts. 1999. Recognition and Management of Pesticide Poisonings. 5th Ed. United States Environmental Protection Agency.
- Reisinger, H.J., D.R. Burris, and J.G. Hering. 2005. Remediating subsurface arsenic contamination with monitored natural attenuation. *Environ. Sci. Technol.* 39: 458A-464A.
- Reynolds, J.G., D.V. Naylor, and S. E. Fendorf. 1999. Arsenic sorption in phosphate-amended soils during flooding and subsequent aeration. *Soil Sci. Am. J.* 63:1149-1156.
- Rochette, E.A., B.C. Bostick, G. Li, and S. Fendorf. 2000. Kinetics of arsenate reduction by dissolved sulfide. *Environ. Sci. Technol.* 34:4714-4720.
- Rodriguez, R.R., N. T. Basta, S.W. Casteel, F.P. Armstrong, and D.C. Ward. 2003. Chemical extraction methods to assess bioavailability arsenic in soil and solid media. *J. Environ. Qual.* 32:876-884.

- Rodriguez, R.R., N.T. Basta, S.W. Casteel, and L.W. Pace. 1999. An in vitro method to estimate bioavailable arsenic in contaminated soils and solid media. *Environ. Sci. Technol.* 33:642-649.
- Roy, W.R., J. J. Hassett, and R.A. Griffin. 1986. Competitive coefficient for the adsorption of arsenate, molybdate, and phosphate mixture by soils. *Soil Sci. Soc. Am. J.* 50:1176-1182.
- Roy W.R., J.J. Hassett, and R.A. Griffin. 1986. Competitive interactions of phosphate and molybdate on arsenate adsorption. *Soil Sci.* 142: 203-210.
- Saada A., D. Breeze, C. Crouzet, S. Cornu, and P. Baranger. 2003. Adsorption of arsenic (V) on kaolinite and on kaolinite-humic acid complexes - Role of humic acid nitrogen groups. *Chemosphere* 51: 757-763.
- Sadiq. M. 1997. Arsenic chemistry in soils: an overview of thermodynamic predictions and field observations. *Water Air Soil Pollut.* 93:117-136.
- Sadiq, M., T .H. Zaidi, and A. A. Mian. 1982. Environmental behavior of arsenic in soils: theoretical. *Water Air Soil Pollut.* 20:369-377.
- Sakata, M. 1987. Relationship between adsorption of arsenic(III) and boron by soil and soil properties. *Environ. Sci. Technol.* 21:1126-1130.
- Sakulpitakphon, T., J.C. Hower, A.S. Trimble, W.H. Schram, and G.A. Thomas. 2003. Arsenic and mercury partitioning in fly ash at a Kentucky power plant. *Energy and Fuels* 2003:1028-1033.
- Scott, M. J., and J. J. Morgan. 1995. Reaction of oxide surface. I. Oxidation of As(III) by synthetic birnessite. *Environ. Sci. Technol.* 29:1898-1905.
- Senn, D.B., and H.F., Hemond. 2002. Nitrate controls on iron and arsenic in an urban lake. *Science* 296, 2373-2376.
- Smedley, P.L., and D.G. Kinniburgh. 2002. A review of the source, behaviour and distribution of arsenic in natural waters. *Applied Geochem.* 17, 517-568.
- Smith, E., R. Naidu, and A.M. Alston. 1998. Arsenic in the soil environment: A review. *Advances in Agronomy.* 64:149-195.
- Smith, E., R. Naidu, and A.M. Alston. 1999. Chemistry of arsenic in soils: I. Adsorption of arsenate and arsenite by selected soils. *J. Environ. Qual.* 28:1719-1726.
- Smith, E., R. Naidu, and A.M. Alston. 2002. Chemistry of inorganic arsenic in soils: I. Effect of phosphorous, sodium, and calcium on arsenic sorption. *J. Environ. Qual.* 31:557-563.
- Smith, S.L., and P.R. Jaffe. 1998. Modeling the transport and reaction of trace metals in water-saturated soils and sediments. *Water Resour. Res.* 34, 3135-3147.
- Sparks, D.L. 1988. Kinetics of soil chemical processes. Academic Press. San Diego, California.

- Sracek, O., P. Bhattacharya, G. Jacks, J.P. Gustafsson, M. von Bromssen. 2004. Behavior of arsenic and geochemical modeling of arsenic enrichment in aqueous environments. *Applied Geochem.* 19:169-180.
- Su, C.M., and R.W. Puls. 2001. Arsenate and arsenite removal by zerovalent iron: Kinetics, redox transformation, and implications for in situ groundwater remediation. *Environ. Sci. Technol.* 35:1487-1492.
- Su, C.M., and R.W. Puls. 2003. In situ remediation of arsenic in simulated groundwater using zerovalent iron: Laboratory column tests on combined effects of phosphate and silicate. *Environ. Sci. Technol.* 37:2582-2587.
- Sun, X., and H.E. Doner. 1996. An investigation of arsenate and arsenite bonding structure on goethite by FTIR. *Soil Sci.* 161:865-872.
- Sun, X., and H.E. Doner. 1998. Adsorption and oxidation of arsenite on goethite. *Soil Sci.* 163:278-287.
- Takahashi, Y., R. Minamikawa, K. H. Hattori, K. Kurishima, N. Kihou, and K. Yuita. 2004. Arsenic behavior in paddy fields during the cycle of flooded and non-flooded periods. *Environ. Sci. Technol.* 38: 1038-1044.
- Tessier, A., P. G. C. Campbell, and M. Bisson. 1979. Sequential extraction procedure for the speciation of particulate heavy metals. *Anal. Chem.* 51:844-851.
- Thomas, J.E., and R.D. Rhue. 1997. Volatilization of arsenic in contaminated cattle dipping vat soil. *Bullte. Environ. Contamin. Toxicol.* 59: 882-887.
- USEPA. 1999. Use of Monitored natural attenuation at superfund, RCRA corrective action, and underground storage tank sites. Report No. 9200.4-17P. <http://www.epa.gov/swrust1/directiv/d9200417.pdf>.
- USEPA. 2001. National primary drinking water regulations; Arsenic and clarifications to compliance and new source contaminants monitoring; Final rule. *Federal Register*. Vol. 66. No. 14. 6975-7066. Jan 22. 2001. U.S. Gov. Print Office, Washington D.C.
- USEPA. 2002. Proven alternatives for aboveground treatment of arsenic in groundwater. Report No. EPA-542-S-02-002. http://www.epa.gov/tio/tsp/download/arsenic_issue_paper.pdf.
- USGS. 2004. The national geochemical survey-Database and documentation. U.S. Geological survey open-file report 2004-1001.
- Violante A., M. Ricciardella, S.D. Gaudio, and M. Pigna. 2006. Coprecipitation of Arsenate with Metal Oxides: Nature, Mineralogy, and Reactivity of Aluminum Precipitates. *Environ. Sci. Technol.*, 40:4961 -4967.
- Violante, A., and M. Pigna. 2002. Competitive sorption of arsenate and phosphate on different clay minerals and soils. *Soil Sci. Soc. Am. J.* 66:1788-1796.

- Voigt, D.E., S.L. Brantley, and R.J.C. Hennet. 1996. Chemical fixation of arsenic in contaminated soils. *Applied Geochem.* 11:633-637.
- Walker, F.P., M.E. Schreiber, and J.D. Rimstidt. 2006. Kinetics of arsenopyrite oxidative dissolution by oxygen. *Geochim. Cosmochim. Acta*, 70: 1668-1676.
- Waltham, C. A., and W.J. Eick. 2002. Kinetics of arsenic adsorption on goethite in the presence of sorbed silicic acid. *Soil Sci. Soc. Am. J.* 66:818-825.
- Wauchope, R.D. 1975. Fixation of arsenical herbicides, phosphate, and arsenate in alluvial soils. *J. Environ. Qual.* 4:355-358.
- Waychunas, G.A., B.A. Rea, C.C. Fuller, and J.A. Davis. 1993. Surface chemistry of ferrihydrite: Part 1. EXAFS studies of the geometry of coprecipitated and adsorbed arsenate. *Geochim. Cosmochim. Acta* 57:2251-2269.
- Waychunas, G.A., J.A. Davis, and C.C. Fuller. 1995. Geometry of sorbed arsenate on ferrihydrite and crystalline FeOOH: Re-evaluation of EXAFS results and topological factors in predicting sorbate geometry, and evidence for monodentate complexes. *Geochim. Cosmochim. Acta* 59:3655-3661.
- Wilkin, R.T., and R.G. Ford. 2002. Use of hydrochloric acid for determining solid-phase arsenic partitioning in sulfidic sediments. *Environ. Sci. Technol.* 36: 4921-4927.
- Williams, L.E., M.O. Barnett, T.A. Kramer, and J.G. Melville. 2003. Adsorption and transport of arsenic(V) in experimental subsurface systems. *J. Environ. Qual.* 32:841-850.
- Woolson, E.A., J.H. Axley, and P.C. Kearney. 1971. The chemistry and phytotoxicity of arsenic in soils: I. Contaminated field soils. *Soil Sci. Soc. Am. Proc.* 35:938-943.
- Woolson, E.A., J.H. Axley, and P.C. Kearney. 1973. The chemistry and phytotoxicity of arsenic in soils: effect of time and phosphorous. *Soil Sci. Soc. Am. Proc.* 37:254-259.
- World Health Organization (WHO). 2004. Arsenic in drinking water. WHO. Geneva.
- Xu, H., B. Allard, and A. Grimvall. 1988. Influence of pH and organic substance on the adsorption of As(V) on geologic materials. *Water Air Soil Pollut.* 40:293-305.
- Zhao, H., and R. Stanforth. 2001. Competitive adsorption of phosphate and arsenate on goethite. *Environ. Sci. Technol.* 35:4753-4757.

CHAPTER 3: KINETICS OF ARSENATE ADSORPTION-DESORPTION IN SOILS

3.1 Introduction

Knowledge of adsorption and desorption of arsenic is necessary for predicting the fate and behavior of As(V) in the soil environments. It is well established that Fe and Al oxides and hydroxides have high affinity to arsenic. Microscopic studies such as extended X-ray adsorption fine structure spectroscopy (EXAFS) (Waychunas et al., 1993) and Fourier transform infrared (FTIR) (Sun and Doner, 1996) have shown that both As(V) and As(III) form mono- or bi-dentate inner-sphere surface complex with iron oxides via a ligand exchange mechanism. Because of their negatively charged surfaces, clay minerals generally have low arsenic adsorption capacity (Manning and Goldberg, 1996). Surface complexation models have been employed to describe the adsorption of arsenic on minerals (Manning et al, 1998; Goldberg and Johnston, 2001). In addition to studies on minerals, several studies have demonstrated that arsenic adsorption on soils is correlated with Al and Fe oxides contents (Jacobs et al., 1970; Wauchope 1975 ; Livesey and Huang, 1981; Elkhatib et al., 1984; Buchter et al., 1989; Manning and Goldberg, 1997; Smith et al., 1999).

Equilibrium experiments carried out in relatively short reaction times (usually 24 h) have widely been used for quantifying the extent of arsenic adsorption in soils. However, the utility of results from short duration studies for predictions of arsenic fate and transport is often limited because equilibrium conditions are rarely achieved in 24 h under laboratory or field conditions due to a wide variety of biological, chemical, and hydrological factors. A literature search revealed that the influence of residence time on retention and release of arsenic in soils has not been adequately investigated.

It has been observed that the sorption rate of As(V) and As(III) on minerals was initially rapid and followed by a slow phase (Fuller et al., 1993; Raven et al., 1998; O'Reilly et al.,

2001; Arai and Sparks, 2002 ; Arai et al., 2004). Fuller et al. (1993) observed that As(V) adsorption on synthesized ferrihydrite had a rapid initial phase (<5min) and adsorption continued for 182 h. Spectroscopic investigation on their samples demonstrated that no surface precipitates were formed during As(V) adsorption on ferrihydrite under alkaline conditions (pH 8-9) and high surface coverage (up to 0.7 mole As pre mole Fe). They proposed that the rate-limiting As(V) adsorption step was controlled by slow diffusion to adsorption sites within aggregates of ferrihydrite crystalline. Raven et al. (1998) studied the temporal dependence of As(V) and As(III) adsorption on ferrihydrite for exposure times 5 min to 96 h. They found that most reactions occurred within the first 2 h and suggested that arsenic adsorption on ferrihydrite were diffusion controlled and well described by a parabolic diffusion equation. Recently, O'Reilly et al. (2001) studied As(V) adsorption on goethite over a period of 4 min up to 1 year. They found 93% (pH=6) and 97% (pH=4) of the As(V) was removed from solution in the initial 24 h, and the rest of the arsenic was slowly adsorbed in the following one year. Arai and Sparks (2002) found that at pH 4.5, it took 3 d to complete As(V) adsorption on aluminum oxide, while at pH 7.8, the reaction continued for over 1 year. And for As(V) adsorption to hematite, Arai et al. (2004) also observed an initially rapid phase and followed a slow approach to equilibrium over the span of 25 h.

Information on the sorption rate of arsenic on soils is limited and somewhat contradictory (Livesey and Huang, 1981; Elkhatib et al., 1984a; Smith et al., 1999; Carbonell-Barrachina et al., 1996). Livesey and Huang (1981) reported that most of As(V) adsorption to soils occurred during the initial 24 h of reaction with a small increase in the amount adsorbed after 24 h. In studies of As(III) adsorption kinetics (0.5-24 h) on surface and subsurface soils, Elkhatib et al. (1984a) concluded that the initial reaction was rapid with more than 50% of As(III) sorbed on

soils in the first 0.5 h. From regression results, they found that reaction rate can be related to soil clay content or Fe oxide content by a multi-linear equation. Smith et al. (1999) showed that As(V) retention by soils attained apparent equilibrium in less than 1 h, followed by a steady, but slow rate for 72 h. However, the effects of longer reaction time (>72 h) on As(V) adsorption were not investigated.

In contrast to adsorption studies, only a limited number of studies have investigated release or desorption of arsenic from minerals and soils (Fuller et al., 1993; Lin and Puls, 2000; O'Reilly et al., 2001; Arai and Sparks, 2002). Fuller et al. (21) suggested that As(V) desorption from ferrihydrite was limited by diffusional processes within soil aggregates. Their data indicated that only a small portion of As(V) desorbed from ferrihydrite after 144 h of reaction. Lin and Puls (2000) found that the desorption rate of As(III) and As(V) from clay minerals was significantly decreased with increasing aging time. They explained this phenomenon with the diffusion of arsenic into internal sorption sites, which may not readily accessible by the bulk solution. O'Reilly (2001) found that a significant amount of As(V) bound to goethite (>60%) was not readily dissociated through exposure to 6 mM phosphate solution after 5 months of exposure. Arai and Sparks (2002) found in their research that the rate of As(V) desorption from aluminum oxide surfaces decreased with increasing initial adsorption time (3 d to 1 year). Furthermore, their EXAFS studies provided microscopic evidence of rearrangement of surface complexes and surface precipitation. Relatively few studies have been conducted to investigate arsenic desorption from soils. For example, Jacobs et al. (1970) found that the extractability of sorbed As(V) by 1 M NH₄OAc and Bray P solution (0.03 M NH₄F and 0.025 M HCl) decreased with increasing sorption time, indicating increased binding strength with increasing reaction time. Elkhatib et al. (1984b) reported that following 24 h sorption, As(III) desorption from soils

was hysteric and only small amounts of the sorbed As(III) was slowly released from five soils. In contrast, Carbonell-Barrachina et al. (1996) reported that As(III) desorption was reversible from three soils having low sorption affinity to As(III). They suggested that different results could be explained through differences in sorption capacities of the soils used.

The objectives of our study were (i) to quantify the kinetics of adsorption and desorption of arsenate in three soils having different physiochemical properties; and (ii) to assess multireaction (equilibrium-kinetic) modeling for its capability of describing the retention as well as the desorption or release behavior of As(V) in different soils.

3.2 Materials and Methods

Surface soils from the Ap horizon (0-10 cm) of Olivier loam (fine-silty, mixed, thermic Aquic Fragiudalf), Sharkey clay (very fine, montmorillonitic, nonacid, thermic, Vertic Haplaquept), and Windsor sand (mixed, mesic Typic Dipsamment) were used in this study (see Table 3.1). The soils were air-dried and passed through a 2-mm sieve before use. They were analyzed for pH using 1:1 soil/water paste, for organic matter using the acid dichromate oxidation method, for free iron oxides by the dithionite-citrate-bicarbonate method, and for cation exchange capacity of the acid soils by exchange with 0.1 M BaCl₂-0.1 M NH₄Cl.

Kinetic batch experiments were conducted to determine adsorption and desorption isotherms for As(V) to the three soils at constant room temperature of 25°C under aerobic conditions. Six initial As(V) concentrations C_0 (5, 10, 20, 40, 80, and 100 mg L⁻¹) of KH₂AsO₄ were prepared in 0.01M KNO₃ background solution to maintain constant ionic strength. Batch experiments were initiated by mixing 3 g of air dry soil with 30 ml of As(V) solution in a 40-mL Teflon tube. For each input concentration C_0 , the tests were performed in triplicate and the average and coefficient of variation in the amount of As(V) adsorbed is reported. The mixtures

were shaken at 150 rpm on a reciprocal shaker and subsequently centrifuged for 10 minutes at 4000 rpm after each specified reaction time. A 1-mL aliquot was sampled from the supernatant at reaction times of 2, 6, 12, 24, 72, 168, 336, and 504 h. After sampling, the slurry was agitated using a vortex mixer and returned to the shaker. The collected samples were analyzed for total arsenic concentration using ICP-AES (Spectro Citros CCD). The amount of arsenate adsorbed by each soil was calculated from the difference between concentrations of the supernatant and that of the initial solutions. The extent of release or desorption of As(V) was also quantified using the batch method described above.

For each initial concentration (C_0), desorption commenced immediately after the last adsorption step (504 h). This was accomplished through sequential or successive dilutions of the slurries to induce As(V) release or desorption. Each desorption step was carried out by replacing the supernatant with 0.01 M KNO_3 background solution and shaking for 48 h. Six desorption steps were carried out with a total desorption time of 288 h. The fraction of arsenate desorbed from the soils were calculated based on the change in concentration in solution (before and after desorption). Moreover, during adsorption as well as desorption experiments, the pH of the supernatant was measured following each reaction time with standard pH meter.

Since arsenic sorbed in soils is bound with the solid phase at different strengths, several sequential chemical extraction methods have been widely proposed to apportion arsenic associated with different soils into various phases based on the types of extractant used. Generally sequential extraction methods can provide an insight into the understanding of the chemical binding of arsenic in soil (Keon et al., 2001; Han et al., 2004). A simplified sequential

Table 3.1 Selected physical and chemical properties of the studied soils.

Soil ^a		Olivier	Sharkey	Windsor
pH		5.80	5.77	6.11
TOC ^b	%	0.83	1.41	2.03

CEC ^c	cmol kg ⁻¹	8.6	29.6	2.0
Sand ^d	%	5	3	77
Silt	%	89	36	20
Clay	%	6	61	3

Selective extraction by

Ammonium oxalate (pH 3.0)

Fe	g kg ⁻¹	0.32	0.83	0.36
Al	g kg ⁻¹	0.08	0.23	0.69

Citrate-bicarbonate-dithionite (CBD)

Fe	g kg ⁻¹	4.09	7.77	3.68
Al	g kg ⁻¹	1.29	2.42	3.65

^a Soil samples were collected from Louisiana (Sharkey and Olivier) and New Hampshire (Windsor).

^b TOC = total organic carbon; CEC = cation exchange capacity.

^d Grain size distribution: sand (2.00-0.05 mm), silt (0.05-0.002 mm), and clay (<0.002 mm).

extraction procedure was carried out here to investigate the amount of arsenic retained at various binding phases following the last desorption step. Three fractions were quantified, referred to here as phosphate extracted ($1M$ NaH_2PO_4), oxalate extracted ($0.2M$ ammonium oxalate, reacted in the dark), and residual ($4N$ HNO_3). The first two phases were measured by mixing the soil with 20 mL of the extractant solution, shaking for 16 h, and centrifuging, whereas the residual arsenic was determined by mixing with $4 N$ HNO_3 solutions and shaking for 2h in a water-bath maintained at $80^\circ C$.

3.3 Multireaction Model

Recent approaches based on soil heterogeneity and kinetics of adsorption-desorption have been proposed for the purpose of describing the time-dependent sorption of heavy metals in the soil environment. The multireaction (MRM) kinetic approach presented here considers several interactions of heavy metals with soil matrix surfaces (Amacher et al., 1988; Selim, 1992; Selim and Ma, 2001; Darland and Inskeep, 1997; William et al., 2003). Specifically, the model assumes that a fraction of the total sorption sites is kinetic in nature whereas the remaining fractions interact rapidly or instantaneously with solute in the soil solution. The model accounts for reversible as well as irreversible sorption of the concurrent and consecutive type (Figure 3.1).

$$S_e = K_e C^n \quad [3.1]$$

$$\frac{\partial S_k}{\partial t} = k_1 \frac{\theta}{\rho} C^m - (k_2 + k_3) S_k \quad [3.2]$$

$$\frac{\partial S_i}{\partial t} = k_3 S_i \quad [3.3]$$

$$\frac{\partial S_s}{\partial t} = k_s \frac{\theta}{\rho} C \quad [3.4]$$

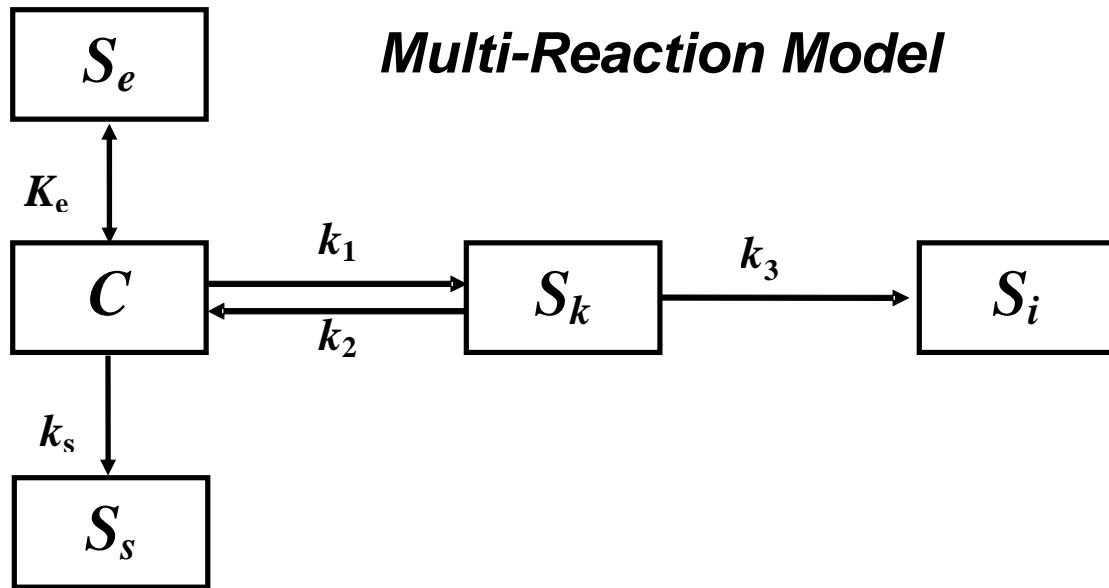


Figure 3.1 A schematic diagram of the multireaction transport model (MRM). Here C is concentration in solution, S_e , S_k , S_i and S_s are the amounts sorbed on equilibrium, kinetic, consecutive and cucurrent irreversible sites, respectively, where K_e , k_1 , k_2 , k_3 and k_s are the respective rates of reactions.

where S_e is the amount retained on equilibrium sites (mg l kg^{-1}), S_k is the amount retained on kinetic type sites (mg kg^{-1}), S_i is the amount retained irreversibly by consecutive reaction (mg kg^{-1}), S_s is the amount retained irreversibly by concurrent type of reaction (mg kg^{-1}), n and m are dimensionless reaction order commonly less than 1, K_e is a dimensionless equilibrium constant, k_1 and k_2 (h^{-1}) are the forward and backward reaction rates associated with kinetic sites, respectively, k_3 (h^{-1}) is the irreversible rate coefficient associated with the kinetic sites, and k_s (h^{-1}) is the irreversible rate coefficient associated with solution. For the case $n = m = 1$, the reaction equations become linear. In the above equations we assumed $n = m$ since there is no known method for estimating n and/or m independently. The total amount of solute retention on soil is:

$$S = S_e + S_k + S_i + S_s \quad [3.5]$$

3.4 Results and Discussion

3.4.1 Nonlinear Sorption Isotherms

Adsorption isotherms describing the distribution between aqueous and sorbed phases for As(V) for all soils at different reaction times are presented in Figure 3.2. Either an equilibrium model of the Freundlich- or Langmuir-type is commonly utilized to describe such adsorption isotherms. The Freundlich equation is an empirical adsorption model that can be expressed as

$$S = K_F C^N \quad [3.6]$$

where S represents the (total) amount of adsorption (mg kg^{-1}), K_F is the distribution or partition coefficient ($\text{mg kg}^{-1} (\text{mg L}^{-1})^{-N}$), and N is the dimensionless reaction order commonly less than one. The Langmuir equation is another widely used equilibrium sorption model. It has the advantage of providing a sorption maximum S_{\max} (mg kg^{-1}) that can be correlated to soil sorption properties. The Langmuir equation has the form:

$$S = S_{\max} \frac{K_L C}{1 + K_L C} \quad [3.7]$$

where K_L (L mg^{-1}) is a Langmuir coefficient related to the binding strength. We utilized nonlinear least square optimization to obtain best-fit parameters which provide best description of the adsorption data. We found that both Freundlich and Langmuir equations gave highly significant ($P < 0.01$) fits to the As(V) adsorption isotherms shown in Figure 3.2 for all three soils. Best-fit parameter values and goodness of fit values are given in Table 3.2 for selected reaction times. The Freundlich model had significantly better agreement to experimental data as indicated by the lower values of mean square errors (MSE) when compared to the Langmuir model for all three soils ($P < 0.01$, paired t-test).

The As(V) isotherms of Figure 3.2 clearly exhibit nonlinear behavior. The nonlinear or concentration-dependent adsorption behavior was characterized by the low values of the Freundlich parameter N , i.e., N much less than 1 (see Table 3.2). After 24 h, which is commonly used in equilibrium batch studies, the N values were 0.270, 0.340, and 0.284 for the Olivier loam, Sharkey clay, and Windsor sand, respectively. Low N values for As(V) adsorption have been reported by others (Buchter et al., 1989; Manning and Goldberg, 1997; Darland and Inskeep, 1997; William et al., 2003). We should emphasize that N is a measure of the extent of heterogeneity of the sorption sites having different affinities for solute retention by matrix surfaces. In addition, N illustrates the dependence of the sorption process on concentration where sorption by the highest energy sites takes place preferentially at the lowest solution concentration. In our study, the N values for all three soils did not vary significantly after 24 h of reaction. This finding is also consistent with those reported earlier by Selim and Ma (2001) for Cu where N was not time-dependent. Therefore, low N values may be indicatives of extensive heterogeneity of sorption sites in these soils. In contrast, the K_F values increased with increasing

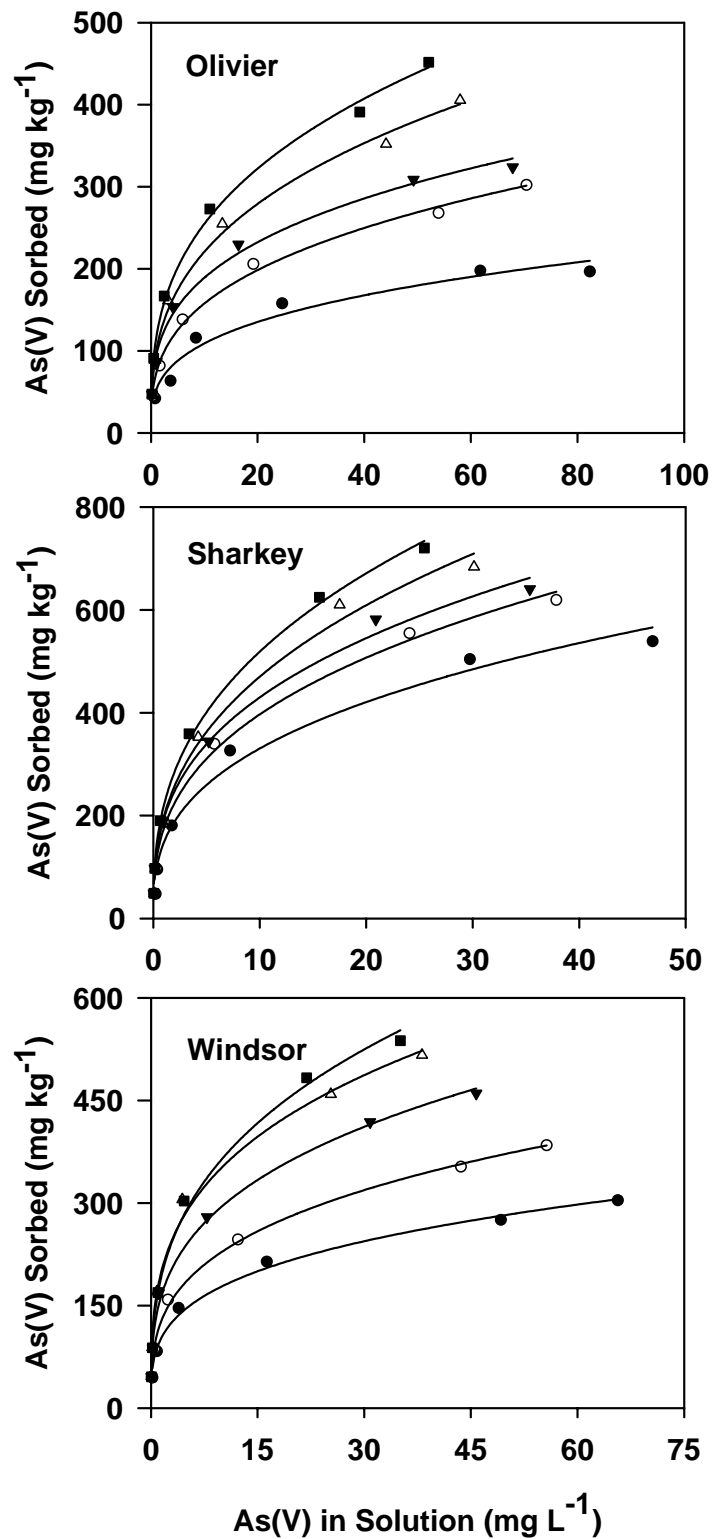


Figure 3.2 Isotherms of arsenate adsorption on different soils. Symbols are for different reaction times of 24, 72, 168, 336, and 504 h (from bottom to top). Solid curves depict results of curve-fitting with Freundlich equation.

Table 3.2 Estimated Freundlich- and Langmuir- equation parameters (with standard error) for arsenate adsorption at different reaction times

Soil	Time h	K_F $\text{mg kg}^{-1} (\text{mg L}^{-1})^{-N}$	N	R^2	S_{max} mg kg^{-1}	K_L L mg^{-1}	r^2
Olivier	6	36.2±6.0	0.206±0.045	0.960	92.2±5.0	0.231±0.058	0.978
	12	43.6±9.6	0.087±0.064	0.892	64.6±6.5	0.830±0.596	0.906
	24	55.3±8.6	0.270±0.042	0.965	183.0±11.6	0.180±0.049	0.972
	72	73.5±4.5	0.309±0.017	0.995	273.6±10.9	0.188±0.033	0.988
	168	95.2±6.8	0.277±0.020	0.991	298.3±12.6	0.274±0.055	0.985
	336	100±6	0.324±0.017	0.994	371.5±16.3	0.229±0.045	0.986
	504	116±6	0.325±0.015	0.995	418.2±20.3	0.245±0.054	0.983
Sharkey	6	58.1±22.3	0.332±0.103	0.856	263.0±45.9	0.106±0.066	0.860
	12	110±5	0.363±0.013	0.997	485.3±16.1	0.167±0.022	0.993
	24	147±9	0.340±0.018	0.993	545.1±16.6	0.257±0.033	0.993
	72	174±7	0.347±0.012	0.997	616.0±26.4	0.303±0.057	0.987
	168	194±7	0.335±0.012	0.997	655.7±32.8	0.288±0.062	0.985
	336	196±7	0.368±0.013	0.997	713.1±28.7	0.292±0.047	0.990
	504	217±5	0.366±0.009	0.999	742.0±31.8	0.345±0.060	0.989
Windsor	6	77.0±11.3	0.189±0.041	0.948	169.2±10.2	0.552±0.183	0.964
	12	85.2±11.0	0.221±0.035	0.963	209.0±12.3	0.492±0.158	0.966
	24	93.1±6.6	0.284±0.020	0.991	294.0±13.7	0.297±0.068	0.982
	72	115±7	0.290±0.018	0.993	358.5±18.0	0.338±0.084	0.978
	192	149±8	0.297±0.015	0.994	441.2±20.8	0.482±0.117	0.979
	336	181±8	0.291±0.014	0.995	510.5±20.9	0.488±0.096	0.985
	504	172±8	0.328±0.015	0.995	554.9±23.2	0.354±0.064	0.987

reaction time, resulting from the increased amount of adsorption (Table 3.2). Langmuir sorption maxima S_{\max} increased significantly with reaction time for all three soils as clearly demonstrated in Table 2. The Langmuir coefficient K_L for Sharkey clay exhibited a continued increase during adsorption, which is indicative of increased binding strength of As(V) in this soil. In contrast, there was no clear trend for K_L versus time for Olivier loam or Windsor sand, possibly due to the low As(V) affinity for both soils (Table 3.2).

Earlier research emphasized the importance of Fe or Al oxides as one of the main factors determining the soils' sorption capacity for arsenic (Jacobs et al., 1970; Wauchope 1975; Livesey and Huang, 1981; Elkhatib et al., 1984a; Buchter et al., 1989; Manning and Goldberg, 1997; Smith et al., 1999). Our results indicate that adsorption parameters, i.e., 504 h Langmuir S_{\max} , K_L , and 24 h Freundlich N exhibited a linear relationship with the total amount of citrate-bicarbonate-dithionite (CBD) extracted Fe and Al oxides (Figure 3.3). Moreover, soil clay contents were not found to be correlated with As(V) adsorption parameters. This relationship between arsenic adsorption and contents of Fe or Al oxides has also been reported by other researchers. For example, Jacobs et al. (1970) found that As(V) adsorption increased with the increasing content of Fe oxide. Livesey & Huang (1981) reported that the Langmuir maxima (S_{\max}) for arsenate adsorptions on five soils are linearly related to the amount of ammonium oxalate extractable Al and, to a lesser extent, to the content of ammonium oxalate extractable Fe. Similarly, Manning and Goldberg (1997) observed that the Langmuir maxima (S_{\max}) of As(V) and As(III) adsorption increased with increasing contents of CBD extractable Fe in soils. Furthermore, Buchter et al. (1989) found that both Freundlich N and K_F for As(V) adsorption in soils were significantly correlated ($P<0.01$) with amorphous Fe_2O_3 and free Al_2O_3 .

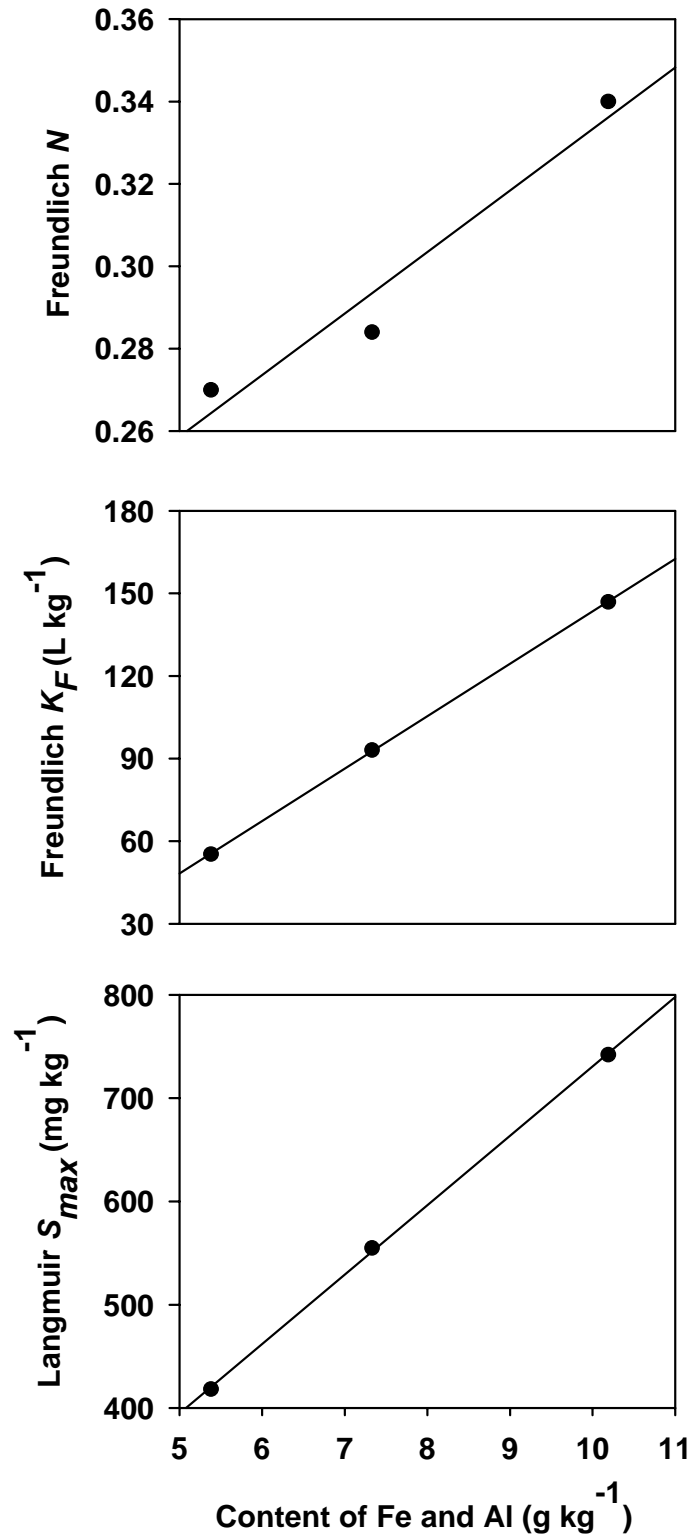


Figure 3.3 Freundlich parameter N (top), coefficient K_F (middle), and Langmuir adsorption maxima S_{max} (bottom) as a function of total amount of citrate-bicarbonate-dithionite (CBD) extractable Fe and Al content.

3.4.2 Adsorption Kinetics

Results from our kinetic batch experiments are presented in Figure 3.4 in order to illustrate the changes in As(V) concentration versus time for the various input concentrations by the different soils. For all three soils, the rate of As(V) retention was rapid during the initial stages of reaction and was then followed by gradual or somewhat slow reactions that are best characterized by continued As(V) retention which are clearly depicted by steady decrease of As(V) concentrations with reaction time. In addition, the kinetic results presented in Figure 3.4 concur with the nonlinear forms of the isotherms of Figure 3.2 which also illustrate the time dependence of As(V) sorption. These findings are in agreement with the biphasic arsenic adsorption behavior observed on several soil minerals (Fuller et al., 1993; Raven et al., 1998; O'Reilly et al., 2001; Arai and Sparks, 2002 ; Arai et al., 2004) as well as whole soils (Elkhatib et al., 1984a; Carbonell-Barrachina et al., 1996) over different time scales (minutes to months).

Several mechanisms may contribute to the kinetics of As(V) retention in the soils shown in Figure 3.4. For example, Fuller et al. (1993) and Waychunas et al. (1993) showed that time-dependent reaction between As(V) and ferrihydrite was controlled by diffusion rather than surface precipitation. Raven et al. (1998) suggested that kinetics of As(V) adsorption on ferrihydrite were diffusion-controlled and best described by a parabolic diffusion equation. However, Arai and Sparks (2002) showed spectroscopic evidence of slow surface precipitation of As(V) on aluminum oxide surface using EXAFS analysis. Nevertheless, in heterogeneous soil systems, non-equilibrium conditions of As(V) adsorption may be due to (1) heterogeneity of sorption sites, (2) slow precipitation at mineral surface, i.e., three dimensional growth of a particular arsenic solid phase, and (3) slow diffusion to sites within the soil matrix, i.e., slowly accessible sites with variable degrees of affinities to As(V) .

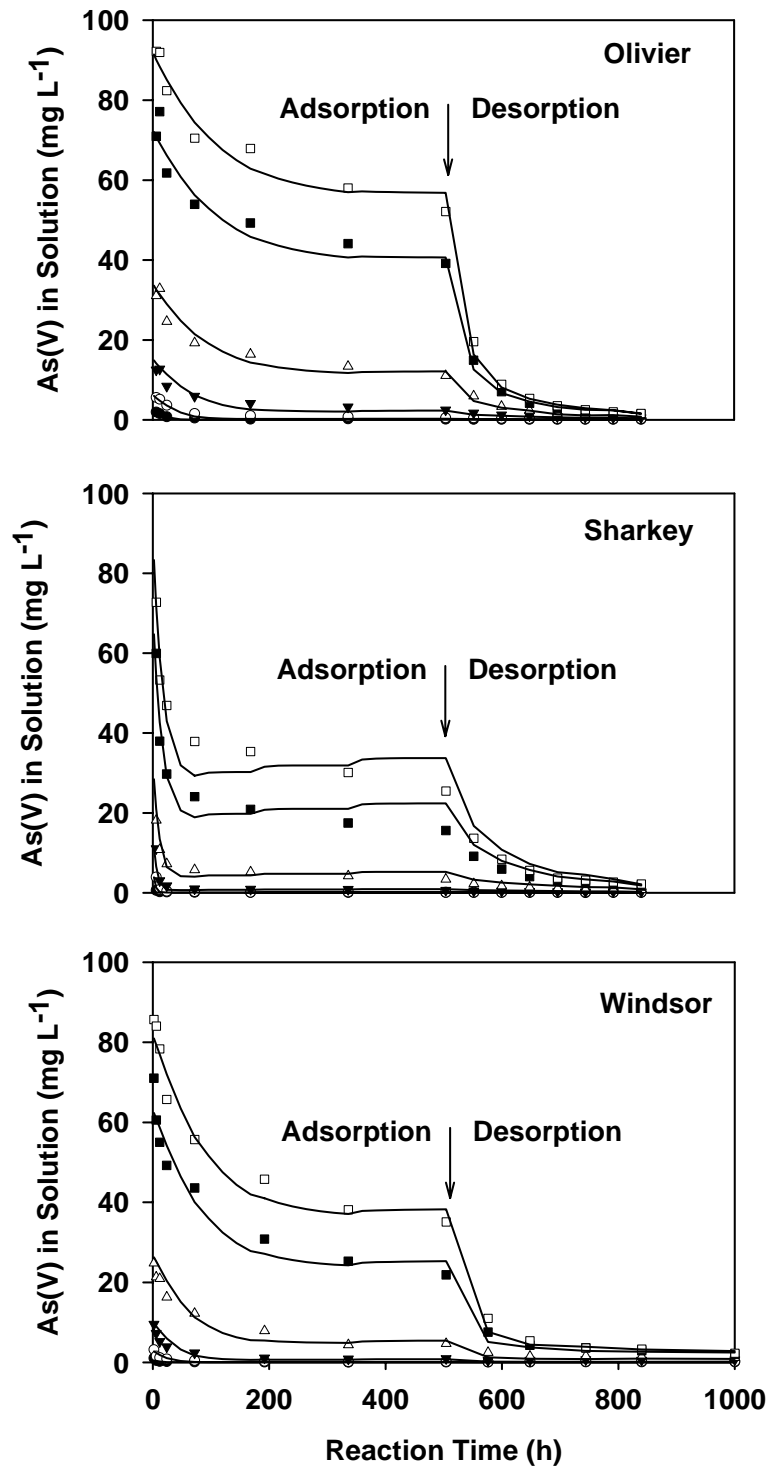


Figure 3.4 Arsenate concentration in solution versus time during adsorption-desorption for different soils. Symbols are for different initial concentrations (C_0) of 5, 10, 20, 40, 80, and 100 mg L^{-1} (from bottom to top). Solid curves are two-phase MRM simulations using parameters obtained from nonlinear optimization with adsorption data.

3.4.3 Desorption Hysteresis and Binding Phases

Desorption or release results which followed adsorption, are presented as isotherms in the traditional manner in Figure 3.5. Distinct discrepancies between adsorption and successive desorption isotherms clearly indicate considerable hysteresis for As(V) release, the extent of which varied among the three soils. This observed hysteresis was not surprising in view of the kinetic retention behavior of As(V) and is also indicative of non-equilibrium behavior of retention mechanisms (31). Since significant irreversibility of arsenic sorbed on mineral surfaces (Fuller et al., 1993; Lin and Puls, 2000; O'Reilly et al., 2001; Arai and Sparks, 2002) and soils (Jacobs et al., 1970; Elkhatib et al., 1984b; Carbonell-Barrachina et al., 1996) has been extensively reported, this observed desorption hysteresis might be due to kinetic retention behavior, such as slow diffusion (Fuller et al., 1993) and irreversible retention (Arai and Sparks, 2002).

The family of desorption curves shown in Figure 3.5 provide the necessary results on the rates of As(V) release and its affinity for the different input concentrations. Release curves demonstrate that at low input As(V) concentrations, i.e., low As(V) surface coverage, only small proportions were desorbed, indicating high sorption affinity between As(V) and the soil matrix. In contrast, at high As(V) input concentrations, as the amounts adsorbed increased, the percentage of desorption for all soils increased, indicating lower As(V) affinities. This corroborated the highly nonlinear adsorption behavior of As(V) in all three soils based on the low values of the Freundlich N indicating relatively high affinity and binding strength at lower As(V) concentrations (Table 3.2). Overall, the total amount of As(V) released, as a percentage of that sorbed, were 12-41%, 4-29%, and 7-35% for Olivier loam, Sharkey clay, and Windsor sand, respectively.

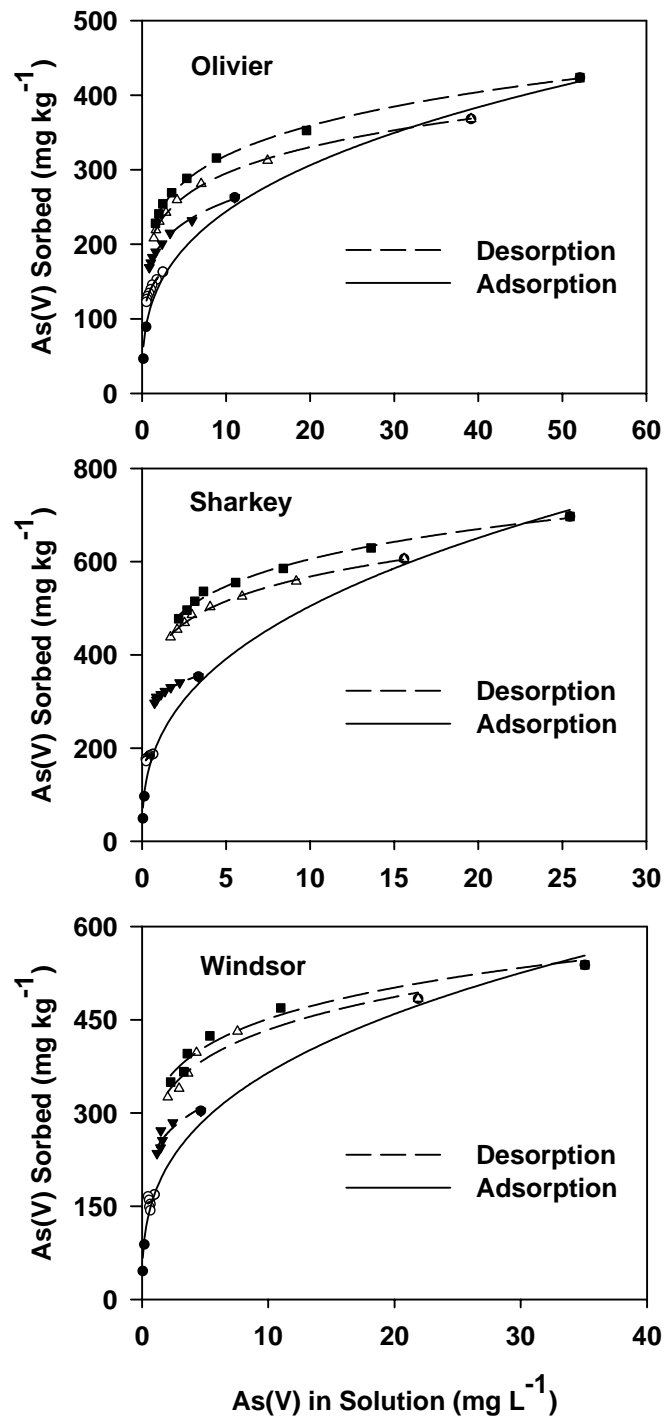


Figure 3.5 Isotherms of arsenate desorption from different soils based on successive dilution after the last adsorption step for different initial concentrations (C_0) of 20, 40, 80, and 100 mg L⁻¹. The solid and dashed curves depict results of curve-fitting with Freundlich equation for 504 h adsorption, and desorption isotherms, respectively.

Three sequential extraction steps were performed on the soil samples from kinetic batch experiment immediately after the last step of desorption as described in the methods section. Amounts of arsenic extracted as percentages of total arsenic sorbed are displayed in Figure 3.6. Our results showed that approximately 32-54%, 28-35%, and 34-50% of the total amounts of arsenic sorbed were replaced by phosphate for Olivier loam, Sharkey clay, and Windsor sand, respectively. Even though arsenic adsorption is not reversible, a large amount of sorbed arsenic can be released by phosphate, since phosphate have similar chemical properties as arsenate and can compete with arsenate for adsorption sites (Jacobs et al., 1970; Livesey and Huang, 1981).

Oxalate extracted arsenic constituted 7-19%, 16-37%, 7-14% of the total amount of arsenic sorbed by Olivier loam, Sharkey clay, and Windsor sand, respectively (Figure 3.6). Ammonium oxalate extractant was used to break up the strong linkage between Fe/Al oxide and As(V). This fraction of arsenic is strongly bound to Fe/Al oxides as surface complexation or precipitation and unlikely to be mobilized unless under extremely reduced conditions (Keon et al., 2001). Beside phosphate-extractable and oxalate extracted phase, other recalcitrant components of arsenic made up 8.7-9.8%, 16-31%, 3.6-9.0% of the total amount of arsenic sorbed by Olivier loam, Sharkey clay, and Windsor sand, respectively, as determined by digestion with strong acid at high temperature.

3.4.4 Multireaction Modeling

We recognize that MRM is an equilibrium-kinetic model which accounts for multiple reactions of the consecutive and concurrent type. As a result, we focused our analysis on a simple MRM model variation which accounts for nonlinear equilibrium and kinetics. Specifically, kinetic data from our batch study was described with MRM models where the parameters K_e , k_1 , k_2 , and n , that provided best-fit were obtained based on Levenberg-

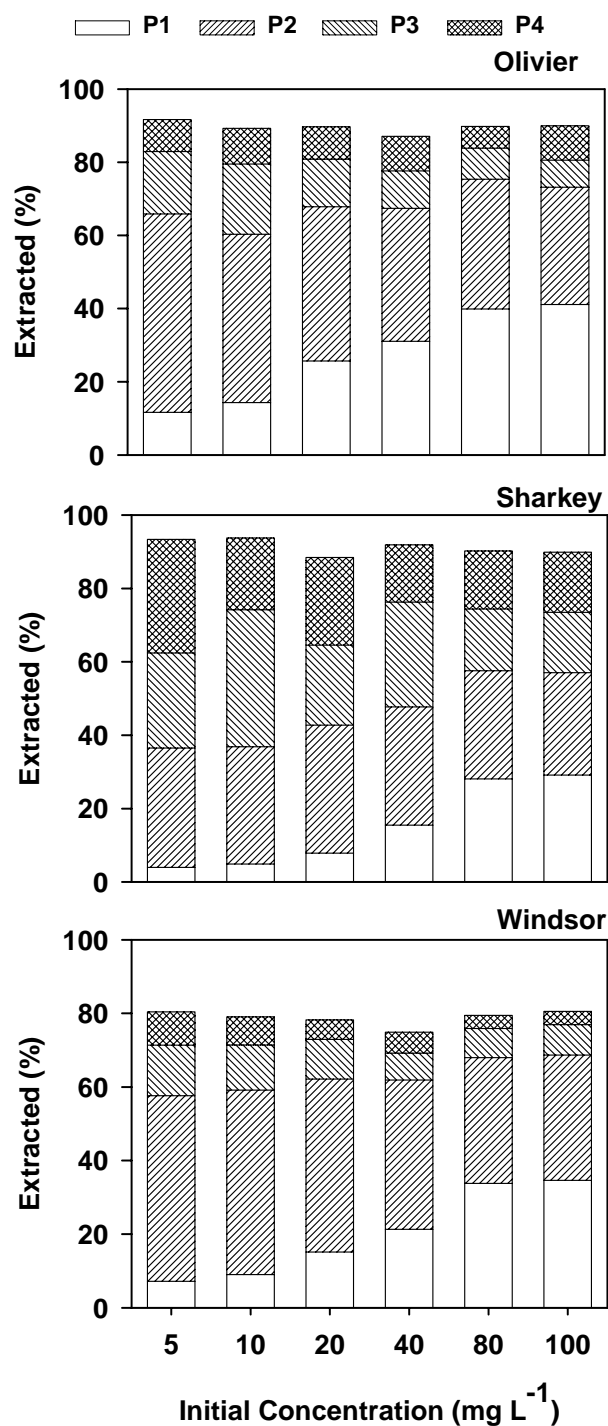


Figure 3.6 Recoveries of arsenic from desorption and sequential extractions as percentages of total adsorption amounts for different soils. Different patterns illustrate arsenic distribution among the following pools: P1 = desorbed during successive desorption, P2 = extracted with 1M NaH₂PO₄, P3 = extracted with 0.2 M ammonium oxalate, and P4 = digested with 4 M HNO₃. Different groups indicate initial concentrations (C₀) of 5, 10, 20, 40, 80, and 100 mg L⁻¹.

Marquardt nonlinear least square optimization method. We refer to this model here as a fully reversible two-phase model. Statistical criteria used for estimating the goodness-of-fit of the models to the data were the coefficients of determination r^2 and the root mean square error (RMSE).

$$RMSE = \sqrt{\frac{\sum (C_{obs} - C_{mod})^2}{n_{obs} - n_{par}}} \quad [3.8]$$

where C_{obs} = observed As(V) concentration at certain time t , C_{mod} = simulated As(V) concentration at time t , n_{obs} = number of measurements, and n_{par} = number of fitted parameters.

From the goodness-of-fit results of Table 3.3, the fully reversible two-phase model described successfully the time-dependent behavior of arsenate adsorption for all soils ($P < 0.01$). Nonlinear reaction orders n determined with kinetic MRM models were close to the Freundlich N for all soils. Such a finding was not surprising since N did not change with reaction time (Table 3.2). Since most sorption experiments commonly reported in the literature are limited to 24 h, it was decided to test whether the use of 24-h Freundlich N in place of n in the MRM model can result in a satisfactory predictions of As(V) kinetic batch data where fewer model parameters are optimized. We found that the resulting simulations were not different when 24-h Freundlich N were used for all three soils compared to optimized n , as can be attested by the similarity of the best-fit values of model parameters are compared (Table 3.3). Therefore, the use of 24-h Freundlich N in MRM kinetic sorption studies for As(V) is recommended.

Based on the model simulations shown in Figures 3.4 and 3.7, one can state that a simple fully reversible model was capable of describing the time-dependent behavior of As(V) sorption for Olivier loam and Windsor sand. It should also be emphasized that the MRM model was applicable for the entire range of input (applied) As(V) concentrations in our experiment (5 to

100 mg L⁻¹). The only set of model parameters needed were K_e , k_1 , k_2 , and n along with the experimental constraints such as initial concentrations, sampling times, decanted volumes, etc. We further tested the model's capability to predict desorption results based on model parameters based on adsorption data of Table 3.3. Specifically, model calculations shown in Figs. 3 and 7 represent adsorption based on optimized parameters as discussed earlier whereas the desorption calculations were based on predictions only. In other words, we utilized adsorption parameters (ADS) to predict desorption or release data as is commonly carried out in the literature. This was compared with the case when the entire adsorption-desorption data set (ADS-DES) for each soil was described using MRM where best-fit model parameters were optimized. There was no significant difference between the kinetic parameters calculated from ADS and ADS-DES data sets (Table 3.3), indicating that the adsorption and desorption processes can be described based on parameters from either data set. Since adsorption rather than desorption data sets are commonly available, it is significant to point out simulations on release or desorption can be obtained where one can rely on parameters based on adsorption data alone.

MRM simulations shown in Figures 3.4 and 3.7 illustrate that an excellent fit of the experimental data was achieved for Olivier loam and Windsor sand. However, the fully reversible two-phase model was not capable of describing the batch results for the Sharkey soil especially at high concentrations (Figure 3.4). In fact, for Sharkey soil, model simulations produced a plateau of As(V) concentration in solution after 200 h, whereas experimental measurements indicated a continued removal of As(V) from solution during the entire adsorption process (see Figure 3.4). Because of this observed high affinity of As(V) for Sharkey clay, surface precipitation may be an important process especially at long retention times. This was recently postulated by other studies such as Arai and Sparks (2002).

Table 3.3 Fitted two-phase fully reversible MRM parameters (with standard error) for adsorption and desorption kinetics of As(V) in soils

Soil	Data set ^a	r^2	$RMSE$	n	K_e	k_1 h^{-1}	k_2 h^{-1}
Olivier	ADS	0.996	2.59	0.276±0.040	2.17±0.49	0.102±0.021	0.0073±0.0010
	ADS-DES	0.996	1.84	0.286±0.025	2.02±0.31	0.103±0.015	0.0078±0.0008
	ADS	0.996	2.56	0.270	2.21±0.37	0.104±0.013	0.0073±0.0010
	ADS-DES	0.996	1.83	0.270	2.14±0.27	0.110±0.010	0.0079±0.0007
Sharkey	ADS	0.982	3.28	0.370±0.055	1.75±1.04	0.709±0.185	0.0347±0.0045
	ADS-DES	0.981	2.37	0.308±0.020	2.64±0.86	0.861±0.032	0.0348±0.0019
	ADS	0.982	3.25	0.340	2.06±0.99	0.790±0.113	0.0353±0.0041
	ADS-DES	0.980	2.37	0.340	2.31±0.46	0.757±0.056	0.0337±0.0023
Windsor	ADS	0.994	2.68	0.242±0.033	5.92±0.86	0.200±0.032	0.0082±0.0009
	ADS-DES	0.993	2.26	0.275±0.026	5.17±0.61	0.181±0.025	0.0085±0.0008
	ADS	0.994	2.69	0.284	5.01±0.35	0.170±0.016	0.0080±0.0009
	ADS-DES	0.993	2.24	0.284	4.98±0.30	0.174±0.015	0.0084±0.0008

^a ADS: only adsorption data was used for parameter optimization; ADS-DES: both adsorption and desorption data was used for parameter optimization.

Table 3.4 Fitted three-phase reversible-irreversible MRM parameters (with standard error) for adsorption and desorption kinetics of As(V) in soils

Soil	Data set ^a	r^2	$RMSE$	K_e	k_1 h^{-1}	k_2 h^{-1}	k_3 h^{-1}
Olivier	ADS	0.998	1.87	0.736±0.496	0.249±0.050	0.0270±0.0059	0.0018±0.0003
	ADS-DES	0.997	1.60	0.908±0.250	0.224±0.022	0.0219±0.0025	0.0012±0.0002
Sharkey	ADS	0.995	1.77	0.361±0.023	1.151±0.035	0.0627±0.0022	0.0011±0.0001
	ADS-DES	0.994	1.35	0.664±0.029	1.083±0.027	0.0579±0.0016	0.0009±0.0001
Windsor	ADS	0.997	1.97	3.426±0.373	0.401±0.051	0.0317±0.0047	0.0020±0.0003
	ADS-DES	0.995	1.92	3.653±0.347	0.357±0.039	0.0266±0.0031	0.0016±0.0002

^a ADS: only adsorption data was used for parameter optimization; ADS-DES: both adsorption and desorption data was used for parameter optimization.

To account for surface precipitation reactions, the irreversible sorption sites were included in order to model our Sharkey clay data set. This resulted in a three-phase reversible-irreversible model with the following parameters, K_e , k_1 , k_2 , k_3 and n , which was subsequently used in nonlinear least square optimization (Table 3.4). This three-phase model, i.e., equilibrium, kinetic, and irreversible sorption phases, provided a significantly improved description of the time dependent As(V) adsorption by Sharkey clay compared to that of the two-phase model. RMSE was reduced from 3.25 based on the two-phase model to 1.77 based on the three-phase model (see Tables 3.3 and 3.4). Based on model simulation, at long residence time, surface precipitation is very likely an important process of As(V) retention on soils with high content of Fe and Al oxides (Figure 3.8). This was corroborated from the evidence that large amount of the arsenic was sorbed at oxalate extracted and residual phase as illustrated by the sequential extraction (Figure 3.6).

3.5 Summary and Conclusions

Adsorption-desorption of arsenic is the primary factor that impacts the bioavailability and mobility of arsenic in soils. To examine the characteristics of arsenate [As(V)] adsorption-desorption, kinetic batch experiments were carried out on three soils having different properties, followed by arsenic release using successive dilutions. Adsorption of As(V) were highly nonlinear with a Freundlich reaction order N much less than 1 for Olivier loam, Sharkey clay, and Windsor sand. Adsorption of arsenate by all soils was strongly kinetic, where the rate of As(V) retention was rapid initially and was followed by gradual or somewhat slow retention behaviour with increasing reaction time. Freundlich distribution coefficients and Langmuir adsorption maxima exhibited continued increase with reaction time for all soils. Desorption of As(V) was hysteretic in nature which is an indication of lack of equilibrium retention and/or

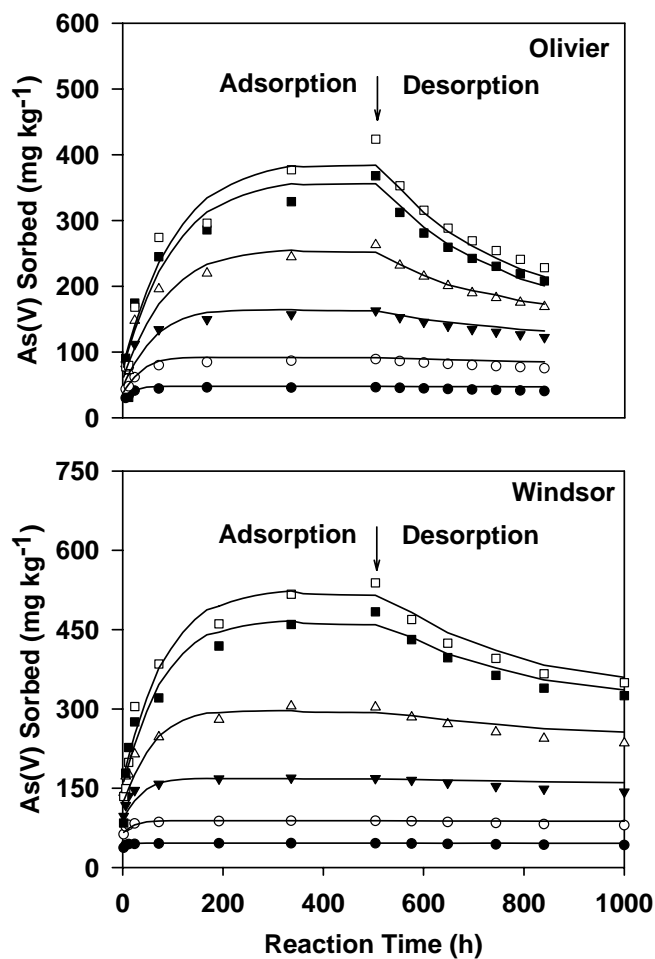


Figure 3.7 Arsenate sorbed versus time during adsorption-desorption for Olivier and Windsor soils. Symbols are for initial concentrations (C_0) of 5, 10, 20, 40, 80, and 100 mg L⁻¹ (from bottom to top). Solid curves are two-phase MRM simulations using parameters obtained from nonlinear optimization with adsorption data.

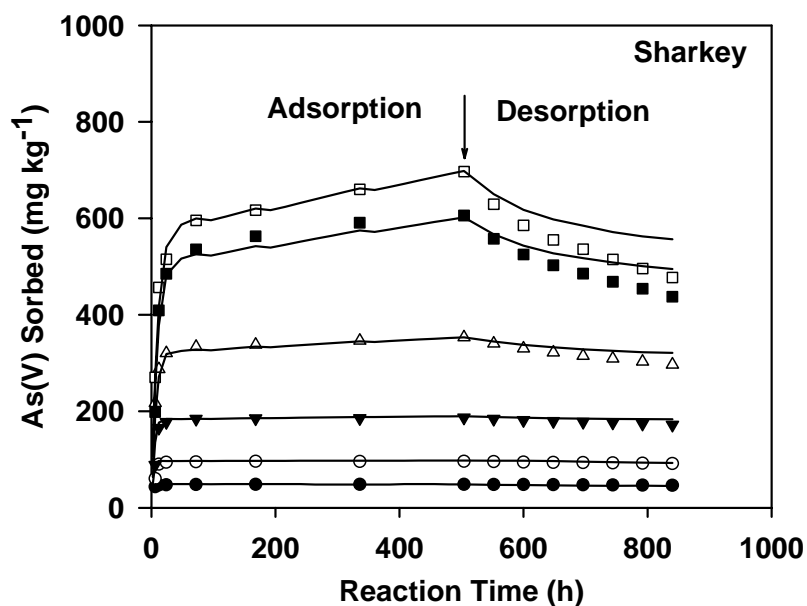


Figure 3.8 Arsenate sorbed versus time during adsorption-desorption for Sharkey soil. Symbols are for different initial concentrations (C_0) of 5, 10, 20, 40, 80, and 100 mg L⁻¹ (from bottom to top). Solid curves are three-phase MRM simulations using parameters obtained from nonlinear optimization with adsorption data.

irreversible or slowly reversible processes. A sequential extraction procedure provided evidence that a significant amount of As(V) was irreversibly adsorbed on all soils. A multireaction model (MRM) with nonlinear equilibrium and kinetic sorption successfully described the adsorption kinetics of As(V) for Olivier loam and Windsor sand. The model was also capable of predicting As(V) desorption kinetics for both soils. However, for Sharkey clay, which exhibited strongest affinity for arsenic, an additional irreversible reaction phase was required to predict As(V) desorption or release with time.

A major implication of this study is that contamination of soils with high concentrations of arsenic could result in slow release for extended period of time, i.e., weeks or months. The rate of such arsenic release parameters were successfully related with soil Fe/Al oxides. A secondary implication is that describing retention (adsorption) and subsequent release or leaching (desorption) by use of a multiple reaction model of the equilibrium-kinetic-irreversible nonlinear MRM type provided good overall predictions of the fate of arsenic in the soils examined in this study. We recognize that this model has several limitations since it does not consider such variables as pH, counter-ion, or ionic strength. Nevertheless, we are not aware of other models which provide predictive capability for arsenic during adsorption and subsequent desorption and for a wide range of input (initial) concentrations (three orders of magnitude) similar to the model presented here. Application of such multireaction models is, therefore, recommended in describing the retention by soils and the spreading in the vicinity of heavy metal spills where high concentrations may be encountered.

3.6 References

Amacher, M.C.; Selim, H.M.; Iskandar, I.K. 1988. Kinetics of chromium(VI) and cadmium retention in soils - a nonlinear multireaction model. *Soil Sci. Soc. Am. J.* 52, 398-408.

- Arai, Y.; Sparks, D.L. 2002. Residence time effects on arsenate surface speciation at the aluminum oxide-water interface. *Soil Sci.* 167, 303-314.
- Arai, Y.; Sparks, D.L.; Davis, J.A. 2004. Effects of dissolved carbonate on arsenate adsorption and surface speciation at the hematite-Water interface. *Environ. Sci. Technol.* 38, 817-824.
- Buchter, B.; Davidoff, B.; Amacher, C.; Hinz, C.; Iskandar, I.K.; Selim, H.M. 1989. Correlation of Freundlich K_d and n retention parameters with soils and elements. *Soil Sci.* 148, 370-379.
- Carbonell-Barrachina, A.; Carbonell, F. B.; Beneyto, J. M. 1996. Kinetics of arsenite sorption and desorption in Spanish soils. *Commun. Soil Sci. Plant. Anal.* 27, 3101-3117.
- Darland, J.E.; Inskeep, W.P. 1997. Effects of pore water velocity on the transport of arsenate. *Environ. Sci. Technol.* 31, 704-709.
- Elkhatib, E.A.; Bennett, O.L.; Wright, R.J. 1984. Kinetics of arsenite adsorption in soils. *Soil Sci. Soc. Am. J.* 48, 758-762.
- Elkhatib, E.A.; Bennett, O.L.; Wright, R.J. 1984. Arsenite sorption and desorption in soils. *Soil Sci. Soc. Am. J.* 48, 1025-1029.
- Fuller, C.C.; Davis, J.A.; Waychunas, G.A. 1993. Surface chemistry of ferrihydrite: Part 2. Kinetics of arsenate adsorption and coprecipitation. *Geochim. Cosmochim. Acta* 57, 2271-2282.
- Goldberg, S.; Johnston, C.T. J. 2001. Mechanisms of arsenic adsorption on amorphous oxides evaluated using macroscopic measurements, vibrational spectroscopy, and surface complexation modeling. *Colloid Interface Sci.* 234, 204-216.
- Goldberg, S. 2002. Competitive adsorption of arsenate and arsenite on oxides and clay minerals. *Soil Sci. Soc. Am. J.* 66, 413-421.
- Han, F. X.; Kingery, W.L.; Selim, H.M.; Gerard, P.D.; Cox, M.S.; Oldham, J.L. 2004. Arsenic solubility and distribution in poultry waste and long-term amended soil. *Sci. Total Environ.* 320, 51-61.
- Jacobs, L.W.; Syers, J.K.; Keeney D.R. 1970. Arsenic sorption by soils. *Soil Sci. Soc. Am. Proc.* 34, 750-754.
- Keon, N.E.; Swartz, C.H.; Brabander, D.J.; Harvey, C.; Hemond, H. F. 2001. Validation of an arsenic sequential extraction method for evaluating mobility in sediments. *Environ. Sci. Technol.* 35, 2778-2784.
- Lin Z.; Puls, R.W. 2000. Adsorption, desorption and oxidation of arsenic affected by clay minerals and aging process. *Environ. Geol.* 39, 753-759.
- Livesey, N.T.; Huang, P.M. 1981. Adsorption of arsenate by soils and its relation to selected chemical properties and anions. *Soil Sci.* 131, 88-94.
- Manning, B.A.; Goldberg, S. 1997. Arsenic(III) and arsenic(V) adsorption on three California soils. *Soil Sci.* 162, 886-895.

- Manning, B.A.; Goldberg, S. 1996. Modeling arsenate competitive adsorption on kaolinite, montmorillonite and illite. *Clays Clay Miner.* 44, 609-623.
- O'Reilly, S.E.; Strawn, D. G.; Sparks, D. L. 2001. Residence time effects on arsenate adsorption/desorption mechanisms on goethite. *Soil Sci. Soc. Am. J.* 65, 67-77.
- Raven, K.P.; Jain, A.; Loeppert, R.H. 1998. Arsenite and arsenate adsorption on ferrihydrite: Kinetics, equilibrium, and adsorption envelopes. *Environ. Sci. Technol.* 32, 344-349.
- Selim, H.M. 1992. Modeling the transport and retention of inorganics in soils. *Adv. Agron.* 47, 331-384.
- Selim, H.M.; Ma, L.W. 2001. Modeling nonlinear kinetic behavior of copper adsorption-desorption in soil. In *Physical and chemical processes of water and solute transport/retention in soil*. Selim, H.M.; Sparks, D. L. Ed. SSSA special publication no. 56. Soil Sci. Soc. A. Madison, WI.; pp 189-212.
- Smith, E.; Naidu, R.; Alston, A.M. 1999. Chemistry of arsenic in soils: I. Adsorption of arsenate and arsenite by selected soils. *J. Environ. Qual.* 28, 1719-1726.
- Sun, X.; Doner, H.E. 1996. An investigation of arsenate and arsenite bonding structure on goethite by FTIR. *Soil Sci.* 161, 865-872.
- Wauchope, R.D. 1975. Fixation of arsenical herbicides, phosphate, and arsenate in alluvial soils. *J. Environ. Qual.* 4, 355-358.
- Waychunas, G.A.; Rea, B.A.; Fuller, C.C.; Davis, J.A. 1993. Surface chemistry of ferrihydrite: Part 1. EXAFS studies of the geometry of coprecipitated and adsorbed arsenate. *Geochim. Cosmochim. Acta* 57, 2251-2269.
- Williams, L.E.; Barnett, M.O.; Kramer, T.A.; Melville J.G. 2003. Adsorption and transport of arsenic(V) in experimental subsurface systems. *J. Environ. Qual.* 32, 841-850.

CHAPTER 4: MODELING THE TRANSPORT AND RETENTION OF ARSENIC(V) IN SOILS

4.1 Introduction

The movement of arsenic in soils and aquifers is highly dependent on the adsorption-desorption reactions in the solid phase. Iron (Fe) and aluminum (Al) oxides and hydroxides in particular have high affinity to As(V) and form inner-sphere surface complex via a ligand exchange mechanism (Waychunas et al., 1993). The adsorption of As(V) on various Fe- and Al-containing minerals have been extensively investigated (e.g., Goldberg, 2002). Equilibrium models of the Freundlich and Langmuir type are commonly used to describe results of arsenic sorption by soils (e.g., Buchter et al., 1989; Manning and Goldberg, 1997). However, the utility of results from short duration studies for predictions of arsenic fate and transport is questionable because equilibrium conditions are rarely achieved for arsenic transport under field conditions due to a wide variety of biological, chemical, and hydrological factors. The occurrence of non-equilibrium conditions can have significant impact on the transport of As(V) in heterogeneous soil systems. The mechanisms behind the rate-limited sorption and transport of As(V) in soils have not been fully explored. In general, rate-limited processes for reactive solutes are due to physical (transport related) and chemical (sorption related) non-equilibriums. Physical non-equilibrium includes processes such as inter- and intra-particle diffusion within soil aggregates and preferential flow through soil macro-pores (Brusseau, 1993). Non-equilibrium sorption of As(V) may be due to (1) heterogeneity of sorption sites on the soil matrix, (2) rate limited precipitation at mineral surfaces, i.e., three dimensional growth of a particular arsenic solid phase, and (3) slow diffusion to sites within the soil matrix (Zhang and Selim, 2005).

Downward movement of arsenic has been observed in contaminated soils. Isensee et al. (1973) investigated arsenate residual in Metapeake silt loam 14 years after massive application

of arsenical herbicides. Their results showed that a large amount of arsenic remained in the soil profile and the concentration decreased with increasing depth, which is indicative of slow leaching processes. In Australia, McLaren et al. (1998) observed considerable downward movement of arsenic through the soils surrounding cattle dips. They concluded that the migration of arsenic was slow and controlled by soils properties. They showed arsenic concentrations in the subsurface (20 - 40 cm) near cattle dip sites ranged from 57 to 2282 mg kg⁻¹.

A number of studies were carried out in the laboratory to investigate the transport of arsenic in soils. For example, Hiltbold et al. (1974) studied MSMA (monosodium methanearsonate) transport in surface and subsurface soils using field profile sampling, batch experiment, and soil column experiments. Arsenic distribution in soil profile after repeated application of MSMA showed no evidence of leaching. Arsenic K_d values based on batch and column experiments showed extensive discrepancies and were attributed to the short residence time of arsenic in the soil columns.

Other transport studies include that of Melamed et al. (1995) who studied effect of phosphate incubation on leaching of arsenate from packed columns of aggregated Oxisol. Asymmetrical breakthrough curves (BTCs) were observed indicative of physical and/or chemical non-equilibrium during arsenic movement through the columns. Darland and Inskeep (1997a,b) demonstrated the effect of pore water velocity, pH, and phosphate on the transport of arsenate through packed columns of sand with Fe oxides. They found at pH 4.5 and 6.5, AsO₄ transport exhibited significant retardation and tailing, while at pH 8.0, BTC of AsO₄ was nearly symmetrical. Increase in added PO₄ content resulted in an increase in arsenic recovery, decrease in retardation, and symmetrical BTC. Increasing pore volume velocity from 0.2 cm h⁻¹ to 90 cm h⁻¹ increased arsenic recovery from 7.24% to 74.3%. Williams et al. (2003) carried out column

experiments to investigate As(V) transport through a heterogeneous soil containing Fe oxide. They concluded that the effect of factors affecting arsenic transport increased in the order $\text{pH} < \text{pore water velocity} < \text{phosphate}$. Attempts to model arsenic BTCs from the soil columns showed that the use of linear or Freundlich (equilibrium) retention mechanisms describe neither the extent of retardation nor the release (desorption) during leaching.

A literature search revealed that only few studies focused on the kinetics of As(V) retention during transport in soils. Kinetic adsorption data have the advantage of accounting for the nonequilibrium sorption behavior which may arise from the heterogeneity of sorption sites on soil surface and slow diffusion process on the interface between liquid phase and soil matrix. The objectives of this study were (i) to determine the adsorption kinetics and transport behavior of As(V) in three soils having different properties; and (ii) to test the applicability of different formulations of a multi-reaction (equilibrium-kinetic) transport model (MRM) in simulating non-equilibrium sorption and transport of As(V) in soils.

4.2 Material and Methods

The transport of As(V) in soils was investigated using the miscible displacement technique as described by Selim et al. (1987). Acrylic columns (5-cm in length and of 6.4-cm i.d.) were uniformly packed with air-dry soil and were slowly water-saturated with a background solution of 0.01 *M* KNO₃ at a low Darcy flux. Input solutions of 0.01 *M* KNO₃ were applied for several pore volumes using a variable speed piston pump, and the fluxes were adjusted to the desired flow rates. Between 10 to 20 pore volumes of 0.01 *M* KNO₃ were applied to each column prior to introduction of As(V) pulse solutions. One or more pulses of 100 mg L⁻¹ As(V) solution (as KH₂AsO₄) in 0.01 *M* KNO₃ as background solution, were introduced to each soil column as indicated in Table 4.1. For columns 101 (Olivier soil) and 103 (Windsor soil) only

one As(V) pulse was introduced, whereas, for all other columns received two consecutive As(V) pulses (see Table 4.1). Each As(V) pulse was approximately 10-12 pore volume and was subsequently eluted by 0.01 *M* KNO₃ solution. During pulse application, column flow was completely stopped for a duration of 3-6 days in order to evaluate the influence of flow interruption on As(V) transport. Flow interruption or stop-flow was accounted for in our model by simply assuming $v=0$ and $D=D_o$ (molecular diffusion coefficient) during flow interruption. The volume of each As(V) pulse along with soil parameters associated with each column (e.g., v , θ and ρ) are given in Table 4.1.

To obtain independent estimates for the dispersion coefficient (D) of Eq. [1], separate pulses of a tracer solution were applied to each soil column prior to As(V) pulse applications. The tracer used was tritium (³H₂O) which is commonly utilized for miscible displacement experiments and the collected samples were analyzed using a Tri-Carb liquid scintillation β counter (Packard-2100 TR) by mixing 0.5 mL aliquot with 5 mL cocktail (Packard Ultima Gold) for 10 minutes on the liquid scintillation counter. The radioactivity was recorded as counts per minute (CMP). Estimates for D values are given in Table 4.1. Selected tritium breakthrough curves (BTCs) which represent relative concentration (C/C_o) versus pore volume (V/V_o) are shown in Figure. 4.1. The tritium data were described using the classical convection-dispersion equation and best-fit parameters for D and the retardation factor R ($= 1 + \rho K_d/\theta$) were obtained using nonlinear least square optimization.

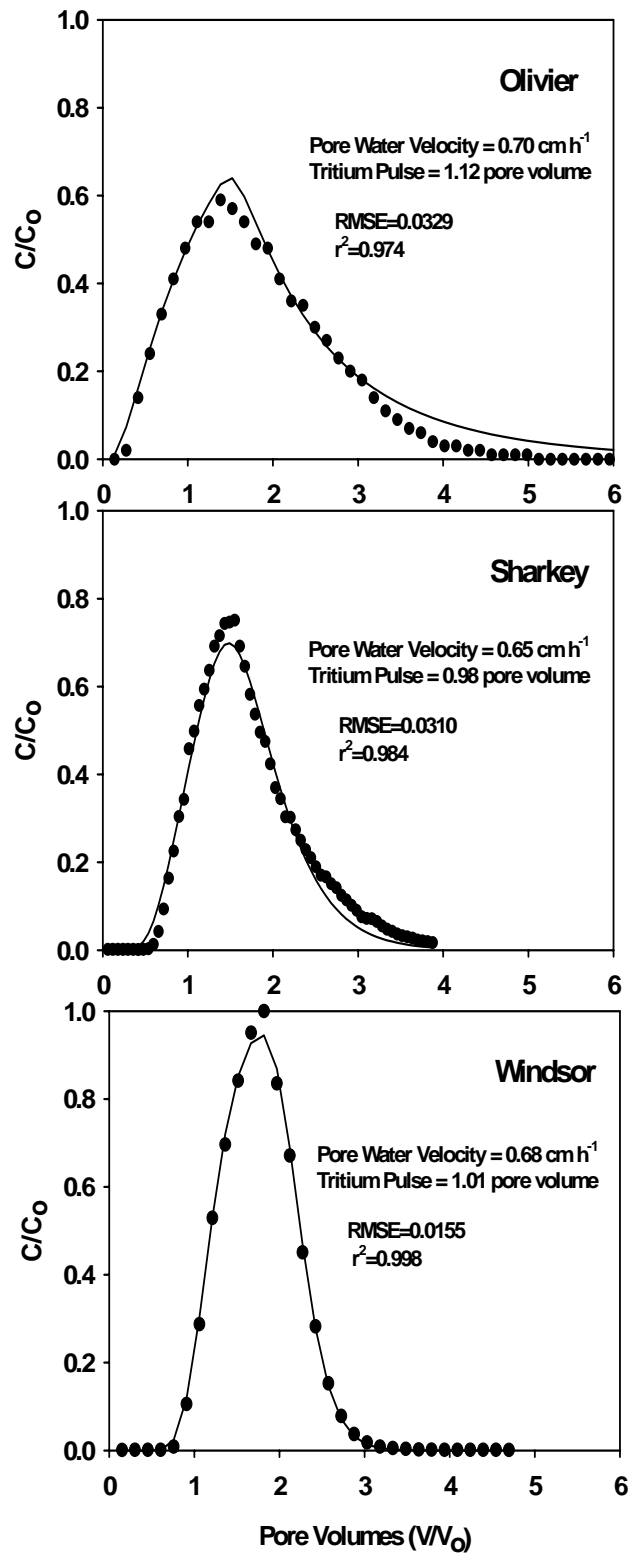


Figure 4.1 Tritium breakthrough curves for soils. Solid curves depict results of curve-fitting with convection dispersion equation (CDE) for non-reactive solutes

Table 4.1 Column soil physical parameters for As(V) and tritium miscible displacement experiments for single and double pulses. Values of the dispersion coefficient were estimated from tritium breakthrough results.

Column No	101	102	103	104	105
Soil type	Olivier	Olivier	Windsor	Windsor	Sharkey
Bulk density (ρ , Mg m ⁻³)	1.25	1.22	1.17	1.17	1.15
Saturated moisture content (θ , %)	53	54	56	56	57
Pore water velocity (v , cm h ⁻¹)	0.34	0.70	0.34	0.68	0.65
First As(V) pulse input (p.v.) ^a	10.35	10.96	10.47	10.94	12.48
First flow interruption (h)	-	120	73	97	120
Second As(V) pulse input (p.v.)	-	10.06	-	10.20	11.40
Second flow interruption (h)	-	144	-	97	144
Dispersion coefficients (D , cm ² h ⁻¹)	0.89	1.65	0.64	0.86	0.31
As(V) mass recovery (%)	70.6	82.1	56.8	64.6	43.0

^a p.v. = pore volumes.

4.3 Results and Discussion

4.3.1 Kinetic Sorption

The capability of the multireaction model (MRM) in describing the kinetics of As(V) adsorption on three soils was investigated for the various initial (or input) concentrations (C_o 's) as well as for the entire data set, i.e., all C_o 's (*Overall*). In our first simulation attempt, we chose a simple MRM model formulation with four parameters n , k_1 , k_2 , and k_3 . Results of nonlinear least-square optimization are given in Table 4.2 for Olivier soil. In general, for individual C_o , this model formulation resulted in poor predictions as indicated by the large values of RMSE. The reaction order n was highly unstable as shown through the large standard errors, especially at high C_o values. Similar results were obtained by Selim and Ma (2001) for Cu sorption. Selim and Ma (2001) indicated that the nonlinear reaction order n was particularly difficult to estimate from individual data sets. Based on parameter estimates from our study, we conclude that the reaction order n could not be determined from kinetic batch data of individual input concentrations.

In our second attempt to describe the As(V) batch data, the entire data set (for all initial concentrations C_o) was used in the nonlinear least square optimization. This resulted in significant improvement in predictions as depicted by the small standard errors associated with all parameters (see Table 4.2). Since the best-fit n of 0.27 ± 0.04 for Olivier soil was not significantly different from that of the 24-h Freundlich b value of 0.284, it was decided to test whether the value of 24 h Freundlich b can be used in place of the nonlinear reaction order n in the MRM model. Based on r^2 and RMSE values, from all three soils, we conclude that the use of 24-h Freundlich b in MRM simulation of adsorption kinetics can be recommended.

Table 4.2 Comparison of the goodness-of-fit of a two-phase kinetic reversible and consecutive irreversible model requires 3 parameters model formulation ($M4 = k_1, k_2$, and k_3) for Olivier soil.

C_0 mg L ⁻¹	r^2	$RMSE$	n	SE^c	k_1	SE	k_2 h ⁻¹	SE	k_3	SE
5	0.990	0.114	2.30	0.17	0.035	0.005	0.0001	0.0003	0.0000	0.0087
10	0.977	0.554	2.83	0.34	0.002	0.001	0.0000	0.0002	0.0000	5.44E3
20	0.989	0.930	3.58	0.53	0.0001	0.0001	0.0000	0.0009	0.0000	1.38E7
40	0.994	1.98	2.50	1.29	0.0001	0.0006	0.0094	0.0119	0.0055	0.0029
80	0.997	3.79	0.892	5.64	0.019	0.462	0.0219	0.0566	0.0020	0.0054
100	0.998	3.38	0.717	3.69	0.040	0.686	0.0286	0.0351	0.0025	0.0045
Overall ^a	0.998	1.91	0.288	0.0300	0.304	0.044	0.0340	0.0041	0.0018	0.0003
Overall ^b	0.998	1.90	0.270	—	0.328	0.027	0.0342	0.0041	0.0018	0.0002

^a All initial concentrations (C_0) were used.

^b n was derived from Freundlich b .

^c SE =standard error.

Table 4.3 Comparison of parameters and goodness-of-fit determined from fitting eight different MRM model formulations to kinetic adsorption data.

<i>MRM</i> ^a	<i>r</i> ²	<i>RMSE</i>	<i>K_e</i>		<i>k</i> ₁ h ⁻¹	<i>SE</i> ^b	<i>k</i> ₂ h ⁻¹	<i>SE</i>	<i>k</i> ₃ h ⁻¹	<i>SE</i>	<i>k</i> _s h ⁻¹	<i>SE</i>
Olivier												
M1	0.985	4.91	4.54	0.30	-	-	-	-	-	-	0.0015	0.0001
M2	0.992	3.52	-	-	0.22	0.14	0.015	0.001	-	-	-	-
M3	0.997	2.31	-	-	0.34	0.02	0.036	0.003	0.0018	0.0002	-	-
M4	0.995	2.83	2.35	0.23	0.10	0.01	0.0074	0.0006	-	-	-	-
M5	0.996	2.65	-	-	0.30	0.02	0.032	0.003	-	-	0.0008	0.0001
M6	0.997	2.25	0.93	0.33	0.25	0.03	0.027	0.004	0.0018	0.0002	-	-
M7	0.996	2.54	1.27	0.31	0.19	0.03	0.021	0.003	-	-	0.0007	0.0001
M8	0.997	2.22	0.93	0.33	0.24	0.03	0.028	0.004	0.0015	0.0003	0.0002	0.0001
Sharkey												
M1	0.926	6.43	11.4	0.5	-	-	-	-	-	-	0.0041	0.0004
M2	0.974	3.80	-	-	1.11	0.04	0.046	0.002	-	-	-	-
M3	0.989	2.47	-	-	1.30	0.03	0.070	0.002	0.0011	0.0001	-	-
M4	0.976	3.67	2.46	0.62	0.79	0.07	0.036	0.003	-	-	-	-
M5	0.987	2.66	-	-	1.25	0.04	0.070	0.003	-	-	0.0021	0.0002
M6	0.989	2.49	0.49	0.04	1.22	0.04	0.067	0.002	0.0011	0.0001	-	-
M7	0.987	2.67	0.00	0.01	1.25	0.04	0.070	0.003	-	-	0.0021	0.0002
M8	0.989	2.50	0.48	0.05	1.22	0.03	0.067	0.002	0.0011	0.0001	0.0000	0.0000
Windsor												
M1	0.972	5.61	7.34	0.35	-	-	-	-	-	-	0.0031	0.0002
M2	0.971	5.70	-	-	0.67	0.04	0.030	0.002	-	-	-	-
M3	0.988	3.64	-	-	1.20	0.04	0.093	0.004	0.0024	0.0001	-	-
M4	0.991	3.11	5.18	0.23	0.17	0.01	0.0081	0.0006	-	-	-	-
M5	0.986	3.02	-	-	1.16	0.09	0.097	0.010	-	-	0.0022	0.0001
M6	0.994	2.53	3.70	0.26	0.40	0.04	0.032	0.003	0.0021	0.0002	-	-
M7	0.993	2.86	3.98	0.28	0.31	0.03	0.027	0.003	-	-	0.0016	0.0001
M8	0.994	2.54	3.70	0.26	0.40	0.04	0.032	0.003	0.0020	0.0002	0.0001	0.0001

^a Required model parameters for different MRM formulations are as follows: M1 = *k*₁ and *k*₂; M2 = *K_e* and *k_s*; M3 = *K_e*, *k*₁, and *k*₂; M4 = *k*₁, *k*₂, and *k*₃; M5 = *k*₁, *k*₂, and *k_s*; M6 = *K_e*, *k*₁, *k*₂, and *k*₃; M7 = *K_e*, *k*₁, *k*₂, and *k_s*; M8 = *K_e*, *k*₁, *k*₂, *k*₃, and *k_s*. Model parameter *n* and *m* was derived from Freundlich b for all model formulations. All initial concentrations (*C*₀) were used.

^b SE = standard error.

To test the capability of MRM describing the retention behavior of arsenic versus time by the three soils, several model formulations were tested. Different formulations of the multireaction model (MRM) of Figure 3.1 represent different reactions from which one can deduce retention mechanisms. Eight model formulations were derived from the general model and denoted as M1 through M8. The required model parameters are dependent on the formulation of the MRM model used. Two model formulations require only 2 parameters (M1 = k_1 and k_2 ; and M2 = K_e and k_{irr}). Another two model formulations require 3 parameters (M3 = K_e , k_1 , and k_2 ; M4 = k_1 , k_2 , and k_3 ; and M5 = k_1 , k_2 , and k_{irr}). Two model formulations require 4 parameters (M6 = K_e , k_1 , k_2 , and k_3 ; and M7 = K_e , k_1 , k_2 , and k_{irr}). One model formulation require 5 parameters (M8 = K_e , k_1 , k_2 , k_3 and k_{irr}). Model formulation M8 may be considered as the full version of the MRM model. In contrast, M1 is the simplest model formulation where As(V) retained in the S_k phase with only reversible kinetics as the governing process (see Figure 3.1). In all model formulations, the nonlinear 24 h Freundlich b was used in place of n and m for each soil as discussed above, and the entire datasets (all C_o 's) were used in the nonlinear least-square optimization.

Estimated parameters and their goodness-of-fit for different MRM model formulations are given in Table 4.3. In general, three- and four-parameter model formulations provided better predictions than two-parameter formulations. However, the goodness-of-fit of the model to experimental data varied among different soils. Based on RMSE and r^2 , model formulations M1 and M2 consistently provided poorest predictions of As(V) retention. As a result, the use of a single fully reversible nonlinear kinetic reaction or two-phase concurrent equilibrium and irreversible processes is not recommended for describing As(V) retention in all three soils. It was observed that several other model formulations (M3-M8) were similar in their capability of

describing the kinetic batch data. Similar to the findings of Selim and Ma (2001), the consecutive irreversible reaction (k_3 in Figure 3.1) provided improvements in description of the kinetic batch data compared to the concurrent irreversible reaction (k_{irr}). Specifically, model formulations M4 and M6 offered similar goodness-of-fit in terms of root mean squared errors and yielded improved predictions when compared to M5 and M7. Since M4 contains only three model parameters, it may be preferred for future application. Therefore, the use of a fully kinetic model (M4) where retention is accounted for by two phases, one reversible (S_k) and one irreversible (S_i) is recommended for describing As(V) kinetics.

4.3.2 Tracer Breakthrough Curves

Selected breakthrough curves (BTCs) of tritium ($^3\text{H}_2\text{O}$), which is employed as a conservative tracer in this experiment, are presented in Figure 4.1 for different soils. These BTCs were fitted with classical convection-dispersion equation (CDE) of the form

$$R \frac{\partial C}{\partial t} = \frac{\partial}{\partial x} \left(D \frac{\partial C}{\partial x} \right) - v \frac{\partial C}{\partial x} \quad [4.1]$$

to obtain solute dispersion coefficient (D) and retardation factor (R). For Sharkey and Windsor soils, tritium BTCs were essentially symmetrical, exhibited no tailing, and conformed to Eq. [4.1]. However, indicative of physical nonequilibrium, significant tailing was observed for tritium BTC of Olivier soil. Similar BTCs for aggregated soil have been observed by Selim et al. (1987) and can be explained with intraparticle diffusion through soil aggregates (Brusseau 1993). Therefore, dispersion coefficient is further interpreted as the combination of hydrodynamic dispersion, and intraparticle diffusion D_w ($\text{cm}^2 \text{h}^{-1}$)

$$D = \alpha v + D_w \quad [4.2]$$

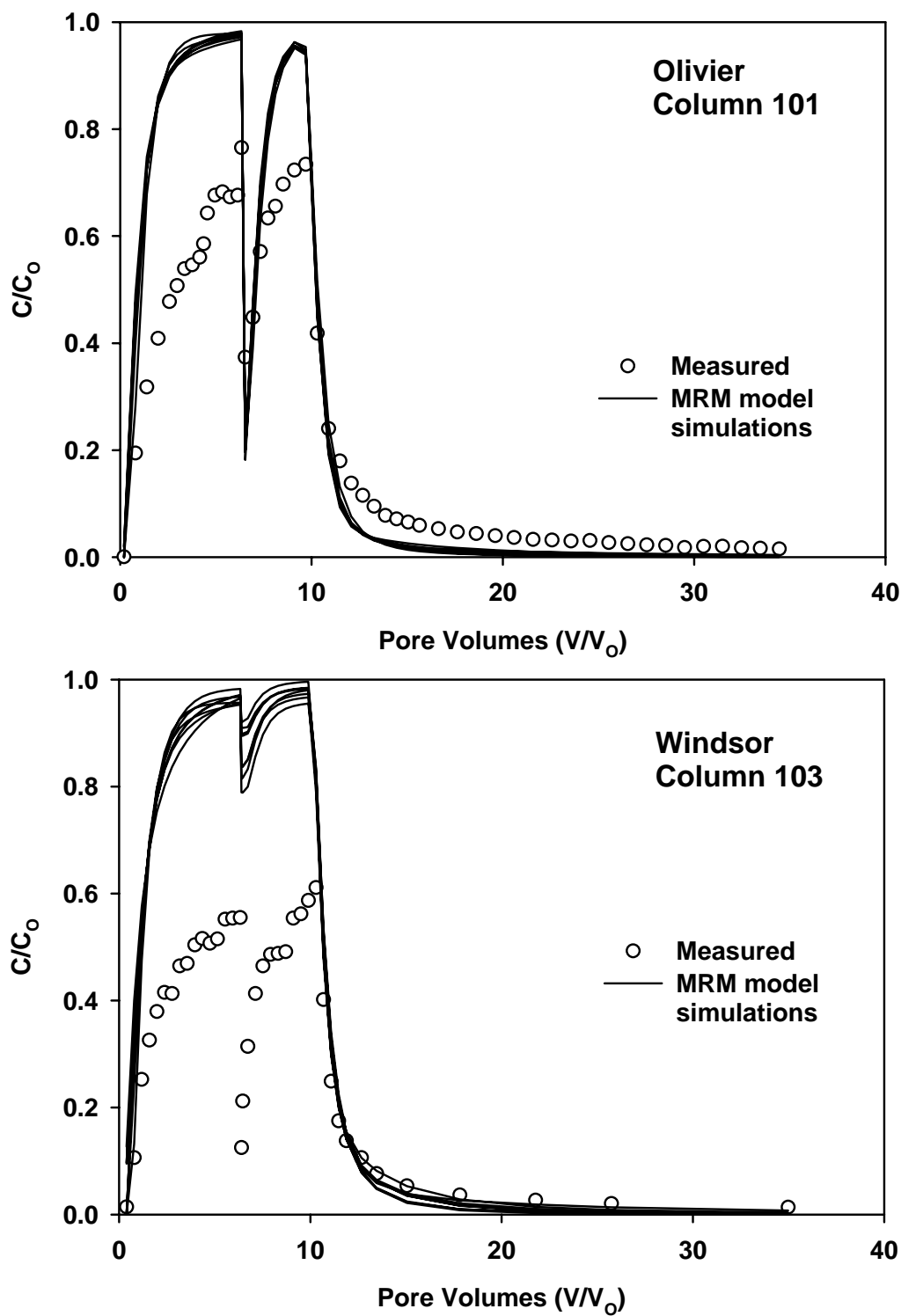


Figure 4.2 Comparison of MRM model formulations M1-M8 for predicting As(V) breakthrough curves for Olivier soil (top) and Windsor soil (bottom). Model parameters were those from the batch kinetic experiment (Table 4.3).

where α (cm) is the longitudinal dispersivity. Values of α and D_w obtained from tritium BTCs were subsequently utilized in the multireaction transport model (MRM) to simulate As(V) transport in soils.

4.3.3 Arsenate Breakthrough Curves

Breakthrough curves (BTCs) of As(V) are presented in Figure 4.2 through 4.7 for all soil columns. The transport of As(V) through all the soil columns was significantly retarded relative to the transport of the conservative tracer tritium. Complete As(V) breakthrough, i.e. 100% recovery of that applied, was not observed in any of the soil columns following application of approximately 10 pore volumes of As(V) pulse. The extent of retardation agrees with the relative degree of adsorption as measured from the As(V) batch isotherms (Figure 3.2). Specifically, highest retardation was observed for Sharkey soil, which has highest As(V) adsorption capacity, while lowest retardation was observed for Olivier with low adsorption capacity. In fact, after two As(V) pulse application and subsequent leaching by arsenic free solution of 20-30 pore volumes, the percentages of As(V) mass recovery from column effluent were 82.1%, 39.2% and 72.5% of that applied for column 102 (Olivier), 105 (Sharkey), and 104 (Windsor), respectively.

All measured As(V) BTCs exhibited extensive asymmetry as illustrated by the difference in the shape of the effluent side from the leaching or desorption side (see Figure 4.2-4.7). This is not surprising if one considers the highly nonlinear and kinetic adsorption behavior observed in our batch experiments (see Figure 3.2-3.4). Similar asymmetry of BTCs for As(V) has been observed by Darland and Inskeep (1997a) and Williams et al. (2003). In addition, the excessive tailing exhibited by all column BTCs demonstrated a continued slow desorption (release) of As(V) from all soils. For Sharkey soil unexpectedly high concentration of As(V) was observed

during the leaching phase; the reason for this remains unclear (Figure 4.7). A possible explanation is the so called colloid facilitated transport, i.e., transport of As(V) associated with mobile colloidal particles in the flowing water. Puls and Powell (1992) have demonstrated that As(V) sorbed on colloidal iron oxides can be transported through aquifer material. It is possible that *in situ* mobilization of colloidal iron oxides increased the concentration of As(V) in the leachate from the Sharkey soil. In our study, colloidal material was visually observed in the effluent during leaching in Sharkey soil.

Flow interruption was used to check for the occurrence of nonequilibrium conditions during solute transport in soils. The purpose of stopping the flow was to provide sufficient time for the solute to diffuse into the soil matrix and/or react with sorption sites on soil matrix surfaces. This technique has been shown to provide estimation of retention parameters when nonequilibrium conditions were dominant (Brusseau et al. 1989). In our column experiments, the influence of flow-interruption on mobility of As(V) through the soil columns is clearly illustrated in the BTCs presented in Figure 4.2-4.7. The sharp drop in As(V) concentration as a result of flow interruptions is indicative of As(V) reactivity during stop flow. This decrease of As(V) concentration in the effluent suggests that extensive nonequilibrium condition exist during As(V) transport for all soil columns. Such behavior during flow interruption was expected because of the kinetic sorption characteristics of As(V) as exhibited by the batch experiments.

4.3.4 Multireaction Transport Modeling

The classical convection-dispersion equation (CDE) was used to describe the one-dimensional steady-state transport of reactive solute through porous media (Selim et al., 1989):

$$\rho \frac{\partial S}{\partial t} + \theta \frac{\partial C}{\partial t} = \frac{\partial}{\partial x} \left(D \theta \frac{\partial C}{\partial x} \right) - v \theta \frac{\partial C}{\partial x} \quad [4.3]$$

where C is solute concentration ($\mu\text{g cm}^{-3}$), S is amount sorbed by the soil matrix ($\mu\text{g g}^{-1}$), x is distance (cm), t is time (h), D is hydrodynamic dispersion coefficient ($\text{cm}^2 \text{h}^{-1}$), ρ is soil bulk density (g cm^{-3}), and θ is volumetric water content ($\text{cm}^3 \text{cm}^{-3}$). In addition, v is pore water velocity (cm h^{-1}) where $v=q/\theta$, and q is Darcy's water velocity (cm h^{-1}). The amounts of arsenic retention in soils (S) were simulated with the multireaction model (MRM) of equation 3.1-3.4.

The multireaction transport model was utilized to describe the transport of As(V) through columns in two different modes, i.e., a fully predictive mode and an inverse modeling mode. In the predictive mode, all necessary model parameters were provided independent of As(V) BTCs results being modeled. Specifically, model retention parameters (n , K_e , k_1 , k_2 , k_3 , etc.) were those given in Table 4.3 for our kinetic batch data, whereas the hydrodynamic dispersivity (α) and intra-particle diffusion (D_w) were obtained from tritium BTCs (Figure 4.1). All other parameters such as column length (L), pore water velocity (v), bulk density (ρ), moisture content (θ), and pulse duration were provided for each individual column (see Table 4.1). The goodness-of-fit of model prediction was evaluated based on RMSE and r^2 values. Examples of model predictions using all model formulations (M1-M8) are shown in Figure 4.2 for Olivier and Windsor soils. Consistent with previous studies (Ma and Selim 1997), the use of batch model parameters overpredicted concentration maxima (peaks) and underestimated the extent of retardation (BTCs shift to the left). The steepness of the BTC fronts was overpredicted and the tailing was underpredicted by all model formulations. Therefore, the use of batch rate coefficients grossly underestimated the extent of As(V) retention in Olivier and Windsor soils. Conversely, overestimation of potential As(V) mobility was predicted by all model formulations used. We thus conclude that BTC predictions based on batch parameters did not adequately predict the breakthrough of As(V) from all soil columns studied (with RMSE ranging from 0.228 to 0.548).

Results of Darland and Inskeep (1997a) based on MRM predictions of As(V) BTCs yielded similar predictions to those of our observation for the soil columns presented here.

Discrepancies between measured and MRM model predictions (using batch parameters) were observed by Barnett et al. (2000) for Uranium(VI) transport through soil columns. They suggested several fundamental differences between batch and column experiments that reduced the applicability of batch experiment data in simulating column transport experiments. In our experiments, the different retention capacities determined from batch and column experiments might result from the following reasons: difference between sorption time used for batch experiment and hydrologic retention time of column experiment; low solid/solution ratio of batch experiments; As(V) was added in one spike for batch study compare to continuous addition in column experiments; and potential buildup of reaction products in closed batch systems.

4.3.5 Inverse MRM Modeling

In an inverse mode, we utilized the multireaction transport model along with nonlinear least-squares optimization scheme to test the capability of MRM for predicting As(V) BTCs without reliance on parameter estimates from the batch experiments. Therefore, one assumes that if the model is incapable of describing measured BTCs, the model is an inaccurate representation of the retention mechanisms. In general, three and four parameter model formulations provided better predictions than two parameter formulations as shown in Figure 4.3 to 4.6. However, the goodness-of-fit of model prediction to experimental data varied among individual columns. Examples using all eight model formulations are given in Table 4.4. The overall goodness-of-fit as evidenced by the root mean squared errors (RMSE) and r^2 were best when k_1 , k_2 , and k_3 , (M4) or k_1 , k_2 , and k_{irr} (M5) were used. M6, M7 and M8 provided similar goodness-of-fit in terms of RMSE and r^2 . Since M4 and M5 contain only three model

Table 4.4 Root mean squared errors (RMSE) of predicted and optimized arsenate breakthrough curves (BTCs) across all soil columns and eight different MRM formulations (M1-M8).

Column	RMSE of Model Formulations ^a							
	M1	M2	M3	M4	M5	M6	M7	M8
PREDICTED^b								
101	0.208	0.209	0.212	0.213	0.210	0.214	0.211	0.216
102	0.248	0.233	0.243	0.246	0.245	0.245	0.244	0.246
103	0.559	0.544	0.563	0.571	0.560	0.576	0.563	0.580
104	0.368	0.346	0.357	0.382	0.363	0.377	0.361	0.380
105	0.436	0.421	0.435	0.449	0.435	0.441	0.431	0.443
OPTIMIZED^c								
101	0.043	0.102	0.044	0.036	0.032	0.038	0.033	0.035
102	0.086	0.117	0.073	0.084	0.085	0.073	0.074	0.075
103	0.105	0.100	0.105	0.090	0.083	0.097	0.086	0.089
104	0.071	0.071	0.069	0.060	0.043	0.060	0.039	0.049
105	0.108	0.123	0.073	0.075	0.079	0.059	0.057	0.071

^a Required model parameters for the different MRM formulations are as follows: M1 = k_1 and k_2 ; M2 = K_e and k_{irr} ; M3 = K_e , k_1 , and k_2 ; M4 = k_1 , k_2 , and k_3 ; M5 = k_1 , k_2 , and k_{irr} ; M6 = K_e , k_1 , k_2 , and k_3 ; M7 = K_e , k_1 , k_2 , and k_{irr} ; M8 = K_e , k_1 , k_2 , k_3 , and k_{irr} . Model parameter n and m was derived from Freundlich b for all model formulations.

^b Model parameters (K_e , k_1 , k_2 , k_3 , and k_{irr}) used were obtained from kinetic batch data (see Table 4).

^c Model parameters (K_e , k_1 , k_2 , k_3 , and k_{irr}) were obtained from nonlinear least-squares optimization of transport data.

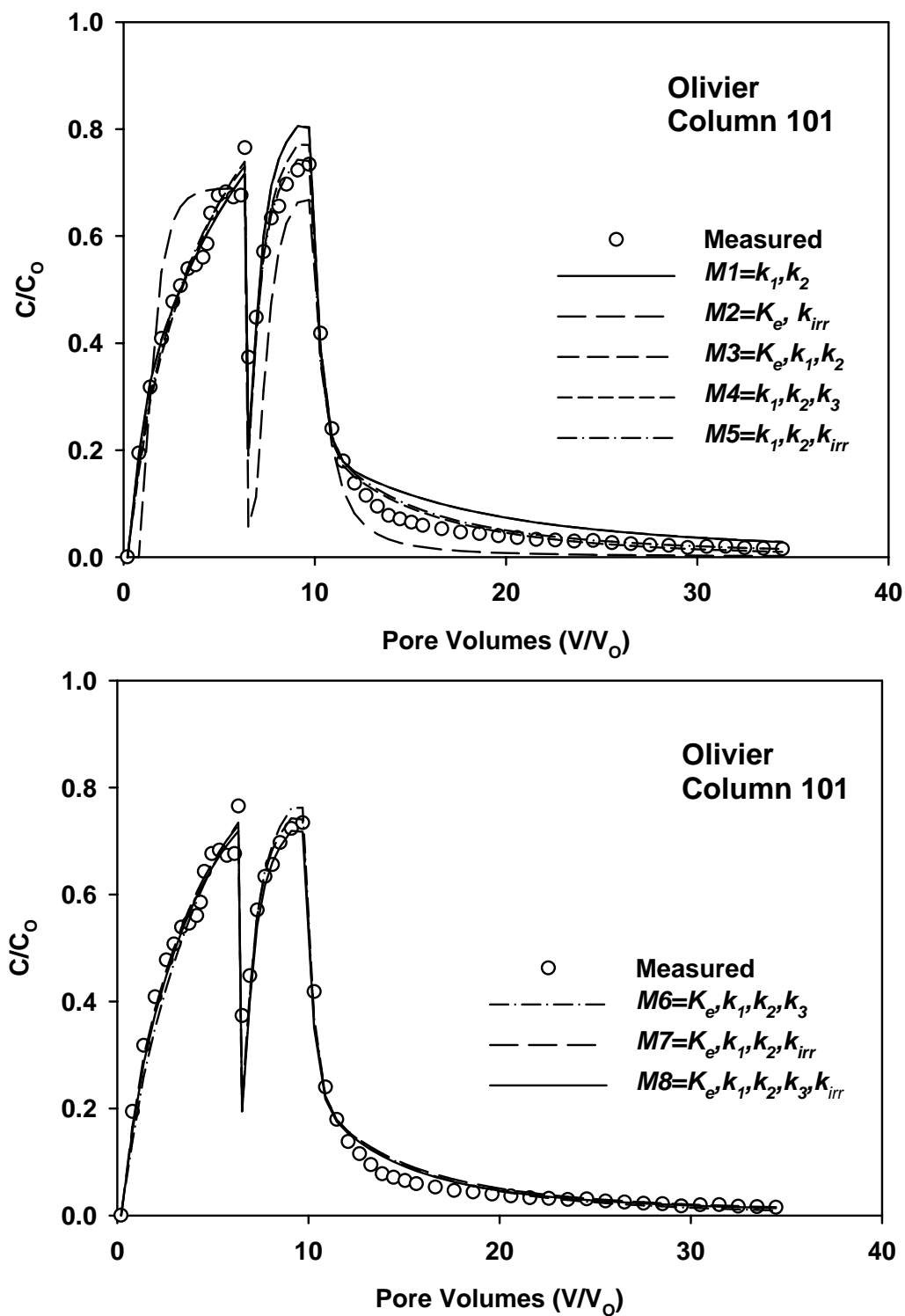


Figure 4.3 Comparison of MRM model formulations M1-M8 model for predicting As(V) breakthrough curves for Olivier soil column 101. Model parameters were obtained using nonlinear inverse modeling.

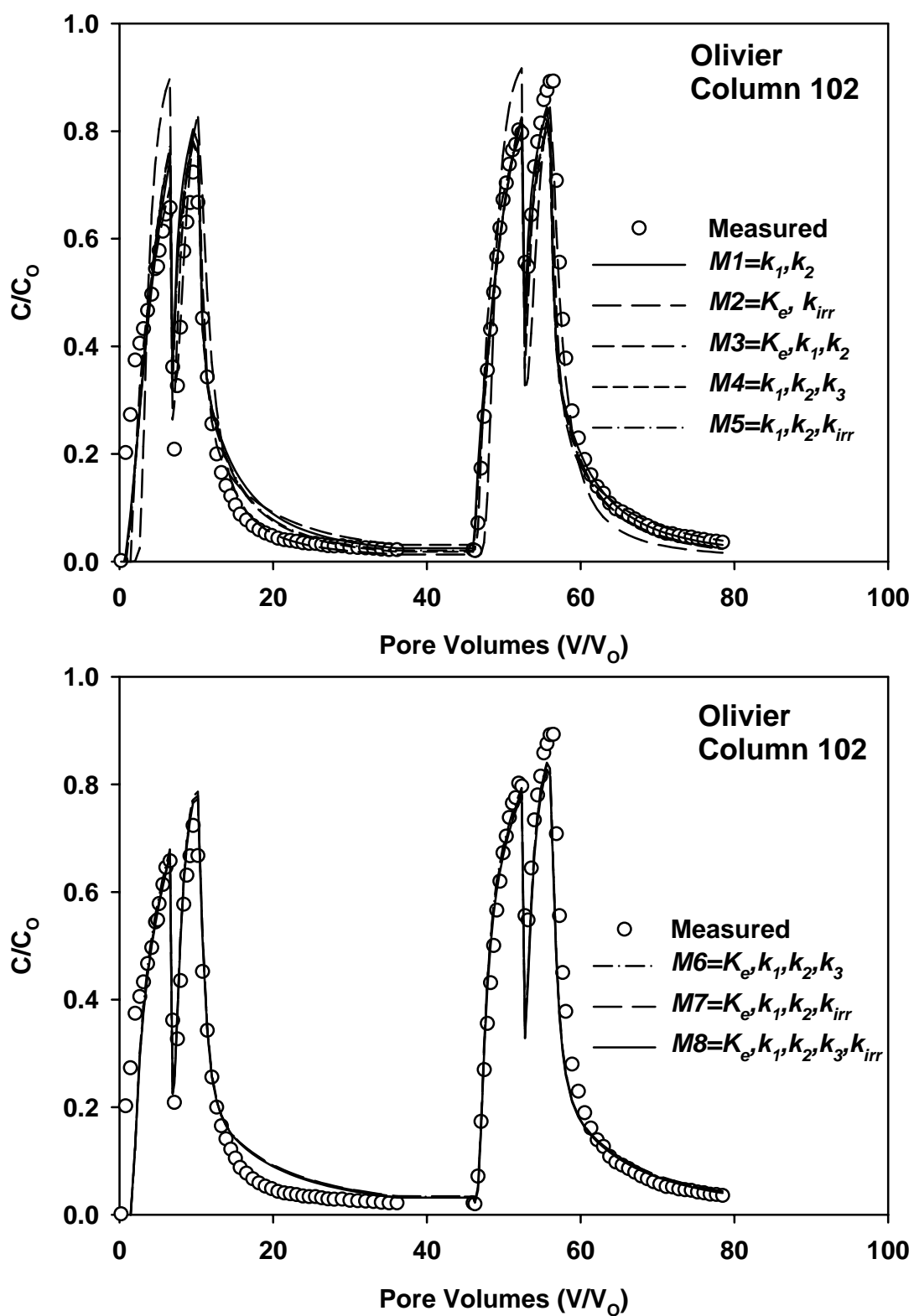


Figure 4.4 Comparison of MRM model formulations M1-M8 for predicting As(V) breakthrough curves for Olivier soil column 102. Model parameters were obtained using nonlinear inverse modeling.

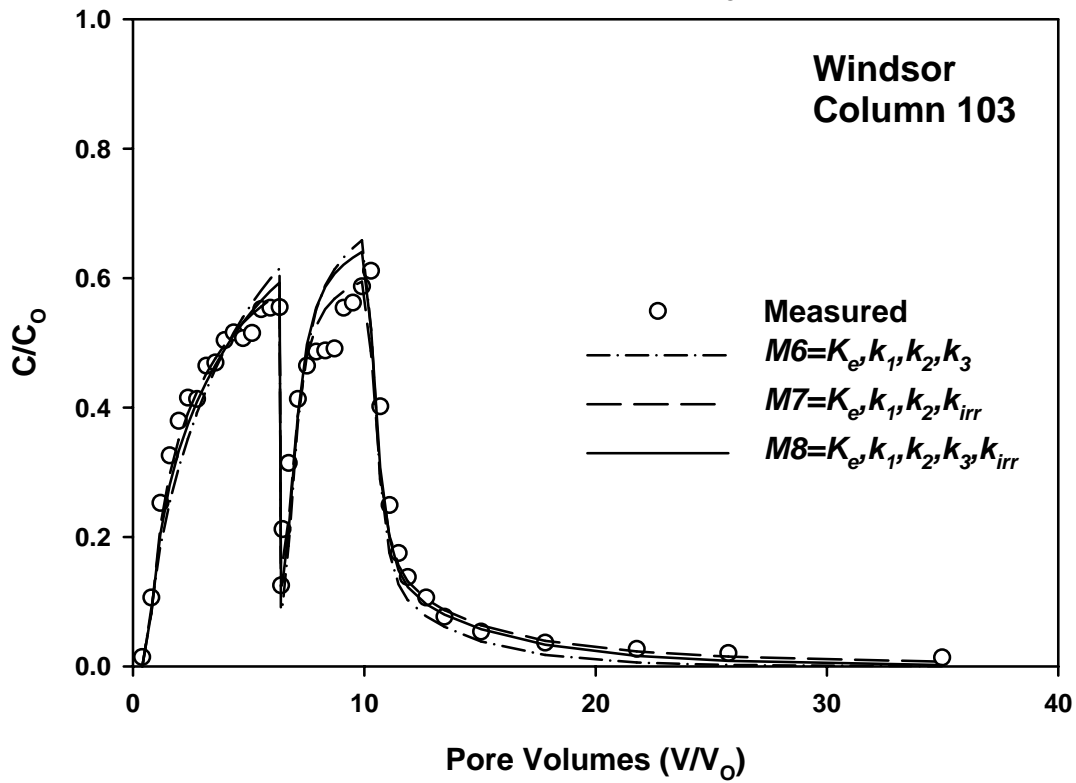
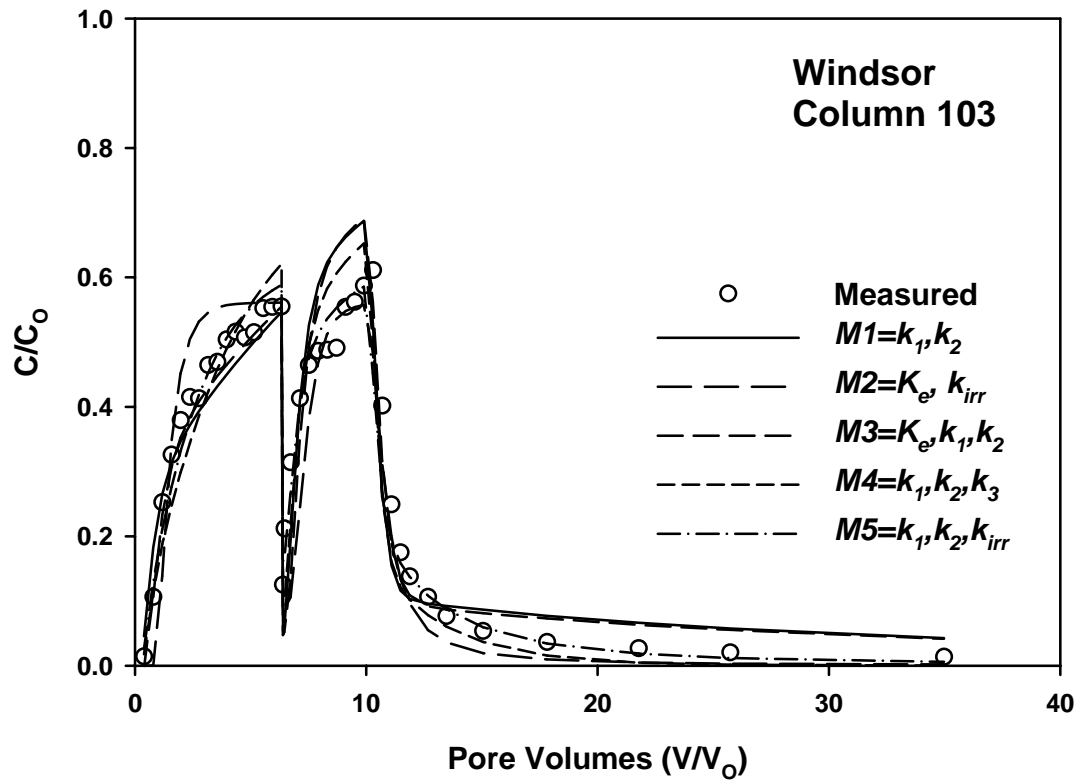


Figure 4.5 Comparison of MRM model formulations M1-M8 for predicting As(V) breakthrough curves for Windsor soil column 103. Model parameters were obtained using nonlinear inverse modeling.

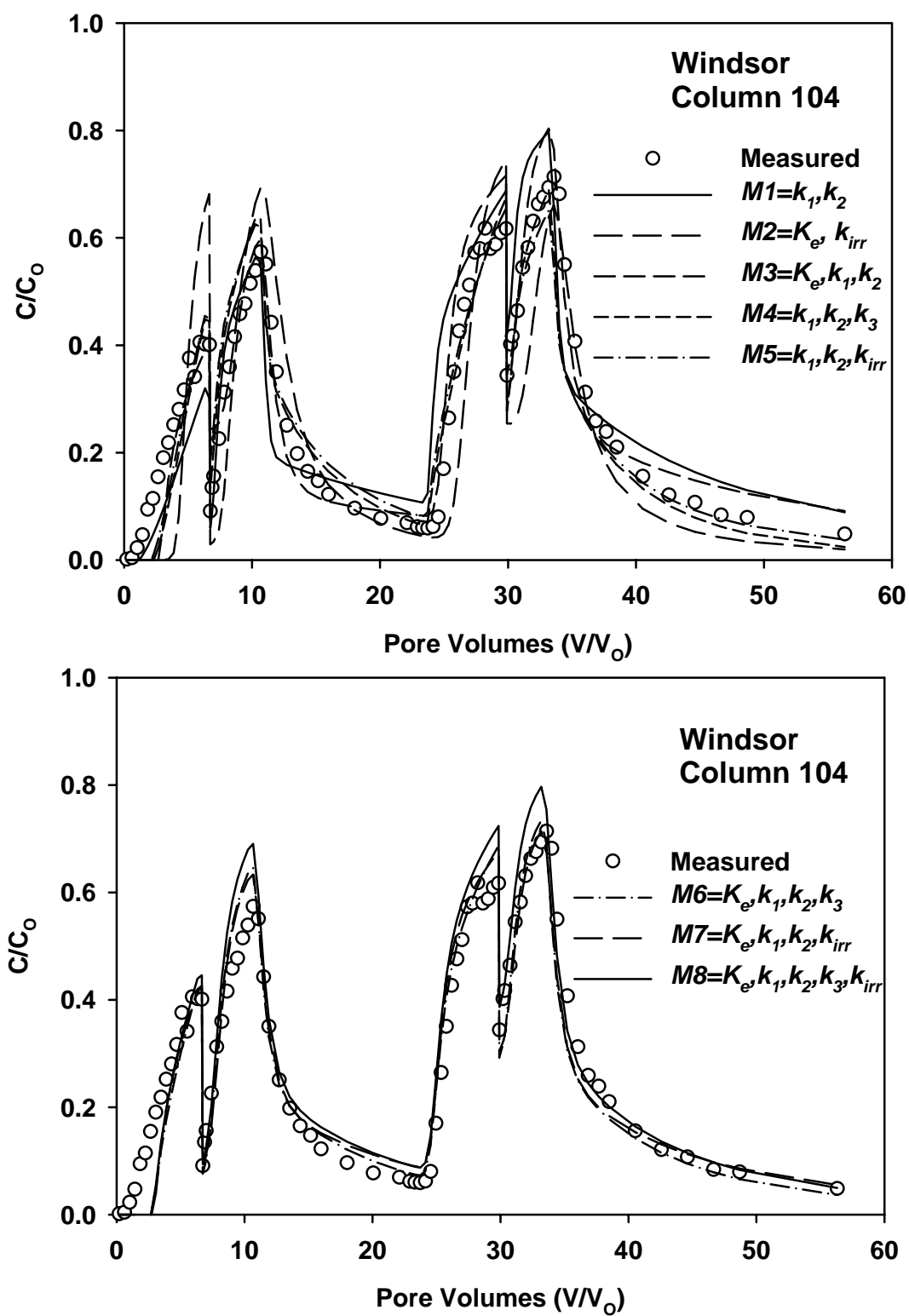


Figure 4.6 Comparison of MRM model formulations M1-M8 for predicting As(V) breakthrough curves for Windsor soil column 104. Model parameters were obtained using nonlinear inverse modeling.

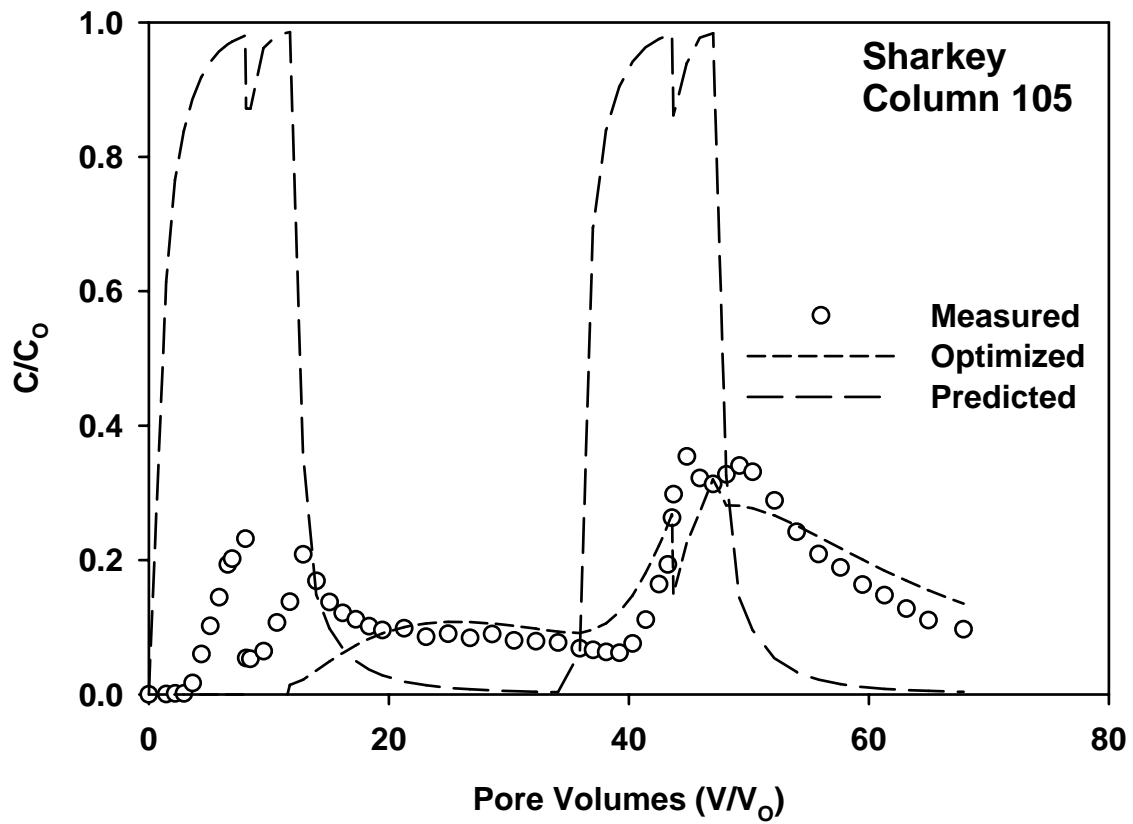


Figure 4.7 Comparison of predictions and simulations using MRM model formulation M8 for predicting As(V) breakthrough curves for Sharkey soil column 105.

parameters, these model formulations are perhaps preferable for future application. Based on batch as well as column transport analysis, we conclude that MRM formulations with three parameters can be recommended.

Overall excellent fits of the model were achieved for As(V) BTCs of Olivier and Windsor columns as indicated by the small values of RMSE (< 0.1) and high r^2 (> 0.95). In addition, the effect of flow interruption was successfully described when several model formulations along with the nonlinear optimization scheme was used. Sorption rate coefficients obtained from column BTCs were much larger than those obtained from batch experiments. This is indicative of higher As(V) sorption for soil columns than batch experiments. The MRM model failed to describe As(V) BTC of Sharkey column (Figure 4.7). It is possible that other processes (e.g., colloid facilitated transport), which is not accounted in our model dominated the transport process.

4.4 Summary and Conclusions

In summary, we evaluated a nonlinear equilibrium-kinetic multireaction (MRM) model for its prediction capability of As(V) retention as well as transport in three soils having different soil properties. Kinetic batch experiments were carried out over a wide range of input concentrations and we concluded that As(V) adsorption was highly nonlinear with a Freundlich reaction order much less than unity for all soils investigated. Adsorption was strongly kinetic, the rate of As(V) retention was rapid initially and was followed by gradual or somewhat slow retention behavior with increasing reaction time. Based on root mean square errors, model formulations having nonlinear reversible reaction along with a consecutive or concurrent irreversible retention (M4 and M5) were considered the most favorable in describing As(V)

retention over time for all three soils. These model formulations are recommended for As prediction and for future application because the fewest number of model parameters.

Column transport experiments indicated extensive As retardation followed by slow release or extensive tailing of the BTCs. The percentages of As(V) mass recovery from column effluent ranged from 82.1% for Olivier soil to as low as 39.2% for Sharkey clay. The use of batch model parameters provided poor overall predictions of all BTCs. The use of batch rate coefficients grossly underestimated the extent of As(V) retention in Windsor and Olivier soils and overestimated As(V) mobility by all model formulations used. We thus conclude that BTC predictions based on batch parameters are not recommended. However, when the multireaction transport model was utilized in an inverse mode, the model was capable of describing As(V) BTCs for Windsor and Olivier soils. Moreover, model formulations which provided best-fit of the BTCs were consistent with those based on kinetic batch data.

4.5 References

- Amacher, M. C., H. M. Selim, and I. K. Iskandar. 1988. Kinetics of chromium(VI) and cadmium retention in soils: A nonlinear multireaction model. *Soil Sci. Soc. Am. J.* 52:398-408.
- Barnett, M.O., P.M. Jardine, S.C. Brooks, and H.M. Selim. 2000. Adsorption and transport of uranium(VI) in subsurface media. *Soil Sci. Soc. Am. J.* 64:908-917.
- Brusseau, M.L., P.S.C. Rao, R.E. Jessup, and J.M. Davidson. 1989. Flow interruption: A method for investigating sorption nonequilibrium. *J. Contam. Hydrol.* 4:223-240.
- Brusseau, M.L. 1993. The influence of solute size, pore water velocity, and intraparticle porosity on solute dispersion and transport in soils. *Water Resour. Res.* 29:1071-1080.
- Buchter, B., B. Davidoff, C. Amacher, C. Hinz, I.K. Iskandar, and H.M. Selim. 1989. Correlation of Freundlich K_d and n retention parameters with soils and elements. *Soil Sci.* 148:370-379.
- Darland, J.E., and W.P. Inskeep. 1997a. Effect of pore water velocity on the transport of arsenate. *Environ. Sci. Technol.* 31:704-709.
- Darland, J.E., and W. P. Inskeep. 1997b. Effects of pH and phosphate competition on the transport of arsenate. *J. Environ. Qual.* 26:1133-1139.

- Fuller, C.C., J.A. Davis, and G.A. Waychunas. 1993. Surface chemistry of ferrihydrite: Part 2. Kinetics of arsenate adsorption and coprecipitation. *Geochim. Cosmochim. Acta.* 57:2271-2282.
- Goldberg, S. 2002. Competitive adsorption of arsenate and arsenite on oxides and clay minerals. *Soil Sci. Soc. Am. J.* 66:413-421.
- Hiltbold, A.E., B.F. Hajek, and G.A. Buchanan. 1974. Distribution of arsenic in soil profile after repeated application of MSMA. *Weed Sci.* 22:272-275.
- Isensee, A.R., W.C. Shaw, W.A. Gretner, C.R. Swansen, B.C. Turner, and E.A. Woollen. 1973. Revegetation following massive application of selected herbicides. *Weed Sci.* 21:409-412.
- Ma, L., and H.M. Selim. 1997. Evaluation of nonequilibrium models for predicting atrazine transport in soils. *Soil Sci. Soc. Am. J.* 61:1299-1307.
- Manning B.A., and S. Goldberg. 1997. Arsenic(III) and arsenic(V) adsorption on three California soils. *Soil Sci.* 162:886-895.
- McLaren, R.G., R. Naidu, J. Smith, and K. G. Tiller. 1998. Fractionation and distribution of arsenic in soils contaminated by cattle dip. *J. Environ. Qual.* 27:348-354.
- Melamed, R., J.J. Jurinak, and L.M. Dudley. 1995. Effect of adsorbed phosphate on transport of arsenate through an oxisol. *Soil Sci. Soc. Am. J.* 59:1289-1294.
- Puls, R.W. and R.M. Powell. 1992. Transport of inorganic colloid through natural aquifer material: implication for contaminant transport. *Environ. Sci. Technol.* 26:614-621.
- Selim, H.M., R. Schulin, and H. Flüer. 1987. Transport and ion exchange of calcium and magnesium in an aggregated soil. *Soil Sci. Soc. Am. J.* 51:876-884.
- Selim, H.M., B., Buchter, C., Hinz, and L. Ma . 1992. Modeling the transport and retention of cadmium in soils - Multireaction and multicomponent approaches. *Soil Sci. Soc. Am. J.* 56:1004-1015.
- Selim, H.M., and L. Ma . 2001. Modeling nonlinear kinetic behavior of copper adsorption-desorption in soil. p. 189-212. *In* Selim, H.M. and D.L. Sparks (ed.) *Physical and Chemical Processes of Water and Solute Transport/Retention in Soil*. SSSA special publication no. 56. Soil Sci. Soc. A. Madison, WI.
- Waychunas, G.A., B.A. Rea, C.C. Fuller, and J.A. Davis. 1993. Surface chemistry of ferrihydrite: Part 1. EXAFS studies of the geometry of coprecipitated and adsorbed arsenate. *Geochim. Cosmochim. Acta.* 57:2251-2269.
- Williams, L.E., M.O. Barnett, T.A. Kramer, and J.G. Melville. 2003. Adsorption and transport of arsenic(V) in experimental subsurface systems. *J. Environ. Qual.* 32:841-850.
- Zhang, H., and H.M. Selim. 2005. Kinetics of arsenate adsorption-desorption in soils. *Environ. Sci. Technol.* 39:6101-6108.

CHAPTER 5: COMPETITIVE SORPTION KINETICS OF ARSENATE AND PHOSPHATE IN SOILS

5.1 Introduction

Phosphate (P) anion has similar chemical properties to arsenate and forms similar types of inner-sphere surface complex with Fe/Al oxide minerals. The competition between As(V) and P for adsorption sites has the potential of increasing arsenic mobility and bioavailability in soil environments (Woolson et al., 1973; Melamed et al., 1995). The competitive adsorption of P and As(V) can be affected by a wide range of factors such as surface properties of the adsorbent, concentration and molar ratio of As(V) to P, solution pH, and residence time. Based on competitive adsorption of anions on goethite and gibbsite, Hingston et al. (1971) proposed two types of adsorption sites on mineral surface; the first type is available for both anions where competition takes place while the second type of adsorption sites is specifically available for either anions.

Results from studies on single ion sorption showed that arsenate and phosphate sorption on Fe and Al oxides were somewhat similar (Hingston et al., 1971; Manning and Goldberg, 1996ab; Jain and Loeppert, 2000; Liu et al., 2001). However, when added simultaneously in equal molar, Violante and Pigna (2002) reported that metal oxides and phyllosilicates rich in Fe were more effective in adsorbing As(V) than P, while more P was adsorbed than As(V) on minerals rich in Al. Adsorption studies on soils often reveal that P is preferentially adsorbed than As(V) whether added separately or added simultaneously in equal molar ratios (Roy et al., 1986ab). Amounts of As(V) sorbed on minerals and soils exhibited a decrease with increasing additions of P in solution. Adsorbed As(V) on soils can be partly displaced by the addition of P, which was used to assess arsenic availability in soils (Keon et al., 2001). Moreover, the sequence of addition might significantly affect the competition between As(V) and P (Liu et al., 2001;

Zhao and Stanforth, 2001). Liu et al. (2001) found that when added sequentially (arsenate before phosphate vs. phosphate before arsenate), more P was replaced by As(V) on goethite than vice versa. Similar results of the displacement of P adsorbed on soils by As(V) additions were reported by Barrow (1974). Due to the similar dissociation constants of phosphate ($pK_a^1=2.23$, $pK_a^2=7.2$, $pK_a^3=12.3$) and arsenate ($pK_a^1=2.20$, $pK_a^2=6.97$, $pK_a^3=11.53$), adsorption of both anions decreases with increasing pH (Hingston et al., 1971; Manning and Goldberg, 1996ab; Jain and Loeppert, 2000). When added simultaneously, Jain and Loeppert (2000) reported that the effect of P on As(V) adsorption on ferrihydrite was greater at high pH than at low pH. Similar results were reported for several metal oxides and clay minerals (Manning and Goldberg, 1996ab).

Attempts have been made to model competitive adsorption between As(V) and P. A Langmuir type of model with parameters of surface sites and reaction constants for each solute was developed by Hingstons et al. (1971) to describe competitive adsorption between multiple ligands. A competitive Freundlich-type equation, known as Sheindorf-Rebhun-Sheintuch (SRS) equation (Sheindorf et al., 1981), was latter adopted by Roy et al. (1986ab) to describe the competitive adsorption isotherms of As(V) and P in several soils. Surface complexation models with one or two adsorption sites were applied by Manning and Goldberg (1996ab) to simulate binary adsorption envelopes on multiple minerals. Using binding mechanisms observed from spectroscopy results, Hiemstra and van Riemsdijk (1999) simulated competitive adsorption of As(V) and P on metal oxides with a multi-site surface complexation model.

For most studies on competitive adsorption, equilibrium conditions are often assumed. Several experiments demonstrated adsorption of arsenate (Fuller et al., 1993; Raven et al., 1998) and phosphate (Barrow, 1992; Gimsing et al., 2004) on minerals and soils are both time-

dependent. A literature search revealed that the influence of residence time on competitive adsorption of arsenate and phosphate in soils was not studied. In this study, kinetic batch experiments were carried out to quantify competitive adsorption-desorption of As(V) and P in soils. Furthermore, release or desorption of As(V) and P was carried out following adsorption using successive dilution. Specifically, the objective of this study were: i) to determine the competitive adsorption kinetics of As(V) and P in several soils of distinctly different properties; ii) to quantify the characteristics of release or desorption of As(V) and P in soils; and iii) to model competitive adsorption using equilibrium (modified Freundlich) and kinetic (multireaction) models.

5.2 Material and Methods

Kinetic batch experiments were conducted to quantify the competitive adsorption and desorption kinetics of As(V) and P in the above soils. Reagent grade KH_2AsO_4 and KH_2PO_4 were used. Mixed solutions at different As/P molar-ratios (0.0/0.32, 0.0/3.2, 0.13/0.0, 0.13/0.32, 0.13/1.3, 0.13/3.2, 1.3/0.0, 1.3/0.32, and 1.3/3.2 mM) were also prepared. All solutions were prepared in 0.01M KNO_3 background solution to maintain a constant ionic strength. Batch experiments were carried out in duplicates where 3.0 g of air dry soil were mixed with 30 ml of solution in a 40-mL Teflon tube. The mixtures were shaken at 150 rpm on a reciprocal shaker and subsequently centrifuged for 10 minutes at 4000 rpm for each specific reaction time. Following this, a 1-mL aliquots were sampled from the supernatant at reaction times of 6, 24, 72, 168, 336, and 504 h and diluted to 6mL for further analysis. After sampling, the pH of the supernatant was measured with standard pH meter and samples were reweighed. The slurry was agitated using a vortex mixer and returned to the shaker. The collected samples were analyzed for total As and P concentrations using ICP-AES (Spectro Citros CCD). The amounts of As(V)

and P retained by each soil was calculated from the difference between concentrations of the supernatant and that of the initial solutions.

Desorption was initiated immediately after the last adsorption step (504 h) for all initial concentrations. Sequential or successive dilutions of the slurries were carried out to induce release or desorption of As(V) and P retained by the soil matrix. Each desorption step was conducted by replacing the supernatant with 0.01 M KNO₃ background solution and shaking for 48 h. Four desorption steps were carried out with a total desorption time of 192 h. The fraction of As(V) and P desorbed from the soils were calculated based on the change in concentration in solution (before and after desorption). Moreover, the pH of the supernatant was also measured following each reaction time.

Following the last desorption step, the soils were mixed with 20 mL of 0.2M ammonium oxalate and shaken for 16 h in dark to determine oxalate extracted arsenic. At the end of the experiment, the residual arsenic was determined by mixing soil with 4 N HNO₃ solutions and shaking for 2h in a water-bath maintained at 80°C.

5.3 Results and Discussion

5.3.1 Adsorption Isotherms

Single anion adsorption isotherms for As(V) and P for the three soils at 24 hours of reaction are presented in Figure 5.1. The Freundlich parameters K_F and N given in Table 5.1 were obtained by fitting the adsorption isotherms to Eq. 3.6 with nonlinear least square optimization.

Sorption behavior for As(V) and P exhibited nonlinear or concentration-dependent patterns. Nonlinearity is characterized by the low values of the Freundlich reaction order N , which ranged from 0.287 to 0.341 for As(V) and 0.387 to 0.486 for P (see Table 5.1). The

parameter N may be regarded as a representation of energy distribution of heterogeneous adsorption sites for solute retention by matrix surfaces (Sheindorf et al., 1981). Nonlinearity and competition are often regarded as characteristics of site-specific adsorption processes. Here adsorption occur preferentially at the sites with higher adsorption affinity and occupy the available sites with lower adsorption potential with increasing concentration. According to Xing et al. (1996), overlapping set of adsorption sites available for the anions results in competitive adsorption.

Consistent with observations by other researchers (Roy et al., 1986ab), our results indicated higher adsorption capacity for P than As(V) on all three soils. Moreover, the relative sorption affinities of the three soils to As(V) and P were distinctly different. Sharkey soil exhibited the highest adsorption for As(V) whereas Windsor soil showed the highest adsorption for P. Olivier soil exhibited the lowest adsorption for both As(V) and P (see Figure 5.1). As suggested by several studies, both As(V) and P are primarily adsorbed on Fe/Al (hydro)oxides as inner-sphere complex and soil sorption capacities for As(V) and P are highly correlated with soil contents of Fe and Al (Smith et al., 2002; De Brouwere et al., 2004). Violante and Pigna (2002) reported that minerals rich in Fe had higher affinity to As(V) than P, while Al oxides had higher affinity to P than As(V). For our three soils, the differences in the soil content of Fe/Al oxides explain the differences in adsorption affinities to As(V)/P. Specifically, Sharkey soil has the highest content of citrate-bicarbonate-dithionite (CBD) and ammonium-oxalate extractable Fe and thus has the highest adsorption capacity to As(V). On the other side, the extractable Al and adsorption capacity to P are the highest for Windsor.

5.3.2 Competitive Adsorption

Competitive sorption of arsenate in the presence of phosphate are depicted in Figure 5.2, which shows amount of arsenate sorbed, after 24 h of reaction, in the presence of different phosphate input concentrations. Our experiment results clearly demonstrate that arsenate adsorption decreased substantially with increasing phosphate concentrations. When 3.2mM phosphate was added, the percent reductions in arsenate adsorption were 38%, 50%, and 37% for Olivier, Sharkey, and Windsor, respectively. In addition, the competition was generally greater at low P concentrations and leveled off with increasing P.

Competition for specific adsorption sites is likely the major cause for the observed competitive effect between arsenate and phosphate shown in Figure 5.2. Formation of surface complexation between Fe/Al (hydro)oxides and As(V)/P restricted the accessibility of those surface sites for further adsorption (Hingston et al., 1971). Because adsorption of both anions takes place preferentially on high affinity sites, the competition is expected to be greatest at low As(V) and P concentrations, which is consistent with our observation.

Sheindorf et al. (1981) introduced a modification of Freundlich equation [1] in order to account for adsorption when more than one competing ions is present in the solution. Specifically, the Sheindorf-Rebhun-Sheintuch (SRS) model was developed to describe competitive equilibrium sorption for multicomponent systems. Here it was assumed that for a single component, sorption isotherms follow the Freundlich equation. The derivation of SRS equation was also based on the assumption of an exponential distribution of adsorption energies for each component. A general form of the SRS equation may be written as

$$S_i = K_{Fi} C_i \left(\sum_{j=1}^l \alpha_{ij} C_j \right)^{N_i-1} \quad [5.1]$$

Table 5.1 Estimated Freundlich and SRS parameters for 24 h adsorption of arsenate and phosphate

Soil	Arsenate			Phosphate			Competition		
	K_f mM mM ^{-N}	N	r^2	K_f mM mM ^{-N}	N	r^2	α_{As-P}^b	α_{P-As}	r^2
Olivier	2.72±0.14 ^a	0.311±0.040 ^a	0.993	4.13±0.11	0.461±0.033	0.997	0.282	1.04	0.998
Sharkey	8.50±0.47	0.341±0.034	0.994	11.2±0.30	0.387±0.027	0.997	0.442	1.56	0.995
Windsor	4.24±0.11	0.287±0.017	0.998	9.76±0.37	0.486±0.039	0.996	0.302	1.90	0.952

^a one standard error

^b competitive coefficients were obtained by fitting 24h competitive adsorption data to SRS equation.

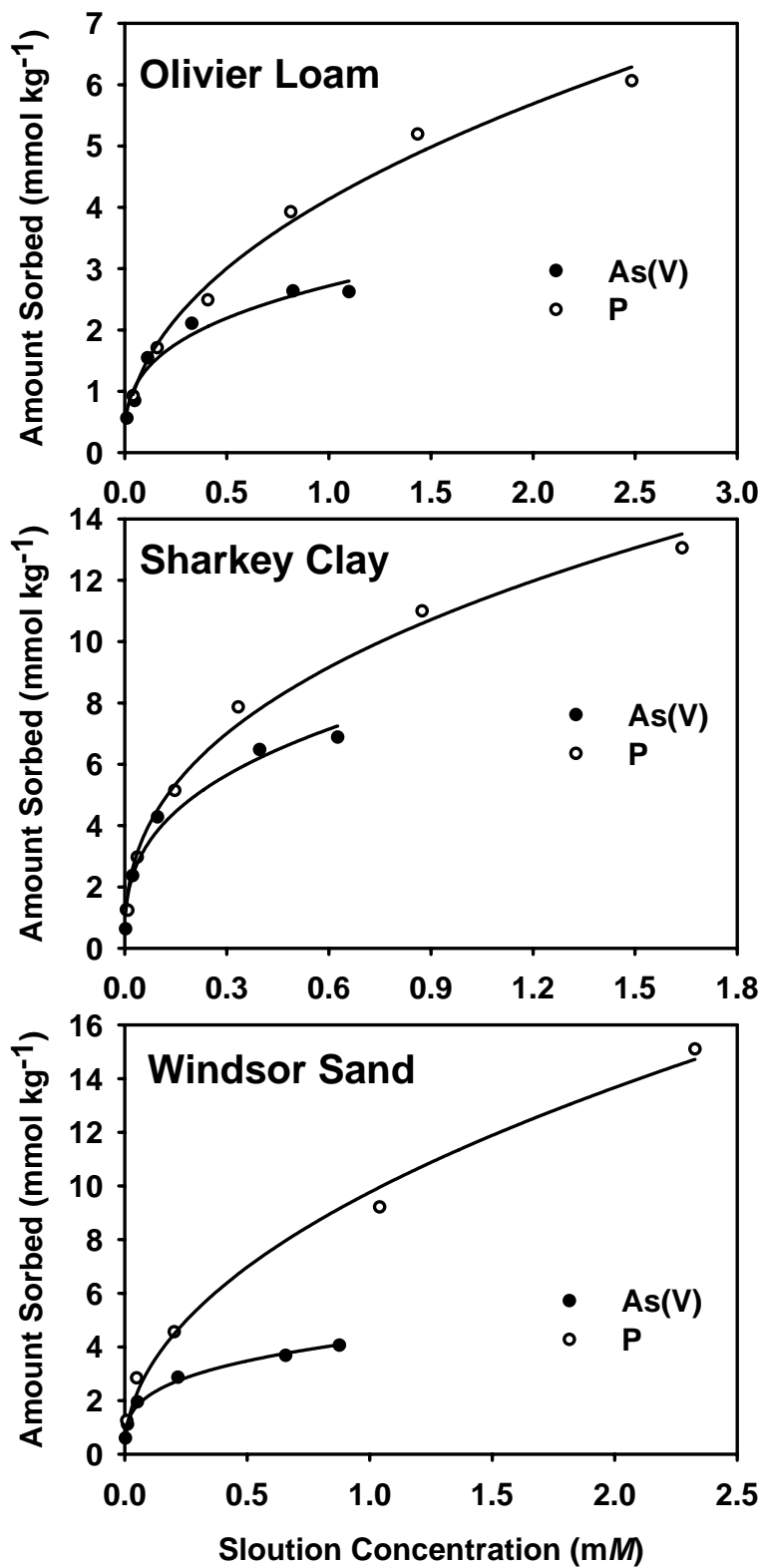


Figure 5.1 Arsenate [As(V)] and phosphate (P) adsorption isotherms at 24 h of reaction for Olivier, Sharkey, and Windsor soils. The lines depict results of curve-fitting with Freundlich equation.

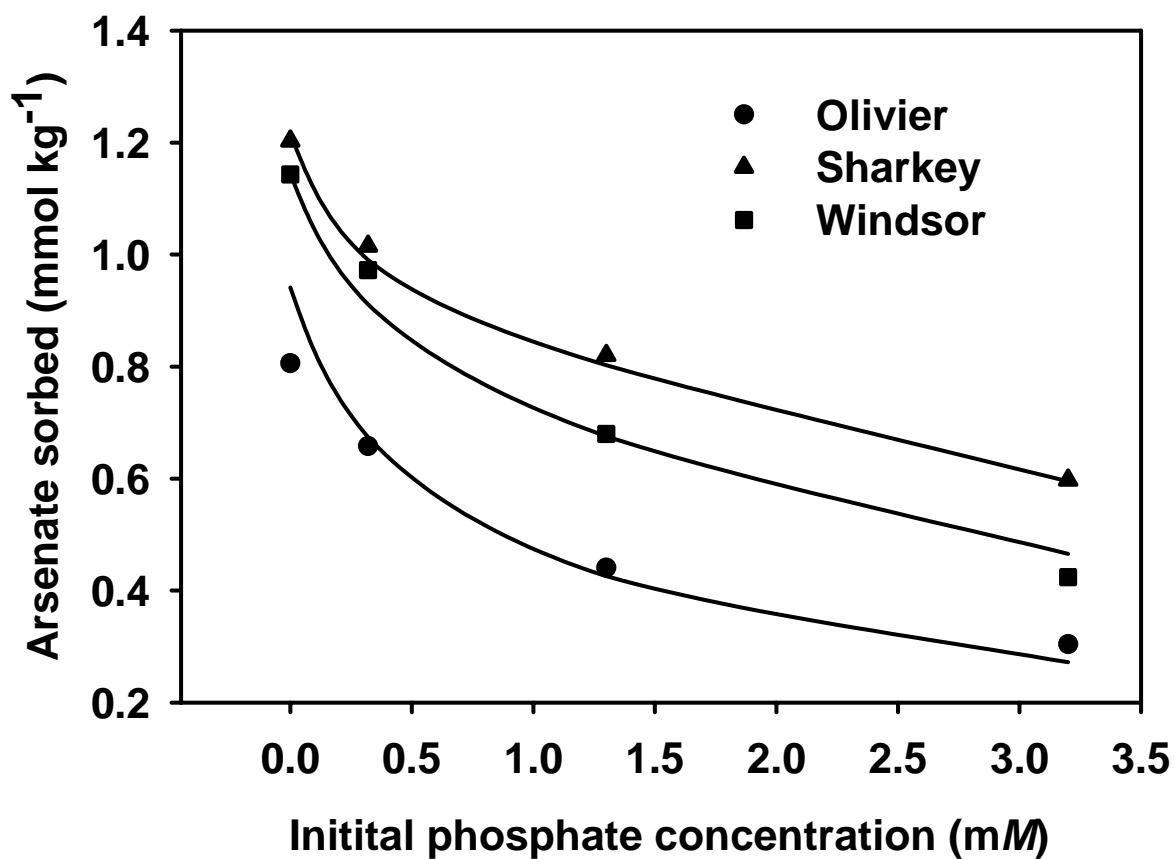


Figure 5.2 Competitive sorption between arsenate and phosphate at 24 h of reactions for Olivier, Sharkey, and Windsor soils. The initial concentrations of arsenate were 0.13 mM.

where l is the total number of components, i and j represent components i and j , α_{ij} is a dimensionless competition coefficient that describes the inhibition by component j to the adsorption of component i where $\alpha_{ij} = 1$ when $i = j$. In the absence of competitive sorption, i.e., $\alpha_{ij} = 0$ for $i \neq j$, equation (2) yields the Freundlich equation [1] for a single component.

The SRS equation was employed to quantify competitive adsorption of As(V) and P. Specifically, the Freundlich K_F and N were taken from the single-anion adsorption data and utilized to obtain the competitive coefficients α_{ij} by fitting the competitive adsorption data to Eq. 2 with nonlinear least square optimization. Estimates for best-fit α_{ij} are given in Table 5.1. We should emphasize that the SRS equation should only be regarded as an empirical model and the conformity of this equation do not imply certain reaction mechanisms. In their original paper, Sheindorf et al. (1981) defined α_{ij} as symmetrical values, i.e., $\alpha_{ij} = 1/\alpha_{ji}$. However, Roy et al. (1986ab) suggested that the coefficients should be regarded as empirical values describing the degree of competition under specific experimental conditions. Furthermore, Barrow et al. (2005) used nonlinear curve fitting to determine the competitive coefficients between arsenate and phosphate and they found that the coefficients were not symmetrical.

5.3.3 Adsorption Kinetics

Results from the kinetic batch experiments are presented in Figure 5.3 in order to illustrate the changes in As(V) concentration versus time in the presence of various concentrations of P by the different soils. Similarly, adsorption kinetics of P at different concentrations of As(V) are presented in Figure 5.4. The extent of As(V) sorbed by all soils were significantly reduced as concentrations of P in the applied solution increased. Moreover, both

As(V) and P exhibited strongly time-dependent adsorption behavior which is depicted by the continued decrease of concentration with reaction time.

Observed retention kinetics of As(V) and P in Figure 5.3 and 5.4 is likely due to the heterogeneity of the soil surface where multiple chemical and physical processes take place. Chemical reaction rates of surface complexation between anions and metal oxides are considered rapid. Using a pressure jump relaxation technique, Grossl et al. (1997) calculated a kinetic rate constant of $10^{6.3} \text{ s}^{-1}$ for the formation of mono-dentate inner-sphere surface complex on goethite surface. In addition, a forward rate constant of 15 s^{-1} was associated with succeeding reaction for the formation of bidentate mononuclear surface complex on goethite surface. Because of their rapid reaction rates, surface complexation is not a rate-limiting step of arsenate and phosphate adsorption in soils. However, different types of surface complexes (e.g., mono-dentate, bi-dentate, mono-nuclear, bi-nuclear) can be formed on oxide surfaces at high or low surface coverage. This heterogeneity of sorption sites may contribute to adsorption kinetics observed in our experiments, i.e., where sorption takes place preferentially on high affinity sites and followed by slow sorption to sites of low sorption affinity. In addition, rearrangement of the surface complexes from high energy state to low energy state may be another factor for the adsorption kinetics.

Recent adsorption studies suggested that surface precipitation, i.e., three dimensional growth of a particular surface phase, may occur for both arsenate and phosphate (Jia et al., 2006). The development of surface precipitate is a slow process involving multiple reaction steps and partially explained the slow As(V) and P retention kinetics. The theory of surface precipitation suggests that anions adsorbed on mineral surfaces attract dissolved Fe or Al. The adsorbed Fe or Al in turn adsorbs more anions, result in a multilayer adsorption. Zhao and Stanforth (2001)

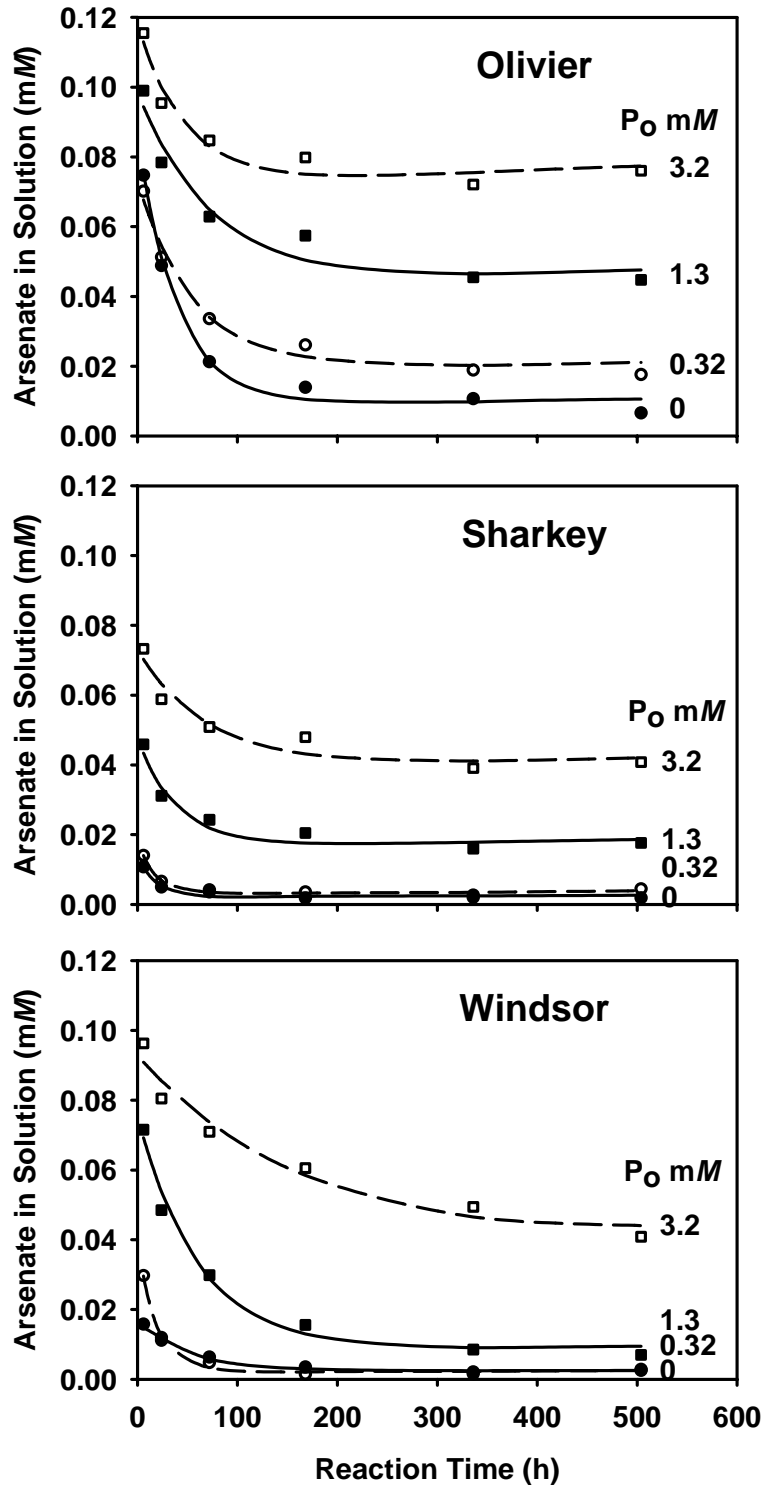


Figure 5.3 Arsenate concentrations in solution as a function of reaction time during adsorption on Olivier, Sharkey, and Windsor soils in the presence of various concentrations of phosphate. The initial concentrations of arsenate were 0.13 mM. The initial concentrations of phosphate were 0, 0.32, 1.3, and 3.2 mM. The lines depict results of MRM simulation.

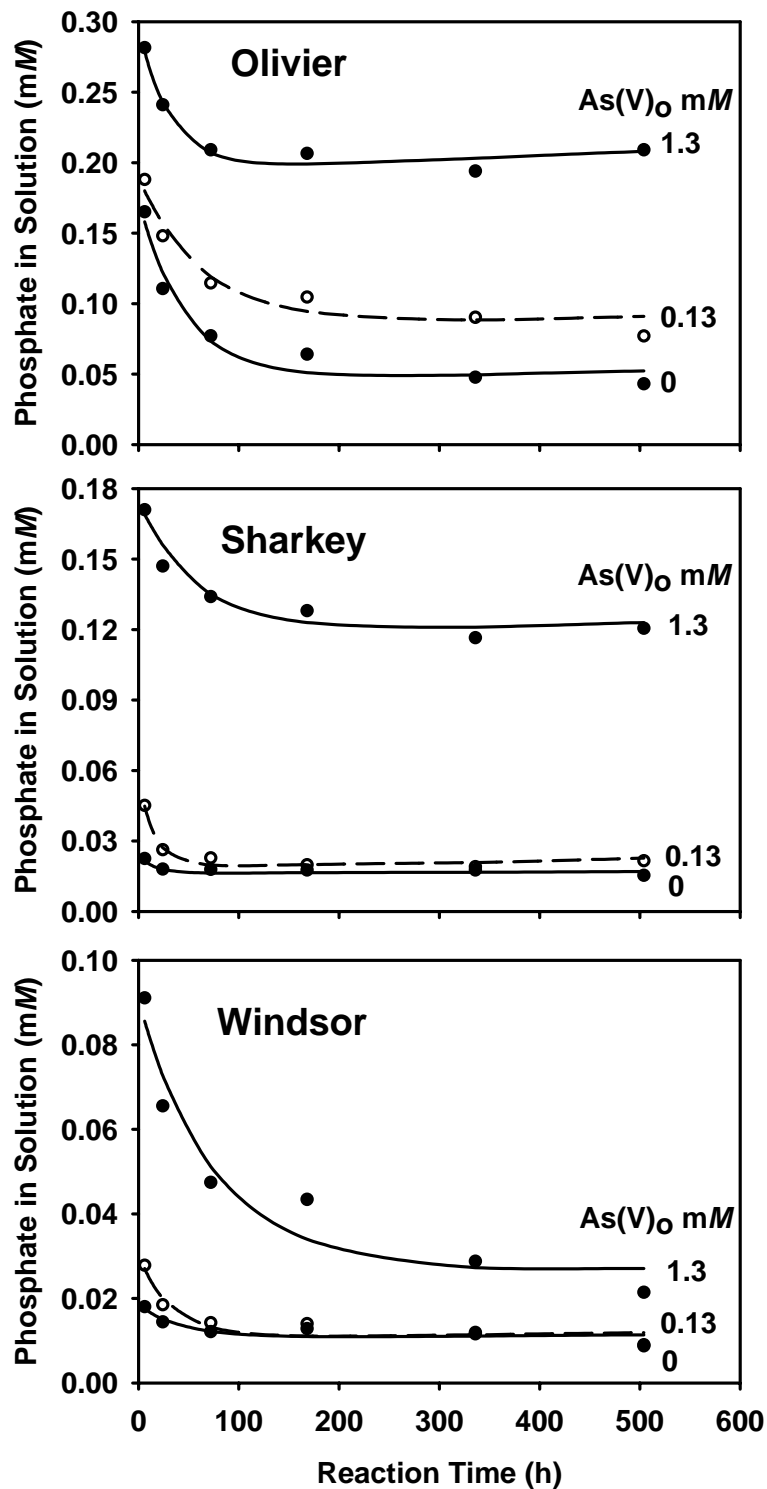


Figure 5.4 Phosphate concentrations in solution as a function of reaction time during adsorption on Olivier, Sharkey, and Windsor soils in the presence of various concentrations of arsenate. The initial concentration of phosphate was 0.32 mM. The initial concentrations of arsenate were 0, 0.13, and 1.3 mM. The lines depict results of MRM simulation.

suggested the slow buildup of surface precipitate as the mechanisms of irreversible As(V) and P retention on goethite. More recently, the XRD and Raman spectroscopy results of Jia et al. (2006) confirmed the formation of poorly crystalline ferric arsenate surface precipitate on ferrihydrite under high As/Fe molar ratio, low pH, and long reaction time.

Diffusion of As(V) and P to reaction sites within the soil matrix was also proposed as the explanation to the time-dependent adsorption (Fuller et al., 1993; Raven et al., 1998). Two-phase process was generally assumed for diffusion controlled adsorption, with the reaction occur instantly on liquid-mineral interfaces during first phase whereas slow penetration or intraparticle diffusion is responsible for the second phase. Pore space diffusion model has been employed by Fuller et al. (1993) and Raven et al. (1998) to describe the slow sorption of As(V) on ferrihydrite. For heterogeneous soil system, the complex network of macro- and micro- pores may further limit the access of solute to the adsorption sites and cause the time-dependent adsorption.

5.3.4 Desorption and Sequential Extraction

As described in the experimental methods section, following last adsorption step, arsenic retained by the soils was desorbed using successive dilution with 0.01 M KNO₃ and subsequently extracted by chemical agents (oxalate, nitric acid). The amounts of arsenic released by desorption and sequential extractions are presented in Figure 5.5. After four steps of successive dissolution, relatively small amounts of Arsenic were released from the soils. This indicates high sorption affinity of arsenic by the solid matrix. Our desorption results are consistent with earlier studies which indicated significant irreversibility and extensive desorption hysteresis of arsenic sorbed by mineral (Fuller et al., 1993; Lin and Puls, 2000; O'Reilly et al., 2001; Arai and Sparks, 2002) and soil (Woolson et al., 1973; Zhang and Selim, 2005). Furthermore, increased phosphate concentrations did not substantially change the fraction of arsenic desorbed by successive

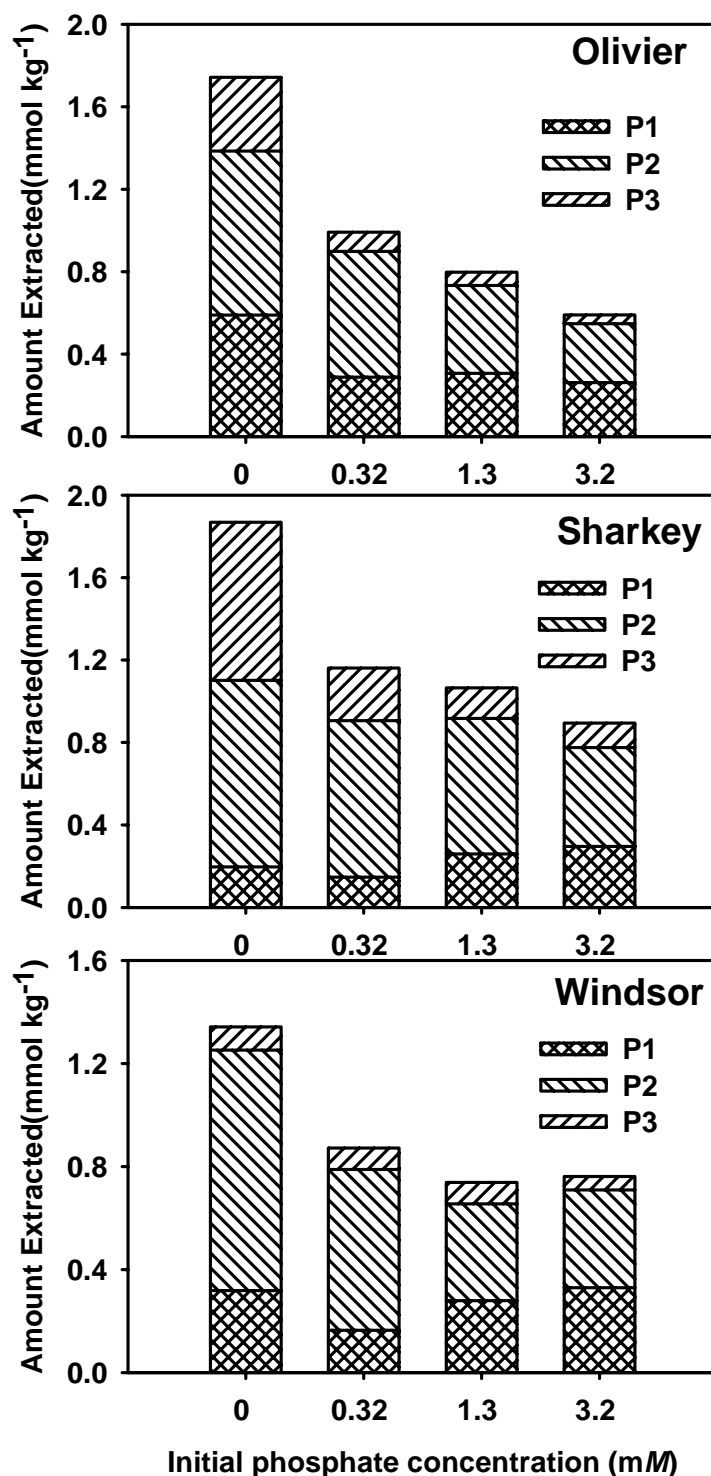


Figure 5.5 Recoveries of arsenic from desorption and sequential extractions for different soils. Different patterns illustrate arsenic distribution among the following pools: P1 = desorbed during successive desorption, P2 = extracted with 0.2 *M* ammonium oxalate, and P3 = digested with 4 *M* HNO₃. Different groups indicate different initial phosphate concentrations of 0, 0.32, 1.3, and 3.2 mM.

dilutions from our soils. This suggests that competition is perhaps weak on the exchangeable phase where arsenic is ionically bound with electrostatic interaction.

Since arsenate and phosphate are mainly adsorbed on the Fe/Al oxides as mono- or bidentate inner-sphere surface complexes through ligand exchange mechanisms, extraction with 0.2 M ammonium oxalate (pH=3) was intended to release arsenic which is strongly bound with Fe/Al oxides through ligand-promoted dissolution (Keon et al., 2001). Our results of Figure 5.5 demonstrate that the oxalate extracted arsenic constituted the major fraction of arsenic adsorbed. This indicates that formation of inner-sphere surface complex with Fe/Al oxides are the dominant mechanisms of arsenic adsorption in our soils. Furthermore, the fractions of oxalate extractable arsenic were significantly reduced when phosphate concentrations in solutions increased in all three soils, suggesting that the competition for adsorption sites on Fe/Al oxides were the major cause of competitive effect of P on As(V) adsorption. Besides electrostatic interaction and inner-sphere surface complexation, coprecipitation with crystalline minerals might also contribute to arsenic adsorption, which was illustrated by the acid extracted fraction of arsenic in Figure 5.5. The formation of precipitation, if any, will certainly cause irreversible retention of As(V)/P.

5.3.5 Selectivity Coefficients

An empirical selectivity coefficient (K_{As-P}) was utilized to evaluate the relative preferences of soil adsorption for As(V) over P (De Brouwere et al., 2004). It was calculated as

$$K_{As-P} = \frac{S_{As}}{S_P} \frac{C_P}{C_{As}} \quad [5.2]$$

Since As(V) and P are both specifically adsorbed on soils, the selectivity coefficient K_{As-P} here is strictly empirical and should not be used to deduce the exchange behavior between As(V)

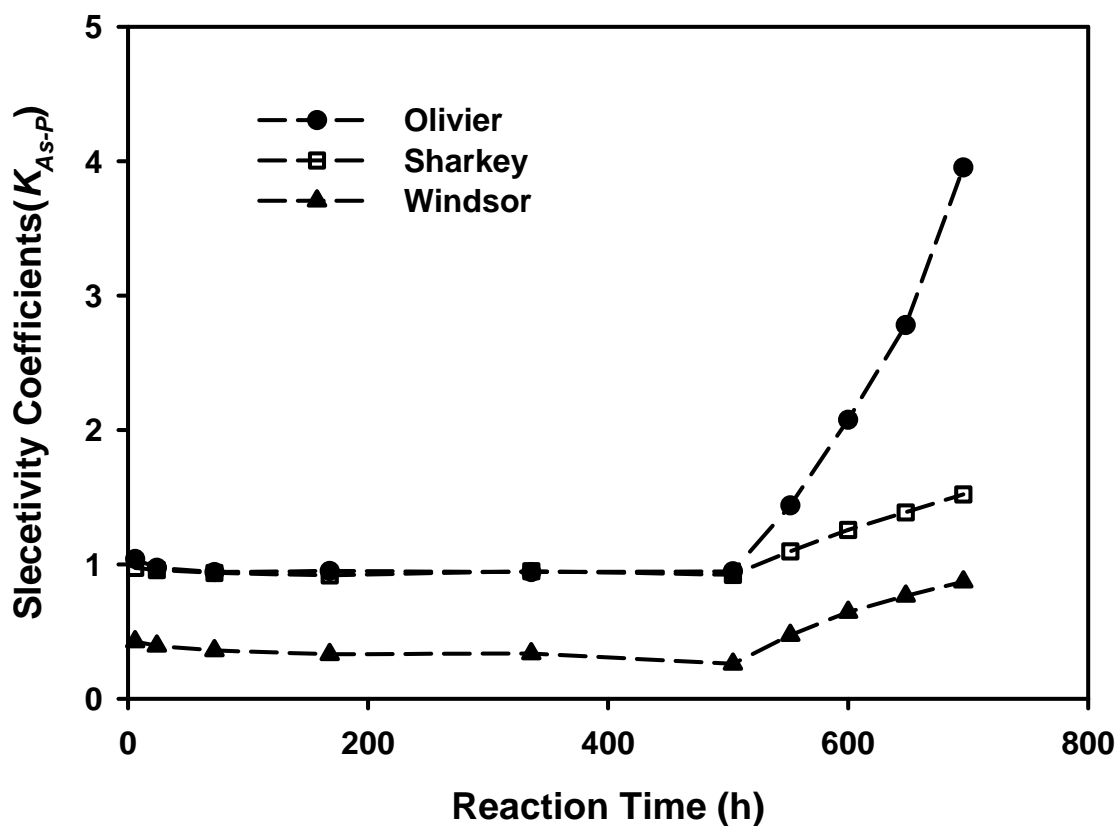


Figure 5.6 Selectivity coefficients of arsenate to phosphate as a function of reaction time for Olivier, Sharkey, and Windsor soils. Initial concentrations were 1.3 and 3.2 mM for arsenate and phosphate, respectively.

and P as commonly conducted for ion exchange reactions. Furthermore, the value of K_{As-P} varies with As/P molar ratio because of the nonlinear (concentration-dependent) adsorption behavior of the anions.

The K_{As-P} values depicted in Figure 5.6 clearly show that the selectivity did not change with reaction time for all three soils. Based on these estimates, there is no preferential adsorption for P over As(V) for Olivier and Sharkey soil. Specifically, K_{As-P} is close to 1 for both soils ($K_{As-P} = 0.95 \pm 0.02$ for Olivier and 0.94 ± 0.02 for Sharkey). However, selective adsorption of P over As(V) was observed for Windsor soil, with an average K_{As-P} of 0.34 ± 0.06 (Figure 5.6). Such difference in their selectivity toward As(V) or P is likely a result of their mineral constituents. Violante and Pigna (2002) showed that As(V) was preferentially adsorbed by minerals rich in Fe whereas P was preferentially sorbed by minerals rich in Al. The higher Al/Fe ratio of Windsor (0.50) soil used in this experiment than Olivier (0.20) or Sharkey (0.24) soil perhaps explain the observed differences in their selectivity toward As or P. Moreover, the increase of K_{As-P} during desorption process (Figure 5.6) suggested that more P than As(V) was desorbed from soils. Liu et al. (2001) suggested that arsenate interacts more strongly on goethite surface than phosphate because arsenate is of larger molecular size and form more bi-dentate complexes with Fe oxides.

5.3.6 Multi-reaction Modeling

Simulations of the time-dependent retention behavior of As(V) and P shown in Figures 5.3 and 5.4 were carried using our multireaction model (MRM). Estimated parameters and their goodness-of-fit for different soils and initial concentrations are given in Tables 5.2 and 5.3. We recognize that the model accounts for a number of reactions and different formulations of MRM represent different reactions from which one can deduce retention mechanisms. In Chapter 3 and

Table 5.2 Estimated MRM parameters for the kinetic adsorption of arsenate in the presence of various concentrations of phosphate

P_o^a mM	Ke	k_1 h ⁻¹	k_2 h ⁻¹	k_3 h ⁻¹	r^2
Olivier					
0	0.94±0.13	0.0055±0.0011	0.016±0.005	0.0012±0.0008	0.986
0.32	1.0±0.1	0.0039±0.0011	0.019±0.007	0.0015±0.0007	0.993
1.3	0.40±0.07	0.0042±0.0010	0.033±0.008	0.0015±0.0003	0.999
3.2	0.12±0.08	0.0038±0.0012	0.038±0.010	0.00080±0.00026	0.999
Sharkey					
0	2.9±0.6	0.023±0.005	0.035±0.007	0.00089±0.00040	0.976
0.32	3.6±0.2	0.013±0.003	0.025±0.008	0.00022±0.00052	0.986
1.3	1.8±0.1	0.0068±0.0013	0.034±0.007	0.0012±0.0003	0.998
3.2	1.0±0.1	0.0047±0.0013	0.041±0.011	0.0014±0.0003	0.999
Windsor					
0	2.9±0.1	0.0046±0.0009	0.015±0.004	0.0016±0.0006	0.994
0.32	1.9±0.1	0.0085±0.0011	0.017±0.004	0.00065±0.00069	0.993
1.3	0.90±0.06	0.0042±0.0007	0.018±0.005	0.0026±0.0007	0.997
3.2	0.45±0.04	0.0035±0.0007	0.043±0.009	0.0031±0.0003	0.999

^a initial concentrations of phosphate.

^b one standard error.

Table 5.3 Estimated MRM parameters for the kinetic adsorption of phosphate in the presence of various concentrations of arsenate

As_o^a mM	Ke	k_1 h ⁻¹	k_2 h ⁻¹	k_3 h ⁻¹	r^2
Olivier					
0	2.2±0.4	0.016±0.005	0.029±0.010	0.0018±0.0007	0.991
0.13	2.0±0.3	0.0096±0.0038	0.027±0.012	0.0018±0.0007	0.995
1.3	0.32±0.14	0.0066±0.0018	0.030±0.008	0.00025±0.00026	0.999
Sharkey					
0	9.3±7.1	0.044±0.218	0.13±0.33	0.00093±0.00137	0.983
0.13	6.3±0.3	0.028±0.005	0.046±0.007	0.00048±0.00018	0.998
1.3	2.2±0.1	0.0064±0.0018	0.040±0.010	0.0011±0.0003	0.999
Windsor					
0	16±2	0.034±0.033	0.058±0.047	0.0019±0.0010	0.993
0.13	12±1	0.042±0.025	0.045±0.026	0.0020±0.0009	0.986
1.3	5.2±0.3	0.019±0.005	0.036±0.009	0.0032±0.0005	0.998

^a initial concentrations of arsenate.

^b one standard error.

4, we found that nonlinear reversible along with consecutive or concurrent irreversible reactions were the dominant mechanisms for describing time-dependent As(V) retention in soils. In this study, the kinetic adsorption data from the batch study were well described with several MRM model versions. Moreover, several model versions results in similar predictions. For As(V), model versions with equilibrium phase (S_e), kinetic reversible phase (S_1) and consecutive irreversible phases (S_i) are recommended, however. Similar findings were obtained for P where model versions with equilibrium and kinetic reactions provided best predictions for all three soils. We should emphasize here that the goodness of fit of the model to the P and As(V) data was based on r^2 and *RMSE*. Mansell et al. (41) utilized MRM with two types of reversible sites to describe P transport in several columns of Florida soils. They concluded that MRM predictions were highly concentration-dependent (C_0).

The effect of the presence of P at different concentration on competitive As(V) adsorption is well depicted by the multireaction model. A major feature of the model is that the rate coefficients associated with reversible reactions (S_e and S_1) exhibited a marked decrease as P concentrations in solution increased. Values of consecutive irreversible reaction rate (k_3) did not significantly change with P addition. The relatively stable irreversible reaction rate is expected because this reaction is assumed to be the rearrangement or transformation of the arsenate adsorbed on mineral surfaces and should not be affected by the competition. Such trends are supportive of our experimental observations shown in Figures 5.3-5.4.

5.4 Summary and Concluions

The competition between arsenate [As(V)] and phosphate (P) has the potential of increasing arsenic mobility and bioavailability in natural soil and water environment. In this study, kinetics of competitive adsorption-desorption of As(V) and P was investigated in batch

systems by introducing their mixed solutions at different molar ratios to three soils having different properties. Sampling was carried out at different adsorption times (up to 504 h) and release or desorption was investigated using successive dilutions following adsorption. The highly nonlinear single-solute isotherms of As(V) and P were observed for Olivier, Sharkey, and Windsor soils. Our results demonstrated that rates and amounts of As(V) adsorption by these soils were significantly reduced by increasing P additions. In addition, the adsorption preferences of the soils to As(V) and P were constant during the adsorption period. The highly time-dependent retention data of both As(V) and P were successfully described with multireaction model (MRM). Only a small fraction of As(V) was desorbed in our experiments and a significant amount of As(V) was irreversibly adsorbed on all soils as demonstrated by the sequential extraction procedure.

In summary, our results indicated that (1) the extent of As(V) adsorption on all soils was substantially reduced by increasing phosphate input concentration and the competitive effect was explained by the competition for specific adsorption sites on Fe/Al oxides; (2) while adsorption of both As(V) and P are highly time-dependent for all three soils, selectivity coefficients of As(V) to P was constant with reaction time during adsorption; (3) MRM rate coefficients for As(V) adsorption on kinetic sites decreased with increasing P additions and indicated the competition on kinetic sites.

5.5 References

- Barrow, N.J. 1974. Displacement of adsorbed anions from soil. 2. Displacement of phosphate by arsenate. *Soil Sci.* 117:28-33.
- Barrow, N.J. 1992. The effect of time on the competition between anions for sorption. *J. Soil Sci.* 43:421-428.
- Barrow, N.J., P. Cartes, and M.L. Mora. 2005. Modifications to the Freundlich equation to describe anion sorption over a large range and to describe competition between pairs of ions. *Euro. J. Soil Sci.* 56:601-606.

- De Brouwere, K., E. Smolders, and R. Merckx. 2004. Soil properties affecting solid-liquid distribution of As(V) in soils. *Euro. J. Soil Sci.* 55:165-173.
- Fuller, C.C., J.A. Davis, and G.A. Waychunas. 1993. Surface chemistry of ferrihydrite: Part 2. Kinetics of arsenate adsorption and coprecipitation. *Geochim. Cosmochim. Acta* 57:2271-2282.
- Gimsing, A.L., O.K. Borggaard, and P. Sestoft. 2004. Modeling the kinetics of the competitive adsorption and desorption of glyphosate and phosphate on goethite and gibbsite and in soils. *Environ. Sci. Technol.* 38:1718-1722.
- Grossl, P.R., M.J. Eick, D.L. Sparks, S. Goldberg, and C.C. Ainsworth. 1997. Arsenate and chromate retention mechanisms on goethite. 2. Kinetic evaluation using a pressure-jump relaxation technique. *Environ. Sci. Technol.* 31:321-326.
- Hiemstra, T., and W.H. Van Riemsdijk. 1999. Surface structural ion adsorption modeling of competitive binding of oxyanions by metal (hydr)oxides. *J. Colloid Interface Sci.* 210:182-193.
- Hingston, F.J., A.M. Posner, and J.P. Quirk. 1971. Competitive adsorption of negatively charged ligands on oxide surfaces. *Disc. Faraday Soc.* 52:334-342.
- Jain, A., and R.H. Loeppert. 2000. Effect of competing anions on the adsorption of arsenate and arsenite by ferrihydrite. *J. Environ. Qual.* 29:1422-1430.
- Jia, Y.F., L.Y. Xu, Z. Fang, and G.P. Demopoulos. 2006. Observation of surface precipitation of arsenate on ferrihydrite. *Environ. Sci. Technol.* 40:3248-3253.
- Keon, N.E., C.H. Swartz, D.J. Brabander, C. Harvey, and H.F. Hemond. 2001. Validation of an arsenic sequential extraction method for evaluating mobility in sediments. *Environ. Sci. Technol.* 35:2778-2784.
- Liu, F., A. De Cristofaro, and A. Violante. 2001. Effect of pH, phosphate and oxalate on the adsorption/desorption of arsenate on/from goethite. *Soil Sci.* 166:197-208.
- Manning, B.A., and S. Goldberg. 1996a. Modeling competitive adsorption of arsenate with phosphate and molybdate on oxide minerals. *Soil Sci. Soc. Am. J.* 60:121-131.
- Manning, B.A., and S. Goldberg. 1996b. Modeling arsenate competitive adsorption on kaolinite, montmorillonite and illite. *Clays Clay Miner.* 44:609-623.
- Mansell, R.S., S.A. Bloom, B. Burgoa, P. Nkedikizza, and J.S. Chen. 1992. Experimental and simulated p-transport in soil using a multireaction model. *Soil Sci.* 153:185-194.
- Melamed, R., J.J. Jurinak, and L.M. Dudley. 1995. Effect of adsorbed phosphate on transport of arsenate through an oxisol. *Soil Sci. Soc. Am. J.* 59:1289-1294.
- Raven, K.P., A. Jain, and R.H. Loeppert. 1998. Arsenite and arsenate adsorption on ferrihydrite: Kinetics, equilibrium, and adsorption envelopes. *Environ. Sci. Technol.* 32:344-349.
- Roy, W.R., J. J. Hassett, and R.A. Griffin. 1986. Competitive coefficient for the adsorption of arsenate, molybdate, and phosphate mixture by soils. *Soil Sci. Soc. Am. J.* 50:1176-1182.

- Roy W.R., J.J. Hassett, and R.A. Griffin. 1986. Competitive interactions of phosphate and molybdate on arsenate adsorption. *Soil Sci.* 142: 203-210.
- Sheindorf, C., M. Rebhun, and M. Sheintuch. 1981. A freundlich-type multicomponent isotherm. *J. Colloid Interface Sci.* 79:136-142
- Smith, E., R. Naidu, and A.M. Alston. 2002. Chemistry of inorganic arsenic in soils: II. Effect of phosphorous, sodium, and calcium on arsenic sorption. *J. Environ. Qual.* 31:557-563.
- Violante, A., and M. Pigna. 2002. Competitive sorption of arsenate and phosphate on different clay minerals and soils. *Soil Sci. Soc. Am. J.* 66:1788-1796.
- Waltham, C. A., and W.J. Eick. 2002. Kinetics of arsenic adsorption on goethite in the presence of sorbed silicic acid. *Soil Sci. Soc. Am. J.* 66:818-825.
- Woolson, E.A., J.H. Axley, and P.C. Kearney. 1973. The chemistry and phytotoxicity of arsenic in soils: effect of time and phosphorous. *Soil Sci. Soc. Am. Proc.* 37:254-259.
- Xing, B., J.J. Pignatello, and B. Gigliotti. 1996. Competitive sorption between atrazine and other organic compounds in soils and model sorbents. *Environ. Sci. Technol.* 30:2432-2440.
- Zhao, H., and R. Stanforth. 2001. Competitive adsorption of phosphate and arsenate on goethite. *Environ. Sci. Technol.* 35:4753-4757.

CHAPTER 6: MODELING ARSENATE-PHOSPHATE RETENTION AND TRANSPORT IN SOILS: A MULTI-COMPONENT APPROACH

6.1 Introduction

Recent studies indicate that phosphate [P] in soils competes with arsenate [As(V)] for available adsorption sites because of their similar chemical properties. Both As(V) and P are specifically sorbed on mineral surfaces by forming similar types of inner-sphere surface complexes through ligand exchange. In fact, it has been shown that the presence of phosphate substantially suppressed the sorption of arsenate on minerals as well as soils (Roy et al., 1986ab; Peryea, 1991; Melamed et al., 1995; Darland and Inskeep, 1997; Jain and Loeppert, 2000; Violante and Pigna, 2002; Williams et al., 2003).

Competitive sorption between phosphate and arsenate generally depends on the surface properties of the adsorbent, concentrations of As and P, pH, sequence of addition, and residence time. Arsenate and phosphate are specifically adsorbed on a similar set of surface sites, although evidence showed some sites are only available for either As(V) or P. Based on competitive adsorption of anions on goethite and gibbsite, Hingston et al. (1971) proposed two types of adsorption sites on mineral surface; the first type is available for both anions where competition takes place while the second type of adsorption sites is specifically available for either anions. Violante and Pigna (2002) demonstrated that minerals rich in aluminium (Al) have a greater affinity of phosphate than arsenate, whereas metal oxides and phyllosilicates rich in Fe were more effective in adsorbing As(V) than P. In general, the adsorption of both phosphate and arsenate on Fe/Al oxides decreases with increasing pH (Manning and Goldberg, 1996). Furthermore, Jain and Loeppert (2000) reported that the effect of phosphate on arsenate adsorption on ferrihydrite was greater at high pHs than at low pHs. Equilibrium conditions are often assumed for competitive adsorption studies. However, time-dependent behavior of As(V)

adsorption on minerals and soils were reported by Raven et al.(1998), Darland and Inskeep (1997) and Williams et al. (2002). Due to the heterogeneous nature of adsorption sites and kinetic behavior of sorption, the sequence of addition, i.e., addition of P to replace As(V) or vice versa, was shown to influence the competition between the two anions (Liu et al., 2001).

Miscible displacement experiments provided evidence that the presence of P greatly enhanced the movement of arsenic in soils. For example, Melamed et al. (1995) observed that the increasing presence of phosphate shifted the As(V) breakthrough curves (BTCs) to the left, indicating reduced As(V) sorption and enhanced mobility of As(V) in soil. Similarly, Darland and Inskeep (1997) found that peak concentration and total recovery of arsenic from a sand column containing free Fe oxides increased with increasing P addition. Moreover, they found that a significant fraction of As(V) was retained even though the P loading exceeded the maximum adsorption capacity for P. In fact, Williams et al. (2003) compared the effects of pH, pore velocity, and phosphate addition on As(V) transport through columns of a subsurface soil and they concluded that the phosphate has the greatest impact on the mobility of As(V) among the three factors. While significant influence of phosphate on the retention and transport of arsenate were well characterized, a literature search revealed that mathematical models were not developed to simulate the competitive retention kinetics and transport of As(V) and P in porous media.

The objectives of this investigation were (i) to study the kinetics of competitive retention of arsenate and phosphate during transport in saturated soil columns; and ii) to test the predictive capability of a multireaction model for describing the time-dependent retention and transport of As(V) and P in soils. Moreover, we extended the existing multireaction kinetic approach to simulate the competitive sorption between As(V) and P during transport in soils. The formulated

multi-component multireaction model accounts for equilibrium, reversible kinetic, and irreversible kinetic reactions which represent various retention mechanisms of As(V) and P.

6.2 Model Formulation

The transport of many chemical compounds in soils and aquifers is largely dependent on sorption processes in soils. Competition between various chemical species for the same set of sorption sites is a common phenomenon for heavy metals [Murali and Aylmore, 1983] as well as organic compounds [Xing et al., 1996]. Enhanced mobility as a result of sorption competition has been widely observed for environmental contaminants [e.g., McGinley et al., 1996]. Therefore, competitive sorption should be considered for the prediction of contaminant transport in the vadose zones and aquifers.

Geochemical models (e.g., MINTEQ, PHREEQC) have been adopted to simulate the reactions between multiple contaminants during their transport in soils and aquifers [e.g., Manning and Goldberg, 1996, Smith and Jaffe, 1998]. Such models require detailed description of chemical and mineral composition of solution and porous media, as well as numerous reaction constants. However, those types of information are either unavailable or unreliable under most circumstances [Nitzsche et al., 2000]. In addition, heterogeneity of the natural porous media also impedes the application of chemical reaction based models. More importantly, sorption processes are often regarded as instantaneous [i.e., equilibrium conditions are assumed] in such geochemical models. In contrast, numerous studies have demonstrated the lack of reaction equilibrium in soils (Selim 1992). Rather than geochemical models, equilibrium sorption reactions are frequently simulated using empirical models. Freundlich equation is a widely used empirical adsorption model that can be expressed as

$$S = \lambda C^N \quad [6.1]$$

where S is the amount of adsorption (mmol kg^{-1}), C is the solution concentration (mmol L^{-1}), λ is the distribution or partitioning coefficient ($\text{mmol kg}^{-1} (\text{mmol L}^{-1})^{-N}$), and N is a dimensionless reaction order commonly less than one.

The sorption of chemicals by soils and sediments may require weeks to months to reach equilibrium. Therefore, the kinetic (time-dependent) sorption models of the Freundlich type have been developed to simulate the sorption of solutes during their transport in soils and aquifers (Selim, 1992). The reversible n th-order (Freundlich-type) kinetic sorption equation is in the form of

$$\frac{\partial S}{\partial t} = k_1 \frac{\theta}{\rho} C^n - k_2 S \quad [6.2]$$

where k_1 and k_2 are the forward and backward reaction rate coefficients (h^{-1}), respectively, n is a nonlinear parameter usually less than 1, t is reaction time (h), ρ is the soil bulk density (g cm^{-3}), and θ is the volumetric water content ($\text{cm}^3 \text{ cm}^{-3}$). Under equilibrium conditions, i.e., $\frac{\partial S}{\partial t} = 0$,

equation (3) yields Freundlich equation (6.1) assuming $\lambda = \frac{k_1}{k_2} \frac{\theta}{\rho}$ and $N = n$.

The Sheindorf-Rebhun-Sheintuch (SRS) equation has been developed to describe competitive or multicomponent sorption where it is assumed that the single-component sorption follows the Freundlich equation (Sheindorf et al., 1981). The derivation of SRS equation was based on the assumption of an exponential distribution of adsorption energies for each component. A general form of the SRS equation can be written as

$$S_i = \lambda_i C_i \left(\sum_{j=1}^I \alpha_{i,j} C_j \right)^{N_i-1} \quad [6.3]$$

where i, j indicate component i and j , l is the total number of components, $\alpha_{i,j}$ is a dimensionless competition coefficient which describe the inhibition by component j to the adsorption of component i . By definition, $\alpha_{i,j}$ equals 1 when $i=j$. If there is no competition, i.e., $\alpha_{i,j}=0$ for all $j \neq i$, equation [6.3] yields a single species Freundlich equation for component i . It should also be pointed out that if the single-species sorption isotherm is linear, i.e., $N_i = 1$, equations [6.3] predict the absence of competition. Equation (3) was successfully employed by Roy et al. (1986ab) to describe the competitive adsorption isotherms of As(V) and P in several soils.

For time-dependent sorption, we extend equation [3] such that for reversible n th-order multi-component kinetic retention, the equation is of the form

$$\frac{\partial S_i}{\partial t} = k_{1,i} \frac{\theta}{\rho} C_i \left(\sum_{j=1}^l \alpha_{i,j} C_j \right)^{n_i-1} - k_{2,i} S_i \quad [6.4]$$

Under equilibrium condition, equation (6.4) yields equation (6.3) assuming $\lambda_i = \frac{k_{1,i}}{k_{2,i}} \frac{\theta}{\rho}$ and $N_i = n_i$. On the other hand, if there is no competition, equation (6.4) yields a single species N th- order kinetic sorption equation (6.3).

The MRM model of equation 3.1-3.5 has been applied successfully to simulate the soil retention of many environmental contaminants [e.g., Amacher et al., 1988; Selim et al., 1992; Barnett et al., 2000]. However, the competitive or multicomponent adsorption is not accounted in the MRM model. In this study, we developed a multi-component formula for the multireaction model to account the competition effect. Specifically, the equilibrium and kinetic adsorption equations were modified in a way similar to the SRS equation. The modified model proposed in this analysis can be described with the following equations:

$$S_{e,i} = K_{e,i} C_i \left(\sum_{j=1}^l \alpha_{i,j} C_j \right)^{n_i-1} \quad [6.5]$$

$$\frac{\partial S_{1,i}}{\partial t} = k_{1,i} \frac{\theta}{\rho} C_i \left(\sum_{j=1}^l \alpha_{i,j} C_j \right)^{n_i-1} - (k_{2,i} + k_{3,i}) S_{1,i} \quad [6.6]$$

$$\frac{\partial S_{2,i}}{\partial t} = k_{3,i} S_{1,i} \quad [6.7]$$

$$\frac{\partial S_{s,i}}{\partial t} = k_{s,i} \frac{\theta}{\rho} C_i \quad [6.8]$$

The notations used above have similar meaning as they are in the MRM model except that subscripts i are added to indicate the i th component. The competitive coefficients $\alpha_{i,j}$ from the SRS equation [3] is used to describe the competition of component j on component i .

Equation 6.5-6.8 can be incorporated into the one-dimensional reactive advective-dispersive transport equation (ADE) under steady water flow (Selim, 1992)

$$\frac{\partial C_i}{\partial t} + \frac{\rho}{\theta} \frac{\partial S_i}{\partial x} = D \frac{\partial^2 C_i}{\partial x^2} - v \frac{\partial C_i}{\partial x} \quad [6.9]$$

where x is distance (cm), D is dispersion coefficient ($\text{cm}^2 \text{h}^{-1}$), v ($=q/\theta$) is average pore water velocity (cm h^{-1}) and q is Darcy's water flux density (cm h^{-1}). The appropriate initial and boundary conditions for a finite soil column are

$$C_i(x) = C_{init} \quad t = 0 \quad [6.10a]$$

$$S_i(x) = S_{init} \quad t = 0 \quad [6.10b]$$

$$\left(-D \frac{\partial C_i}{\partial x} + v C_i \right) \Big|_{x=0} = \begin{cases} v C_{o,i} & t \in T_{pi} \\ 0 & t \notin T_{pi} \end{cases} \quad [6.10c]$$

$$\frac{\partial C_i}{\partial x} \Big|_{x=L} = 0 \quad t > 0 \quad [6.10d]$$

where C_{init} is the initial solution concentration (mg L^{-1}), S_{init} is the initial amount of sorption (mg kg^{-1}), C_o is the input solute concentration (mg L^{-1}), T_p is the duration of applied solute pulses, L is the length of column (cm). The dispersion coefficient is further interpreted as the combination of hydrodynamic dispersion, and intraparticle diffusion coefficient D_w ($\text{cm}^2 \text{h}^{-1}$)

$$D = \delta v + \frac{D_w}{\tau} \quad [6.11]$$

where δ (cm) is the longitudinal dispersivity and τ is the tortuosity factor (Brusseau, 1993; Ma and Selim, 1994). Flow interruption or stop-flow is accounted for in the proposed models by simply assuming $v=0$ and $D=D_w/\tau$ during flow interruption. The above equations (11-16) were solved numerically using finite difference approximations (Selim et al., 1990). Specifically, the solute transport (equation 15) was simulated using Crank-Nicholson explicit-implicit method. The kinetic retention processes (equation 11-14) were solved with 4-th order Runge-Kutta method. Mass balance at each step of the simulation was used to check the numerical results. The single-species simulation results were further tested with the analytical solution for the two-site non-equilibrium transport model provided by CXTFIT (Toride et al., 1995).

6.3 Materials and Methods

Competitive transport of As(V) and P in soils was investigated using the miscible displacement technique as described by Selim et al. (1987). Acrylic columns (5-cm in length and of 6.4-cm i.d.) were uniformly packed with air-dry soil and were slowly water-saturated with a background solution of 0.01 M KNO_3 at a low Darcy flux. Input solutions of 0.01 M KNO_3 were applied for several pore volumes using a variable speed piston pump, and the fluxes were adjusted to the desired flow rates. To maintain constant ionic strength, between 10 to 20 pore volumes of 0.01 M KNO_3 were applied to each column prior to introduction of As(V) or P pulse solutions. Two pulses of 1.33 mM As(V) solution in 0.01 M KNO_3 as background solution were

introduced to column 101 and 104. For column 102 and 105, an 1.33 mM As(V) input pulse was followed immediately by a 3.23 mM phosphate input pulse, whereas two pulses of mixed solution of 1.33 mM As(V) and 3.23 mM P were supplied to column 103 and 106. During pulse application, column flow was completely stopped for a duration of 4-6 days in order to evaluate the influence of flow interruption on As(V)/P transport. The volume of each As(V)/P pulse along with soil parameters associated with each column (e.g., v , θ and ρ) are given in Table 6.1.

To obtain independent estimates for the dispersion coefficient (D), separate pulses of a tracer solution were applied to each soil column prior to As(V) pulse applications. The tracer used was tritium ($^3\text{H}_2\text{O}$) and the collected samples were analyzed using a Tri-Carb liquid scintillation β counter (Packard-2100 TR) by mixing 0.5 mL aliquot with 5 mL cocktail (Packard Ultima Gold) for 10 minutes. The radioactivity was recorded as counts per minute (CMP). Estimates for D values are given in Table 6.1. The tritium data were described using the classical convection-dispersion equation and best-fit parameters for D and the retardation factor R ($= 1 + \rho K_d/\theta$) were obtained from nonlinear least square optimization using CXTFIT (Toride et al., 1995).

6.4 Results and Discussion

6.4.1 Competitive Sorption Isotherms

Single component sorption isotherms for the arsenate and phosphate at 24 h of reaction are shown in Figure 5.1 for the Olivier and Windsor soils. These isotherms were fit to the Freundlich equation (eq 1) using nonlinear least square optimization. The estimated parameters (λ and N) along with coefficient of determination (r^2) are given in Table 5.1. Those highly nonlinear sorption isotherms for As(V) and P are characterized by Freundlich N much less than 1, indicating the high sorption affinity at low concentrations. The similar shape of the As(V)

Table 6.1 Soil physical parameters for miscible displacement experiments. Values of the dispersion coefficient were estimated from tritium breakthrough results.

No	Soil	ρ_b^a g cm ⁻³	θ cm ³ cm ⁻³	v cm h ⁻¹	D cm ² h ⁻¹	Solute	P.V. ^b	No flow ^c h	Solute	P.V.	No flow h	As % recovery	P
101	Olivier	1.22	0.54	0.70	1.65	As	11.0	120	As	10.1	144	82.1	-
102	Olivier	1.19	0.55	0.75	1.91	As	10.9	-	P	10.5	120	92.7	89.9
103	Olivier	1.15	0.57	0.66	1.13	As&P	9.8	120	As&P	11.3	120	91.0	99.9
104	Windsor	1.17	0.56	0.68	0.86	As	10.9	97	As	10.2	97	72.5	-
105	Windsor	1.51	0.43	0.89	0.21	As	10.1	-	P	10.1	120	83.8	48.0
106	Windsor	1.44	0.46	0.80	0.20	As&P	10.4	120	As&P	9.5	120	89.5	72.5

^a ρ_b = Bulk density, θ = saturated water content, v = pore water velocity, D = Dispersion coefficient.

^b P.V. = total pore volumes of input pulse.

^c Duration of flow interruption.

and P sorption isotherms also suggests the similarities in sorption mechanisms for these two anions.

The estimated Freundlich parameters λ and N for As(V) and P were used in the SRS equation (eq 3) to simulate the competitive adsorption between As(V) and P. Since only two components [As and P] were considered, the nonlinear set of equations needs to be solved are

$$S_{As} = \lambda_{As} C_{As} (C_{As} + \alpha_{As,P} C_P)^{N_{As}-1} \quad [18a]$$

$$S_P = \lambda_P C_P (C_P + \alpha_{P,As} C_{As})^{N_P-1} \quad [18b]$$

The unknown variables (C_{As} , C_P , S_{As} , and S_P) were solved simultaneously from the initial experiment conditions (i.e., initial As(V) and P concentrations, solid/solution ratios).

Specifically, the nonlinear set of equations was solved through iterative improvements, similar to the approach of Barrow et al. (2005). The competitive coefficients $\alpha_{As,P}$ and $\alpha_{P,As}$ given in Table 5.1 were obtained by fitting the competitive adsorption data to equation [18] using nonlinear least square optimization. In Figure 6.1 we presents an example of the SRS simulation results for competitive adsorption isotherms of As(V) and P on Olivier soil.

6.4.2 Sorption Kinetics

Results from our single component kinetic batch experiments are presented in Fig 6.2 and 6.3 for arsenate and phosphate, respectively. Highly time-dependent retention behavior of the two anions are clearly illustrated by the decreasing concentrations of As(V) or P in soil solution versus reaction time for the two soils. The rate of As(V) or P retention was rapid initially and was followed by slow reactions. The kinetic adsorption data of As(V) and P from our batch study was described using single component MRM models. Previous studies demonstrated that the use of 24-h Freundlich N in place of n in the MRM satisfied the simulation need and the same

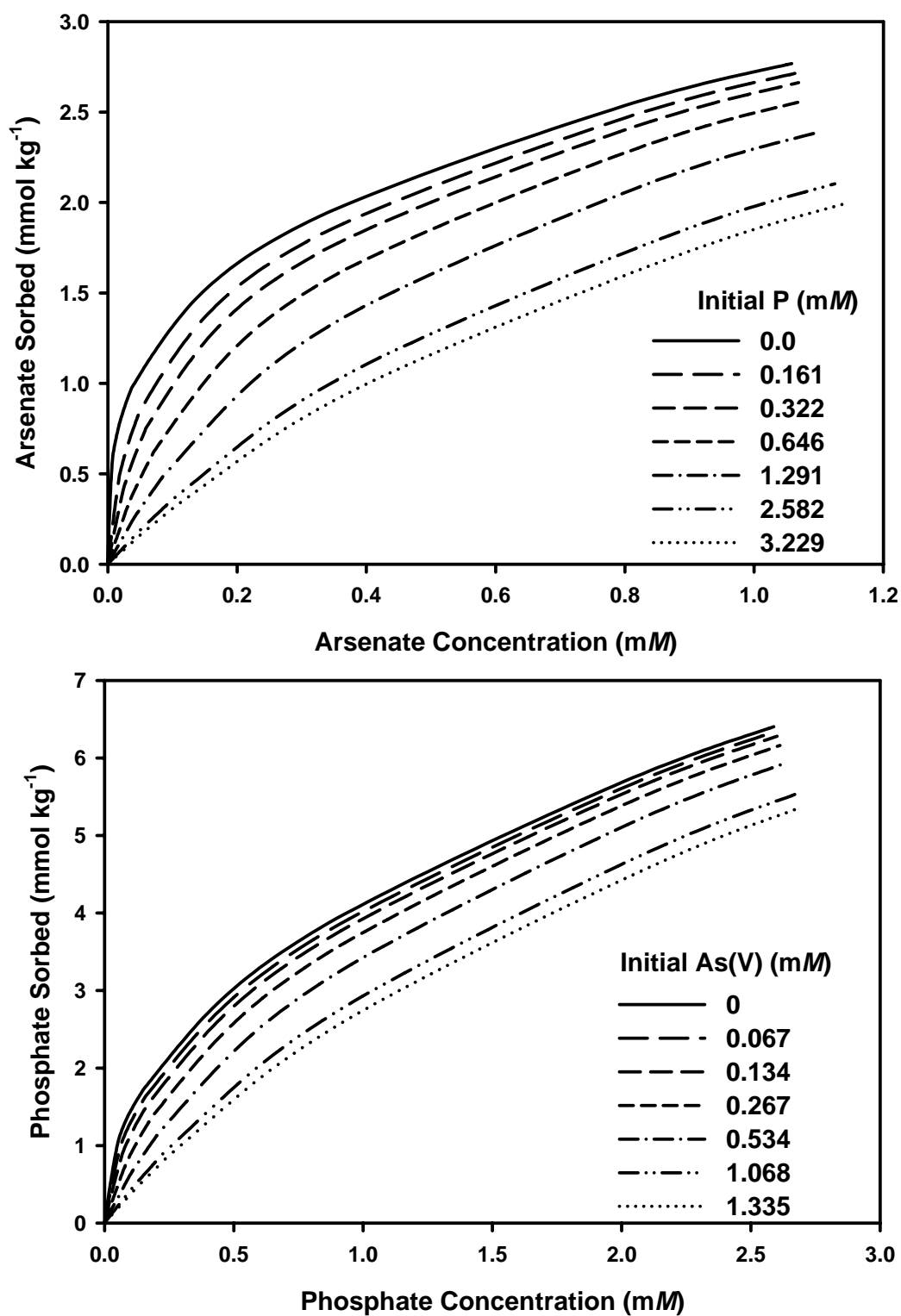


Figure 6.1 Calculated competitive sorption isotherms for Olivier soil using SRS equation with sorption parameters given in Table 5.1.

practices were carried out in our simulation (Zhang and Selim, 2006). Specifically, nonlinear reaction order of 0.311 and 0.287 were used in MRM simulation of arsenate adsorption by Olivier and Windsor soils, respectively. Similarly, nonlinear reaction orders of 0.461 and 0.486 were used for the simulation of P adsorption by Olivier and Windsor soils, respectively (see Table 5.1). Other parameters (K_e , k_1 , k_2 , k_3 , and k_s) were obtained through Levenberg-Marquardt nonlinear least square optimization of the kinetic batch data to the MRM model.

The MRM kinetic parameters (K_e , k_1 , k_2 , and k_3) obtained from nonlinear optimization with kinetic batch data are given in Table 6.2 along with their goodness-of-fit. Excellent fit of the experimental data was achieved for both As(V) and P, as shown by the high coefficients of determination (r^2) and the low root mean square errors (*RMSE*) given in Table 6.2. MRM simulations with kinetics parameters provided in Table 6.2 are depicted as solid and dashed lines in Figure 6.2 and 6.3. It should also be emphasized that the MRM model was applicable for the entire range of input concentrations for both arsenate (0.067 to 1.333 mM) and phosphate (0.32 to 3.23 mM).

6.4.3 Multi-Component Retention Kinetics

Results from the multi-component kinetic batch experiments are presented in Figure 6.4 and 6.5 in order to illustrate the changes in As(V) or P concentration versus reaction times in the presence of various concentrations of competing anion for the different soils. Rates and amounts of As(V) adsorption were significantly reduced by increasing P additions. Furthermore, we observed that the competitive effects of P on As(V) adsorption were small at the initial stage of the reaction and steadily increased with reaction time.

The multi-component multi-reaction model (MCMRM) was employed to simulate the competitive adsorption kinetics between As(V) and P in a fully predictive mode. Specifically, the

Table 6.2 Estimated single component MRM parameters (with standard errors) for adsorption kinetics of arsenate and phosphate

Soil	Solute	r^2	RMSE	n	K_e	k_1 h^{-1}	k_2 h^{-1}	k_3 h^{-1}
Olivier	Arsenate	0.998	0.0249	0.311	0.40±0.21	0.0106±0.0023	0.0270±0.0061	0.0019±0.0003
	Phosphate	0.999	0.0454	0.461	1.52±0.39	0.0202±0.0060	0.0390±0.0105	0.0011±0.0003
Windsor	Arsenate	0.997	0.0258	0.287	1.61±0.15	0.0163±0.0022	0.0300±0.0048	0.0021±0.0003
	Phosphate	0.994	0.0598	0.486	6.11±1.27	0.0634±0.0284	0.0579±0.0240	0.0040±0.0007

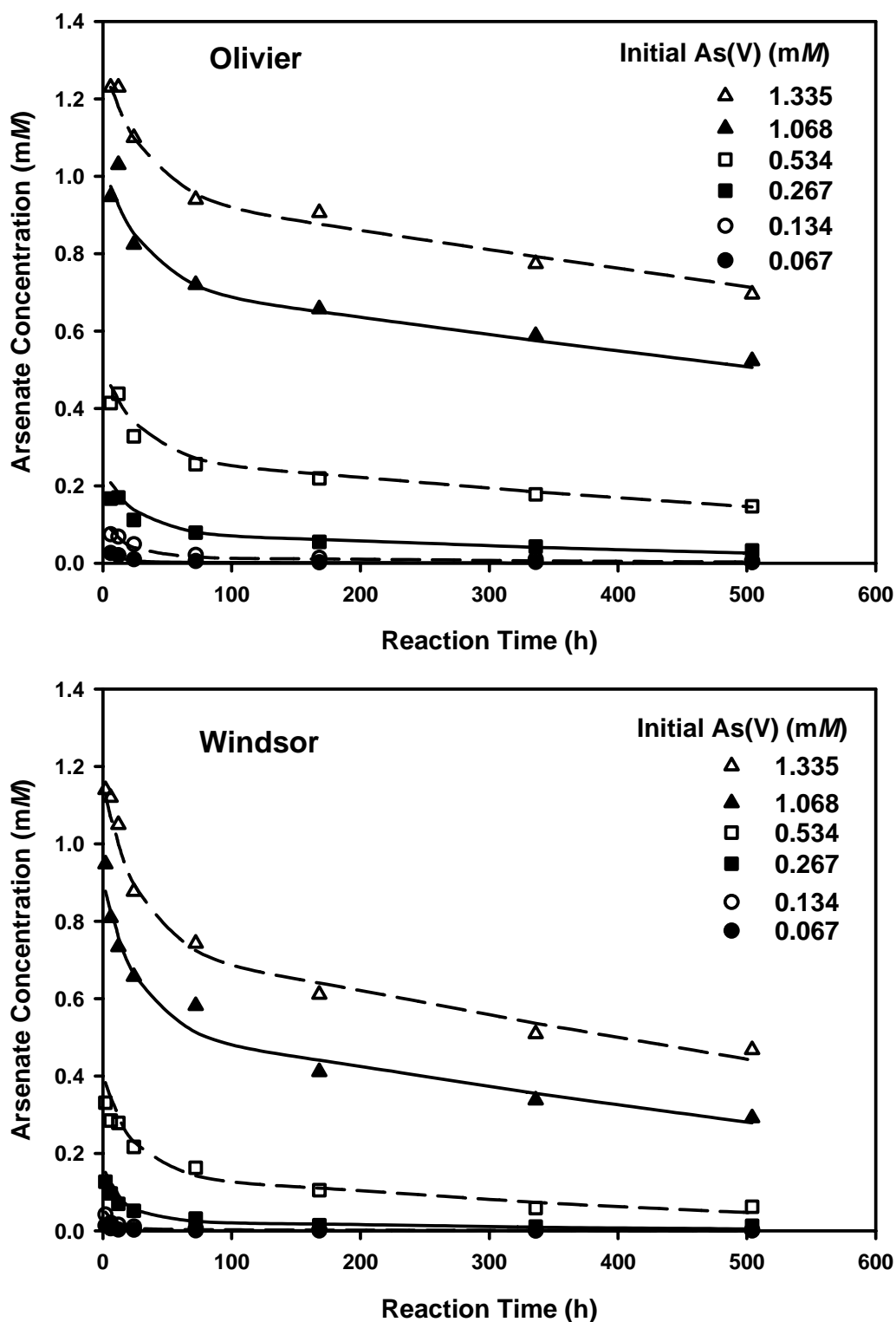


Figure 6.2 Arsenate concentrations versus reaction times for Olivier and Windsor soils. Symbols are for different initial As(V) concentrations of 0.067, 0.13, 0.27, 0.53, 1.07, and 1.33 mM. Solid and dashed curves are single component multireaction model (MRM) simulations with kinetic parameters given in Table 6.2.

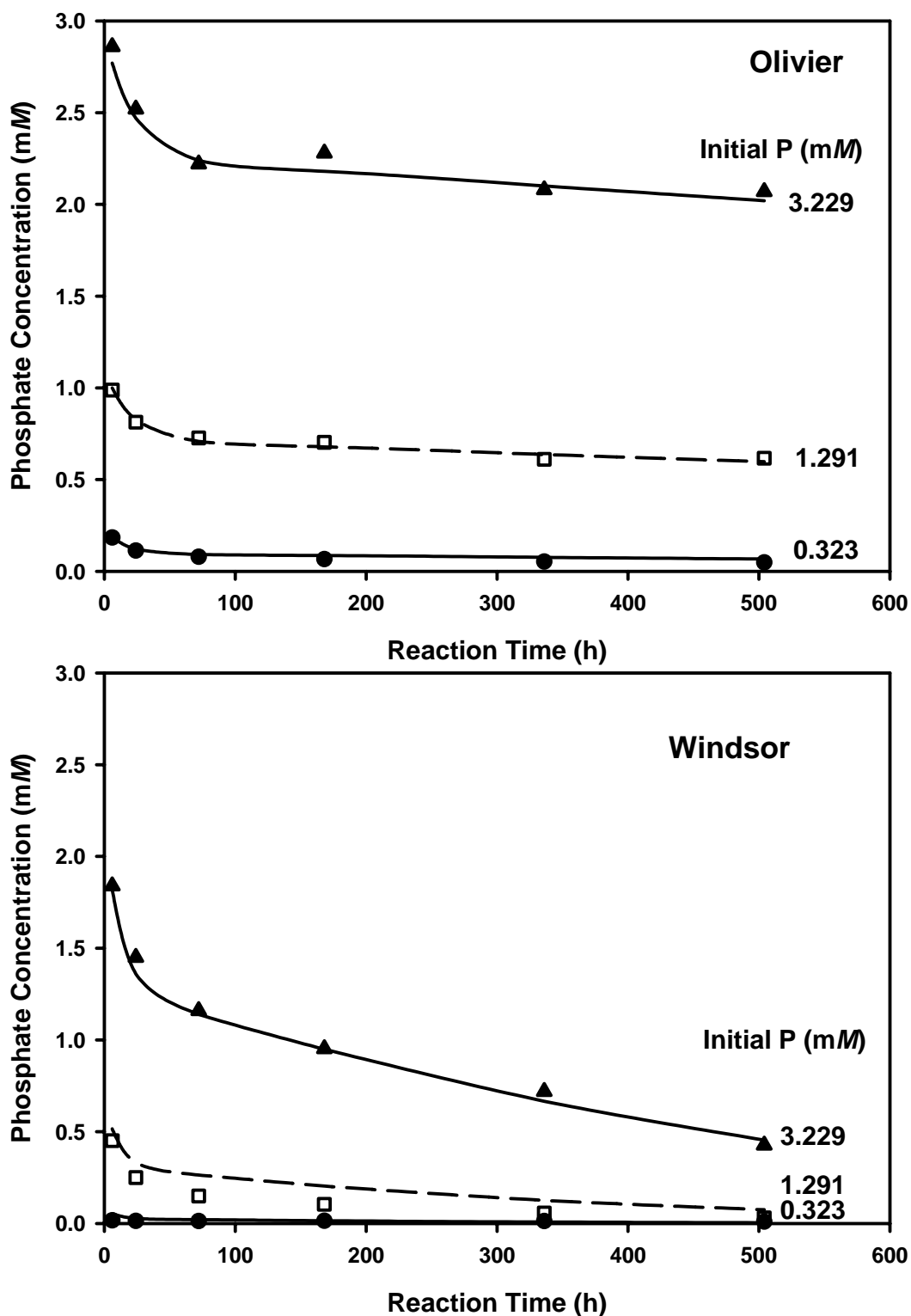


Figure 6.3 Phosphate concentrations versus reaction times for Olivier and Windsor soils. Symbols are for different initial phosphate concentrations of 0.32, 1.29, and 3.23 mM. Solid and dashed curves are single component multireaction model (MRM) simulations with kinetic parameters given in Table 6.2.

MCMRM modeling was carried out using kinetic sorption parameters (K_e , k_1 , k_2 , k_3 , and n) obtained from single component MRM simulation (see Table 6.2), and the competitive coefficients (α_{As-P} and α_{P-As}) obtained from nonlinear optimization of the SRS equation to the 24 hour competitive adsorption data (see Table 5.1), along with the experimental constraints such as initial conditions, sampling times, decanted volumes, etc. The results of MCMRM predictions are depicted as the solid and dashed lines in Figure 6.4 and 6.5. Surprisingly good descriptions of the As(V) kinetic sorption data were achieved with this purely predictive model for both Olivier and Windsor soils, as shown through the close resemblance between the prediction and measured retention curves. The MCMRM predictions of the arsenate competition on phosphate sorption on Olivier soils were acceptable. However, the prediction of the competitive effect of As(V) on P sorption on Windsor soil was not successful. The use of the 24 h SRS competitive coefficients grossly overestimated the extent of As(V) competition on phosphate sorption. In addition, we tested the MCMRM simulation in an inverse modeling mode, where the competitive coefficients ($\alpha_{As,P}$ and $\alpha_{P,As}$) were obtained from nonlinear least square optimization. Significant improvement in the MCMRM prediction was observed with the optimized $\alpha_{As,P}$ and $\alpha_{P,As}$. Furthermore, the value of $\alpha_{P,As}$ obtained from this optimization process was much less than the 24h SRS $\alpha_{P,As}$, indicating the effect of reaction time on the competition between the two anions. In general, the simulation results demonstrated that the multi-component multi-reaction model with right competitive coefficients had the capability of predicting the competitive sorption kinetic between As(V) and P.

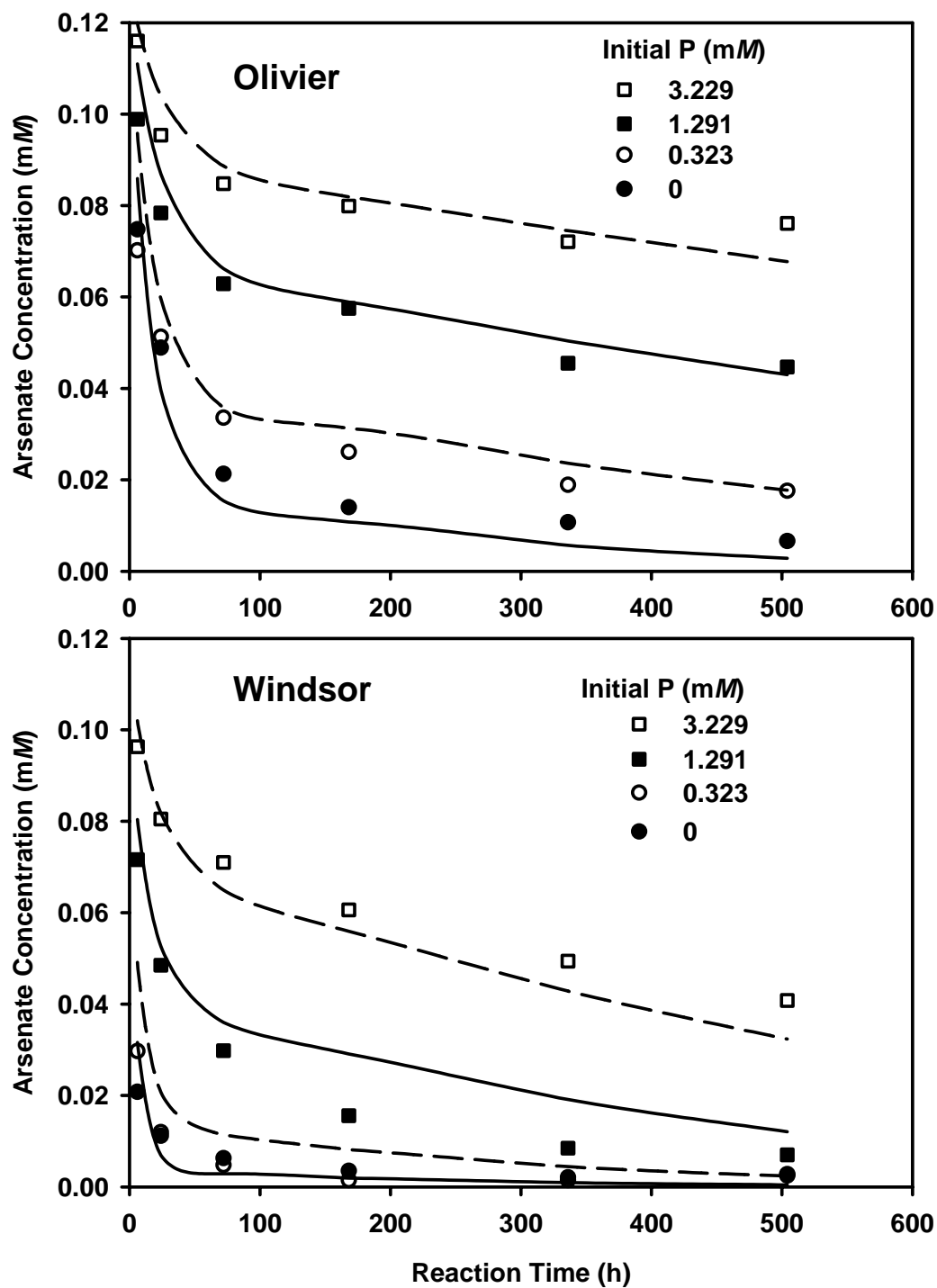


Figure 6.4 Arsenate concentrations versus reaction times with the presence of various concentrations of phosphate for Olivier and Windsor soils. The initial concentrations of arsenate were 0.13 mM. Symbols are for different initial phosphate concentrations of 0, 0.32, 1.3, and 3.2 mM. Solid and dashed curves are multi-component multi-reaction model (MCMRM) simulations with parameters given in Table 6.2.

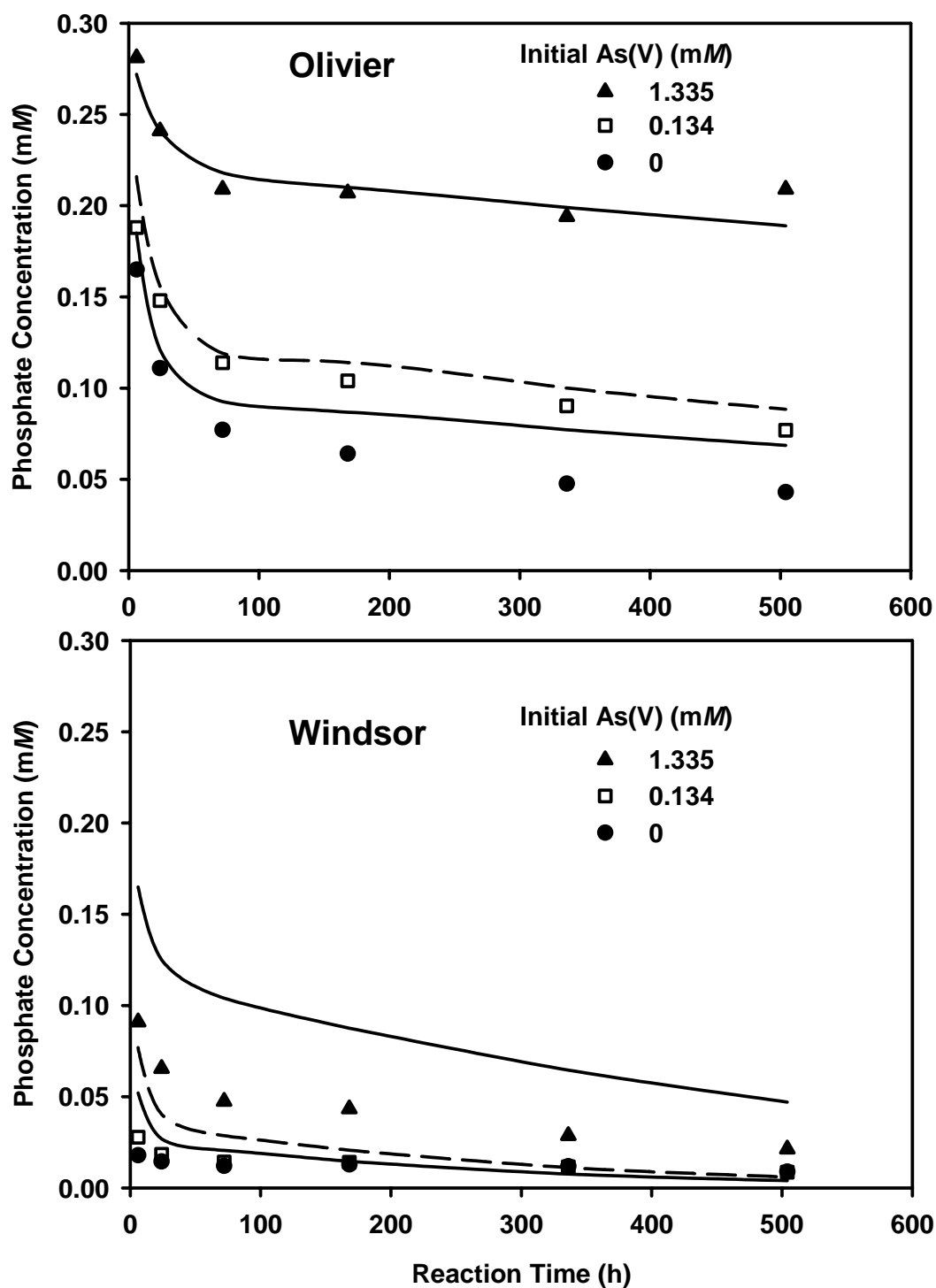


Figure 6.5 Phosphate concentrations versus reaction times with the presence of various concentrations of arsenate for Olivier and Windsor soils. The initial concentration of phosphate was 0.32 mM. Symbols are for different initial arsenate concentrations of 0, 0.13, and 1.3 mM. Solid and dashed curves are multi-component multi-reaction model (MCMRM) simulations with parameters given in Table 6.2.

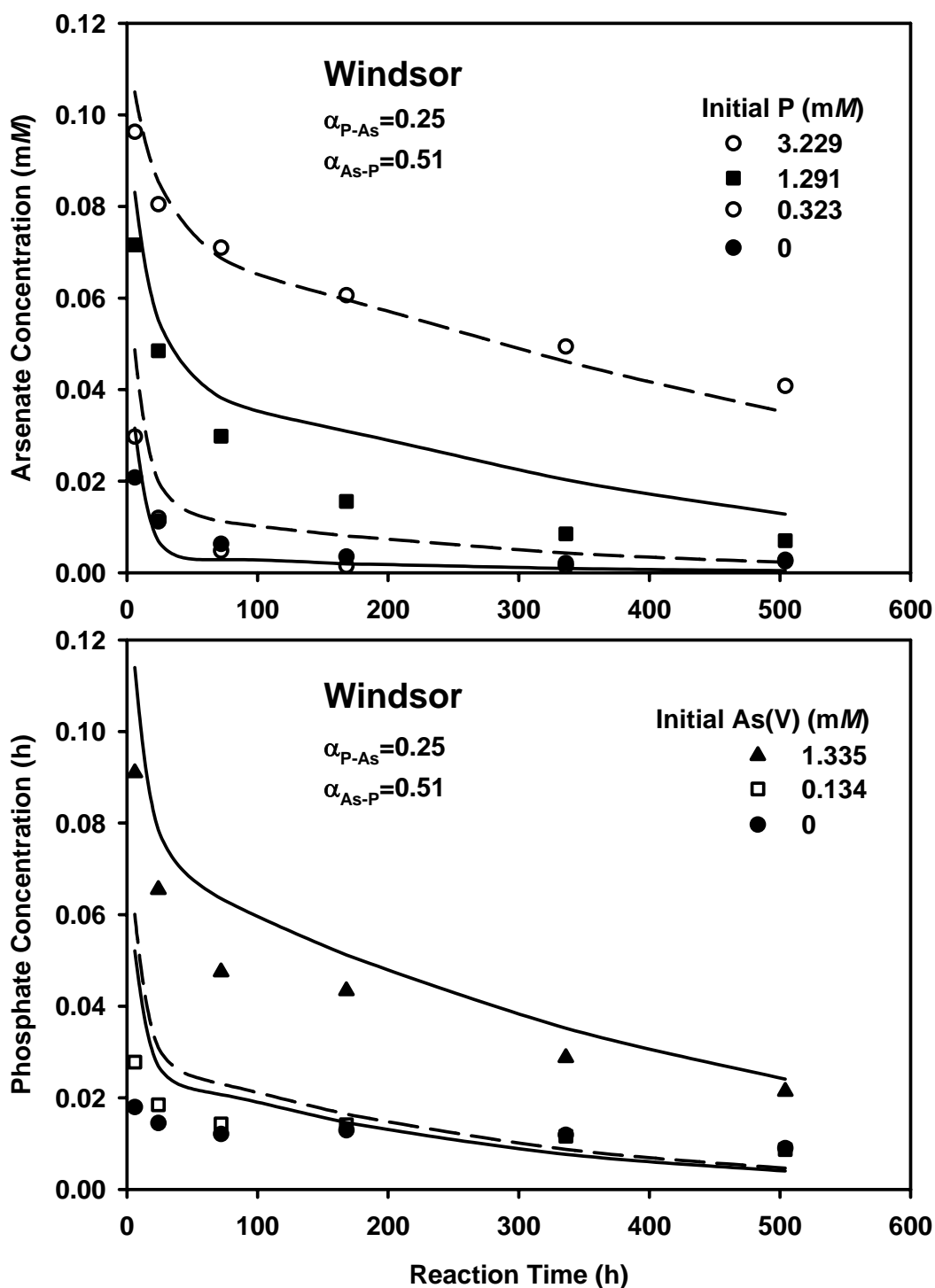


Figure 6.6 Competitive sorption kinetics of arsenate and phosphate on Windsor soils. a) The initial concentrations of arsenate were 0.13 mM. Symbols are for different initial phosphate concentrations of 0, 0.32, 1.3, and 3.2 mM. b) The initial concentration of phosphate was 0.32 mM. Symbols are for different initial arsenate concentrations of 0, 0.13, and 1.3 mM. Solid and dashed curves are multi-component multi-reaction model (MCMRM) simulations with parameters given in Table 6.2.

6.4.4 Breakthrough Curves

Results from saturated miscible displacement experiments are presented as breakthrough curves (BTCs) in Figure 6.7 to 6.12. The single component BTCs shown in Figure 6.7 and 6.8 (Column 101 and 104) indicate extensive retention during As(V) transport in Olivier and Windsor soils. A comparison of BTCs from Columns 101 (Olivier) and 104 (Windsor) demonstrate that the extent of sorption determined from column experiments was in general agreement with adsorption isotherms, that is, high sorption capacity of Windsor soil resulted in the low peak concentration and low mass recovery of As(V) in BTC of column 104. After two As(V) pulse applications and subsequent leaching by arsenic free solution of 20-30 pore volumes, the As(V) mass recoveries in the effluent were 82.1% and 72.5% of that applied for column 101 (Olivier), and 104 (Windsor), respectively. This suggests that a fraction of As(V) was irreversibly retained by each soil. The BTCs for As(V) transport was asymmetrical, showing excessive tailing at the desorption side. Similar asymmetry As(V) BTCs were reported by other researchers [Kuhlmeier 1997; Darland and Inskeep 1997; Williams et al. 2003] and were attributed to the rate-limited or time-dependent adsorption-desorption. Flow interruptions were carried out in our column experiments to check the extent of non-equilibrium conditions during arsenic transport. The sharp drop in As(V) concentration due to flow interruption indicates dominance of time-dependent retention during As(V) transport. Such results are in agreement with the highly kinetic sorption behavior observed from our batch experiments.

For Column 103 (Olivier) and 106 (Windsor) shown in Figure 6.10 and 6.12, application of pulses of mixed solutions of As(V) and P were carried out to study the impact of phosphate on As(V) transport. Consistent with results from other studies [Melamed et al., 1995; Darland and Inskeep 1997; Williams et al. 2003], the addition of phosphate significantly increased peak

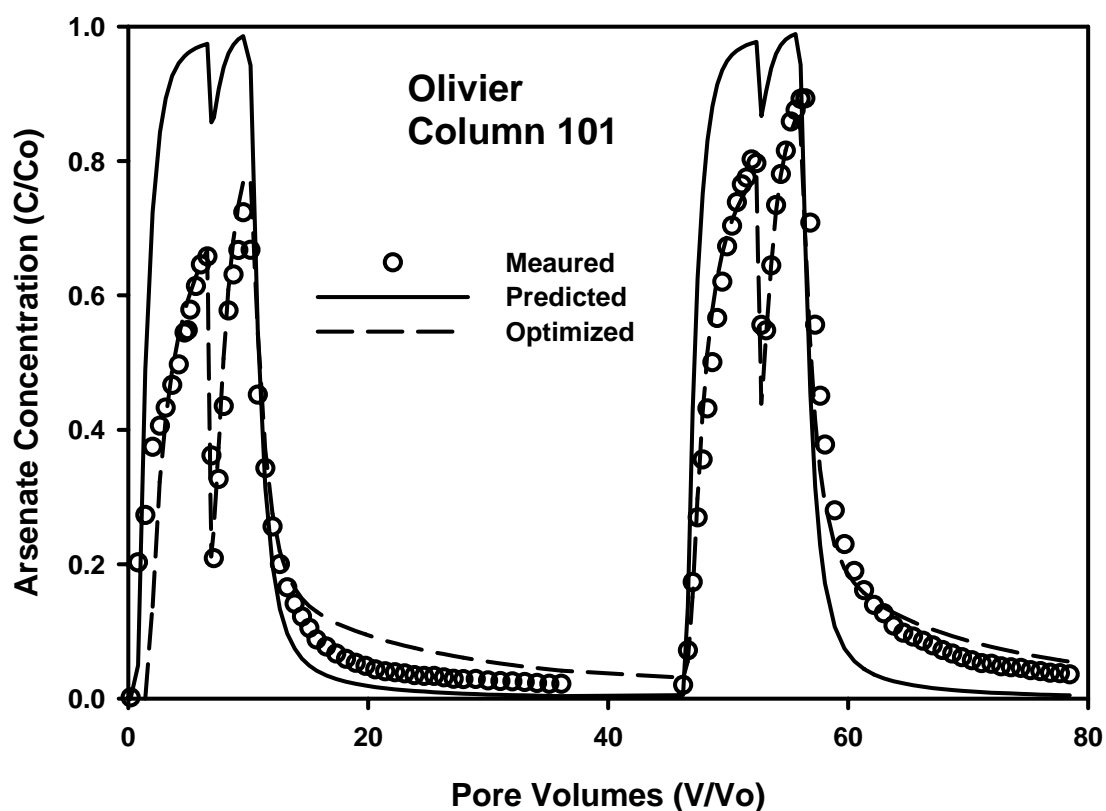


Figure 6.7 Experimental As(V) breakthrough curves (BTCs) in Olivier soil without addition of phosphate. Solid curves are single-component multi-reaction model (MRM) predictions made with the kinetic parameters derived from the batch experiment data (Table 6.2), whereas the dashed curves depicts the results of nonlinear optimization of BTCs to the MRM model.

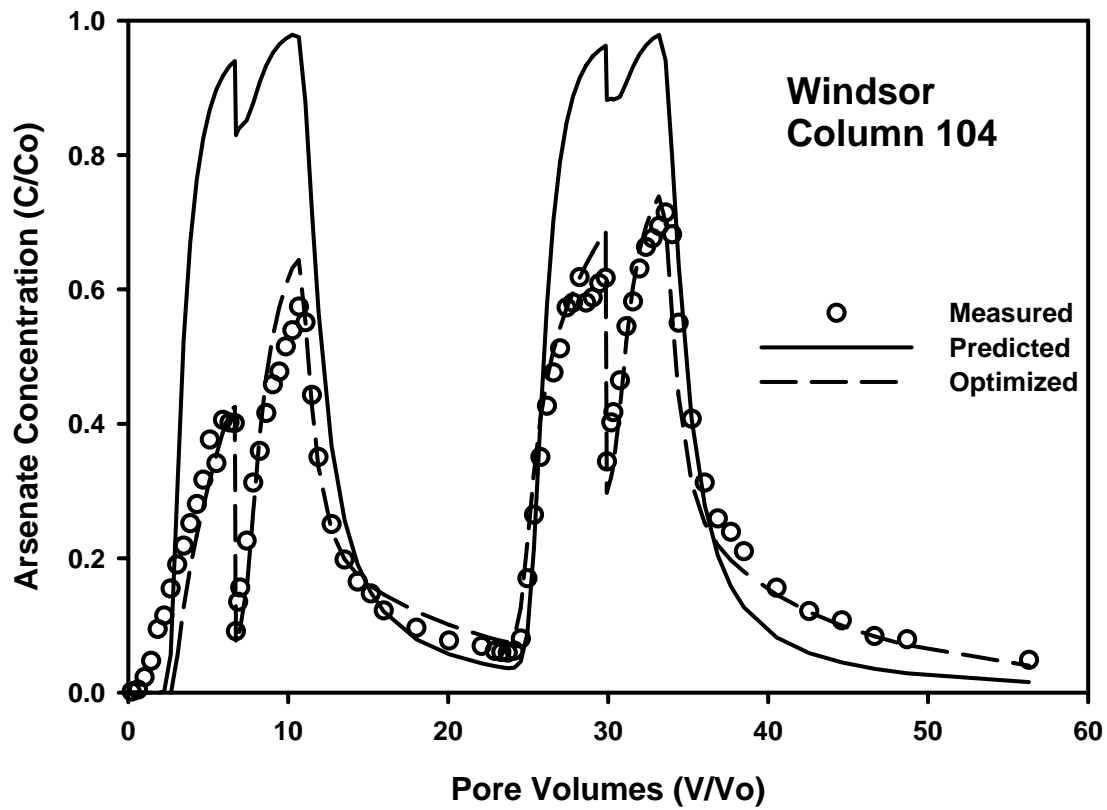


Figure 6.8 Experimental As(V) breakthrough curves (BTCs) in Olivier soil without addition of phosphate. Solid curves are single-component multi-reaction model (MRM) predictions made with the kinetic parameters derived from the batch experiment data (Table 6.2), whereas the dashed curves depicts the results of nonlinear optimization of BTCs to the MRM model (Table 6.3).

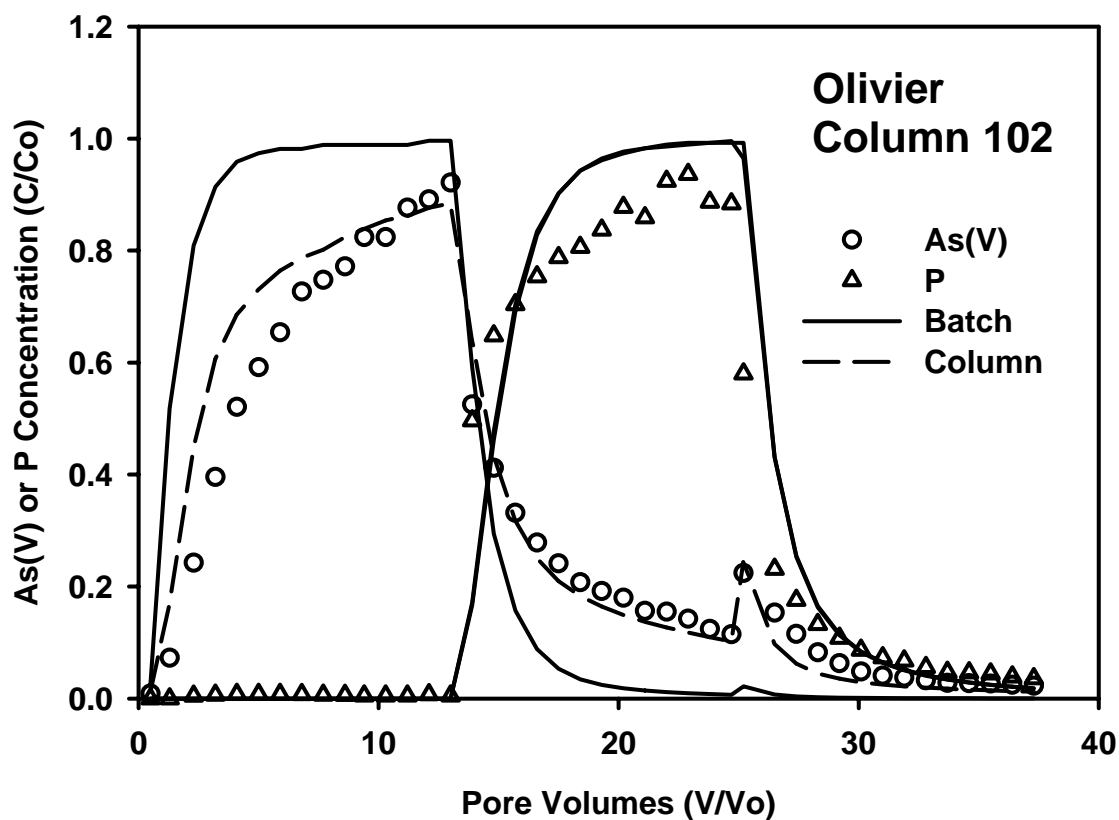


Figure 6.9 Experimental As(V) and P breakthrough curves (BTCs) in Olivier soil (column 102). Solid curves are multi-component multi-reaction model (MCMRM) predictions made with the kinetic parameters derived from the batch experiment data (Table 6.2), whereas the dashed curves are MCMRM simulation with kinetic parameters obtained from single component As(V) transport experiment (column 101, see Table 6.3).

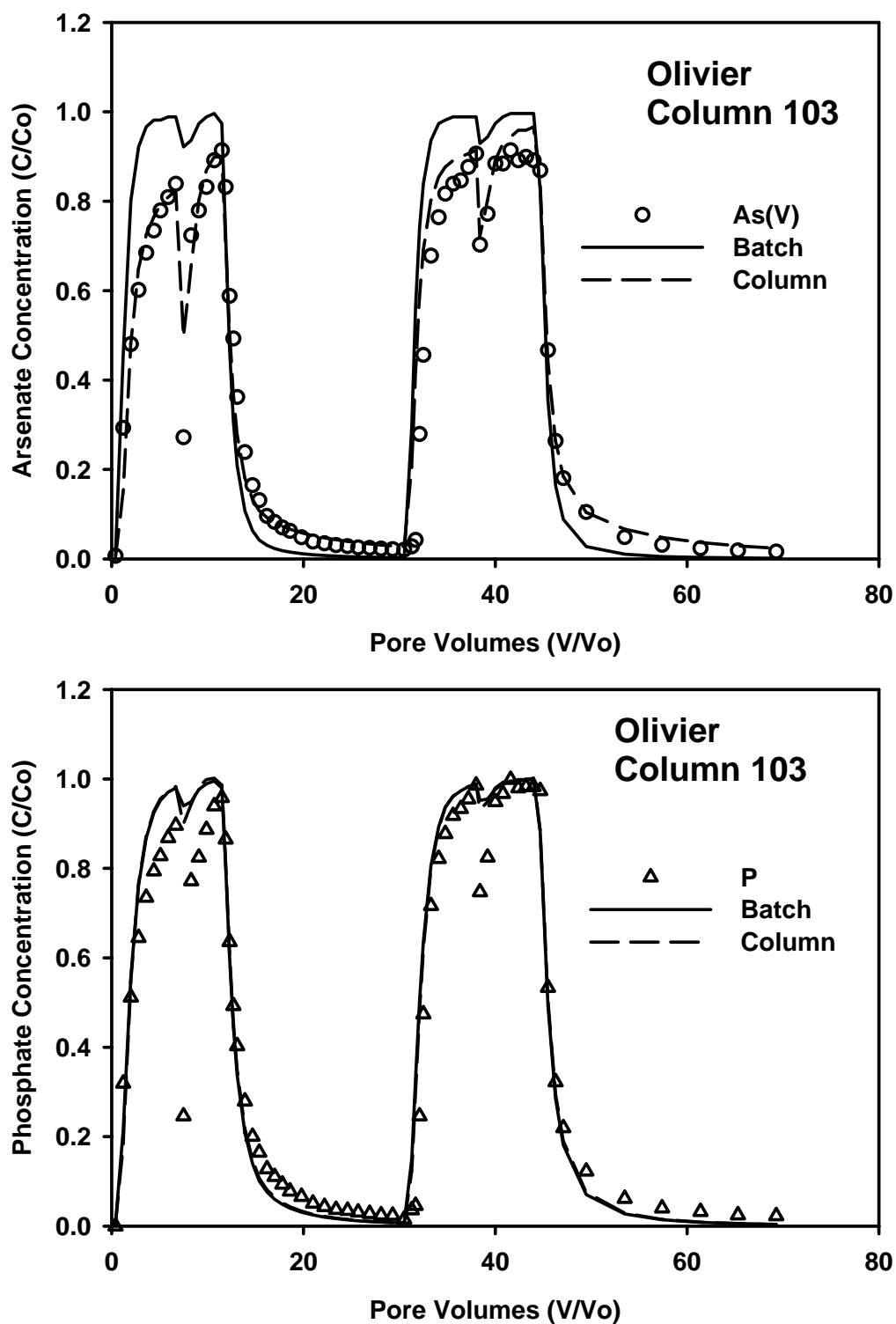


Figure 6.10 Experimental As(V) and P breakthrough curves (BTCs) in Olivier soil (column 103). Solid curves are multi-component multi-reaction model (MCMRM) predictions made with the kinetic parameters derived from the batch experiment data (Table 6.2), whereas the dashed curves are MCMRM simulation with kinetic parameters obtained from single component As(V) transport experiment (column 101, see Table 6.3).

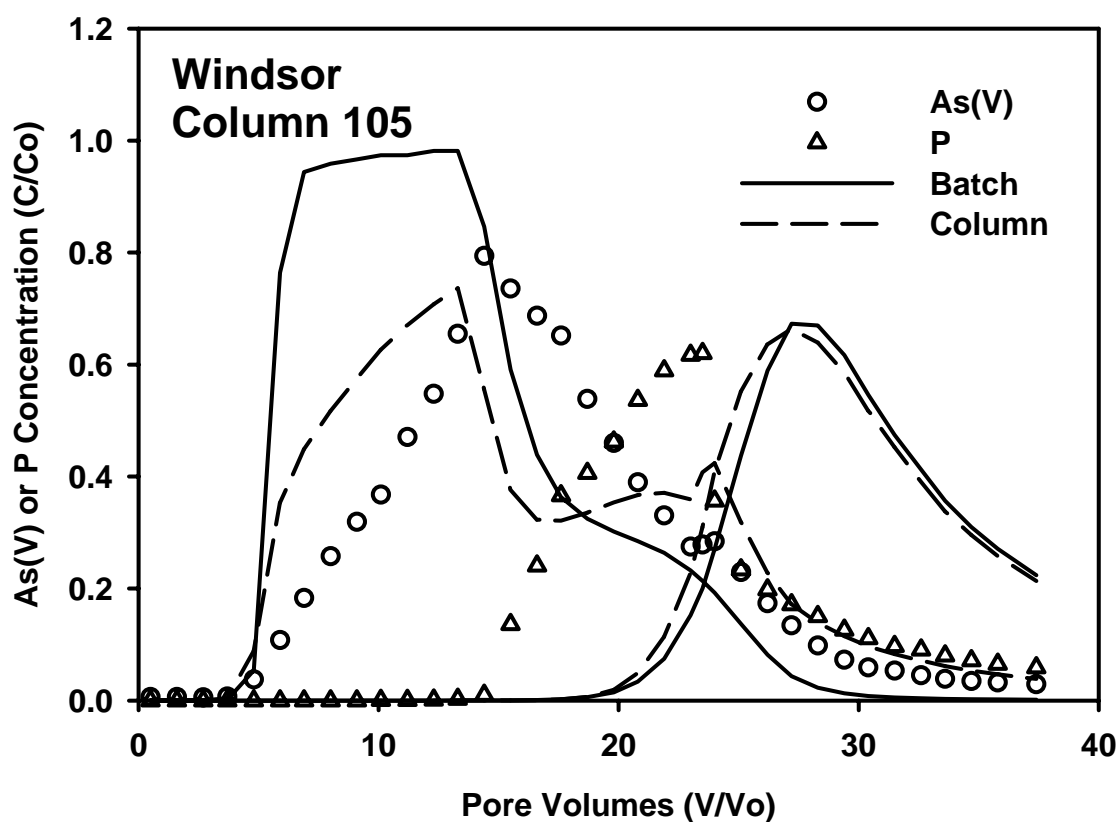


Figure 6.11 Experimental As(V) and P breakthrough curves (BTCs) in Windsor soil (column 105). Solid curves are multi-component multi-reaction model (MCMRM) predictions made with the kinetic parameters derived from the batch experiment data (Table 6.2), whereas the dashed curves are MCMRM simulation with kinetic parameters obtained from single component As(V) transport experiment (column 104, see Table 6.3).

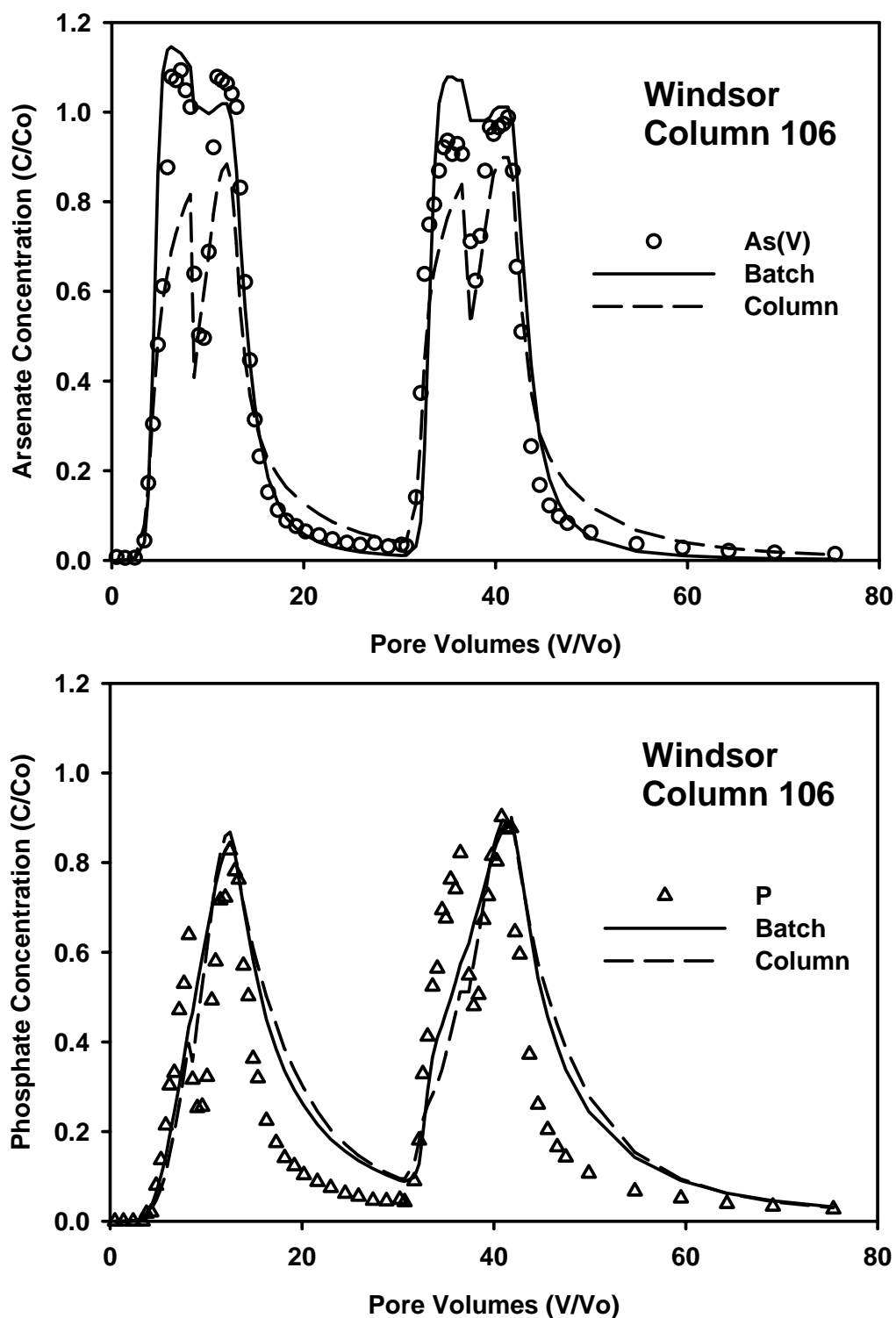


Figure 6.12 Experimental As(V) and P breakthrough curves (BTCs) in Windsor soil (column 106). Solid curves are multi-component multi-reaction model (MCMRM) predictions made with the kinetic parameters derived from the batch experiment data (Table 6.2), whereas the dashed curves are MCMRM simulation with kinetic parameters obtained from single component As(V) transport experiment (column 104, see Table 6.3).

concentrations and mass recoveries (see Table 6.1) of As(V) eluted from Olivier and Windsor soil columns. In the presence of phosphate, As(V) BTC from Column 106 (Windsor) had a peak concentration which exceeded the input concentration ($C/C_0 \approx 1.2$). This is indicative of chromatographic or snow-plow effect. High peak concentration of As(V) in the presence of P was also reported by Darland and Inskeep (1997). Selim et al. (1992) observed snow-plow effect for Cd transport and suggested that this was a result of the release of sorbed species in response to the large increase in total solute concentrations in solution. While arsenate recoveries was significantly enhanced by the addition of phosphate, a large fraction of As(V) was retained in the column at the end of the experiment as indicated by recoveries less than 100% (91.0% and 89.5% for column 103 and 106, respectively) .

The BTCs shown in Figure 6.10b and 6.12b (Column 103 and 106) illustrated the transport of P in the presence of As(V). Similar to As(V), BTCs for P transport exhibited extensive asymmetry as illustrated by the difference in the shape of the sorption side from the desorption side. The extensive non-equilibrium conditions were indicated by the sharp drop in P concentration as a result of flow interruption. This is not surprising if one considers the time-dependent sorption behavior of P demonstrated by our kinetic batch results. For Olivier soil (Column 103), more As(V) than P was sorbed during transport as illustrated by the lower peak concentration and mass recovery of As(V) than P. In contrast, P was preferentially sorbed during transport in Windsor soil. The selective sorption of P to As(V) may be partially responsible for the snow plow effect of As(V) observed in Column 106.

The displacement of As(V) by P is shown in Figure 6.9 and 6.11 (Column 102 and 105). In comparison with single component As(V) BTCs (Column 101 and 104), increased release of As(V) was observed in Column 102 and 105 as a result of P addition. The exchange of sorbed

As(V) by the application of P was clearly illustrated by the increased As(V) concentration at the desorption side of the BTCs. Moreover, As(V) concentration increased due to flow interruption. This increase is indicative of the kinetic competitive sorption between As(V) and P (Fig 12 and 14).

6.4.5 Transport Modeling

Our modeling efforts were first carried out on each individual As(V) BTCs with a single component multi-reaction transport model (MRM) in a fully predictive mode. Specifically, the model retention parameters (n , K_e , k_1 , k_2 , and k_3) from our kinetic batch data (Table 6.2) were used, coupled with the hydrodynamic dispersivity (δ) obtained from tritium BTCs (Table 6.1), along with other measured parameters such as column length (L), pore water velocity (v), bulk density (ρ), moisture content (θ), and pulse durations (see Table 6.1). Results of multi-reaction transport model predictions are shown as the solid curves in Figure 6.7 and 6.8. Consistent with previous studies (Selim, 1992; Selim et al., 1992; Hinz and Selim 1994), the use of batch model parameters overpredicted concentration maxima (peaks) and underestimated the extent of retardation (BTCs shift to the left). This fully predictive model also underestimated the influence of the flow interruption on As(V) transport. In general, the use of batch rate coefficients grossly underestimated the extent of As(V) retention in Olivier and Windsor soils and overestimated the potential As(V) mobility. In addition, we evaluated several MRM formulations in their capability to predict the BTCs and found no significant difference between the MRM formulations. Zhang and Selim (2006) arrived at a similar finding based on batch kinetic data from three soils.

Table 6.3 Estimated single component MRM parameters (with standard error) obtained from nonlinear optimization with As(V) BTCs

Column	Soil	Solute	r^2	RMSE	n	K_e	k_1 \mathbf{h}^{-1}	k_2 \mathbf{h}^{-1}	k_3 \mathbf{h}^{-1}
101	Olivier	Arsenate	0.976	0.0657	0.311	0.91±0.07	0.10±0.01	0.017±0.002	0.0001±0.0003
103	Windsor	Arsenate	0.979	0.0567	0.287	1.0±0.1	0.23±0.02	0.028±0.003	0.0017±0.0002

We further utilized the MRM model in an inverse modeling mode, where nonlinear least-squares optimization scheme were adopted to obtain the necessary kinetic retention parameters through best-fit of the As(V) BTCs. The kinetic retention parameters and the goodness-of-fit for the nonlinear optimization are given in Table 6.3 for column 101 (Olivier) and 104 (Windsor). The MRM simulation results are shown as dashed curves in Figure 6.7 and 6.8. Overall excellent fits of the model were achieved for As(V) BTCs for Olivier and Windsor columns as indicated by the small values of RMSE (< 0.1) and high r^2 (> 0.95). In addition, the effect of flow interruption and extended tailing (slow release) was successfully described with MRM in inverse modeling mode. We found that the forward reaction rate (k_1) associated with kinetic retention sites (S_1) were approximately one magnitude higher of column transport experiments than batch kinetic experiments (see Table 6.2 and 6.3), indicating that the kinetic retention under dynamic flow conditions were stronger than that of the well mixed batch system. This explains in part the early arrival of BTCs based on fully predictive mode.

The competitive transport of As(V) and P was initially simulated with multi-component multi-reaction transport model (MCMRM) with parameters obtained from the kinetic batch results given in Table 6.2 and the SRS competitive coefficients of Table 5.1. Model results are shown by the solid curves in Figure 6.9-6.12. BTCs of As(V) and P were calculated simultaneously in the computer program, i.e., one simulation produces BTCs for both As(V) and P at each time step. Consistent with the single component MRM simulations, we found the use of batch rate coefficients underestimated As(V) retention and overestimated the extent of As(V) mobility in columns 102, 103 and 105. The model BTCs exhibited higher peak concentrations, steeper BTC fronts, and lack of tailing of the BTCs (Figure 6.9-6.11). However, the competitive model with batch kinetic rates successfully predicted the snow-plow effect [$C/C_0 > 1.0$ for

As(V)] observed in Column 106 (Windsor). Moreover, the predicted BTC closely followed that measured except at flow interruption, where the concentration drop was grossly underestimated. The MCMRM model predicted phosphate BTCs for Olivier and Windsor columns with moderate success. Specifically, our model well described the peak concentration and the extensive tailings. However, the predicted BTCs for Windsor soils had a much longer retardation period than the experimental observation, which was probably resulted from the high equilibrium distribution constant (Ke) from the batch results. Moreover, the effects of flow interruptions were underestimated in all model simulations, suggesting that extent of kinetic sorption during transport was underrepresented by the kinetic reaction rates obtained from our batch experiment results.

In an effort to further test the capability of the proposed competitive model in describing As(V) transport in the presence of P, we decided to implement As(V) parameters derived from column BTCs where As(V) alone was applied (a single component) (see Table 6.3). Specifically, model parameters derived from As(V) BTCs as single component were used in an effort to predict the transport of As(V) where both As (V) and P were applied. The resulting model predictions are shown by the BTCs (dashed curves) in Figure 6.9-6.12, for column 102, 103, 105, and 106. Based on visual observations, as well as r^2 and RMSE, the use of such As(V) parameters significantly improved the prediction of As(V) BTCs for column 102, 103, and 105 where P was also present. Such improved predictions were a result of the fact that similar experimental conditions during transport were maintained. For Olivier soil (Column 102 and 103), the competitive model successfully predicted the concentration increase of the sorption side and the extensive tailing of the desorption side in the BTCs. Furthermore, the effect of flow interruption was successfully described with the kinetic reaction rates from separate column

experiments. Based on the overall prediction of the measured BTCs, we conclude that our model provides an overall representation of possible retention mechanisms for Olivier soil during competitive As(V) and P transport.

The use of column kinetic parameters improved model prediction of As(V) BTC for Column 105 but somewhat with much less success. There were apparent discrepancies between predicted and measure BTCs in the desorption side. In addition, the use of column rate coefficients resulted in better prediction of the effect of flow interruption but failed to predict the snow-plow effect observed in As(V) BTCs for column 106. The poor predictions observed in Windsor soil (Column 105 and 106) was probably due to inaccurate parameters used for the simulation of kinetic retention during P transport.

6.5 Summary and Conclusions

The nonlinear equilibrium-kinetic multireaction (MRM) model was extended in order to describe competitive sorption and transport of multiple species in soils. We evaluated this multi-component multireaction model (MCMRM) for its prediction capability of As(V)-P retention as well as transport in soils. Results from kinetic batch experiments demonstrated that the rate and amounts of As(V) sorption was significantly reduced when applied P concentrations in solution increased. Competitive retention for As(V) and P over time was successfully predicted using MCMRM where model coefficients were based on single component kinetic batch results.

Results from miscible displacement experiments indicated that the presence of P increased mobility of As(V) in all soil columns. The use of batch rate coefficients provided poor prediction of As(V) BTCs from the competitive column transport experiments. The multi-component model adequately predicted the measured BTCs for competitive As(V)-P transport in Olivier and Windsor soil when rates coefficients obtained from inverse modeling of single

component As(V) BTCs were used. The competitive approach was also capable of predicting flow interruptions as well as the chromatographic effect of the As(V) pulse due to the competition of P.

6.6 References

- Amacher, M. C., H. M. Selim, and I. K. Iskandar. 1988. Kinetics of chromium(VI) and cadmium retention in soils: A nonlinear multireaction model. *Soil Sci. Soc. Am. J.* 52:398-408.
- Barnett, M.O., P.M. Jardine, S.C. Brooks, and H.M. Selim. 2000. Adsorption and transport of uranium(VI) in subsurface media. *Soil Sci. Soc. Am. J.* 64:908-917.
- Barrow, N.J., P. Cartes, M.L. Mora. 2005. Modifications to the Freundlich equation to describe anion sorption over a large range and to describe competition between pairs of ions. *Euro. J. Soil Sci.* 56, 601-606.
- Brusseau, M.L. 1993. The influence of solute size, pore water velocity, and intraparticle porosity on solute dispersion and transport in soils. *Water Resour. Res.* 29:1071-1080.
- Darland, J.E., and W. P. Inskeep. 1997. Effects of pH and phosphate competition on the transport of arsenate. *J. Environ. Qual.* 26:1133-1139.
- Hingston, F.J., A.M. Posner, and J.P. Quirk. 1971. Competitive adsorption of negatively charged ligands on oxide surfaces. *Disc. Faraday Soc.* 52, 334-342.
- Kuhlmeier, P.D. 1997. Sorption and desorption of arsenic from sandy soils: Column studies. *J. Soil Contam.* 6: 21-36.
- Ma, L.W., and H.M. Selim. 1994. Tortuosity, mean residence time, and deformation of tritium breakthroughs from soil columns. *Soil Sci. Soc. Am. J.* 58, 1076-1085.
- Manning, B.A., and S. Goldberg. 1996. Modeling competitive adsorption of arsenate with phosphate and molybdate on oxide minerals. *Soil Sci. Soc. Am. J.* 60:121-131.
- McGinley, P.M., L.E. Katz, and W.J. Weber. 1996. Competitive sorption and displacement of hydrophobic organic contaminants in saturated subsurface soil systems. *Water Resour. Res.* 32:3571-3577.
- Melamed, R., J.J. Jurinak, and L.M. Dudley. 1995. Effect of adsorbed phosphate on transport of arsenate through an oxisol. *Soil Sci. Soc. Am. J.* 59:1289-1294.
- Murali V. and L.A.G. Aylmore. 1983. Competitive adsorption during solute transport in soils: 3. A review of experimental evidence of competitive adsorption and an evaluation of simple competition models. *Soil Sci.* 136, 279-290.
- Nitzsche, O., G. Meinrath, and B. Merkel. 2000. Database uncertainty as a limiting factor in reactive transport prognosis. *J. Contam. Hydrol.* 44:223-237.

- Peryea, F.J. 1991. Phosphate-induced release of arsenic from soils contaminated with lead arsenate. *Soil Sci. Soc. Am. J.* 55:1301-1306.
- Raven, K.P., A. Jain, and R.H. Loeppert. 1998. Arsenite and arsenate adsorption on ferrihydrite: Kinetics, equilibrium, and adsorption envelopes. *Environ. Sci. Technol.* 32:344-349.
- Roy, W.R., J. J. Hassett, and R.A. Griffin. 1986. Competitive coefficient for the adsorption of arsenate, molybdate, and phosphate mixture by soils. *Soil Sci. Soc. Am. J.* 50:1176-1182.
- Roy, W.R., J.J. Hassett, and R.A. Griffin. 1986. Competitive interactions of phosphate and molybdate on arsenate adsorption. *Soil Sci.* 142: 203-210.
- Selim, H.M., M.C. Amacher, and I.K. Iskandar. 1990. Modeling the transport of heavy metals in soils. CRREL Monograph 2, U.S. Government Printing Office (152 p).
- Selim, H.M. 1992. Modeling the transport and retention of inorganics in soils. *Adv. Agron.* 47:331-384.
- Selim, H.M., B. Buchter, C. Hinz, and L.W. Ma. 1992. Modeling the transport and retention of cadmium in soils: Multireaction and multicomponent approaches. *Soil Sci. Soc. Am. J.* 56:1004-1015, 1992.
- Sheindorf, C., M. Rebhun, and M. Sheintuch. 1981. A freundlich-type multicomponent isotherm. *J. Colloid Interface Sci.* 79:136-142.
- Smith, S.L., and P.R. Jaffe. 1998. Modeling the transport and reaction of trace metals in water-saturated soils and sediments. *Water Resour. Res.* 34:3135-3147.
- Toride, N., F.J. Leij, and M.Th. van Genuchten. 1995. The CXTFIT code for estimating transport parameters from laboratory or field tracer experiments, Version 2.0, Research Report No. 137, U.S. Salinity Laboratory, USDA-ARS, Riverside, CA.
- Violante, A., and M. Pigna. 2002. Competitive sorption of arsenate and phosphate on different clay minerals and soils. *Soil Sci. Soc. Am. J.* 66:1788-1796.
- Williams, L. E., M. O. Barnett, T. A. Kramer, and J. G. Melville. 2003. Adsorption and transport of arsenic(V) in experimental subsurface systems. *J. Environ. Qual.* 32:841-850.

CHAPTER 7: COLLOID MOBILIZATION AND ARSENITE TRANSPORT IN SOIL COLUMNS

7.1 Introduction

A wide range of interactions including ion exchange, surface complexation, and precipitation contribute to the removal of arsenic from aquatic solution by solid constituents. In general, adsorption to soil and sediment is the major pathway of attenuating arsenic bioavailability and toxicity in natural environments. Numerous studies have demonstrated that iron oxides/hydroxides have particularly high affinity for arsenic. The spectroscopic studies of Sun and Doner (1998) and Manning et al. (1998) indicated that As(III) formed bidentate binuclear inner-sphere complexes on goethite surface, whereas Goldberg and Johnson (2001) reported that arsenite forms both inner- and outer-sphere surface complexes on amorphous Fe oxides and outer-sphere surface complexes on amorphous Al oxides. Dixit and Hering (2003) reported that As(V) have higher affinity to iron oxides than As(III) below pH 5-6, whereas more As(III) was sorbed above pH 7-8. In addition, the kinetic study of Raven et al. (1998) demonstrated that arsenite adsorption was more rapid than arsenate and they suggest the adsorption kinetics was diffusion controlled. Adsorption studies on soils demonstrated that the amounts of arsenite adsorption were less than arsenate (Manning and Goldberg, 1997; Smith et al., 1999). The kinetic or time-dependent adsorption behavior of arsenite on soils was demonstrated by the studies of Elkhatib et al. (1984a). In addition, Elkhatib et al. (1984b) found that the arsenite adsorption on soils were essentially irreversible.

Most of the researches on the mobility of arsenite were conducted in well mixed batch experiments, whereas only a few studies have investigated the mobility of arsenite under dynamic flow conditions. Radu et al. (2005) studied the effect of pH and pore water velocity on the transport of As(III) in saturated columns of goethite-coated sand. They reported that As(III)

was more mobile at pH 4.5 than pH 9, and that increasing pore water velocity increased the mobility of As(III), an indication of rate dependent adsorption.

Traditionally, the transport of arsenic is assumed to occur entirely in aqueous or soluble phase. However, significant portion of mobile arsenic in the groundwater is present in colloidal form, i.e., arsenic minerals or adsorbed on mineral surfaces. For example, Le et al. (2000) observed that more than 50 % of the arsenic presented in the particulate fraction ($>0.45\mu\text{m}$) for the well water samples collected from northern Alberta. Ishak et al. (2002) investigated arsenic leaching from fly ash through an intact Appling loamy sand column. Their result showed that arsenic levels present in the leachates roughly correlated with effluent turbidity, which support the supposition that arsenic movement was generally associated with mobilized colloids. The important role of colloid in facilitating contaminant transport in porous media has been recognized since the early 1990s. There is evidence indicating that non-aqueous, mobile colloid could transport low solubility contaminants for a considerable distance (Kretzschmar et al., 1999; Bertsch and seaman, 1999).

The potential of colloids mobilized from natural soils or sediments in facilitating the transport of strongly sorbed contaminants have been studied by several researchers. Grolimund et al. (1996) observed substantial colloids release and Pb^{2+} mobilization in a column of an aquic dystic Eutrochrept when input solution was switched from 50mM NaCl to 0.15mM CaCl_2 . Recently, they developed a mathematical transport model coupling the transport of colloids and solutes, where a large array of reactions was considered (Grolimund and Borkovec, 2005). Similarly, Roy and Dzombak (1997) conducted systematic laboratory investigations on the transport of Ni^{2+} in Lincoln sand in the presence of colloids mobilized by flushing with low ionic

strength solution. They observed substantial transport of strongly sorbed Ni^{2+} as a result of colloid mobilization.

Iron oxides have long been recognized as important soil constituents affecting the retention and transport of inorganic arsenic [As(V) and As(III)] in soils. If colloidal iron oxides with adsorbed arsenic were mobilized in the soil system, it may cause colloidal facilitated transport of arsenic. Puls and Powell (1992) conducted column experiments with aquifer material to investigate possible effects of colloidal iron oxide on facilitating As(V) transport. They observed the substantial mobilization of colloid associated arsenate when flushing the column with deionized water. Moreover, they evaluated several factors (particle size, pH, velocity, ionic strength, and anions) on the transport of colloidal iron oxides. Their result demonstrated that the presence of HAsO_4^{2-} and HPO_4^{2-} anions substantially increased the mobility of iron oxides due to increased particle-particle repulsive forces. Such repulsive forces are a result of charge reversal on initially positively charged iron oxide surfaces.

The reductive dissolution of iron oxide and subsequent release of sorbed or precipitated arsenic were proposed as the mechanisms of arsenic contamination of aquifers in Bangladesh (Smedley and Kinniburgh, 2002; Pedersen et al., 2006). Herbel and Fendorf (2006) investigated the mobilization of arsenic under dynamic flow conditions in ferric hydroxide coated sands inoculated with arsenate reducing bacteria (*Surfurosprillum barnesii* strain SES-3). They suggested that the release of arsenic into the aqueous phase is associated with the mineralogical transformation of iron oxides resulted from the microbial reduction. From their reductive dissolution experiment with iron oxides, Pedersen et al. (2006) demonstrated that As(V) was not released from surfaces of ferrihydrite and goethite until the surface area became too small.

In addition to the release of dissolved arsenic, the reduction of iron(III) (hydr)oxides may mobilize colloidal arsenic by dissolving the ferric oxyhydroxide coatings cementing the aggregates (Ryan and Gschwend, 1990; Thompson et al., 2006). Ryan and Gschwend (1990) observed the presence of colloidal clay particles in anoxic groundwater. Their field evidence indicated the depletion of oxidized iron coating mobilized colloids. Recently, Thompson et al. (2006) studied the colloid mobilization during iron redox oscillations with a Hawaiian soil. They suggested that the colloid dynamics were dependent on pH shifts due to the Fe redox reaction. Peretyazhko and Sposito (2005) found Fe(II) produced from reductive reaction was mainly particulate due to the possible precipitation of siderite and vivianite.

The motivation of this study was to determine the relationships between the mobilization of colloidal Fe oxides and transport of As(III) in natural soils with different properties. Specifically, we conducted sorption/mobilization column experiments to explore the potential for rapid mobilization of contaminants from porous medium by the release of colloids upon reducing ionic strength of the influent.

7.2 Material and Methods

7.2.1 X-ray Diffraction

Random powder samples were prepared by grinding in isopropyl alcohol using an agate mill micronizer. Sodium dispersed samples were prepared by immersing overnight 40g soil in 320mL Na_3PO_4 . Water dispersible clay (WDC) samples were treated by mixing 40g soil in 320mL deionized water and shaking for 16h on a reciprocal shaker. The coarse (0.2-2 μm) and fine (<0.2 μm) clay of both sodium dispersed and water dispersed samples were extracted by gravity settling and centrifugation, respectively. The oriented slides for clay mineral analysis were treated after K saturation with heat treatment at 300 and 550 °C and Mg saturation with

salvation using glycerol and ethylene glycol. Oriented and random powder samples were analyzed by X-ray diffraction (XRD) using a Siemens D500 with Cu-K α radiation at 40 kV and 30 mA in the 2-36°2 θ and 2-70°2 θ range, respectively, with a step size of 0.02°2 θ and a count time of 1.0s. Compensation variable-slit, sample spinning, and position reflection correction with quartz (100) internal standard were used. X-ray diffraction scanning of oriented slides further treated with ethylene glycol (EG), and heated (at 300 and 500 for 1h) was performed. MacDiff 4.2.5 software written by Petschick (2000) was used for peak decomposition and qualitative identification of minerals.

7.2.2 Miscible Displacement Experiments

Saturated column transport experiments were conducted to study arsenite transport in the soils. Acrylic columns (6.4cm i.d. and 10cm in length) were uniformly packed with <2mm air dried soil samples resulting in bulk density of 1.05 to 1.35 g cm⁻³. Influent was supplied by a piston pump to the bottom of each column to sustain a steady-state flow, and the effluent was collected using a fraction collector. Columns were saturated from the bottom with 0.01 M NaCl background solution. Input solution of 10 mg L⁻¹ arsenite (in the form of NaH₂AsO₃) in 0.01 M NaCl was then applied. After about 10 pore volumes of arsenite pulse application, the flow was completely stopped. This 5-day flow interruption was to evaluate non-equilibrium or kinetic controlled arsenic retention during transport and colloid mobilization. Some 8-10 pore volumes of arsenite solution were applied subsequent to flow interruption and were then leached with deionized water. Another 5-d flow interruption was carried out during leaching with DIW. Electrical conductivity (EC), turbidity, and pH of column effluent were monitored over time. The samples collected from column experiment were analyzed by inductively coupled plasma atomic emission spectrometry (ICP-AES). Total (<20 μ m) concentrations of As, Fe, and Al in effluent

samples were measured by digestion using 16M HNO₃, whereas the dissolved (<0.20µm) concentrations were determined after filtration with 0.20 µm membrane filter. The particulate (0.2µm-20µm) As, Fe, and Al concentrations were calculated from the difference between total and dissolved concentrations. The volume of arsenite pulse along with soil parameters associated with each column is given in Table 7.1.

7.2.3 Sequential Extraction

At the end of each miscible displacement column experiment, the 10 cm long soil column was dismantled and sectioned into 5 pieces segments (2cm each). The amounts of arsenic bound at different strengths by the soil matrix were determined through sequential extraction. A simplified version of the extraction procedures proposed by Keon et al. (2001) was used. Specifically, four fractions were quantified, referred to here as exchangeable (extracted with 1M MgCl₂, pH=8), strongly bound (extracted with 1M NaH₂PO₄, pH=5), coprecipitated with Fe/Al oxides (0.2M ammonium oxalate, pH=3, reacted in dark), and recalcitrant fraction (extracted with 16N HNO₃). The first three phases were measured by mixing 3.0g of soil with 20 mL of the extractant solution, shaking for 24 h, and centrifuging, whereas residual arsenic was determined by mixing with 20mL of 16 N HNO₃ solutions and shaking for 2h in a water-bath maintained at 80°C.

7.3 Results

7.3.1 Soil Characteristics

XRD analysis of bulk soil samples indicated that both Olivier and Windsor soils consisted mainly of quartz, with much less plagioclase feldspar, and clay minerals. The mineralogy of the fine clay (<0.2µm) and coarse clay (0.2-2µm) fractions determined with

Table 7.1 Column soil physical parameters for miscible displacement experiments. Values of the dispersion coefficient were estimated from tritium breakthrough results.

No	Soil	ρ_b^a g cm ⁻³	θ cm ³ cm ⁻³	ν cm h ⁻¹	D cm ² h ⁻¹	P.V. ^b
101	Olivier	1.05	0.61	0.83	1.65	17.25
102	Windsor	1.35	0.49	1.03	0.21	21.33

^a ρ_b = Bulk density, θ = saturated water content, ν = pore water velocity, D = Dispersion coefficient.

^b P.V. = total pore volumes of arsenic input pulse.

Table 7.2 XRD determined mineral composition of coarse (0.2-2 μ m) and fine (<0.2 μ m) fractions of sodium-dispersible clay (SDC) and water-dispersible clay (WDC) for Olivier and Windsor soils

		size (μ m)	Smectite	Illite	Chlorite	Kaolinite	Quartz
Olivier	SDC	0.2-2	28	30	0	31	11
	SDC	<0.2	45	31	0	22	2
	WDC	0.2-2	34	30	0	24	11
	WDC	<0.2	52	20	0	24	3
Windsor	SDC	0.2-2	12	33	15	29	10
	SDC	<0.2	24	49	24	0	4
	WDC	0.2-2	0	41	36	15	8
	WDC	<0.2	0	61	33	0	6

sodium dispersion and desionized water dispersion are given in Table 7.2. Based on XRD results, smectite, illite, kaolinite, and quartz were found in the fine clay fraction ($<0.2\mu\text{m}$) of both soils, whereas chlorite was only found in Windsor soil.

7.3.2 Arsenite Transport

The results from saturated miscible displacement experiments are presented in Figure 7.1 as breakthrough curves (BTCs) for Olivier and Windsor soils. The transport of arsenite in Olivier soil column was relatively fast, the breakthrough of arsenite was observed shortly following the injection of arsenite solution and after approximately 17 pore volumes of arsenite pulse, the total concentration of arsenic in the effluent gradually increased to 3.5 mg L^{-1} . A sharp increase of arsenic concentration was observed as a result of and after the input solution was replaced to deionized water. The total arsenic concentration in the effluent approximately doubled due to leaching using deionized water. After approximately 20 pore volumes of leaching with deionized water, the total arsenic concentration in the effluent was approximately 0.4 mg L^{-1} and with extensive tailing, i.e., slow and continued desorption.

Flow interruption during arsenic input pulse resulted in a decrease of arsenic concentration by about 1.0 mg L^{-1} , whereas stopping the flow during leaching phase resulted in an increase of arsenic concentration for approximately 0.6 mg L^{-1} . The particulate arsenic (difference between $<20\mu\text{m}$ and $<0.2\mu\text{m}$ arsenic) was observed only when the input solution was replaced by deionized water. The peak concentration of particulate arsenic was about 2 mg L^{-1} .

The breakthrough of arsenite from Windsor column showed extensive retardation (>15 pore volumes) with a sharp front at about 25 pore volumes. The peak concentration of dissolved arsenic ($<0.2\mu\text{m}$) occurred after the column was leached with more than 10 pore volumes of DIW. At the end of the experiment (leached with DIW for >25 pore volumes), relatively high

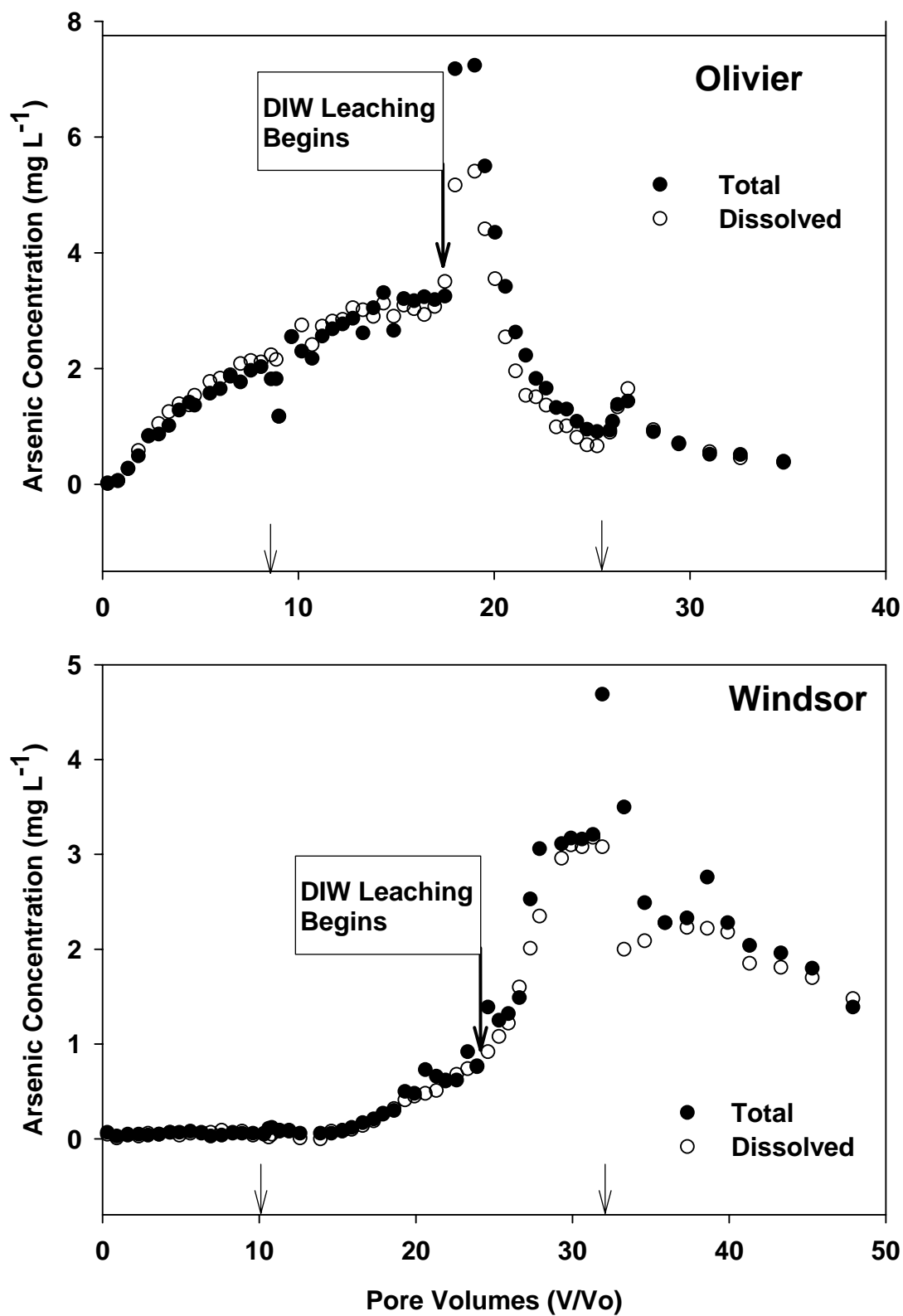


Figure 7.1 Breakthrough curves (BTC) of total ($<20\mu\text{m}$) and dissolved ($<0.2\mu\text{m}$) arsenic for Olivier and Windsor soil columns. Arrows indicate pore volumes when flow interruptions occur.

Table 7.3 Cumulative amount of As, Fe, and Al leached out and amount of As retained in soil columns

No	Soil	Fe		Al		As					
		<20µm	<0.2µm	<20µm	<0.2µm	<20µm	<0.2µm	P1 ^a	P2	P3	P4
		-----mg-----									
101	Olivier	16.6	15.7	12.2	9.7	13.1 ^b (40.8%)	12.3 (38.3%)	0.30 (0.9%)	8.1 (25.2%)	9.6 (29.9%)	1.3 (4.0%)
102	Windsor	75.4	50.8	5.8	1.7	9.8 (29.1%)	8.5 (25.2%)	0.36 (1.1%)	7.3 (21.7%)	12.1 (35.9%)	0.73 (2.2%)

^a: P1= Exchangeable (1M NaCl), P2 = Strongly sorbed (1 M NaH₂PO₄), P3 = Precipitated (0.2 M ammonium oxalate), and P4 = Recalcitrant (16 N HNO₃).

^b: Percent of the total arsenic applied to the soil column.

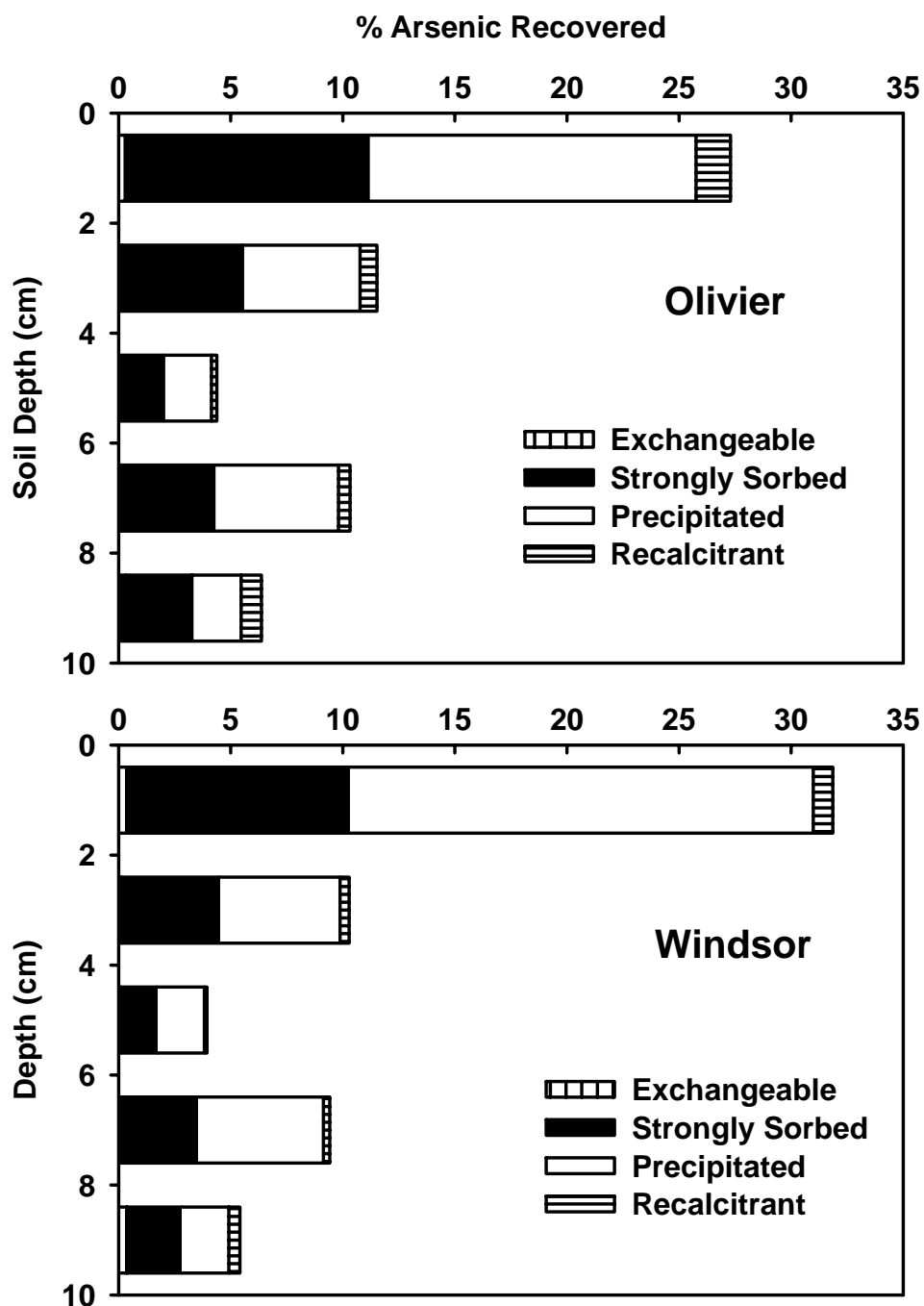


Figure 7.2 The percentage recoveries of arsenic as against to the total input as determined from sequential extractions of soils from different column depths. Agents used for extractions were: Exchangeable ($1M$ $NaCl$), Strongly sorbed ($1M$ NaH_2PO_4), Precipitated ($0.2M$ ammonium oxalate), and Recalcitrant ($16 N$ HNO_3).

concentration (around 1.4 mg L^{-1}) of arsenic still present in the effluent. Release of particulate arsenic was not observed after introducing deionized water. However, flow interruption during leaching phase resulted in the release of particular arsenic with peak concentration of 1.5 mg L^{-1} .

7.3.3 Arsenic Retention in Soils

The amount of arsenic retained by the soils as determined using sequential extraction are presented in Figure 7.2 in terms of concentration versus soil depth. In addition, the percentages of arsenic recovered in the effluent and sequential extraction are given in Table 7.3. Our results demonstrated extensive retention during arsenite transport in Olivier and Windsor soils. After leaching with DIW for 20-30 pore volumes, the mass recoveries from column effluents were 40.8% and 29.1% of that applied for column 101 (Olivier), and 102 (Windsor), respectively. The sequential extraction result further revealed that large fractions of arsenic were strongly bound (extracted with NaH_2PO_4) or coprecipitated with Fe/Al oxides (extracted with ammonium oxalate). Based on the results illustrated in Figure 7.2, more than 60% of arsenic was retained in both Olivier and Windsor, indicating the strong retention of arsenic by both soils.

7.3.4 Mobilization of Colloidal Particles

The turbidity of the effluent, which represents the concentration of colloidal particles in the effluent solution, is illustrated as breakthrough curves in Figure 7.3. For Olivier soil, the initial effluent turbidity was around 50 NTU and decreased rapidly to less than 10 NTU after 3 pore volumes of arsenic application. Flow interruption implemented during arsenic input phase resulted in a small increase of turbidity to 22 NTU. Rapid release of large amounts of colloidal particles was observed when the input solution was replaced by deionized water, as illustrated by sharp increase in turbidity in the effluent ($>100 \text{ NTU}$). In addition, the flow interruption during

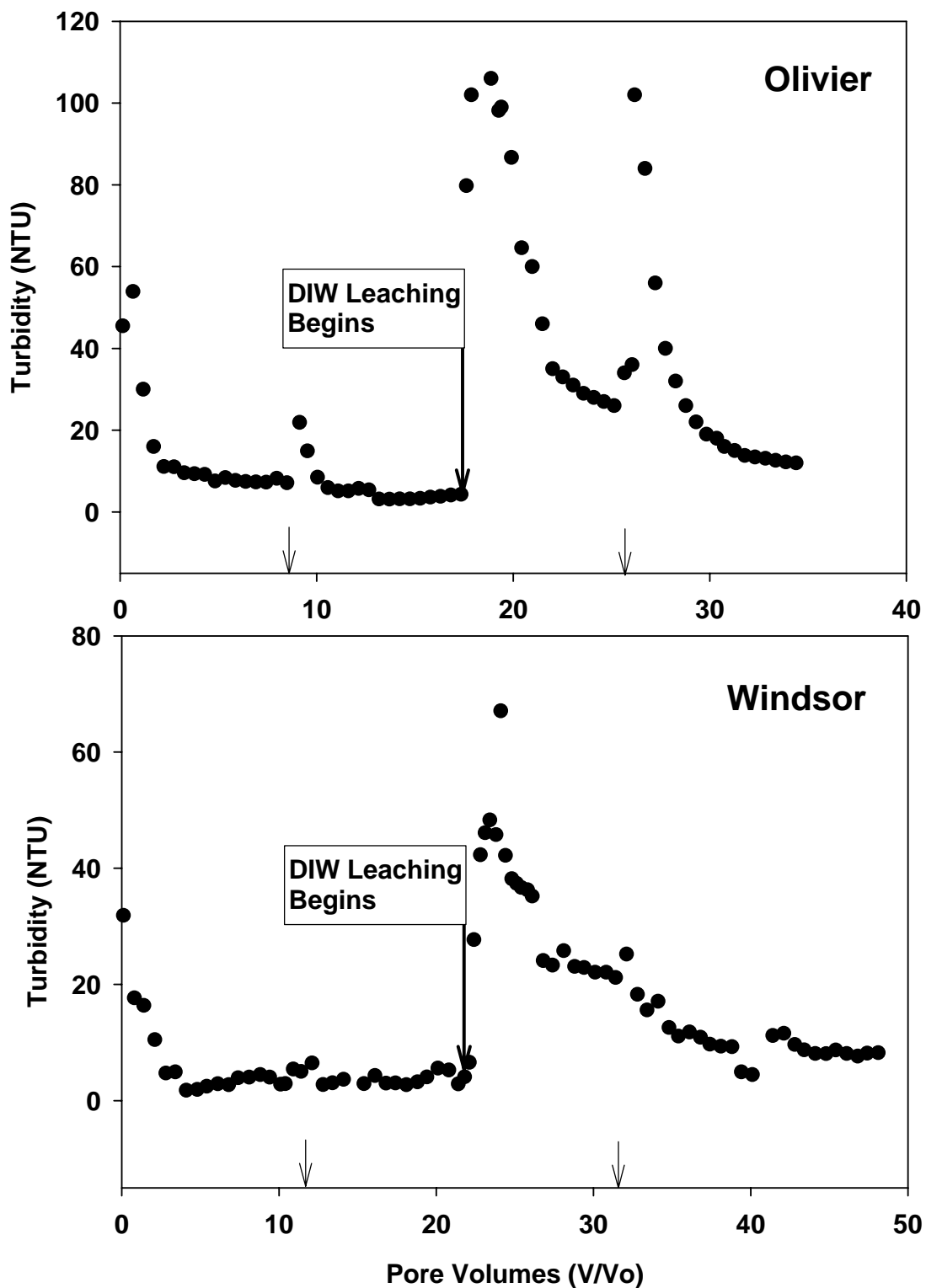


Figure 7.3 Effluent turbidity during injection of 10 mg L^{-1} As(III) in $0.01M$ NaCl followed by leaching with deionized water for Olivier and Windsor soil columns. Arrows indicate pore volumes when flow interruptions occur.

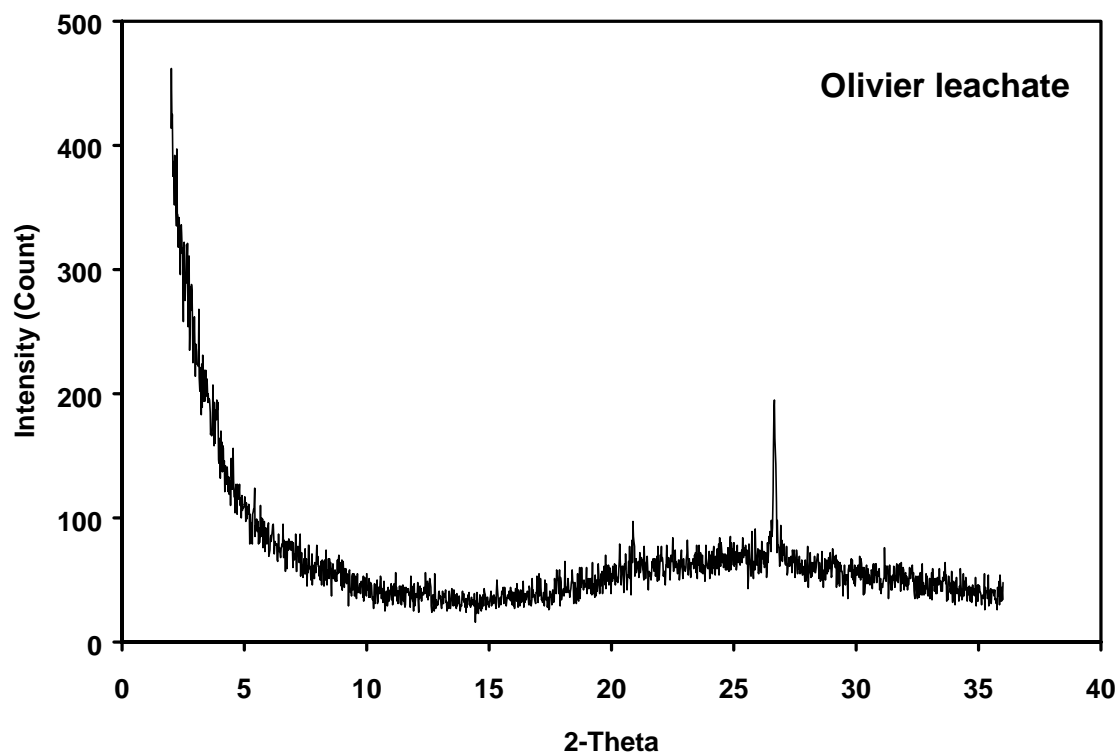


Figure 7.4 X-ray diffractograms (XRD) of colloids in the composite effluent solution of Olivier soil column.

leaching with deionized water resulted in a substantial release of colloidal particles with peak turbidity > 100 NTU. For Windsor soil, the release of colloidal particles was observed when the deionized water was introduced, was reflected by the peak turbidity around 50 NTU. However, flow interruptions did not result in the increase of turbidity. The XRD pattern shown in Figure 7.4 demonstrated that the major portion of the mobile particles in the effluent solution from Olivier soil was amorphous, with trace amounts of quartz particles.

7.3.5 Release of Fe and Al

Elution of Fe and Al from soil columns are illustrated as BTCs in Figure 7.5 and 7.6 for Olivier and Windsor Soils. For both soils, large amounts of Fe were released during the initial stage (first 10 pore volumes) of the experiment. The peak concentrations were 10 and 52 mg L⁻¹ for Olivier and Windsor soils, respectively. Flow interruption during arsenic input phase resulted in the release of Fe from both soils. However, the amount release from Windsor soil (peak concentration of 41 mg L⁻¹) was much higher than that from the Olivier soil (peak concentration of 3.6 mg L⁻¹). Replacing the input solution with deionized water resulted in a rapid increase of total Fe concentration in the effluent from Olivier column. In contrast, total Fe concentration in the eluent from Windsor column continued to decrease during leaching with DIW. Furthermore, flow interruption during the DIW leaching phase resulted in rapid release of Fe (peak concentration of 8.5 mg L⁻¹) from Olivier soil but not from the Windsor soil. For Olivier column, particulate Fe fraction was only observed after the arsenic input solution was replaced with DIW. In contrast, a small fraction of particulate Fe was observed for the Windsor soil through out the arsenic input phase.

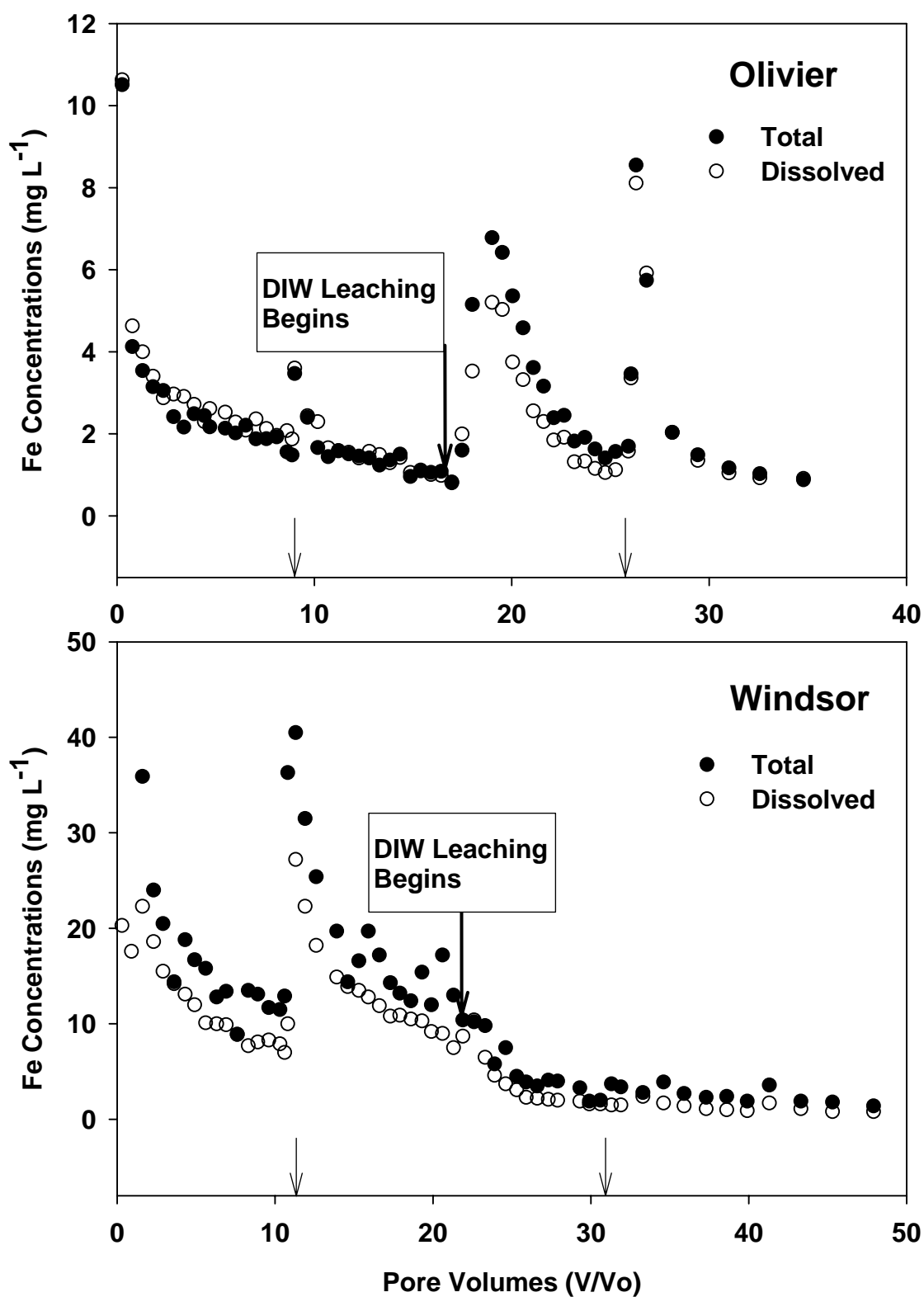


Figure 7.5 Mobilization of total ($<20\mu\text{m}$) and dissolved ($<0.2\mu\text{m}$) iron fractions from Olivier and Windsor soil columns. Arrows indicate pore volumes when flow interruptions occur.

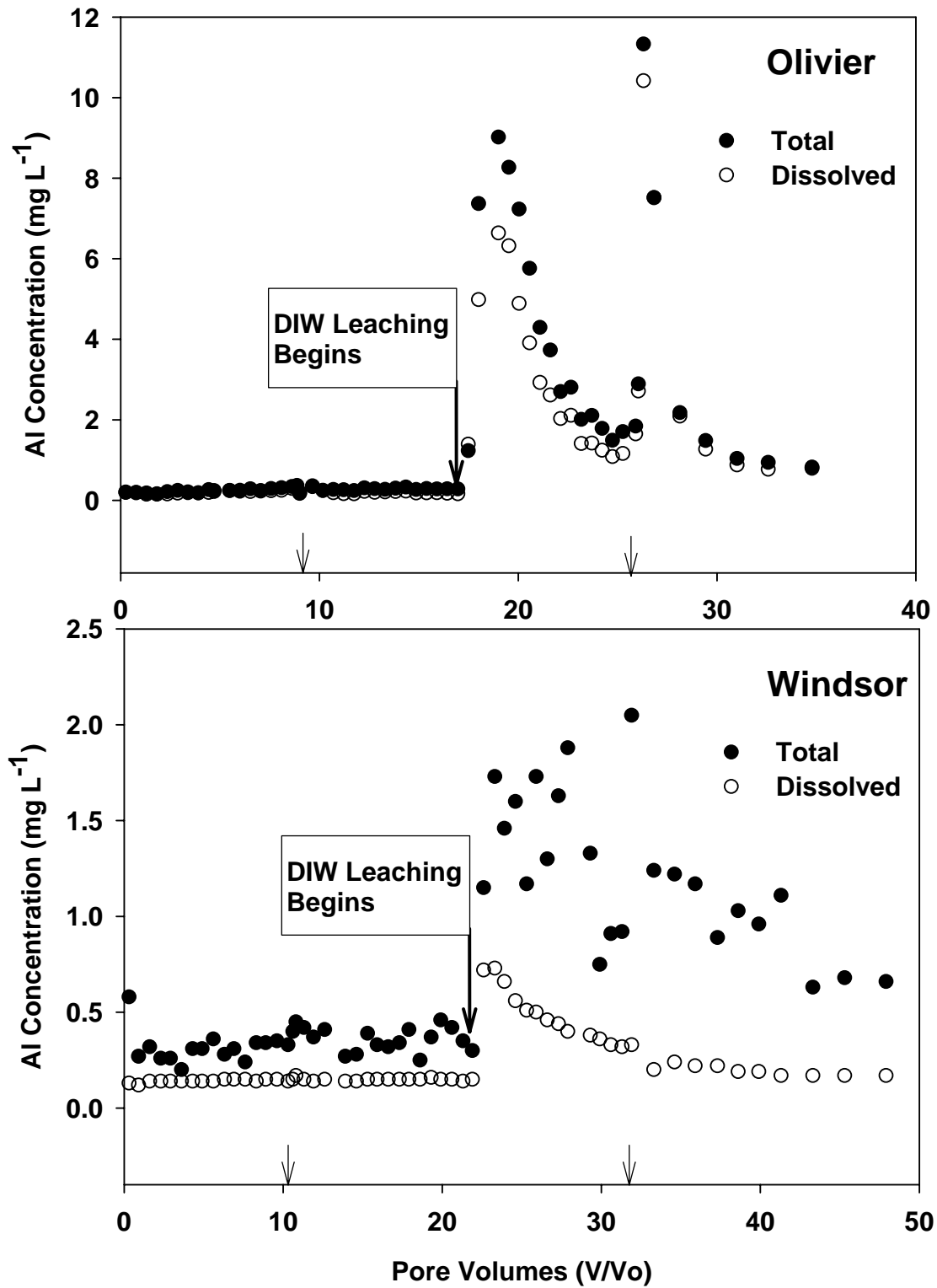


Figure 7.6 Mobilization of total ($<20\mu\text{m}$) and dissolved ($<0.2\mu\text{m}$) aluminum fractions from Olivier and Windsor soil columns. Arrows indicate pore volumes when flow interruptions occur.

During the arsenic input pulse, Al concentration in the effluent was consistently low for both Olivier and Windsor soil (see Figure 7.6). Significant mobilization of Al was observed only after the DIW was introduced. Flow interruption during DIW leaching resulted in significant release of Al from Olivier column. Furthermore, Al was more mobile in Oliver, illustrated by the higher Al concentration of the effluent than that for Windsor soil. A significant amount of Al was present in the particulate fraction, especially for Windsor soil.

7.4 Discussion

7.4.1 Colloid Mobilization

For Olivier soil, there was no apparent difference between the mineralogical composition of sodium dispersed colloids (SDC) and water dispersed colloids (WDC), which is in general agreement with Seta and Karathanasis (1996) and is believed to be a result of low organic content in this soil. However, the significant impact of dispersion agent (sodium vs. DIW) was observed in the XRD patterns of Windsor soil. Specifically, smectite constitute a significant fraction of SDC but was completely missing in WDC, indicating that the aggregates between smectite particles were relatively stable. Similarly, much less kaolinite was found in WDC than in SDC. In addition, for Windsor soil, kaolinite was only found in the coarse clay fraction (0.2-2 μm), indicating the large size of kaolinite aggregates. The relative stability of smectite and kaolinite aggregates were explained with the high content of organic matter in Windsor soil. The important role of organic matter as major binding agent for water stable aggregates has been well documented (Tisdall and Oades, 1982).

Even though the XRD analysis demonstrated that the clay minerals in Olivier soil was readily dispersed by DIW, we did not observe significant mobilization of clay minerals in our column study based on the XRD pattern of colloidal particles in the effluent (Figure 7.4). The

peaks of colloid BTCs coincided with peaks of Fe BTCs (Figure 7.3 and 7.5) for Olivier column, suggesting that a fraction of the amorphous material were colloidal Fe oxides. Relatively few studies have been carried out to investigate the mineral composition of colloid particles mobilized from natural soils and sediments. Kretzschmar et al. (1999) suggested that mobilized colloids were representative of the mineralogy composition of the clay fraction. However, Seaman et al. (1997) found the colloids mobilized from southeastern coastal plain sediments consisted mainly of Al-rich goethite, with lesser amounts of kaolinite, and some crandallite, which is different from the mineral composition of bulk sediment. Several studies have reported that a wide range of chemical and physical factors could impact the attachment-detachment, flocculation-dispersion, and transport of colloids in natural environment (Bertsch and Seaman, 1999; Kretzschmar et al., 1999). Our results also indicated that the characteristics of colloids mobilized from natural soil might significantly different from that of the clay fraction in the bulk soils.

Minor variation of the chemistry of the pore water may have profound influence on colloid generation and transport in natural soils (Bertsch and Seaman, 1999). The dispersive effects of monovalence cations (Na^+ , K^+ , NH_4^+) on clay aggregates have been known by soil scientists for several decades. In our column experiments, the initial release of colloidal particles might partly due to the dispersion of colloidal particles induced by increasing exchangeable sodium percentage (ESP). Another possible mechanism for colloid mobilization during the initial stages was the formation of inner-sphere surface complexes between arsenite and Fe/Al oxides. It is demonstrated that the specific (inner-sphere) sorption of phosphate anions reduces repulsive forces between positively charged particles and decreases aggregates stability (Gillman 1974).

Therefore, the extensive adsorption of arsenite anions might contribute to the initial release of colloids observed in our column experiment.

Based on the classical DLVO theory, low concentration of background electrolytes increases repulsive electrostatic force between colloids and therefore leads to their dispersion (Sposito, 1989). Kuhn et al. (2000) demonstrated the increasing transport of hematite colloids in packed quartz sand with reduced ionic strength. Using columns of a highly weathered aquifer material, Seaman et al. (1995) observed the mobilization of colloidal particles with positive electrophoretic mobility when the pore solution (CaCl_2 , NaCl , and MgCl_2) was replaced with deionized water. Results from our experiments clearly demonstrate that significant amounts of colloidal particles were mobilized when the background solution (0.01 M NaCl) was displaced with DIW. This was based on the subsequent sudden increase in the level of turbidity in the effluent solution. A comparison between columns indicate that significantly more colloids were mobilized from Olivier soil than Windsor soil, which is in general agreement with the relative stability of aggregates observed by the mineralogical analysis. Moreover, flow interruption on Olivier column resulted in significant increase of turbidity in the effluent, which indicates strong time-dependent behavior of the colloid mobilization processes. However, the colloid concentration did not increase as a result of stop-flow for Windsor column, suggesting a different mechanism of colloid mobilization.

7.4.2 Release of Fe Oxides under Anaerobic Condition

Assessment of Fe and Al release indicated the importance of these elements in the mobilization of colloids and transport of arsenite in soil columns. In our analysis, $0.2\mu\text{m}$ filters were used to separate total and dissolved fraction of Fe. However, particle size of colloidal iron

oxides might $<0.2\mu\text{m}$ and pass through the pores of these filters. Advanced analytical methods are required to further separate the dissolved fractions from colloidal fractions.

The shape of Fe BTCs (Figure 7.5a) from Olivier column closely followed the BTC of colloid mobilization (Figure 7.3a). Based on these similarities, the amorphous particles appeared in the effluent from Olivier columns may be ferric hydroxide minerals (Ryan and Gschwend, 1990). Moreover, we suggest that the mechanisms used to explain colloid mobilization can also be applied to the release of Fe/Al oxides observed for Olivier column.

High concentrations of Fe were observed in the effluent from Windsor column during the arsenite input pulse. Flow interruption after approximately 10 pore volumes resulted in further release of Fe. Total Fe release declined to a steady level of approximately 2.5 mg L^{-1} after extensive leaching and was not affected by changes in ionic strength or flow interruption around 33 pore volumes. Our results suggest that iron released from the Windsor column was the result of reductive Fe(III) dissolution (see also Ryan and Gschwend, 1990). The dissolution of Fe minerals might contribute to the mobilization of colloidal particles as suggested by Thompson et al. (2006). Furthermore, we suggest that the differences between the observed Fe behavior in Olivier and Windsor columns can be explained based on the presence of high amount of organic matter in Windsor soil. For Olivier soil, iron oxides were associated with clay particles or quartz grains. Changing ionic strength resulted in the dispersion of particles and exposed iron oxides in the aggregates to a reductive solution, which stimulated the reduction of iron oxides. In contrast, complexes were formed between iron hydroxides and the organic matter in Windsor soil (Davis, 1982). Organic coating on those iron oxides modified its reaction and protected it from dispersion by low ionic solution. The role of organic matter in controlling the release of Fe oxides under reduced condition is an interesting issue that warrants further investigation.

In our experiment, substantial release of Al was only observed after the input solution was displaced by deionized water, which further supports the notion of reductive dissolution as the mechanisms of iron release during arsenite input pulse. While free Al content of Windsor soil was approximately three times that of Olivier soil, substantially less Al was released from Windsor column than from Olivier column. We suggest that the Al oxides in Windsor soil was immobilized by complexation with organic matter.

7.4.3 Arsenite Transport

The transport of arsenite was largely controlled by the adsorption-desorption on the surfaces of Fe/Al oxides (Radu et al., 2005). Our sequential extraction results demonstrated that a large fraction of the input arsenic was strongly retained on Fe/Al oxides, which was similar to the sequential extraction results of Keon et al. (2001). In addition, the sorption of As(III) in the soils were rate-limited, illustrated by the long tailing and concentration change after flow interruption.

In our experiment, the transport of As(III) in Olivier column was greatly enhanced by the introduction of DWI water and the subsequent decrease in ionic strength. Goldberg and Johnson (2001) observed that the arsenite adsorption on amorphous Fe and Al oxides actually increased with decreasing ionic strength. Other studies have shown that ionic strength have relatively little effect on the As(III) adsorption (Manning and Goldberg, 1997; Smith et al., 1999). Therefore, desorption is unlikely the cause of the release of arsenic after the high ionic strength input solution was replaced with deionized water. In fact, high concentration of particulate arsenic was observed after introducing of DIW and accounted for a significant portion of the enhanced arsenic concentration in the effluent. In conclusion, the changing ionic strength dispersed colloidal particles and released colloidal arsenic into solution.

7.4.4 Environmental Implications

A major implication of this study is that changes in chemical composition of solutions in aquifer and vadose zones might result in colloid facilitated transport of contaminants such as As (Grolimund and Borkovec, 2005). For example, landfill leachate often contains high concentrations of heavy metals with high ionic strength. Displacement by rainfall or irrigation water which typically has low ionic strength could result in mobilization of arsenic associated with colloidal particles and the potential contamination of surface or groundwater. Another possible case is the freshwater intrusion to a contaminated coastal aquifer, which is often saturated with saltwater. Moreover, the extent of colloid generation and its effect on contaminant transport is heavily relied on the chemical and mineralogical composition of the natural geological materials.

7.5 Summary and Conclusions

Colloid generation and transport in soils is of great concern because of the suspected colloid-facilitated transport of contaminants to groundwater. In this study, colloid mobilization and its effect on the transport of arsenite [As(III)] were investigated with Olivier and Windsor soil columns. Input solution of 10 mg L⁻¹ As(III) in 0.01 M NaCl was first applied to saturated columns, followed by leaching with deionized water (DIW). Turbidity, electrical conductivity (EC), and pH of column effluents were monitored. Total and dissolved concentrations of As, Fe, and Al were analyzed. Mobilization of colloidal amorphous material and enhanced transport of As(III) was observed when the input solution was replaced with DIW. The peak of colloid generation coincided with peak concentrations of Fe, indicating mobilization of Fe oxides and facilitated transport of As(III) adsorbed on oxide surfaces. Mobilization of colloidal particles was observed due to flow interruption in Olivier column which suggests the kinetically controlled

colloid generation. Moreover, our results indicate significant effect of organic matter in stabilizing aggregates of colloidal particles.

7.6 References

- Bertsch, P.M., and J.C. Seaman. 1999. Characterization of complex mineral assemblages: Implications for contaminant transport and environmental remediation. *PNAS* 96:3350-3357.
- Davis, J.A. 1982. Adsorption of natural dissolved organic-matter at the oxide water interface. *Geochim. Cosmochim. Acta* 46:2381-2393.
- Dixit S., and J. G. Hering. 2003. Comparison of arsenic(V) and arsenic(III) sorption onto iron oxide minerals: implication for arsenic mobility. *Environ. Sci. Technol.* 37:4182-4189.
- Elkhatib, E.A., O.L. Bennett, and R.J. Wright. 1984a. Kinetics of arsenite adsorption in soils. *Soil Sci. Soc. Am. J.* 48:758-762.
- Elkhatib, E.A., O.L. Bennett, and R.J. Wright. 1984b. Arsenite sorption and desorption in soils. *Soil Sci. Soc. Am. J.* 48:1025-1030.
- Goldberg S., and C.T. Johnston. 2001. Mechanisms of arsenic adsorption on amorphous oxides evaluated using macroscopic measurements, vibrational spectroscopy, and surface complexation modeling. *J. Colloid Interface Sci.* 234:204-216.
- Grolimund, D., M. Borkovec, K. Barmettler, and H. Sticher. 1996. Colloid-facilitated transport of strongly sorbing contaminants in natural porous media: a laboratory column study. *Environ. Sci. Technol.* 30:3118-3123.
- Grolimund, D., and M. Borkovec. 2005. Colloid-facilitated transport of strongly sorbing contaminants in natural porous media: Mathematical modeling and laboratory column experiments. *Environ. Sci. Technol.* 39:6378-6386.
- Herbel, M., and S. Fendorf. 2006. Biogeochemical processes controlling the speciation and transport of arsenic within iron coated sands. *Chem. Geol.* 228:16-32.
- Ishak, C.F., J.C. Seaman, W.P. Miller, and M. Summer. 2002. Contaminant mobility in soils amended with fly ash and flue-gas gypsum: Intact soil cores and repacked columns. *Water Air. Soil Pollut.* 134:287-305.
- Keon, N.E., C.H. Swartz, D.J. Brabander, C. Harvey, and H.F. Hemond. 2001. Validation of an arsenic sequential extraction method for evaluating mobility in sediments. *Environ. Sci. Technol.* 35:2778-2784.
- Kretzschmar, R., M. Borkovec, D. Grolimund, and M. Elimelech. 1999. Mobile subsurface colloids and their role in contaminant transport. *Adv. Agron.* 66:121-193.

Le, X.C., S. Yalcin, and M. Ma. Speciation of submicrogram per liter levels of arsenic in water: On-site species separation integrated with sample collection. *Environ. Sci. Technol.* 2000, 34:2342-2347.

Manning, B.A., S.E. Fendorf, and S. Goldberg. 1998. Surface structure and stability of arsenic(III) on goethite: Spectroscopic evidence for inner-sphere complexes. *Environ. Sci. Technol.* 32:2383-2388.

Manning, B.A., and S. Goldberg. 1997. Arsenic(III) and arsenic(V) adsorption on three California soils. *Soil Sci.* 162:886-895.

Masscheleyn, P.H., R.D. Delaune, and W.H. Patrick. 1991. Effect of redox potential and pH on arsenic speciation and solubility in a contaminated soil. *Environ. Sci. Technol.* 25:1414-1419.

Pedersen, H.D., D. Postma, and R. Jacobsen. 2006. Release of arsenic associated with the reduction and transformation of iron oxides. *Geochim. Cosmochim. Acta* 70:4116-4129.

Peretyazhko, T., and G. Sposito. 2005. Iron(III) reduction and phosphorous solubilization in humid tropical forest soils. *Geochim. Cosmochim. Acta* 69:3643-3652.

Petschick R. 2000. MacDiff 4.2.5 manual. http://www.geologie.uni-frankfurt.de/Staff/Homepages/Petschick/PDFs/MacDiff_Manual_E.pdf

Puls, R.W., and R.M. Powell. 1992. Transport of inorganic colloids through natural aquifer material: Implication for contaminant transport. *Environ. Sci. Technol.* 26:614-621.

Radu, T., J.L. Subacz, J.M. Phillippi, and M.O. Barnett. 2005. Effects of Dissolved Carbonate on Arsenic Adsorption and Mobility. *Environ. Sci. Technol.* 39:7875 – 7882.

Raven, K.P., A. Jain, and R.H. Loeppert. 1998. Arsenite and arsenate adsorption on ferrihydrite: Kinetics, equilibrium, and adsorption envelopes. *Environ. Sci. Technol.* 32:344-349.

Roy, S.B., and D.A. Dzombak. 1997. Chemical factors influencing colloid-facilitated transport of contaminants in porous media. *Environ. Sci. Technol.* 31:656-664.

Ryan, J.N., and P.M. Gschwend. 1990. Colloid mobilization in 2 Atlantic coastal-plain aquifers - field studies. *Water Resour. Res.* 26:307-322.

Seaman, J.C., and P.M. Bertsch. 1997. Characterization of colloids mobilized from southeastern coastal plain sediments. *Environ. Sci. Technol.* 31:2782-2790.

Seaman, J.C., P.M. Bertsch, and W.P. Miller. 1995. Chemical control on colloid generation and transport in a sandy aquifer. *Environ. Sci. Technol.* 29:1808-1815.

Seta A.K. and A.D. Karathanasis. 1997. Stability and transportability of water-dispersible soil colloids. *Soil Sci. Soc. Am. J.* 61:604-611.

Smedley P.L., and D.G. Kinniburgh. 2002. A review of the source, behaviour and distribution of arsenic in natural waters. *Applied Geochem.* 17:517-568.

- Smith, E., R. Naidu, and A.M. Alston. 1999. Chemistry of arsenic in soils: I. Adsorption of arsenate and arsenite by selected soils. *J. Environ. Qual.* 28:1719-1726.
- Sposito, G. 1989. *The chemistry of soils*. Oxford University Press, New York.
- Sun, X., and H.E. Doner. 1998. Adsorption and oxidation of arsenite on goethite. *Soil Sci.* 163:278-287.
- Thompson, A., O.A. Chadwick, S. Boman, and J. Chorover. 2006. Colloid mobilization during soil iron redox oscillations. *Environ. Sci. Technol.* 40: 5743-5749.
- Tisdall, J.M., and J.M. Oades. 1982. Organic-matter and water-stable aggregates in soils. *J. Soil Sci.* 33:141-163.

CHAPTER 8: SUMMARY AND CONCLUSIONS

Adsorption and desorption of arsenic are the primary factors that impact the bioavailability and mobility of arsenic in soils. Adsorption of arsenate [As(V)] were highly nonlinear with a Freundlich reaction order N much less than 1 for Olivier loam, Sharkey clay, and Windsor sand. As(V) adsorption coefficients were successfully related with total content of soil Fe and Al oxides. Adsorption of arsenate by all soils was strongly kinetic, where the rate of As(V) retention was rapid initially and was followed by gradual or somewhat slow retention behaviour with increasing reaction time. Freundlich distribution coefficients and Langmuir adsorption maxima exhibited continued increase with reaction time for all soils. Desorption of As(V) was hysteretic in nature which is an indication of lack of equilibrium retention and/or irreversible or slowly reversible processes. A sequential extraction procedure provided evidence that a significant amount of As(V) was irreversibly adsorbed on all soils.

Results from saturated column transport experiments demonstrated that all measured As(V) breakthrough curves (BTCs) were asymmetric as illustrated by the difference in the shape of the effluent side from the leaching or desorption side. Specifically, arsenic retardation or adsorption was followed by slow release or extensive tailing. The sharp drop in As(V) concentration during arsenic pulse application as a result of flow interruptions is indicative of the dominance of rate-limited As(V) retention. After extended leaching, the percentages of As(V) mass recovery from column effluent ranged from 82.1% for Olivier soil to as low as 39.2% for Sharkey clay, indicative of slow release or irreversible As(V) retention.

A multireaction model (MRM) with nonlinear equilibrium and kinetic sorption successfully described the adsorption kinetics of As(V) for Olivier loam and Windsor sand. The model was also capable of predicting As(V) desorption kinetics for both soils. However, for Sharkey clay, which exhibited strongest affinity for arsenic, an additional irreversible reaction

phase was required to predict As(V) desorption or release with time. We further evaluated several formulations of MRM model for its prediction capability of As(V) retention as well as transport in soils. Based on root mean square errors (RMSE) and coefficients of determination (r^2), model formulations having nonlinear reversible reaction along with a consecutive or concurrent irreversible retention were considered the most favorable in describing As(V) retention over time for all three soils. These model formulations are recommended for As prediction and for future application because of the fewest number of model parameters. The use of batch model parameters provided poor overall predictions of all BTCs. The use of batch rate coefficients grossly underestimated the extent of As(V) retention in Windsor and Olivier soils and overestimated As(V) mobility by all model formulations used. We thus concluded that BTC predictions based on batch parameters are not recommended. However, when the multireaction transport model was utilized in an inverse mode, the model was capable of describing As(V) BTCs for Windsor and Olivier soils. Moreover, model formulations which provided best-fit of the BTCs were consistent with those based on kinetic batch data.

The competition between arsenate [As(V)] and phosphate (P) has the potential of increasing arsenic mobility and bioavailability in soil and water environment. Kinetic batch and saturated miscible displacement experiments were further conducted to evaluate the competitive effect of P on As(V) sorption and transport. Nonlinear single-solute isotherms of As(V) and P were observed for Olivier, Sharkey, and Windsor soils. Competition for specific adsorption sites is likely the major cause for the observed competitive effect between arsenate and phosphate. The relative adsorption affinity of As(V) over P was explained with the Fe/Al ratio of the soils. The Sheindorf-Rebhun-Sheintuch (SRS) equation successfully described the competition between As(V) and P with optimized competitive coefficients. The kinetic batch results

demonstrated that rates and amounts of As(V) adsorption by these soils were significantly reduced by increasing P additions. In addition, the adsorption preferences of the soils to As(V) and P were constant during the adsorption period. Only a small fraction of As(V) was desorbed in our experiments and a significant amount of As(V) was irreversibly adsorbed on all soils as demonstrated by the sequential extraction procedure. Miscible-displacement experiments were conducted to determine the extent of As(V)-P competition when the anions were introduced simultaneously or consecutively to saturated soil columns. The results from column experiments demonstrated that the addition of phosphate significantly increased peak concentrations and mass recoveries of As(V) eluted from soils. Increasing As(V) was released when P was introduced to displace sorbed As(V). Concentration changes during flow interruptions in column studies verified the dominance of time-dependent sorption during As(V) and P transport in soils.

We extended the equilibrium-kinetic multireaction model (MRM) to quantitatively simulate competitive retention kinetics of multiple chemical species. Competitive coefficients from Sheindorf-Rebhun-Sheintuch (SRS) equation were adopted to describe the extent of competition between chemical species. We evaluated this multi-component multireaction model (MCMRM) for its prediction capability of As(V)-P retention as well as transport in soils. Competitive retention for As(V) and P over time was successfully predicted using MCMRM where model coefficients were based on single component kinetic batch results. The use of batch rate coefficients provided poor prediction of As(V) BTCs from the competitive column transport experiments. The multi-component model adequately predicted the measured BTCs for competitive As(V)-P transport in Olivier and Windsor soil when rate coefficients obtained from inverse modeling of single component As(V) BTCs were used. The competitive approach was

also capable of predicting flow interruptions as well as the chromatographic effect of the As(V) pulse due to the competition of P with As(V).

Colloid generation and transport in the natural soil is of great concern because of the suspected colloid-facilitated transport of contaminants to groundwater. XRD analysis demonstrated that the clay minerals in Olivier soil was readily dispersed by deionized water (DIW). However, mineral composition of water dispersible clay (WDC) was substantially different from that of sodium dispersible clay (SDC) of Windsor soil. This is possibly resulted from the high organic matter content of Windsor soil. Mobilization of colloidal amorphous material and enhanced transport of As(III) was observed when the input solution was replaced with DIW. The peak of colloid generation coincided with the peak concentrations of Fe, indicating mobilization of Fe oxides and facilitated transport of As(III) adsorbed on oxide surfaces. We have observed substantial mobilization of colloidal particles after flow interruption in Olivier column, suggesting the kinetically controlled colloid generation. Moreover, our results indicated a significant effect of organic matter in stabilizing aggregates of colloidal particles. Our experiment results demonstrated that changes in chemical composition of solutions in aquifer and vadose zones might result in colloid facilitated transport of contaminants such as arsenic.

VITA

Mr. Hua Zhang was born in a small village in People's Republic of China on January 22, 1977, as the second son of Mr. Yongxiang Zhang and Mrs. Yuping Gu. He graduated from HuaZhong Agricultural University, Wuhan, China, in 1999 with the degree of Bachelor of Science in agricultural environmental protection. In this college he fell in love with his future wife, Xueli Gao, and they married in 2002. He obtained his degree of Master of Science in soil science from the Institute of Soil Science, Chinese Academy of Sciences, Nanjing, China, in 2002. He began his doctoral studies in soil physics in 2002 at the Department of Agronomy and Environmental Management, Louisiana State University. Mr. Zhang has a lovely daughter, Rudi Zhang, who was born in November 17, 2005.